T and B lymphocyte crosstalk in autoimmune diabetes

Félix Lombard-Vadnais

Department of Microbiology & Immunology
McGill University, Montreal

A thesis submitted to McGill University in partial fulfillment of the requirements of the degree of Doctor of Philosophy

Abstract

The development of type 1 diabetes (T1D), an autoimmune disease affecting the pancreas in susceptible individuals, is controlled by a variety of environmental and genetic factors. While the pathogenesis of T1D has been studied for more than 100 years, the cellular events leading to pancreatic beta cell loss are incompletely understood. Two principal actors in the autoimmune responses promoting diabetes are T and B lymphocytes, both of which are necessary for diabetes development in NOD mice, a mouse model of T1D. While the importance of both cell subsets has been clearly established, the consequences of their interplay on diabetes development are not fully understood. Therefore, we evaluated the contribution of T and B lymphocyte crosstalk in the context of autoimmune diabetes. With this project, we identified a locus on chromosome 9 of the mouse (the *Idd2* locus) containing genetic variants that promote T and B cell interactions, by influencing the level of MHC expression on immune cells. Genes in this locus are highly implicated in diabetes susceptibility, as modification of this locus on the NOD background greatly reduce diabetes onset. We also show that *Pou2af1*, a candidate gene is the *Idd2* locus, promotes the differentiation of Tfh by participating in the crosstalk between T and B cells. Lastly, we uncover a novel role for AID expression in thymic B cells in supporting their participation in the selection of thymocytes and the control of autoimmunity. Together, these data highlight the multi-faceted consequences of the crosstalk between T and B cells in the context of autoimmune diabetes.

Résumé

Le développement du diabète de type 1 (DT1), une maladie auto-immune affectant le pancréas chez les individus à risque, est contrôlé par divers facteurs génétiques et environnementaux. Bien que la pathogénèse de cette maladie soit étudiée depuis plus de 100 ans, les mécanismes cellulaires menant à la perte des cellules betas du pancréas ne sont pas complètement compris. Les deux acteurs principaux participant aux réactions auto-immunes qui causent le DT1 sont les lymphocytes T et B, deux types cellulaires nécessaires au développement de la maladie chez la souris NOD, un modèle murin de DT1. Bien que l'importance des cellules T et B dans le développement du DT1 soit établie, les conséquences des interactions entre ces cellules ne sont pas totalement connues. Conséquemment, notre but était de caractériser les interactions entre les cellules B et T dans le développement du diabète auto-immun. Grâce à ce projet, nous avons identifié un locus sur le chromosome 9 de la souris (le locus *Idd2*) comportant des variants génétiques qui favorisent les interactions entre cellules B et T, via la modulation de molécules du CMH. La modification de ce locus chez la souris NOD réduit fortement le développement du diabète, confirmant que des gènes de ce locus sont impliqués dans la susceptibilité au diabète auto-immun. Nous avons aussi montré que le gène *Pou2af1*, un gène candidat du locus *Idd2*, favorise le développement des cellules T folliculaires en modulant les interactions entre les cellules B et T. Pour terminer, nous avons identifié un nouveau rôle pour l'expression de AID dans les cellules B thymiques, permettant à ces cellules de participer à la sélection des thymocytes et au contrôle de l'auto-immunité. Ensemble, ces résultats soulignent les conséquences diverses qui surviennent suite aux interactions entre les cellules B et T dans le contexte du diabète auto-immun.

Acknowledgments

Adrien, Cindy, Victor, ce doctorat aurait été très différent sans vous. Toutes ces longues soirées auraient été beaucoup plus pénibles sans nos karaokés de Mariah Carey et nos playlists de flute de Pan. Peut-importe où vous êtes rendu sur la planète, je suis très chanceux de toujours être en contact avec vous, pour parler de tout, de rien et rire ensemble. J'ai bien hâte qu'on se retrouve tous ensemble en personne. Merci du fond du cœur pour ces belles années!

Erin, je me rappellerai toujours mon premier stage, en 2015. C'est un moment stressant pour quelqu'un qui ne connait pas du tout le milieu de la recherche. Tu as rendu ce stage enrichissant et très plaisant, une des raisons pourquoi j'étais de retour au labo deux ans plus tard. Merci aussi pour toutes les discussions scientifiques pendant la première partie de mes études. Au plaisir d'avoir d'autres belles discussions dans le futur.

Geneviève, toujours là pour aider les gens au laboratoire, autant au début de mon parcours quand je ne savais rien faire, que maintenant. Une bonne humeur constante qui rend nos journées au laboratoire très agréable. L'équipe ne serait pas du tout la même sans toi. Merci pour toutes ces années, ainsi que celles à venir !

Bien sûr, tous les autres membres du laboratoire. Merci pour la bonne ambiance au laboratoire, c'est toujours agréable de venir travailler avec vous tous.

Ianula et Catherine, merci beaucoup pour votre travail acharné à l'animalerie. Sans vous, nos expériences seraient impossibles. Vous être toujours disponibles pour nous donner un coup de main et c'est énormément apprécié.

Merci à mes parents et mon frère. Merci de me supporter lorsque le doctorat est stressant et que je deviens moins agréable. Merci pour les mots d'encouragement quand ça devient difficile ; de m'encourager à persévérer et de regarder un jour à la fois. Merci aussi d'avoir été là pour célébrer chaque petite victoire ensemble. Et merci à Ariane pour le champagne à chaque étape.

Martine et Frédéric, merci pour ces cinq années (même plus) d'aide à la cytométrie, de discussions et de conseils. Nous en avons passé des heures ensemble… juste à regarder les figures de cette thèse, on s'en rend rapidement compte ! Et ce fut toujours agréable.

Claire, je te remercie pour tout ton aide et les moments passé ensemble. Mon mentor pour la microscopie, j'ai fort apprécié toutes les petites collaborations que nous avons eu.

Virginy, partager les joies et les frustrations des études graduées ensemble fut très libérateur. Merci aussi pour tes conseils de biologie moléculaire !

À tous les organismes subventionnaires (FRQS, IRSC, Fondation HMR, Diabète Québec, The Cole Foundation, Montreal Immunology Meetings), merci pour votre support qui m'a permis de me consacrer à temps plein à ma recherche.

Dr King, thank you for giving me a chance even though you didn't know me at all. It gave me the opportunity of discovering another part of the Montreal research world. Thank you for the scientific and non-scientific discussions and for always being available to help. Your questions, comments and advice greatly helped me pushed myself. Thank you for all these years.

Sylvie, comment te remercier? Merci d'avoir cru en moi dès le début, après à peine une année d'étude au baccalauréat. Je te remercie pour ton ouverture, de m'avoir laisser explorer un domaine de l'immunologie qui n'était pas celui prévu pour moi au début de mes études. Je te remercie pour ta patience exemplaire ainsi que pour m'avoir laissé partager mes idées et opinions. Ceci m'a permis d'apprendre énormément. Merci de m'avoir poussé à me dépasser constamment. Et bien sûr, merci de me faire confiance pour la suite !

Et toutes les souris qui ont permis les nombreuses découvertes décrites ici et les autres à venir, je ne vous oublie pas, merci !

Table of content

Contribution to original knowledge

The work presented in this thesis significantly contributes to the advancement of knowledge by tackling original questions related to the biology of germinal center (GC) and extrafollicular immune responses. GCs are dynamic cellular structures composed mainly of T and B lymphocytes that play critical roles in the humoral response. While extensively studied, the crosstalk between T and B cells in GCs and extrafollicular responses are not completely understood.

Using an unbiased approach in Chapter 2, we reveal that genetic variants linked to autoimmune diabetes susceptibility in mice contribute to GC formation. In Chapters 3 and 4, we investigate the non-conventional roles of genes previously identified as key determinants of the GC response, namely *Pou2af1* and *Aicda*. In Chapter 3, we demonstrate that *Pou2af1* plays significant cell-intrinsic roles in GC B cell differentiation, but only indirectly affects T cells. In Chapter 4, we explore the impact of *Aicda* expression by thymic B cells and reveal its role in the induction of thymocyte negative selection, an important process in the control of immune tolerance.

In the published manuscript-based Chapter 2, we demonstrate that genetic variants inside the *Idd2* locus:

1. Drastically determine autoimmune diabetes susceptibility in mice
2. Impact the formation of spontaneous and induced germinal centers
3. Modulate MHC I expression on most immune cells and MHC II expression on B cells

In the published manuscript-based Chapter 3, we resolve a long-lasting controversy regarding the impact of *Pou2af1*/OCA-B expression in T cell biology. We demonstrate that:

1. While *Pou2af1* is induced in T cell following activation, *Pou2af1* expression in T cells does not impact T cell differentiation or function
2. Deletion of *Pou2af1* in T cells does not significantly impact the T cell transcriptome
3. Expression of *Pou2af1* in B cells indirectly promotes maturation of preTfh into mature Tfh

In the manuscript-based Chapter 4, in preparation for submission, we demonstrate that AID expression by thymic B cells:

1. Promotes interactions between thymic B cells and CD4SP thymocytes
2. Promotes negative selection of self-reactive CD4SP thymocytes
3. Limits T cell-mediated inflammation and autoimmune diabetes development

Contribution of authors

Chapter 1:

F.L.V wrote the introduction

Chapter 2:

F.L.V performed experiments, analyzed data, and wrote the manuscript. R.C., G.C.R and J.F.D. performed experiments. N.L. provided reagents and conceptual inputs and wrote the manuscript. S.L. performed experiments, supervised the study, and wrote the manuscript.

Chapter 3:

F.L.V performed experiments, analyzed data, and wrote the manuscript. J.L. and G.C.R. performed experiments. M.F. provided reagents and conceptual inputs. S.L. supervised the study and wrote the manuscript.

Chapter 4:

F.L.V performed experiments, analyzed data, and wrote the manuscript. G.C.R performed experiments. J.D.N. provided reagents and conceptual inputs. S.L. supervised the study and wrote the manuscript.

List of abbreviations

AID: Activation-induced cytidine deaminase

APC: Antigen presenting cell

BioID: Biotin identification

BCR: B cell receptor

CD4SP: CD4 Single Positive

CD8SP: CD8 Single Positive

CSR: Class switch recombination

cTEC: Cortical thymic epithelial cell

CXCR5: C-X-C chemokine receptor type 5

DC: Dendritic cell

DZ: Dark zone

FDC: Follicular dendritic cell

GC: Germinal center

IFNγ: Interferon gamma

IL: Interleukin

KO: Knock Out

LN: Lymph node

LncRNA: Long non-coding RNA

mLN: Mesenteric lymph node

mTEC: Medullary thymic epithelial cell

pLN: Pancreatic lymph node

LZ: Light zone

MHC: Major Histocompatibility Complex

miRNA: microRNA

NOD: Non-Obese Diabetic

PD-1: Programmed cell death protein 1

PP: Peyer's patches

RORγt: RAR-related orphan receptor gamma T

SHM: Somatic hyper mutation

SNPs: Single nucleotide polymorphisms

SRBC: Sheep red blood cell

TCR: T cell receptor

Tc: Cytotoxic T cell

Tfh: Follicular helper T cell

Th: T helper cell

Th17: T helper type 17 cell

TLR: Toll-like receptors

Treg: T regulatory cell

TNFα: Tumor necrosis factor α

WT: Wild type

Chapter 1:

Literature review

The immune system is composed of a wide array of immune cells that protect from infection and cancer. Cells of the innate immune system, such as neutrophiles and macrophages, provide rapid protection against invading microbes, while cells of the adaptive immune system, such as T and B lymphocytes, provide specialized protection against a variety of pathogens and transformed cells. This thesis will focus on the adaptive immune responses, as breach of tolerance from T and B cells lead to autoimmunity and, in some individuals, development of autoimmune diseases. Specifically, we will touch on different aspects of the crosstalk between T and B cells, with a particular interest on germinal center (GC) reactions. GCs are complex cellular structures composed mostly of B and T cells. The biology of GCs is discussed in chapters 1.4 and 1.10. Before addressing the complexity of T and B cell crosstalk, let's start by examining the development of those lymphocyte populations.

1.1 Thymic development of T cells

T lymphocytes are part of the adaptive immune system, in which they play critical roles as helper ($CD4^+$) and cytotoxic ($CD8^+$) T cells. T cell lineage specification takes place in the thymus, via signals present in the thymic environment (1). After entry at the cortico-medullary junction (2), early T cell precursors follow the CXCL12 gradient that lead them into the cortex, where they begin their differentiation process (2). In addition to developing immature T cells, called thymocytes, the thymic cortex is mainly composed of cortical epithelial cells (cTECs), macrophages and fibroblasts. Cells defining the earliest stages of thymocyte differentiation lack

expression of both CD4 and CD8; following productive TCR β rearrangement, they differentiate into $CD4^+CD8^+$ (DP) thymocytes. At the DP stage, thymocytes start expressing a functional αβTCR (3). TCR expression allows recognition of peptide-MHC (pMHC) complexes present on the surface of cTECs and macrophages. Recognition of such complexes have different outcomes, depending on the strength and duration of the TCR-pMHC interaction. Low affinity interactions (or absence of interaction) lead to death by neglect, while medium and high affinity interactions lead to conventional and unconventional T cell differentiation, respectively (4, 5), via processes called positive and agonist selection. In addition, negative selection to ubiquitous antigens also takes place in the cortex, resulting in the elimination of some self-reactive DP thymocytes by induction of cellular apoptosis (6).

Following positive selection, DP thymocytes migrate to the thymic medulla, where they differentiate into CD4SP or CD8SP thymocytes. The cellular composition of the medulla varies from the cortex, with an increase in the density of DCs and B cells, as well as the presence of specialized epithelial cells (mTECs) (7, 8). At this stage, self-reactive semi-mature thymocytes are still susceptible to apoptosis (9). Depending on the signals they receive from medullary antigen presenting cells (APCs), thymocytes can survive or be eliminated by negative selection. If they continue to receive tonic TCR signals, thymocytes continue their maturation and become resistant to apoptosis (9). At this stage, the most mature thymocytes exit the thymus and reach the periphery, where they confer protective immunity (10).

1.2 Central T cell tolerance

The T cell repertoire has evolved to allow the generation of considerably diverse TCR sequences (1×10^{15}) (11). This enormous diversity enables the recognition of an almost infinite number of antigens. Microbial pathogens and transformed cells express antigens that can be recognized by TCRs, enabling anti-microbial and anti-tumoral immune responses.

It is, however, not infrequent that the random generation of a TCR results in recognition of self-antigens. Recognition of self-antigens by mature T cells can lead to immune responses against healthy cells and tissues, and at times, can promote the development of autoimmune diseases. To prevent autoimmunity, there are mechanisms that limit the generation of self-reactive T cells. Indeed, impaired elimination of autoreactive thymocytes has been documented in multiple mouse models of autoimmunity as well as patients suffering from autoimmune diseases (12-15). As mentioned above, the primary mechanism allowing the elimination of autoreactive thymocytes is called negative selection (or clonal deletion) and takes place directly during thymocyte differentiation.

While death by neglect is a passive form of cell death, caused by absent or insufficient TCR signaling, negative selection is an active process. It was initially estimated, using various $MHC^{-/-}$ chimeras, that 90% of all developing thymocytes die by neglect, while 5% are clonally deleted, leaving only 5% of remaining thymocytes to fully complete their thymic maturation (16). However, this estimation has been recently challenged, where most death were reported to be due to negative selection rather than death by neglect (6). Indeed, using $BIM^{-/-}$ and $NUR77^{GFP}$ mice, it

was estimated that the majority (75%) of negatively selected cells die at the DP stage in the cortex, with the remaining 25% being deleted at the SP stage in the medulla (6). Thymic selection therefore enables, in two distinct steps, the generation of a T cell repertoire composed of cells expressing functional TCRs, while limiting the presence of highly self-reactive T cells.

A hypothesis for the importance of affinity of the TCR for pMHC complexes in determining thymocyte selection outcome (death or survival) lies in the duration of the interactions between the thymocyte and the APC. While low affinity ligands result in short interactions, leading to only early TCR signals, ligands with stronger affinity allow longer interactions and induce both early and late TCR signals, inducing thymocyte death (17-19). At the molecular level, few differences have been identified between signaling inducing positive and negative selection. Those include MAP kinase signaling (specifically necessary for positive selection (20)) and the nuclear receptor NUR77 (necessary for negative but not positive selection (21)).

Still, TCR engagement by itself is not sufficient to induce negative selection (22). Indeed, a second signal is necessary for the induction of thymocyte apoptosis during negative selection. In combination with TCR signaling, engagement of multiple surface receptors has been demonstrated to promote negative selection (17, 23, 24). Of those, CD28-CD80/CD86 interactions have been the most studied. Expression of CD80 and CD86 on thymic APCs promotes clonal deletion of autoreactive CD4SP thymocytes, thereby limiting the development of T cell-mediated autoimmune diseases (25). Furthermore, expression of CD80 and CD86 promote the generation of thymic Tregs through a distinct molecular mechanism (25), which are important mediators of T cell tolerance in the periphery (26). While cTECs do not express the co-stimulatory molecules

necessary to induce negative selection (CD80/CD86), cortical macrophages and the rare cortical dendritic cells (DCs) can induce negative selection of a high number of thymocytes in the cortex (6, 27). In the thymic medulla, mTECs and DCs are the most abundant APCs. An important characteristic of mTECs is their ability to express tissue-restricted antigens (TRAs) (28). Expression of proteins normally only expressed in specific tissues, such as insulin, enables mTECs to induce deletion of potentially autoreactive thymocytes that could drive tissue-specific autoimmune responses in the periphery. Two main transcription factors have been identified as master regulators of TRAs expression in mTECs: Aire and FEZF2. It was however estimated that only 60% of all TRA genes are regulated by either AIRE, FEZF2 or a combination of both (29), suggesting that at least one other transcription factor is implicated in TRA expression in mTECs. Interestingly, it was reported that, in addition to mTECs, thymic B cells represent an important population of AIRE-expressing APCs (30). The role of thymic B cells in negative selection of thymocytes is further discussed in chapter 1.5.

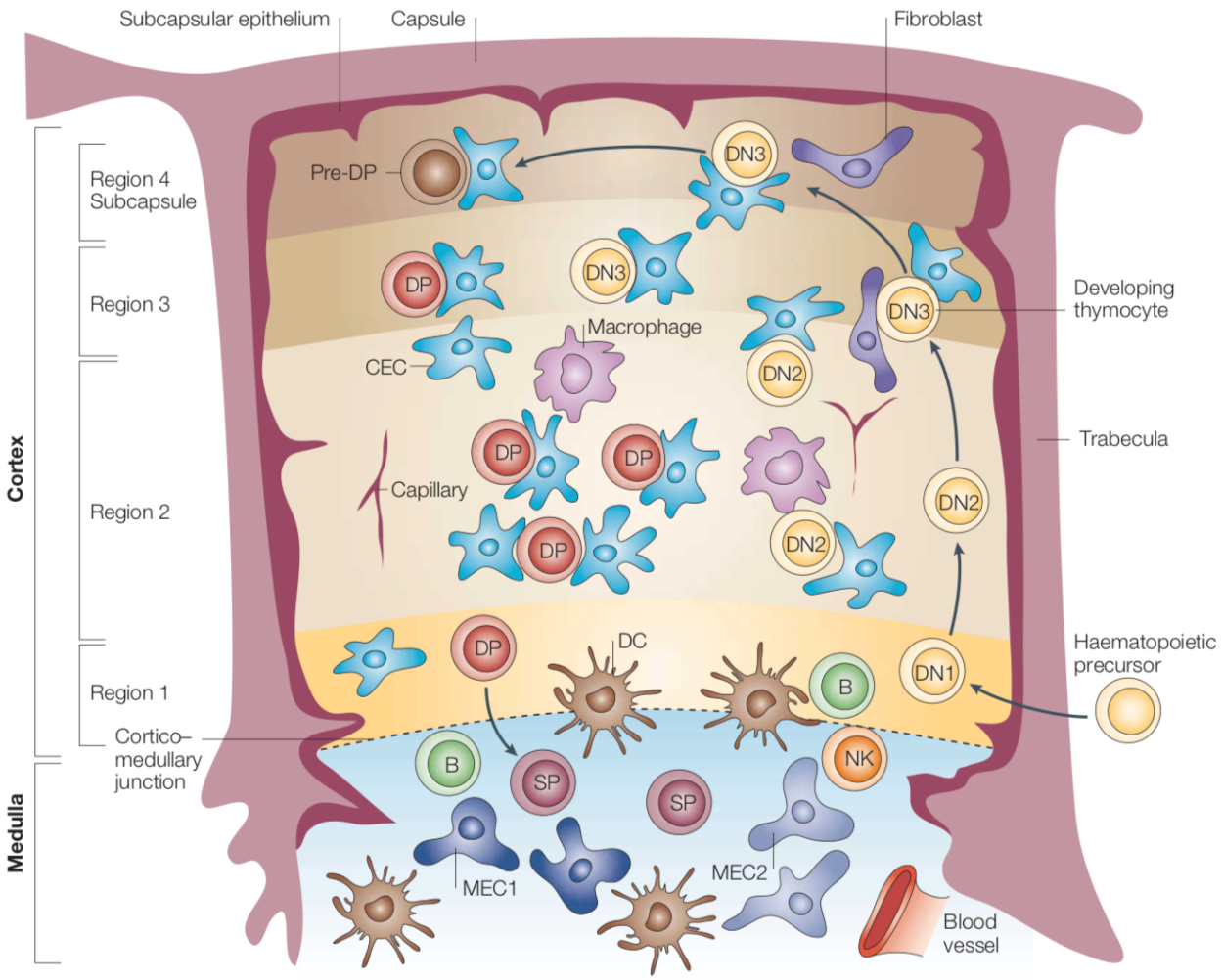

Figure 1: Schematic representation of the thymus and the cellular populations present in this organ. On the right, precursors enter the thymus at the cortico-medullary junction. Thymocytes then undergo a series of guided steps by interacting with various cellular and molecular components in the thymus. This ultimately leads to the production of functional T cells, where most potentially autoreactive T cells have been purged from the repertoire.Source: Adapted from (31).

1.3 B cell development

1.3.1 B cell development after birth

B cells originate from common lymphoid progenitors present in the bone marrow, which can give rise to T and B lymphocytes, DCs, Natural Killer (NK) cells and innate lymphoid cells (32-34). The first committed stage in the B cell lineage, characterized by the expression of the surface marker B220/CD45R, is the pre-pro-B cells (35). Similar to T cell precursors in the thymus, developing B cells displaying self-reactivity are eliminated in the bone marrow. This selection process takes place at the immature B cell stage, when IgM is first expressed at the cell surface, through the combination of the heavy and light chain of the BCR (36). Immature B cells bearing BCRs that strongly react to antigens present in the bone marrow are estimated to represent 50-75% of all immature B cells in mice and humans (37). This number drops to 20-40% in the transitional and naïve B cell populations (37), demonstrating that clonal deletion at the immature stage is responsible for the elimination of around 50% of self-reactive B cells. Cells that survive this selection process then migrate from the bone marrow to the spleen, through sphingosine-1-phosphate (S1P)–mediated chemoattraction (38). In the spleen, immature B cells complete their differentiation into follicular or marginal zone B cells. B cells are also able to recirculate to the thymus via the bloodstream. The origin and phenotype of thymic B cells are further discussed in section 1.3.4.

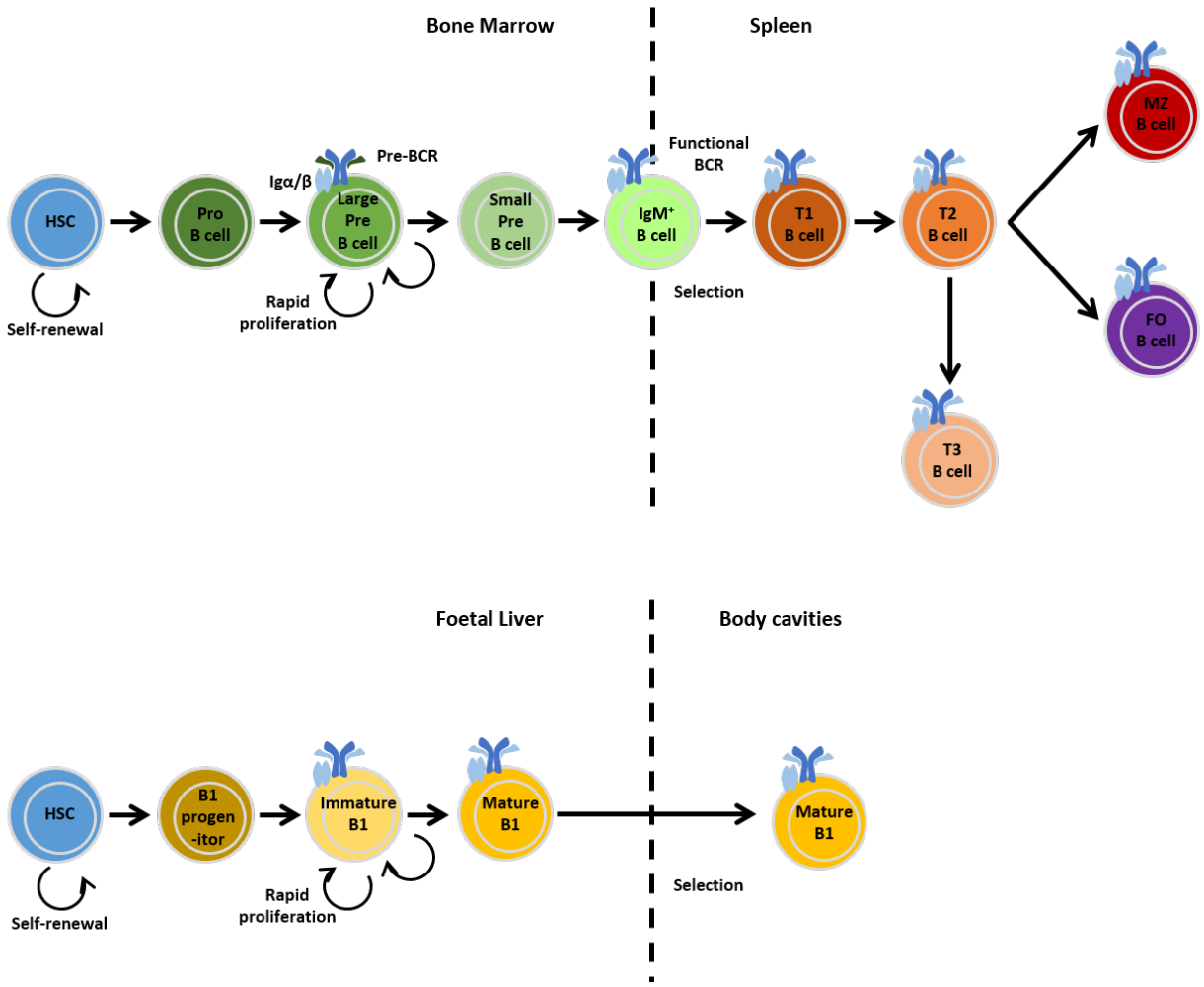

Figure 2. Schematic representation of the developmental stages of B cells in the bone marrow and fetal liver. At the pro-B cells stage, cells start expressing the B cell specific marker CD19, as well as RAG-1/2 and TDT, for the recombination of their B cell receptor (BCR) (36). At this stage, pro-B cells rearrange the heavy chain of their BCR (36). Association of the newly generate heavy chain with the surrogate light chain (identical in all B cells), leads to their differentiation into large pre-B cells. RAG expression is halted in large pre-B cells, which proliferate massively, giving rise to B cells clones with the same heavy chains of the BCR (36). After proliferation, pre-B cells (now referred to as small pre-B cells) regain RAG expression and complete the rearrangement of their BCR through the V-J joining of the light chain (36). Source: Adapted from https://www.immunology.org/public-information/bitesized-immunology/cells/b-cells

1.3.2 Transcription factors:

As for other cell types, B cell development is tightly regulated through the expression and repression of several transcription factors. The transcription factor PAX5 is first expressed at the pro B cell stage and its expression is maintained throughout the B cell life, until plasma cell differentiation (39). PAX5 is regarded as the master regulator of B cell development as its expression in pro B cells drives B cell lineage commitment. Indeed, in absence of PAX5, differentiation of pro B cells is arrested and these cells can differentiate in other hematopoietic lineages, such as NK cells, granulocytes and DCs (40). PAX5 exerts multiple roles during B cell differentiation, such as the promotion of the V-DJ recombination events, the expression of B-cell specific genes and the repression of genes associated with other hematopoietic cell types (39). Interestingly, PAX5 expression is downregulated in plasma cells, allowing expression of PAX5-repressed genes, such as *Blimp-1*, *Xbp1,* and *Jh*, which all have important roles in plasma cells (39).

In addition to PAX5, many other transcription factors contribute to B cell differentiation. For example, *E2a*, encoding for E12 and E47, is necessary for the differentiation of pro-B cells into pre-B cell, such that $E2a^{-/-}$ mice lack almost all mature B cells (41). Similarly, $Ebf^{-/-}$ mice lack mature B cells because of the requirement of EBF (Early B cell factor) for the recombination of the heavy chain at the pro-B cell stage (42). In addition, the transcription factors PU.1 and IRF8 are important during the later stages of B cell differentiation, notably for the development and survival of follicular and germinal center B cells (43). OCA-B (also known as BOB.1 or OBF-1) is another important protein involved in the transcriptional regulation of B cell development. OCA-B is encoded by the *Pou2af1* gene and is a transcriptional co-activator highly expressed in B cells

(44, 45). OCA-B binds to the transcription factors OCT-1 and OCT-2 and activate the transcription of target genes (44). OCA-B is expressed in B cell precursors and mature B cells, although its expression varies between the different stages and with the activation status of the cell (46). In *Pou2af1*$^{-/-}$ mice, mature B cell numbers are severely reduced, possibly due to a reduction of *Bcl2* expression, resulting in an increase in apoptosis of B cell precursors (46). OCA-B deficiency also impairs BCR signaling, leading to reduced calcium mobilization (46), a crucial factor during B cell selection in the bone marrow. Therefore, OCA-B might promote B cell development by allowing optimal BCR signaling in B cell precursors, leading to efficient B cell selection and maturation. OCA-B also promotes the differentiation and migration of transitional B cells to the spleen (46, 47), thereby participating in the last stage of B cell maturation. Interestingly, OCA-B deficiency seems to impair the development of follicular B cells more significantly than marginal zone B cells or B-1 B cells, suggesting a subset-dependent requirement for OCA-B during development (46). The other roles of OCA-B in B cell biology are further discussed in chapter 1.4 and 4.

1.3.3 Fetal development of B cells

As opposed to B cell development after birth, which takes place in the bone marrow, B cell development in the fetus takes place in the liver. B cell-restricted precursors have been isolated in the mouse fetal liver at day 11 post conception (48), and week 7 in humans (49) . Similar to B cell differentiation in the bone marrow, these fetal liver precursors are dependent on Pax5 and EBF for their differentiation (48). The main difference between fetal and bone marrow B cell development is the phenotype and function of the B cell subsets they generate. While fetal liver precursors mainly give rise to B1-B cells, bone marrow precursors are responsible for the development of B2-

B cells (50). In contrast to the main B2-B cell subset, B1-B cells are characterized by the expression of CD5 (specifically B1a-B cells), exhibit innate immune cell traits and display high levels of BCR cross-reactivity and self-reactivity (51). Of interest, thymic B cells do not accurately fit the criteria for either of these B cell subsets.

1.3.4 Thymic B cell development

In contrast to peripheral B cells, the origin of thymic B cells is still poorly understood. Thymic B cells represent a small population of B cells in the thymus of mice and humans. They appear in the mouse thymus after birth and accumulate with age, accounting for approximately 0.1-1% of total thymocytes in adult mice (data in chapter 4). Current hypotheses suggest that thymic B cells can either arise from migration from the periphery or from in situ differentiation. There is some experimental evidence supporting that mature circulating B cells can populate the thymus. Indeed, intravenous injections of large numbers of tagged B cells showed that mature B cell can migrate via the blood and seed the thymus (30). More convincingly, parabiosis experiments have shown that some thymic B cells arise from the circulation, although to lower levels than splenic B cells (8). Still, whether this is due to the migration of mature B cells or of cellular precursors that seed the thymus and generate B cells in situ is unclear. Alternatively, multiple groups have identified B cell precursors directly in the thymus, corresponding to pro and pre-B cells (8, 52). In addition, these B cell precursors show active intra-thymic BCR rearrangement (8), strongly supporting the notion of intra-thymic B cell development. While thymic B cells express the B1a-B cell marker CD5, they lack the expression of other B1a-B cell markers (CD43 and CD11b), which challenges their classification in the classical B1 and B2-B cell groups. In addition, thymic B cells display a unique surface phenotype, with increased

expression of MHCII, CD80 and CD86, compared to peripheral B cells (8). The unique function of thymic B cell will be discussed in chapter 4.

1.4 Crosstalk between T cells and B cells in secondary lymphoid organs

T cells and B cells both play unique roles in the immune system. Still, crosstalk between these two distinct cell types is crucial for the optimal execution of immune responses.

1.4.1 Antigen presentation

Similar to DCs and macrophages, B cells are considered professional APCs, with constitutive expression of MHC II molecules. Still, several differences exist between B cells and other professional APCs. One major difference between B cells and DCs/macrophages is the absence of expression of co-stimulatory molecules at steady state, with the exception of CD40. Indeed, while mature DCs and macrophages express CD80 and CD86 at steady state, naïve B cells do not (53). However, activation of B cells through binding of the BCR, CD40 or Toll-like receptors (TLR) induces CD80 and CD86 expression (54-56). Therefore, once activated, B cells possess all the necessary molecules (MHC I/II, CD40, CD80, CD86) to efficiently activate naïve T cells. Another significant difference between B cells and other professional APC types lies in the method of antigen capture. Compared to DCs and macrophages, which acquire antigens through efficient phagocytosis, B cells are not considered professional phagocytes. However, B cells take advantage of their BCR to efficiently capture antigens (57). High affinity BCRs enable the capture of antigens present at very low concentration, either soluble in the environment or at

the surface of other cells (57-59). Binding of antigens to the BCR induces a signaling cascade that leads to the activation of the B cells. This signaling cascade induces the expression of several genes implicated in BCR internalization and antigen processing (57), therefore initiating the process of antigen presentation.

In secondary lymphoid organs such as lymph nodes (LNs) and the spleen, B cells and T cells are clustered in different locations. B cell aggregates, termed follicles, are located under the LN capsule or adjacent to the marginal zone of the spleen (60). In the follicles, follicular B cells are the most abundant cell type, followed by follicular dendritic cells (FDCs) (60); the latter are cells of mesenchymal origin that support B cell functions (further discussed in section 1.4.2). In the lymph nodes, T cells are distributed in the paracortex adjacent to the follicles, also known as the T cell zone (60). In the context of immunization, B cells can capture antigen in less than 8 hours (61) and migrate to the T-B cell border of lymph nodes in less than 24h to present antigens to T cells (60), establishing B cells as important APCs in the initiation of adaptive responses.

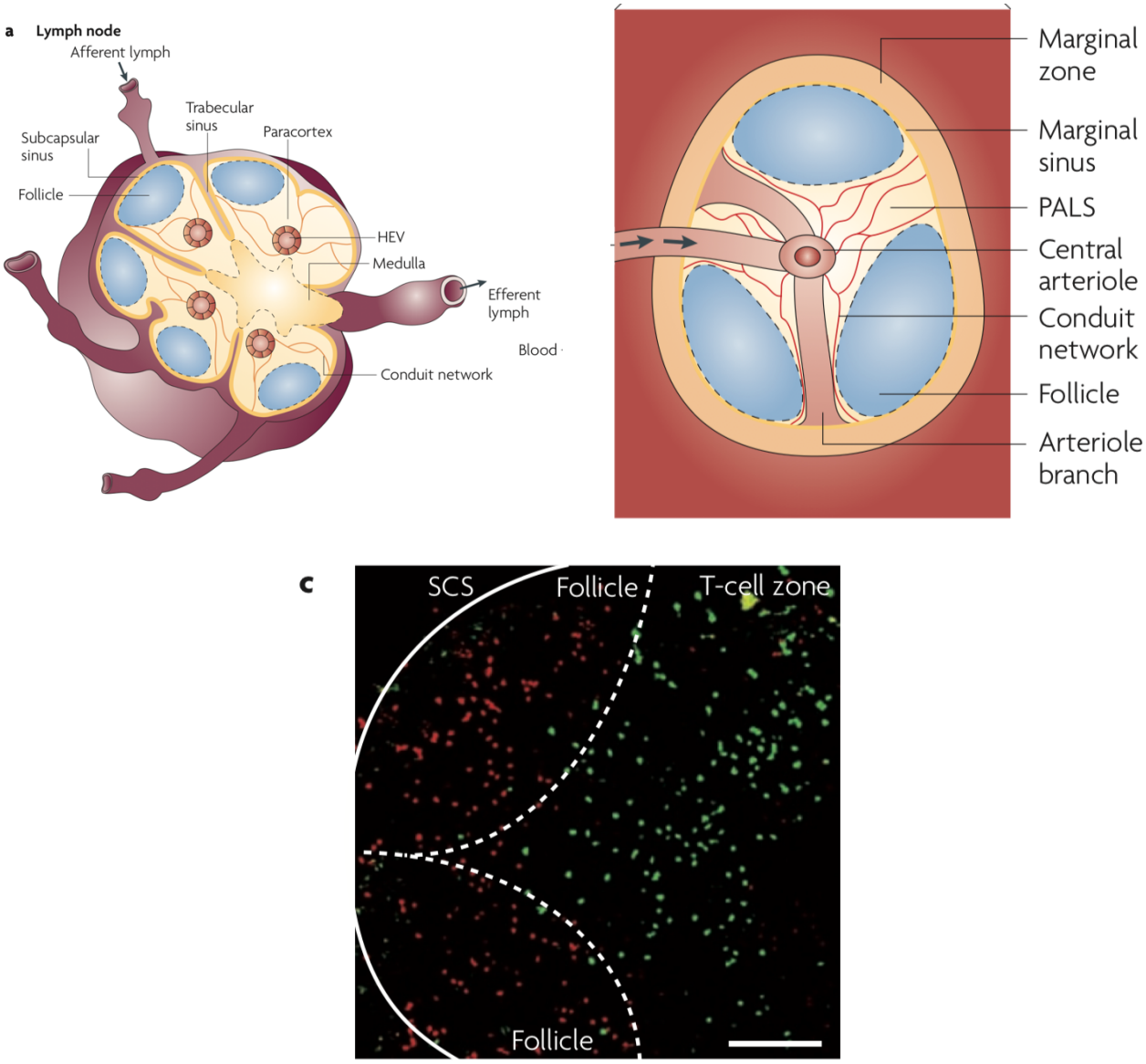

Figure 3: Anatomy of lymphoid organs and cellular organization. A) Schematic representation of lymph nodes. **B)** Schematic representation of the white pulp of the spleen. **C)** Snapshot of a video generated using multiphoton microscopy on a lymph node. Red elements represent seminaphtho-rhodafluor-labelled B cells within follicles and green elements represent CFSE-labelled T cells in the paracortex. Source: Adapted from (60)

As mentioned, B cells are located within the follicles of the lymph nodes and spleen. Various groups have investigated how different types and size of antigens can reach B cells within these follicles. For small soluble antigens, it is believed that those can reach B cell follicles by

diffusing through afferent lymph vessels (60). Access of larger antigens to follicular B cells, however, require other mechanisms. One of the proposed mechanisms involve specialized macrophages that reside in the subcapsular sinus of LNs or marginal zone of the spleen. These macrophages can bind antigens from the subcapsular sinus and retain them in their original form at the cellular surface for long periods of time (60, 62). Those specialized macrophages can present larger antigens at neighboring follicular B cells, initiating antigen-specific B cell activation. Dendritic cells present around high endothelial venules (HEVs) of LNs are also suggested to present antigens to B cells. As circulating B cells enter lymph nodes through HEVs, presentation of antigens from DCs to B cells has been investigated (60). Interestingly, it was demonstrated that these DCs can internalized antigens and recycle them to the cell surface in their intact form, allowing recognition by B cells (60, 63). Antigen recognition on the surface of DCs could induce extrafollicular plasma cell differentiation or B cell migration to the follicle to initiate germinal centers. In addition to macrophages and DCs, FDCs represent an important source of antigens for B cells. FDCs express high levels of FC receptors and complement receptors, enabling them to bind immune complexes and antigens coated with complement fragments (60, 64). FDCs are abundant in the B cell follicles (65) and are a crucial source of antigens in germinal center reactions (discussed in the section below).

In addition to antigen capture methods, antigen processing differs between APC types. Indeed, when incubated with to the same protein, the peptidome presented by B cells and macrophages differed quantitatively but also qualitatively (66), demonstrating that differences in antigen processing between different APC types lead to presentation of different peptides. Interestingly, binding of antigens by immunoglobulins can enhance or inhibit presentation of

specific peptides to T cells (67). Other elements, such as cell type-specific protease also impact the antigen processing and presentation to T cells (68). Together, these different characteristics establish B cells as unique APCs that have important roles in supporting T cell-mediated responses.

1.4.2 Germinal centers

In addition to signal induction in T cells, antigen presentation from B cells to T cells also have significant impacts on the B cells. A great example of this important crosstalk between T and B cells takes place in GCs and will be detailed below. First, we will briefly overview GC structures and dynamics.

GCs are complex and dynamic cellular structures that form in lymphoid organs. Around six days after immunization in mice, aggregates of proliferating B cells appear in the B cell follicles of spleen or LNs (69). Those structures rapidly increase in size and peak at around 7-14 days after initial antigen challenge (70, 71). GCs are the primary site of BCR affinity maturation, which is mediated by the Activation-induced cytidine deaminase (AID) enzyme. The detailed role of AID is further discussed below.

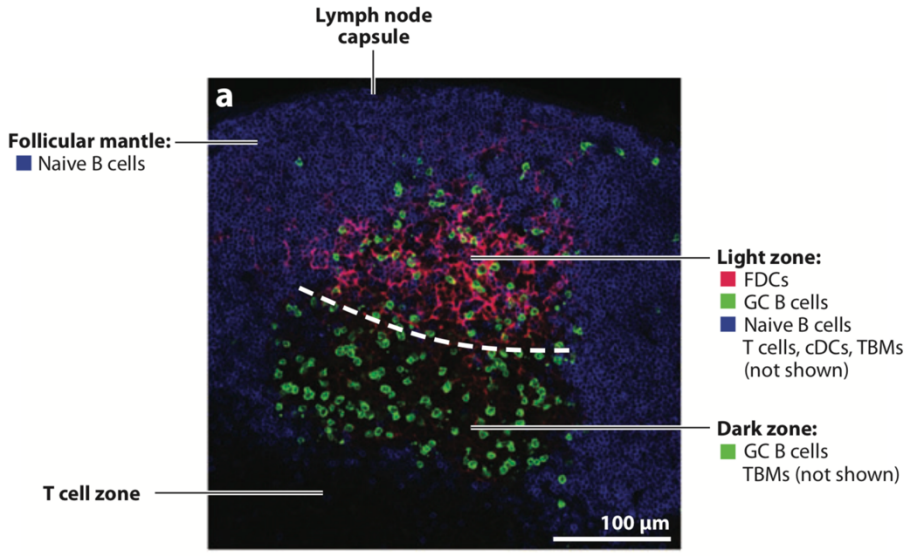

Figure 4: Germinal center anatomy. Cellular composition of a GC, captured by fluorescence microscopy. GC B cells (green) are present in the DZ and LZ of the GC. FDCs (red) are present exclusively in the LZ of the GC. Surrounding the GC, naïve B cells (blue) form a B cell follicle. Source: Adapted from (69).

Mature GCs can be divided in two distinct zones, the dark and light zones. The dark zone (DZ) is almost uniquely composed of rapidly proliferating B cells (69). In contrast, the light zone (LZ) is composed of various cell types, such as B cells, follicular helper T cells (Tfh) and FDCs (see figure 4) (69). The light zone also contains $CD8^+$ T cells, conventional DCs and tingible-body macrophages, but in a lesser abundance (69). GC B cells are activated B cells, and can be distinguished from naïve B cells by their expression of Fas (CD95) and *n*-glycolylneuraminic acid (the ligand of the GL-7 antibody), as well as their binding to peanut agglutinin and loss of expression of IgD BCR (69). Another marker frequently used to identify GC B cells is the transcription factor BCL6. BCL6 is highly expressed in GC B cells and is considered the master regulator of GCs. Mice lacking BCL6 are incapable of mounting a GC response, leading to an

absence of high affinity antibodies (72). BCL6 play multiple roles in GC B cells, some of which are still under investigation. BCL6 modulates the expression of mediators of BCR signaling and CD40 signaling, which have central roles in B cell activation (69). BCL6 also repress the expression of the transcription factor Blimp-1, the master regulator of plasma cell differentiation (69). This repression limits the differentiation of GC B cells into antibody secreting plasma cells. In addition to BLIMP-1, BCL6 represses P53 (69), allowing GC B cells to tolerate DNA damage mediated by AID without undergoing apoptosis. Lastly, BCL6 silences the anti-apoptotic molecule BCL-2 in order to keep GC B cells in a pro-apoptotic state, which is important for the process of affinity-based selection discussed below (69). Interestingly, BCL6 is not restricted to B cells in GCs. Indeed, Tfh also express BCL6. Through repression of various genes, BCL6 repress the differentiation of $CD4^+$ T cells into non-Tfh susbets (Th1, Th2, Th17) (73). Through repression of Id2, BCL6 also promotes expression of CXCR5 (73), a chemokine receptor that is crucial for migration of T cells to the T-B border and into germinal centers. BCL6 is therefore the master regulator of GCs, for its expression in both B cells and T cells.

As a transcriptional co-activator, OCA-B is also crucial for differentiation of B cells into GC B cells (74). While the mechanisms of action of the OCA-B/OCT1/2 complexes are not fully understood, a recent report demonstrated that a complex composed of OCA-B, OCT2 and MEF2B indirectly regulate the promoter of BCL6 (75). This observation may explain why OCA-B-deficient B cells are incapable of differentiating into GC B cells. Expression of OCA-B in $CD4^+$ T cells has also been reported to promote Tfh differentiation through the induction of BCL6 (76). The role of OCA-B in T cells in further discussed in chapter 3.

Crosstalk between T and B cells is required for GC formation

GCs are initiated at the T-B border. After priming of $CD4^+$ T cells by DCs in the T cell zone, via production of IL-6 and IL-21, $CD4^+$ T cells begin their differentiation into Tfh cells (77-79). At this point considered immature or early Tfh, T cells express low levels of BCL6 and CXCR5, initiating their migration to the B cell follicle (77). At the border of the follicle, early Tfh interact with antigen-specific B cells that are presenting antigens on MHC II. Interaction mediated by the co-stimulatory molecule ICOS (on T cells) and its ligand ICOSL (on B cells) lead to further differentiation of early Tfh into mature Tfh and the migration of the Tfh and the activated B cell further into the B cell follicle, where they initiate a GC (77, 80).

In the dark zone, GC B cells (termed centroblasts) divide extremely rapidly (cell cycle estimated between 6-12h (81)) and acquire mutations at every division. This process, termed somatic hyper mutation (SHM), is mediated by AID. Highly expressed in centroblasts (82), AID initiates two important processes in B cells: class-switching (CS) and SHM. AID initiate both of these processes by directly modifying the DNA, converting cytidine (C) to uracil (U) in immunoglobulin genes, either in variable regions for SHM or in Switch (S) regions for CS (83). In the case of SMH, the resulting U-G mismatch can have multiple fates, leading to DNA mutations. If the mismatch is not repaired before DNA replication, the polymerase will insert an adenosine (A) opposing the U, resulting in G > A / C > T mutation (83). Another pathway is the removal of the U by the uracil-DNA glycosylase (UNG) enzyme, creating a site lacking a nucleotide (abasic site). During replication of the DNA, this abasic site is subjected to error-prone repair, leading to a possible C > T/G/A mutation (83). In addition, U-G mismatch also recruits the mismatch repair machinery (MMR), a complex of proteins that create mutations at A-T sites near the U-G mismatch (83). Mutations generated by AID and its downstream cofactors are restricted to the V regions of the immunoglobulin genes. Mutations are almost entirely detected in a 1-2 Kb

region, starting approximately 150bp downstream of the V gene promoters and stopping before the constant region (83). The explanation for the restriction of mutations in this particular region is still unknown, but it is hypothesized that unknown mutator elements (possibly Ty or Spt5) are coupled to the RNA polymerase and guide AID specifically to transcribed regions (84, 85). Random or guided dissociation of these factors during transcription may explain why mutation rates are higher close to the promoter (the initiation site of SHM) and gradually decrease with distance from the promoter (83). High expression of AID in rapidly dividing centroblasts results in efficient hypermutation of the BCR. Indeed, it is estimated that the mutation rate in centroblasts is 10^{-3} per base pair per generation (86), 10^{6} fold higher than the normal rate of random somatic mutations (69).

As mutations are random, SHM alone is not sufficient to promote affinity maturation. Affinity-based selection of B cells is the primary function of GCs. GC B cells are in a constant state of pre-apoptosis; they express high levels of the death receptor Fas and lose expression of the anti-apoptotic molecule BCL-2 (69). Whereas B cell clones with high affinity for antigens survive, clones with lower affinity die by apoptosis (69). While proliferation and SHM takes place mostly in the dark zone, selection of high affinity clones takes place in the light zone (69).

In the light zone, B cells interact with two main cell types, FDCs and Tfh. In GCs, FDCs act as a depot of antigens for B cells. As mentioned above, FDCs bind antigens coated with complement fragments or immune complexes. These antigens are “presented” to GC B cells in the light zone. It is believed that competition between GC B cells for antigen access importantly contributes to the selection process. While high affinity B cells are able to capture the antigens via

their high affinity BCR, lower affinity B cell are left without antigens, leading to an absence of BCR signaling, therefore triggering apoptosis (69). Another factor contributing to B cell selection in the light zone is the access to Tfh signals. After binding antigens on FDCs, B cells internalize these antigens through their BCR, process them and present the resulting peptides to Tfh on MHC II molecules (77). Interactions between Tfh and B cells provide important signals for B cell survival. These signals are mediated by cytokines as well as surface molecules.

The most important surface molecules for T-B crosstalk in GCs are CD40/CD40L and ICOS/ICOSL. CD40 is expressed by B cells and CD40L by Tfh. In $CD40^{-/-}$ mice, germinal centers fail to develop following antigen challenge (87, 88). Blocking CD40 signals also induce rapid dissolution of already formed GCs (89). Specifically in GC B cells, BCR and CD40 signaling synergize to induce c-Myc induction, a critical regulator of GC initiation, maintenance, and selection (90). In cooperation with signals from the BCR, the strength of CD40 signaling controls the differentiation fate of GC B cells (91). $ICOS^{-/-}$ mice also show a reduction of GC formation after antigen challenge (92). ICOS/ICOSL interactions are crucial for the maturation and migration of Tfh, leading to severely disturbed GCs in ICOS-deficient patients and mice (93). Interestingly, ICOS and CD40 signaling cooperate in a feed-forward loop in GC B cells, where signaling from both receptors increases expression of the other (94).

In addition to costimulatory molecules, cytokines contribute to the biology of GCs. The two main cytokines produced by Tfh are IL-4 and IL-21 (77). Both cytokines have multiple effects on B cells, which are not yet fully understood. In GCs, IL-21 signaling causes diverse effects, depending on the context. For example, IL-21 signaling in naïve B cells leads to differentiation

into short-lived plasma cells (95). In contrast, IL-21 signaling in GC B cells favors high expression of AID and BCL6, inducing more rounds of proliferation and mutations (95). IL-4 has critical roles in GCs, as observed by the reduction of GCs in the gut of IL-$4^{-/-}$ mice (96). In GCs, Tfh-derived IL-4 promotes the proliferation of B cells (97), as well as affinity maturation (98). In addition to its roles in GCs, IL-4 promotes the class switching of B cells to IgG1 (77, 98), and in some cases to IgA (99) or IgE (100). CS however takes place mostly outside of germinal centers. B cell CS is discussed below in this section.

Tfh provide signals to B cells presenting antigen-derived peptides (77), based on the amount of peptide-MHC II at the B cell surface. Therefore, B cells that most effectively access antigens through their high affinity BCR receive these survival signals. After selection in the light zone, B cell can differentiate into plasmablasts (precursors to plasma cells), memory B cells or return to the dark zone for subsequent rounds of proliferation and mutations (69). The general affinity for a specific antigen in a GC therefore increases with each round of proliferation and selection.

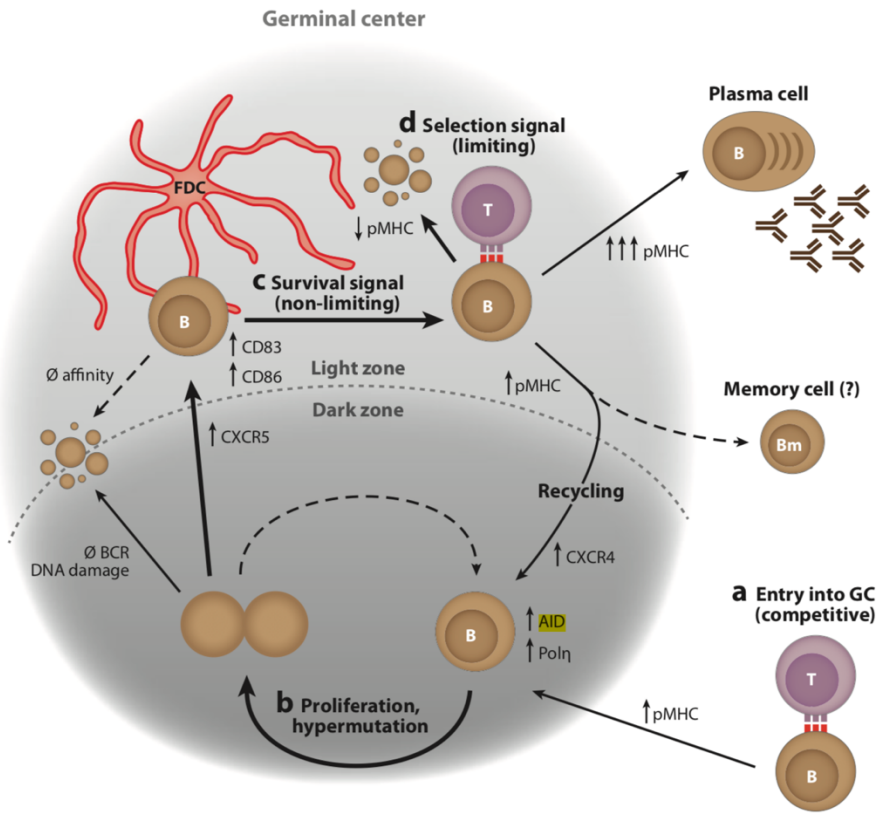

Figure 5: Model of affinity-based selection in germinal centers. During proliferation in the DZ, B cells accumulate mutations in the V regions of their BCR, leading to specificity and affinity changes. These cells then migrate to the LZ, where they compete for antigen access on FDCs and Tfh-derived survival signals. In absence of signals, low affinity B cells undergo apoptosis. B cells that receive survival signals can differentiation into plasma cells, memory B cells or return to the DZ for further proliferation and mutation cycles. Source : Adapted from (69)

1.4.3 Class switching (CS)

In addition to SHM, AID also initiate CS, an important process in the humoral response. In contrast to SHM, which changes the variable (V) regions of the BCR/antibodies, CS targets the constant (C) regions. The C regions of immunoglobulin genes code for different C_H exons, organized in a specific order: Cμ (IgM) > Cδ (IgD) > Cγ (IgG) > Cε (IgE) > Cα (IgA) (101). During CS, the first C_H exon transcribed (Cμ/Cδ) is excised, resulting in a change of isotype from IgM/D

to IgG, IgE or IgA. Contrary to IgG, IgE and IgA, IgD is generated by alternative splicing of the transcript coding for IgM, rather than CS (101). Similar to SHM, initiation of CS by AID requires transcription at the immunoglobulin genes (101). AID initiate CS by converting cytosines into uracils in specific regions upstream of the C_H genes, termed Switch (S) regions (101). The uracils in S regions are then processed, leading to double strand breaks in the downstream (Sμ) and upstream (Sγ, Sε or Sα) S regions. Finally, during the DNA repair process of these double strand breaks, the DNA between these S regions is excised, forming extrachromosomal DNA switch circle (101). Since the Cμ exon is excised in this process, the switched B cell can now only express IgG, IgE or IgA isotypes, depending on which S region was targeted by AID. During this process, only the C regions are affected, meaning that the regions responsible for antigen binding remains intact and that the BCR/antibody specificity is not altered (101). During T-dependent responses, CSR is initiated by CD40 signaling, which is provided by Tfh (101) or other activated $CD4^+$ T cells. Deficiency in CD40 or CD40L lead to significant reduction in CS and in antibodies of the IgG, IgE or IgA isotype (101). During T-independent responses, TLR and BCR signaling induce CS initiation (101). In addition to those signals, cytokines shape CS by dictating which S region will be targeted by AID, leading to switching to specific isotypes. For example, IL-4 signal (mediated by STAT6) favors CS to IgG1 and IgE, while TGFβ signal (mediated by SMAD3/4) mostly favors CS to IgA (102). Importantly, each isotype confers distinct properties to antibodies, contributing to different aspects of the humoral response. While the variable region is unaffected by CS, the change of constant region does impact the resulting BCR or antibody. In the case of secreted antibodies, IgM, IgG, IgE and IgA antibodies all have distinct functions. Although of generally low affinity, IgM antibodies are efficient at opsonizing antigens, due to their pentameric nature (103). In contrast to all other isotypes, IgD is almost exclusively present at the surface of B

cells and is rarely secreted as soluble antibodies. Some hypotheses for its specific functions have been proposed, but the roles of IgD as a BCR or a soluble antibody is still largely unknown (104). In the case of IgGs, which can be divided into four subclasses (IgG1, IgG2, IgG3 and IgG4), several specific characteristics have been associated with these isotypes. IgG antibodies are the most abundant in the serum, due to their long half-life (103). With the exception of IgG4, IgG antibodies bind the Cq1 fragment of the complement, leading to activation of the complement cascade (103). IgGs are also the only antibodies that can bind to FCγRs. In mice, four different FCγRs have been identified and binding of IgG-coated antigens to these receptors can initiate activating or inhibitory signaling cascades, depending on the context and the cell type (105). Another unique characteristic of IgG antibodies is their ability to cross the placenta barrier, due to their binding of the FcRn (Neonatal Fc Receptor), allowing passive transfer of humoral immunity to the fetus (106). At the BCR level, differences in the cytoplasmic tail of the IgM and IgG BCR also impact B cell functions, mostly through modulation of BCR signaling (107, 108). The unique characteristics of IgG BCR signaling are further discussed in chapter 4. The second most abundant antibody isotype in the serum is IgA (103). However, at mucosal surfaces, IgA is the most abundant isotype. At those surfaces, IgA antibodies protect against viruses, bacteria and toxins by neutralization or inhibition of binding to the mucosal surfaces (103). In addition, neutrophils express the IgA receptor, which may promote antibody-dependent cellular cytotoxicity (ADCC) (103). Soluble IgAs can promote tolerance to gut antigens by inducing anti-inflammatory functions in DCs (109).

The least abundant isotype in the serum is IgE, with a short half-life (103). Nevertheless, IgE antibodies play important roles, especially in Th2 responses. In helminth infections, IgE antibodies are particularly important for the removal of the parasites from the gut, either by

inducing smooth muscle contractility or by mediating killing of the larvae (110). IgEs are also implicated in allergies and asthma, mainly via their strong affinity for the FCεRI, expressed on mast cells and basophils (103). Finally, binding of IgE on the FCεRII on B cells have been suggested to participate in the antigen uptake by B cells, leading to the presentation of antigens to T cells (111). Initially believed to take place in GCs, we now know that CS rarely occurs in GCs (81). Rather, CS mostly takes place prior to GC onset, at the T-B border or at extrafollicular sites (81).

1.5 Crosstalk between thymocytes and B cells in the thymus

As mentioned above, B cells represent a small cellular population in the thymus of mice and humans. Still, thymic B cells may play an important role in shaping the T cell repertoire. As other thymic APC types (DCs, cTECs and mTECs), thymic B cells express MHC I and MHC II molecules, suggesting that they can participate in thymocyte development through presentation of antigens. Using BCR and TCR transgenic mice, thymic B cells have been shown to promote the elimination of self-reactive thymocytes (8, 30, 112). For example, transgenic expression of a self-peptide on the MHC II molecule of thymic B cells causes severe deletion of CD4SP thymocytes that recognize this specific peptide, leading to a reduction of autoimmune reactions in the periphery (112). Interestingly, transgenic expression of a TCR and BCR specific for epitopes of the same self-antigen favored efficient negative selection of the self-reactive CD4SP thymocytes, without the need for forced expression of the peptide on B cell MHC II (8). This suggests that thymic B cells acquire self-antigens via their BCR, process the antigens and present the resulting peptides to thymocytes, leading to negative selection of self-reactive thymocytes. It was also demonstrated

that the thymic B cell population is enriched in self-reactive B cells (8, 113) and that these naturally occurring self-reactive B cells are sufficient to induce negative selection of self-reactive CD4SP thymocytes, without the need for transgenic BCRs (8). While thymic B cells express the surface receptors necessary to participate in the elimination of self-reactive thymocytes, the mechanisms and context around this thymic selection by B cells, especially in non-transgenic settings, has yet to be elucidated.

In order to carry out their function in thymic selection, thymic B cells must interact, directly or indirectly, with developing T cells. By studying thymic B cells in various transgenic and KO mice, it has become clear that B cells and thymocytes interact directly and that this crosstalk is crucial for thymic B cell development and maintenance. CD40 signaling is crucial for thymic B cell development and/or survival. Genetic elimination of CD40 or CD40L drastically reduces B cell number in the thymus, while having no effect on peripheral B cell numbers (30). Inhibition of CD40 signaling also drastically impacts the phenotype of the remaining thymic B cells. While thymic B cells typically show high expression of CD80, AIRE and IgG BCRs, thymic B cells in $CD40^{-/-}$ or $CD40L^{-/-}$ have reduced expression of both CD80 and AIRE, and only express the IgM isotype (30, 113). Considering that CD4SP thymocytes are the main source of CD40L in the thymus (30), it is tempting to postulate that crosstalk between thymic B cells and CD4SP thymocytes is responsible for the maintenance of B cells in the thymus and for their unique phenotype. Indeed, in $TCR\alpha^{-/-}$ mice, which lack mature CD4SP and CD8SP thymocytes, thymic B cells carry a similar phenotype to those present in $CD40^{-/-}$ mice (30, 113), confirming the importance of crosstalk between thymic B cells and mature thymocytes. In addition, expression of isotype-switched BCRs (IgG or IgA) by thymic B cells requires the expression of MHC II

molecules on the B cells (113). Therefore, thymic B cells and CD4SP thymocytes interact through both the CD40/CD40L and MHC II/TCR. The role of thymic B cell in thymocyte selection is further discussed in chapter 4.

1.6 Type 1 diabetes (T1D)

The main role of the immune system is to prevent or overcome infections and cancers. To do so, complex mechanisms have evolved to allow efficient humoral and cellular responses by immune cells. However, in some individuals, the regulation of immune responses is not perfect, leading to the development of autoimmune or inflammatory diseases. T1D is one of these diseases.

T1D is a chronic autoimmune disease characterized by the destruction of insulin-producing pancreatic beta cells by the immune system. The gradual loss of beta cell leads to a deficiency of insulin production and consequently, hyperglycemia. While considered a disease with juvenile onset (most cases being diagnosed before the age of 14), T1D can occur at any age (114). Patients with T1D often present with symptoms of polyuria (excessive urine production), polydipsia (excessive thirst) and weight loss. Although many pharmacologic agents are now available for glycemia control (115, 116), there is still no definitive cure for T1D. People living with T1D must inject insulin (or insulin analogs) on a daily basis, either manually or with the help of an insulin pump (115). While life-saving, insulin therapy is not perfect and people living with T1D often still exhibit strong variations in blood glucose levels. Severe hypoglycemic events are frequent and often life-threatening, accounting for 5-10% of type 1 diabetes-related death (114). In addition, chronic variations in glycemia are associated with several complications such as cardiovascular

diseases, nephropathy, retinopathy and decline of cognitive functions (114), reducing overall life expectancy of people living with T1D.

The incidence of T1D is highly variable between countries, with the lowest incidence in Asian countries (<1/100 000) and highest in Scandinavian countries (>35/100 000) (117). As of 2014, the incidence of T1D in Canada was >25/100 000 (118). Regardless, a worldwide trend has been observed, with the incidence of T1D increasing around 2-3% every year (114). Although the reasons for this increasing incidence are still unknown, multiple environmental factors have been suggested, such as changes in diet, pollution, early-life exposures to viruses and reduction of microbiota diversity (114, 119). Other factors contributing to T1D are discussed below (section 1.8).

1.7 Generation of the NOD strain

First described in 1980 (120), Non-Obese Diabetic (NOD) mice represent, still to this day, the only mouse strain to spontaneously develop autoimmune diabetes. Autoimmune diabetes is the mouse equivalent of T1D. The NOD strain was derived from Cataract Shinogi (CTS) mice, an inbred subline of the ICR mouse strain, which develop cataracts (120, 121). To generate an insulin-dependent diabetes mouse model, CTS mice were interbred based on their fasting glucose levels. Eventually, some mice presented with diabetic symptoms, such as polyuria and glycosuria. These mice were selected and interbred, establishing the original NOD mouse colony (120). The main pathology observed in NOD mice (autoimmune diabetes) shares several characteristics with human T1D (120, 122-124). Studies using NOD mice have considerably improved our

understanding of autoimmune and type 1 diabetes. The generation of the NOD strain has facilitated the identification of genetic and environmental factors contributing to disease susceptibility, as well as the discovery of cellular and molecular mechanisms leading to pancreatic beta cell destruction (122, 123, 125).

We now know that T1D and autoimmune diabetes are complex diseases controlled by a combination of different genetic and environmental factors. In addition to studying broad cellular phenotypes in the NOD mouse, the generation of genetically modified NOD mice, such as congenic or KO mice, allows the evaluation of the role of specific loci or genes in disease pathogenesis. The importance of different NOD congenic strains is discussed in chapter 1.8 below.

1.8 Genetic factors contributing to T1D in NOD mice and humans

T1D is a polygenic disease with a strong genetic component. Concordance rates of T1D in monozygous twins is over 50%, compared to less than 10% in dizygous twins (126, 127). Furthermore, siblings of patients living with T1D have a 15 times higher chance of developing T1D than the general population (6% vs. 0.4%, in the United-States) (126), demonstrating the importance of genetic factors in T1D susceptibility. For this reason, identification of genetic factors contributing to disease susceptibility has been a central element of T1D research in the last decades. Genome wide association studies (GWAS) have identified more than 60 loci associated with T1D susceptibility in humans (termed IDDM, for Insulin Dependent Diabetes Mellitus) (128). Although they represent a powerful tool for the identification of potential risk loci, GWAS often do not allow the identification of specific gene or genes in the loci of interests, as well as the molecular or cellular context regarding its link to T1D. Investigating the mechanisms of action of

the candidate genes are often complicated due to the difficulty of obtaining relevant human samples, as well as the limitations of in vitro experiments. For this reason, the NOD mouse represents an extremely useful tool for the characterization of risk loci and their impact on diabetes susceptibility. As in humans, genetic studies using NOD mice identified more than 30 risk loci (termed *Idds*, for Insulin-dependent diabetes) (129, 130). In addition, the use of NOD mice and related congenic strains allows to confirm the implication of specific loci in autoimmune diabetes and are permissive to a more thorough investigation of the cellular and molecular mechanisms at play. To generate congenic NOD mice, NOD mice are crossed to a diabetes-resistant strain, such as B6, B10 or NOR mice. At each generation, the mice are backcross to NOD mice and the pups are genotyped using multiple chromosomal markers to identify the origin of certain DNA sequences. Only the mice retaining the locus of interest are selected for further backcrossing. After 8-12 generations, most of the remaining genetic background is of NOD origin, excepted for the locus of interest, which comes from the diabetes-resistant strain used at the original cross. However, even after 12 backcrosses to NOD mice, contaminating DNA may still be present in the genetic background of the congenic mice, emphasizing the need to sequence the genome (DNA or RNA) of the newly generated congenic mice to confirm genomic purity.

1.8.1 The MHC locus (*Idd1* / *IDDM1*)

The MHC locus is unequivocally the most important risk factor for diabetes susceptibility, accounting for 40-50% of genetic susceptibility in humans (131). Referred to as *IDDM1* in humans and *Idd1* in mice, the MHC locus was the first risk loci linked to autoimmune diabetes in NOD mice (132). Interestingly, while most congenic NOD mice are only partially protected from diabetes, replacement of the MHC locus on the NOD genetic background completely prevents

pancreatic infiltration (insulitis) and diabetes onset (133). Genetic variants associated with T1D have been identified in the MHC I, II and III regions (134, 135). Still, most studies have focused on the specific association between MHC II and autoimmune/type 1 diabetes. In humans, the haplotypes conferring the highest risk for T1D are termed DR3-DQ2 and DR4-DQ8. Children with these haplotypes have approximately 12 times higher risks of developing T1D, compared to the general population (126). While around 40% of the white population of the United-States have at least one of these alleles, 95% of the diabetic population present with at least one allele of HLA-DR3 or HLA-DR4 (126). Conversely, some MHC II haplotypes, such as DR6, are underrepresented in the diabetic population, suggesting their protective role against T1D (136).

In NOD mice, the MHC haplotype ($H2^{g7}$) is composed of the MHC I molecules H2-D^{b} and H2-K^{d}, as well as the unique MHC II molecule I-A^{g7}. Interestingly, a single amino acid in the beta chain of the I-A^{g7} molecule in NOD mice and in DQ2 or DQ8 in human seems to be critical for diabetes susceptibility. Indeed, these three molecules possess a small polar amino acid at position 57, rather than the normally conserved aspartic acid (137). In NOD mice, replacement of the normally coded serine at position 57 of I-A^{g7} by an aspartic acid protect mice from diabetes (137), demonstrating the importance of this specific amino acid in the I-A^{g7} molecule and possibly in the DQ2 and DQ8 molecules. It was later demonstrated that this specific amino acid of I-A^{g7} and DQ2/8 significantly impact peptide loading, allowing for presentation of a more promiscuous peptide repertoire, as well as peptides with negatively charged residues (138). In addition, binding of self-peptides (including insulin peptides) to I-A^{g7} is suggested to be relatively weak, potentially favoring escape from negative selection of insulin-specific thymocytes (139, 140). Finally, transgenic expression of the normally absent I-E molecules in NOD mice completely prevent diabetes onset (141), reminiscent of the protective HLA molecules in humans.

1.8.2 Non-MHC loci

Although the MHC locus is clearly the single locus with the strongest implication in T1D susceptibility, it cannot by itself predict diabetes development. Indeed, while more at risk of developing T1D than people with different haplotypes, the large majority of children with the DR3 or DR4 haplotypes will never develop T1D (126). In addition, mouse strains expressing the H-2^{g7} haplotype such as the B6^{g7} (congenic B6 mice bearing the H-2^{g7} haplotype) or NOR strains remain diabetes free (142, 143). Diabetes susceptibility is therefore controlled by a combination of MHC and non-MHC loci.

For example, a genetic study using NOD mice published in 1987 identified, in addition to the MHC locus (*Idd1*), one other loci linked to diabetes development, named *Idd2* (144). The missing heredity was suggested to be conferred by a third locus for which the chromosomal position was not identified. The contribution of the *Idd2* locus to diabetes susceptibility had not yet been characterized. The role of the *Idd2* locus in autoimmune diabetes is further discussed in chapter 2.

Among the various identified *Idds*, few have been studied as much as the *Idd1* locus. One example of a well characterized non-MHC locus is *Idd3*. Located on chromosome 3 of the mouse, the importance of the *Idd3* locus in diabetes susceptibility has been confirmed in congenic mice, where insertion of the *Idd3* locus of B6 origin into NOD mice (NOD.*Idd3*) partially inhibits diabetes onset (145). Because of its important role in the immune system, the *IL-2* gene, encoded inside the *Idd3* locus, was an obvious candidate gene. It was initially observed that sequence

variations in the NOD *IL-2* gene caused a different glycosylation pattern compared to the *IL-2* gene from B6 mice, suggesting a functional impact on the IL-2 protein in vivo (146). However, further experiments using the *IL-2* gene from 129S mice, which carry the same glycosylation pattern as the NOD IL-2, showed that glycosylation patterns did not explain the impact of the *Idd3* locus in diabetes susceptibility (147). Rather, it is suggested that the NOD *IL-2* gene sequence affects gene expression, causing a two-fold reduction of IL-2 expression compared to B6 mice (148). The reduced production of IL-2 by T cells in NOD mice strongly impacts Treg functions in vitro and in vivo (148), which is crucial for the maintenance of T cell tolerance and the control of diabetes development (149, 150).

In humans, multiple non-MHC candidate genes have been associated with T1D susceptibility, including genes coding for insulin, LYP, CTLA-4, CD25 and others (136). Because of its central role in glucose metabolism and glycemia control, the insulin gene has been extensively studied in the context of T1D susceptibility. Sequencing of the *INS* gene, coding for insulin, revealed a polymorphic region in its promoter where tandem repeat sequences are present in variable copy numbers, from 26 to more than 200 (136, 151). The number of tandem repeat elements is suggested to impact the level of transcription (152), impacting insulin expression in the pancreas but also in the thymus (136). High number of tandem repeats in the insulin gene, which is protective against T1D, is associated with high transcription levels in the thymus. In contrast, low number of tandem repeats, associated with T1D susceptibility, is associated with lower levels of insulin transcription in the thymus (136, 151). This difference in insulin expression in the thymus strongly supports the hypothesis that polymorphism in the insulin gene control T1D susceptibility through its impact on negative selection of self-reactive T cells.

Another non-MHC candidate gene associated with T1D susceptibility is *IL2RA*, encoding for CD25, the alpha chain of the IL-2 receptor (153). Disease-associated polymorphisms in *IL2RA* are also associated with a reduced concentration of circulating IL-2RA (153) and a reduction of Tregs functions (154), which require IL-2 signaling for their development and suppressive functions (155). Interestingly, the association between *IL2RA* and T1D in human is reminiscent of the contribution of the *IL-2* gene in *Idd3* in NOD mice. While CD25 and IL-2 are not the same protein, both participate in the IL-2 signaling pathway, a central element of T cell homeostasis (156).

The *PTPN22* gene represents another candidate genetic risk factor shared between NOD mice and people living with T1D. Encoding for the LYP (lymphoid tyrosine phosphatase) protein, polymorphisms in *PTPN22* are linked T1D diabetes susceptibility, as well as to other autoimmune diseases (157). This phosphatase is expressed in various immune cell types (T cells, B cells, NK cells and myeloid cells), but its expression is highest in activated $CD4^+$ and $CD8^+$ T cells (158). In T cells, LYP acts as a negative regulator of TCR signaling. LYP can directly interact with various intermediate of the TCR signaling pathway, such as Zap70, LCK, CD3, PI_3K and others (158-160). Different single nucleotide polymorphisms (SNPs) have been identified in *PTPN22*, some being linked to T1D susceptibility and others to disease protection (158). The most common allele of *PTPN22* linked to T1D presents with a tryptophan substitution at residue 620 ($PTPN22^{620W}$) and was identified in multiple independent studies (158, 161, 162). Although the impact of this particular SNP was extensively studied, it remains unclear if this genetic variant of *PTPN22* causes a gain or loss of function for this phosphatase in T cells (158). Regardless, polymorphisms in

PTPN22 have significant impacts on T cells responses, such as modulation of IL-2, IL-10 and IFNv production, proliferation and Th1 differentiation (158), which could all impact T1D development. In NOD mice, *Ptpn22* (ortholog to the human *PTNP22* gene), is a candidate gene for the diabetes-associated locus *Idd18* (137). Interestingly, insertion of $Ptpn22^{R616W}$ (the mouse equivalent of the $PTPN22^{620W}$ allele) in the NOD genome caused an acceleration of diabetes development in female mice (163).

In addition to MHC II, insulin, CD25/IL-2 and LYP, multiple other genetic variants are linked to diabetes susceptibility in both humans and NOD mice, such as *CTLA4*, *mt-ND2* and *Slc11a1* (133, 137). The NOD mouse represents a useful model to confirm the impact of candidate genes or variants, as well as to define their mechanistic contribution to diabetes susceptibility. Advances in CRISPR technology, allowing base substitution, should accelerate these discoveries (137).

1.9 The contribution of T cells in T1D

1.9.1 Pathogenic roles of T cells in diabetes

T cells were rapidly established as pathogenic effectors in T1D. One of the first histological analysis of human pancreatic tissue from a child with T1D reported that T cells were the major immune cell type contributing to pancreatic infiltration (164). Since then, it has been established that $CD4^+$ and $CD8^+$ T cells play central roles in the destruction of pancreatic beta cells. The generation of the NOD.scid mouse, which completely lack mature T and B cells, revealed that autoimmune diabetes is a T cell-mediated disease (165). Indeed, adoptive transfer of T cells from

diabetic or prediabetic NOD mice into NOD.scid recipients is sufficient to promote diabetes development (166), revealing that T cells are necessary for T1D onset. These experiments also highlighted the contribution of both $CD4^+$ and $CD8^+$ T cells, as diabetes development was higher when NOD.scid mice received a combination of both $CD4^+$ and $CD8^+$ T cells (166). $CD8^+$ T cells are thought to be the direct effector of pancreatic beta cell death, promoting their apoptosis through TCR-MHCI interactions and perforin secretion, as well as Fas-FasL mediated killing (167). $CD4^+$ and $CD8^+$ T cells also produce cytokines implicated in beta cell apoptosis. In addition to promoting infiltration of immune cells in pancreatic islets, pro-inflammatory cytokines such as IFNγ and TNFα directly induce caspase-dependent apoptosis of beta cells (168). Therefore, in NOD mice and in people living with T1D, $CD4^+$ and $CD8^+$ T cells participate in the pathology through direct and indirect killing of pancreatic beta cells.

The demonstration that injection of anti-CD3 antibodies reversed diabetes in NOD mice (169) confirmed the importance of T cells in the pathology and opened the avenue for clinical trials on diabetic patients. Two different anti-CD3 antibodies have been tested in the clinic for the treatment of T1D, teplizumab and otelixizumab (170). Treatment with otelixizumab significantly preserved beta cell functions, with higher levels of insulin secretion at 6 and 48 months, compared to placebo treated patients (170, 171). This treatment resulted in a reduction of the need for insulin injection, at least during the study period (170, 171). Unsurprisingly, however, anti-CD3 treatment resulted in adverse effects such as flu-like symptoms and virus reactivation, associated with lymphopenia and cytokine release (170, 172). Because of these side effects, a new trial was conducted using far lower concentration of the monoclonal antibody, which, unfortunately, showed no efficacy (172). Other therapies targeting T cells in the context of T1D have also been

tested, such as antithymocyte globulin, anti-CD40L and others, with promising results for most of them (173, 174).

It is also clear, when looking back at T1D-associated genetic variants (MHC II, CD25, IL-2, LYP, CTLA4, and others), that most candidate genes that contribute to T1D susceptibility affect T cell responses directly or indirectly. It is also possible that, since we know that T1D is a T cell-mediated disease, genes associated with T cell functions have been preferentially selected by researchers for more extensive studies.

1.9.2 Protective roles of T cells in diabetes

Although T cells play central roles in beta cell killing, it is becoming increasingly clear that some T cell subsets also promote T cell tolerance and limit diabetes development. The most obvious example of regulatory T cells is FoxP3$^+$ CD4$^+$ T cells (Tregs). In NOD mice, Treg depletion through anti-CD25 antibody injection or genetic deletion of FoxP3 greatly accelerate autoimmune diabetes development (175). In addition, adoptive transfer experiments revealed that the presence of Tregs in the T cell pool significantly delayed diabetes onset in transgenic and non-transgenic NOD mice (176). Treg development does not seem to be deficient in NOD mice, as Treg thymic output and peripheral Treg numbers are not reduced in NOD mice compared to diabetes-resistant strains (177, 178). Conflicting results have, however, been reported, with some groups observing a reduction of Treg numbers in lymphoid organs of NOD mice (179). Regardless, the consensus generally points to an impairment of Treg suppressive capacity rather than a quantitative deficiency. In the classical in vitro suppression assay, NOD Treg show a reduction of suppressive capacity compared to Treg from B6^{g7} mice (178). Specifically in the pancreatic islets,

Tregs from NOD mice are more prone to apoptosis than effector T cells, likely because of a reduction of IL-2 production by intra-pancreatic $CD4^+$ T cells (180). This is reminiscent of the impact of the NOD IL-2 genetic variant, encoded in the *Idd3* locus, which shows low expression of IL-2. Interestingly, while high dose IL-2 injections in prediabetic NOD mice accelerates diabetes onset, likely through the unspecific enhancement of immune cell proliferation, low dose IL-2 treatment specifically targets Tregs and reduces diabetes onset (180, 181). This can be explained, at least in part, by the different forms of the IL-2R. Indeed, while naïve immune cells express a low affinity receptor for IL-2 composed of CD122 and CD132 heterodimer, Tregs express a high affinity receptor composed of CD25, CD122 and CD132. Therefore, high dose IL-2 activate all immune cells, whereas low dose IL-2 treatment preferentially stimulates Tregs and enhances immune tolerance (182, 183). Similar to NOD mice, conflicting results have been reported regarding an alteration of Tregs numbers in the peripheral blood of people living with T1D, with most studies reporting similar numbers between patients and controls (175, 184, 185). However, differences in phenotype and function of human Tregs have been noted in the context of T1D. A reduction in Tregs with an activated or exhausted phenotype as well as changes in chemokine receptor expression and cytokine secretion were reported in children newly diagnosed with T1D (184, 186). Because of the important role of Tregs in the prevention of autoimmune diabetes, multiple therapies using Tregs have been designed in the hope of treating or preventing T1D. Autologous transfer of ex vivo expanded Tregs is safe in humans and multiple clinical trials showed efficacy in at least some participants, with stable C-peptide levels (a marker of insulin production) for up to two years after the initial injection (187). Other therapies targeting Tregs, such as low-dose IL-2 therapy or chimeric antigen receptor (CAR) Tregs are currently under investigation (188).

Tregs are not the only regulatory T cells implicated in T1D. A rare population of $CD4^-$ $CD8^-TCR\alpha\beta^+$ T (DN T cells) have been studied in the context of autoimmune diabetes. DN T cells represent a population of $FoxP3^-$ T cells that possess regulatory properties. While incompletely understood, DN T cells have demonstrated suppressive functions in multiple inflammatory settings, such as graft-versus-host disease and T1D (189). Of relevance to T1D, adoptive transfer of TCR-transgenic or non-transgenic DN T cells prevents autoimmune diabetes onset in NOD mice (190-192). Interestingly, NOD mice display reduced numbers of DN T cells, a trait associated with the *Idd13* diabetes susceptibility locus (193). We are currently investigating the mechanism by which DN T cells promote immune tolerance, in the hope of potentially developing DN T cell-based therapies for the treatment of T1D.

1.9.3 Autoantigens in type 1 diabetes

As T cells are central players in the pathology of T1D, much effort has been geared towards the identification of autoantigens responsible for the specific loss of tolerance against pancreatic tissues. The main autoantigens in T1D include insulin, glutamic acid decarboxylase 65 (GAD65), islet cell antigen 2 (I-A2), Chromogranin A, zinc transporter 8 (ZnT8), islet-specific glucose-6-phosphatase catalytic subunit-related protein (IGRP) and others (194, 195). Unsurprisingly, many of the autoantigens identified are strongly expressed by beta cells, the primary target of diabetogenic T cells. Many of the T1D-associated autoantigens have been identified by testing the reactivity of blood-derived T cells from people living with T1D (194). Years later, studies using T cell from pancreatic tissue of people living with T1D confirmed previous results and identified

new antigenic targets. Interestingly, most of the autoantigens mentioned above are targeted by T cells, but also B cells, through production of autoantibodies (194).

Of the numerous T1D-associated antigens, insulin was the first to be identified and the most studied (196, 197). Insulin, the primary hormone for glycemic control, is initially formed as proinsulin composed of three chains; the A and B chain joined together by the C domain (198). In secretory granules, the C domain is cleaved (becoming the C-peptide, a biomarker commonly used for the monitoring of T1D), giving rise to insulin, composed of the A and B chains (198). Early on, the dominant peptide recognized by insulin-specific T cells was shown to be composed of residues 9-23 of the B chain of insulin, insulin B:9-23 (199). In NOD mice, T cell reactive to the insulin B:9-23 peptide participate in the initiation of the break of tolerance towards beta cells (197). Transgenic replacement of the insulin genes with a mutated sequence modifying the B:9-23 peptide (without impacting the metabolic activity of insulin) completely blocked insulitis and diabetes onset in NOD mice (200). The principal hypothesis as to why this specific insulin peptide is critical in the initiation of T1D is that insulin B:9-23-reactive T cells are not properly eliminated in the thymus during negative selection (197). Indeed, multiple studies have shown that beta cells secrete unique peptides derived from the B:9-23 sequence of insulin, which are then presented by intra-islets APCs (201, 202). As beta cells are absent from the thymus (insulin is produced by mTECs in this organ), thymic APCs do not present these specific peptides to developing thymocytes (202), leading to their escape into the periphery.

In addition to specific insulin peptides, hybrid peptides and modified epitopes have also been implicated in the breach of tolerance in T1D. As in other autoimmune diseases,

posttranscriptional modifications of T1D-associated antigens have been reported. For example, RNA splice variations have been detected in the pancreas for IA-2 and IGRP, resulting in expression of neopeptides in the pancreas but not in the thymus (195). Hybrid peptides are formed by the fusion of two peptides derived from distinct antigens. In the case of T1D, most hybrid peptides are formed of insulin peptides, fused to peptides from proteins present in the secretory granules of beta cells (194). T cell recognizing hybrid insulin peptides are present in both NOD mice and patients with T1D (203). A good example of the importance of hybrid insulin peptides is the highly diabetogenic BDC2.5 T cell clone. Widely used to study the role of $CD4^+$ T cell in diabetes, it was finally reported after decades of investigation, that BDC2.5 T cell clones recognize a hybrid peptide composed of a fragment of the C-peptide fused to a peptide from Chromogranin A (203, 204).

With promising results in NOD mice (205, 206), antigen-based therapies using insulin, GAD65 and other antigens have been tested with the goal of inducing tolerance and limiting T1D development. Use of antigens and adjuvant to divert the pathogenic Th1 response to a Th2 response has been tested but failed to preserve beta cell function (207). Also, contrary to insulin-treatment in NOD mice, insulin therapies failed to show any clinical efficacy in humans (206, 208), highlighting the difficulty in translation of animal therapies to humans.

1.10 The contribution of B cells in T1D

B cells are present in the pancreatic islets of NOD mice and of people living with T1D, where they accumulate with age (209, 210). The observation that B cell-deficient NOD mice were

almost completely protected from diabetes (211) opened the door to multiple studies on the role of B cells in T1D and autoimmune diabetes.

1.10.1 Autoantibodies

The first proposed mechanism of B cell participation in T1D was through their ability to secrete autoantibodies. Together with HLA haplotype, autoantibodies are the most used biomarkers for prediction of T1D in the clinic. The most common autoantibodies detected are directed against insulin, GAD65, IA-2 and ZnT8 (212). More than 95% of people living with T1D are positive for the presence of one or more of these autoantibodies (212). Children with one type of autoantibody show a 15% risk of progression to T1D over 10 years, whereas children with two or more types of autoantibodies have approximately 70% chance of developing T1D in the same time frame (213). Interestingly, different autoantibody profiles associate with different HLA haplotype. For example, anti-insulin antibodies are more prevalent in people with HLA-DR4, while anti-GAD65 antibodies are more prevalent in people with HLA-DR3 (214). Antibody titer, affinity and isotype also impact the risk of developing T1D, and these characteristics can be used to optimize prediction of T1D development (215). In addition to revealing a breach in B cell tolerance, presence of autoantibodies allows for the prediction of T1D development. Predicting the risk of developing T1D is crucial for the design of clinical studies aiming at diabetes prevention. For this reason, detection of autoantibodies (in addition to HLA genotyping) is a central element in the recruitment process for clinical trials enrolling young children at high risks of developing T1D. Insulin specific antibodies, which are the earliest detectable autoantibodies, can be detected in children as early as 6 months of age (214, 216).

The implication of autoantibodies in T1D have been investigated in NOD mice. B1-a B cells, likely through the production of IgG antibodies, have been implicated in immune crosstalk that is crucial for the initiation of autoimmune diabetes (217). Even more compelling, using B cell-deficient NOD mice and embryo transfers into diabetes-resistant strains, it was demonstrated that maternal transmission of autoantibodies to NOD pup influences diabetes development (218). However, the possibility that other factors secreted by B cells are responsible for the difference in diabetes incidence, rather than autoantibodies, remains. In contrast, multiple studies argue against a significant role of antibodies in diabetes susceptibility. Passive antibody transfer do not affect diabetes development in mice, rats or humans (219) and T1D has been reported in a patient with X-linked agammaglobulinemia (220). Furthermore, antibody removal in prediabetic individuals through plasmapheresis do not influence T1D susceptibility (219). Lastly, a human study demonstrated that offspring who showed detectable levels of autoantibodies at birth (likely maternally transmitted antibodies) were less at risk of developing T1D, compared to offspring who were autoantibody negative at birth (221), arguing against a pathogenic role of maternally transmitted autoantibodies.

1.10.2 Antigen presentation in the context of T1D

Generation of a NOD strain in which B cells express a transgenic IgM BCR that cannot be secreted (i.e. no production of antibodies) revealed that B cells participate in the pathology of autoimmune diabetes through antibody-independent mechanisms. Indeed, these transgenic mice showed insulitis and considerable diabetes onset, as opposed to B cell-deficient NOD mice (222). It is now clear that B cells play a key role in diabetes development as APCs. While antibody

transfer into B cell-deficient mice did not enhances diabetes onset, repopulation of the B cell population through adoptive transfer restored diabetes susceptibility and the T cell response against autoantigens (223). Deletion of the MHC II molecule I-A^{g7} specifically in B cells abrogated diabetes development (224), demonstrating the importance of MHC II-mediated antigen presentation by B cells for autoimmune diabetes development. Also, in a BCR transgenic mouse model, insulin-specific B cells enhance diabetes onset without differentiating into antibody-secreting plasma cells (225). In addition to the presentation of antigens to $CD4^+$ T cells via MHC II, B cells participate in the priming of auto-reactive $CD8^+$ T cells through cross-presentation, enhancing diabetes onset (226). Secretion of cytokines by B cells, particularly the anti-inflammatory cytokine IL-10 by regulatory B cells, has also been reported to be impaired in NOD mice and people living with T1D (227-229), suggesting a potential role in the pathology.

The pathogenic potential of NOD B cells has been linked to the *Idd5* and *Idd9/11* locus. Using congenic NOD strains, it was demonstrated that genetic variants inside both *Idd5* and *Idd9/11* impact the pathogenicity of B cells by influencing their proliferation and the induction of anergy (230). The genes responsible for those phenotypes have not yet been identified.

1.10.3 Germinal centers in the context of T1D

Spontaneous GCs (i.e. GC forming in the absence of infection or immunization) have been detected in autoimmunity-prone mice. Indeed, in lupus-prone strains such as PN, MRL/lpr, B6/lpr, NZB and male BXSB mice, spontaneous germinal centers can be observed in the spleen, starting at one month of age (231). Similarly, spontaneous GCs were observed in the spleen of NOD mice, as well as in NOD.*H-2*^{h4} mice, a model of thyroiditis (231, 232). In contrast, non-autoimmune-prone strains, such as DBA/2 or female BXSB mice show complete absence of spontaneous GCs

in the spleen (231). In NOD mice, ectopic GCs can also be observed directly in the pancreatic islets (233, 234). Like classical GCs, those intra-islets GCs are composed of $GL7^+$ B cells and a network of FDCs, and can support SHM, as seen with the strong expression of AID (234).

As mentioned above, IL-2 is the main candidate gene in the *Idd3* locus. However, in addition to IL-2, other groups have suggested that IL-21, also encoded in the *Idd3* locus, may be an important gene contributing to autoimmune diabetes susceptibility (235). Polymorphism in the NOD *IL-21* gene favors strong production of IL-21, which correlates with diabetes incidence (235). As IL-21 is a critical cytokine for GC B cell proliferation and differentiation, polymorphism in the NOD *IL-21* gene may explain the spontaneous induction of GCs in lymphoid and non-lymphoid organs. However, as IL-21 signaling also impacts GC-independent T cell responses (236), it is unclear if the impact of IL-21 on diabetes development is, at least in part, mediated through GCs.

Using single-cell transcriptomic and epigenomic approaches of human tonsil samples, an enrichment of autoimmune disease-associated variants was observed in regions where chromatin is mostly accessible in GC-associated cell subsets (GC B cells and Tfh) (237). Those variants were present in genes coding for IL21, IL-21R, IL4R, BCL6, OCA-B and others. These findings suggest that GC dysregulation may be a feature of genetic-driven autoimmune susceptibility.

Still, these observations do not show that GCs participate in T1D pathology. While is it hard to investigate the role of GCs in disease, because of the lack of genes or pathways that specifically impact GC formation without affecting other aspects of immune responses, some

strategies have been tested. As CD40/CD40L interactions are central in T-B cell crosstalk, inhibition of CD40 signaling was tested in NOD mice. Using anti-CD40L antibodies or small molecule inhibitors, it was shown that inhibition of this pathway completely prevents insulitis and diabetes in NOD mice (238), and can even reverse hyperglycemia in recently diabetic mice (239). However, as CD40 is also expressed on DCs, mTECs and some macrophages, it is unclear if the impact of CD40 blockade on diabetes onset is mediated by inhibition of GCs. Similarly, inhibition of lymphotoxin-α, a cytokine essential for GC formation (240), completely protected NOD mice from diabetes (241). However, inhibition of lymphotoxin-α drastically impairs lymph node development (241), such that it is impossible to conclude whether the diabetes inhibition results from GC inhibition alone.

GCs can participate in autoimmune diseases through the generation of high affinity antibodies, epitope spreading and proliferation of autoreactive B cells (242, 243). More work is needed in order to better understand the contribution of GCs in the pathology of T1D.

1.10.4 Targeting B cells in T1D

The increasing knowledge of the importance of B cells in autoimmune diabetes and T1D lead to the investigation of therapies targeting B cells. In NOD mice, multiple pharmacological strategies have been used to deplete B cells or modulate their functions. Injection of anti-CD20 monoclonal antibodies in young (5-week-old) NOD mice depleted more than 95% of B cells and significantly reduced diabetes onset, likely through a reduction of $CD4^+$ and $CD8^+$ T cells activation (244). However, the effect of anti-CD20 injection on diabetes onset were attenuated when injected into older (15-week-old) NOD mice (244). It was later demonstrated that islet-

infiltrating B cells, which are present in high numbers in older NOD mice, are resistant to anti-CD20 antibody-mediated depletion (245), likely because of CD20 downregulation following migration into the pancreatic islets (246). This observation may explain the reduced efficacy of anti-CD20 antibody therapy in older NOD mice and highlights the importance of timing during the design of therapies against T1D. Another strategy to modulate B cell function focused on the B-cell-activating factor (BAFF) pathway. BAFF plays a central role in B cell development, survival and activation (247). Pharmacological disruption of BCMA signaling, one of the BAFF receptor, in NOD mice drastically reduced B cell numbers and completely inhibited diabetes onset (248). Interestingly, disruption of BAFF signaling showed greater diabetes inhibition than anti-CD20 antibody treatment despite showing reduced efficacy of B cell depletion (249). This observation was explained by the specific enrichment of IL-10 producing regulatory B cells in BAFFR-FC treated mice (249).

With promising data in NOD mice, depletion of B cells by anti-CD20 antibodies was investigated in humans. Rituximab, an anti-CD20 monoclonal antibody, can successfully deplete B cells in humans (250). In a phase 2 clinical trial on the use of Rituximab for patients newly diagnosed with T1D, treatment with Rituximab successfully depleted B cells for 6 months and preserved beta cell function for the following year (250, 251). Unfortunately, the efficacy of treatment was restricted to the early period, with C-peptide levels catching up to the controls 30 months after treatment (250, 251). Other studies using Rituximab after islet transplantation also showed modest efficacy (250), highlighting the importance of B cells in T1D, but also the difficulty of developing therapies with long term efficacy. These disappointing results are potentially explained by the limited window of opportunity for treatment of T1D. Anti-CD20

antibody treatment show the best efficacy when injected into young prediabetic NOD mice, and the impact on diabetes onset is reduced when treatment is initiated in older mice. In contrast, Rituximab treatment in human is initiated after diagnosis of T1D, meaning that beta cell destruction is already significant. It is therefore possible that initiation of Rituximab treatment in individuals already showing symptoms of T1D is simply too late to have long lasting effects. This difference in treatment kinetics may explain the discrepancies between anti-CD20 antibody treatment in NOD mice and humans. Furthermore, increasing dosage of Rituximab or repeating treatment is complicated in humans, as broad and long-term depletion of B cells results in severe immunosuppression, leading to various adverse events (250). The development of more targeted therapies to specifically eliminate autoreactive B cells or boost the function of regulatory B cells may represent a more successful option to treat or delay T1D.

1.11 Hypothesis and objective of my PhD

100 years after the discovery of insulin and its implication in the pathology of diabetes (252), there is still no definitive cure for people living with T1D. Still, our understanding of the events leading to insulin deficiency and the different factors implicated have greatly increased.

We now know that T and B lymphocytes are central players in the pathology of T1D, with clear roles to play in the breach of tolerance against pancreatic beta cells. However, the interplay between these two immune cell subsets in the context of T1D is only partly understood. Furthermore, the genetic factors contributing to T1D susceptibility are also incompletely characterized.

This thesis investigates the crosstalk between T and B lymphocytes in the context of autoimmune diabetes in mice via three principal objectives:

1. Characterize the impact of the T1D-associated locus *Idd2* on autoimmune diabetes susceptibility and on the function of T and B cells
2. Investigate the cell-intrinsic roles of the main candidate gene in the *Idd2* locus, *Pou2af1*, in T and B cells and on the crosstalk between them
3. Investigate the impact of thymic B cell class-switching on the development of T cells and the subsequent impact on autoimmune diabetes susceptibility

Preface to chapter 2

As stated in the introduction, the NOD mouse has been used extensively to understand how genetic variants contribute to the pathology of T1D. The implication of many of the identified loci has been confirmed in congenic strains. Still, the characterization of genetic factors contributing to T1D remains incomplete.

In a previous study, our group performed a linkage analysis to identify genetic loci linked to DN T cells, an immunoregulatory T cell subset (189). We determined that a locus on chromosome 9, coinciding with part of the *Idd2* locus, is linked to DN T cells in TCR-transgenic mice (253). Resistance alleles at this locus also decreased the incidence of autoimmune diabetes in this TCR transgenic setting (253). These results, together with additional studies (190, 254), suggested that resistance alleles at the *Idd2* locus conferred protection from autoimmune diabetes, likely via their impact on DN T cell number.

Based on this work, we set out to determine if the phenotypes observed in the TCR transgenic model were applicable in a non-transgenic, more physiological, setting. Indeed, T cell development is greatly impacted by the forced expression of a rearranged TCR in TCR-transgenic mice (255), skewing the differentiation in favor of DN T cells. Therefore, to determine the impact of *Idd2* resistance alleles on DN T cells and autoimmune diabetes susceptibility, we generated the congenic NOD.*Idd2* strain. This chapter will demonstrate that DN T cell and autoimmune susceptibility are not linked. Instead, we find that non-NOD alleles at *Idd2* locus confers autoimmune resistance, impacts GC formation and influences MHC expression.

Chapter 2:

The *Idd2* locus confers prominent resistance to autoimmune diabetes

Félix Lombard-Vadnais*, †, Roxanne Collin*, ‡, Jean-François Daudelin*, Geneviève Chabot-Roy*, Nathalie Labrecque*, ‡, §, Sylvie Lesage*, ‡

* - Immunology-oncology axis, Research Center, Maisonneuve-Rosemont Hospital, Montreal, Quebec, H1T 2M4, Canada;

† - Department of Microbiology and Immunology, McGill University, Montreal, Quebec H3A 0G4, Canada;

‡ - Département de microbiologie, infectiologie et immunologie, Université de Montréal, Montréal, Québec H3C 3J7, Canada;

§ - Département de médecine, Université de Montréal, Montréal, Québec H3C 3J7, Canada;

Correspondence address:
Sylvie Lesage
Maisonneuve-Rosemont Hospital
Research Center
5415 l'Assomption Blvd
Montréal, Québec
Canada, H1T 2M4
Phone number 1-514-252-3400 x 4649
sylvie.lesage@umontreal.ca

2.1 Abstract

Type 1 diabetes (T1D) is an autoimmune disease characterized by pancreatic β cell destruction. It is a complex genetic trait driven by over 30 genetic loci with parallels between humans and mice. The NOD mouse spontaneously develops autoimmune diabetes and is widely used to identify insulin-dependent diabetes (*Idd)* genetic loci linked to diabetes susceptibility. While many *Idd* loci have been extensively studied, the impact of the *Idd2* locus on autoimmune diabetes susceptibility remains to be defined. To address this, we generated a NOD congenic mouse bearing B10 resistance alleles on chromosome 9 in a locus coinciding with part of the *Idd2 locus* and find that NOD.*B10-Idd2* congenic mice are highly resistant to diabetes. Bone marrow chimera and adoptive transfer experiments show that the B10 protective alleles provide resistance in an immune cell-intrinsic manner. While no T cell-intrinsic differences between NOD and NOD.*B10-Idd2* mice were observed, we find that the *Idd2* resistance alleles limit the formation of spontaneous and induced germinal centers. Comparison of B cell and dendritic cell (DC) transcriptome profiles from NOD and NOD.*B10-Idd2* mice reveal that resistance alleles at the *Idd2* locus affect the expression of specific MHC molecules, a result confirmed by flow cytometry. Altogether, these data demonstrate that resistance alleles at the *Idd2* locus impair germinal center formation and influence MHC expression, both of which likely contribute to reduce diabetes incidence.

Keywords: autoimmune diabetes, genetic susceptibility, *Idd2* locus, B cells, germinal centers, MHC.

Key points:

NOD.*Idd2* mice are strongly protected from autoimmune diabetes

Idd2-mediated diabetes protection is immune cell-intrisic

Idd2 locus genetic variants impact germinal center formation and MHC expression

2.2 Introduction

Autoimmune or type 1 diabetes (T1D) is a complex genetic trait involving many loci in both mice and humans (121, 256-259). The locus that contributes most to T1D susceptibility is the MHC locus, named *Insulin-dependent diabetes 1 (Idd1)* in mice and *Insulin-Dependent Diabetes Mellitus 1* in humans (259-261). Interestingly, variant MHC class II molecules linked to susceptibility in both mice and humans do not code for the otherwise conserved aspartic acid at codon 57 (262, 263). Apart from the MHC locus, many other susceptibility loci are orthologous between mice and humans (121, 256-259). The NOD mouse strain, which spontaneously develops autoimmune diabetes, facilitates the dissection of the role of genetic loci in T1D susceptibility (121, 124, 264). Unravelling the biological importance of these genetic loci not only guides the identification of genetic variants, it contributes to our overall understanding of T1D pathology.

In addition to presenting as a complex trait, T1D develops as a result of intricate immune cellular interactions (121, 123, 265). Whereas autoreactive T cells are necessary and sufficient to drive this autoimmune disease, they interact with other immune cells that can either facilitate or impede disease progression (121, 123, 265). Among these, there is a growing body of evidence that B cells and dendritic cells (DCs) significantly contribute to T1D (123, 244, 249, 266-272). The initial study demonstrating a reduced diabetes incidence in NOD mice lacking B cells strongly supported their role in facilitating disease progression (211). Follow-up studies showed that B cells promote diabetes development mostly by their ability to present self-antigens to T cells (222-224). Similarly, NOD.Batf3$^{-/-}$ mice, which lack a subset of DCs, are completely protected from diabetes as a consequence of a reduction in antigen presentation to T cells (268). Moreover, both T1D patients and NOD mice exhibit altered cDC phenotype and function (271, 273-275)**.** Altogether,

the enhanced activation of autoreactive T cells by B cells and DCs in NOD mice facilitate a break in immune tolerance contributing to autoimmune diabetes susceptibility.

In our previous work, we exploited double transgenic mice bearing both the 3A9 TCR transgene and its cognate antigen, hen egg lysozyme (HEL), where the expression of the latter is driven by the rat insulin promoter (233). When both transgenes are expressed in NOD.$H2^k$ mice, the mice progress to overt diabetes, whereas 3A9 TCR:insHEL B10.BR mice are relatively resistant to disease (233). In one of our T cell linkage analyses exploiting these two strains, we obtained linkage to the *Idd2* locus (253). To validate the impact of this locus, we generated a 3A9 TCR:insHEL NOD.$H2^k$-*Idd2* congenic mice (253). The incidence of diabetes was reduced in these mice (253). In addition, they showed an increase of regulatory $CD4^-CD8^-$ T cells and a reduction of IgG autoantibodies (253). It is however unclear if either of these two traits contribute to diabetes resistance. Considering the constraints of transgenic models, we decided to outcross the *Idd2* locus to the NOD strain to determine its impact on the incidence of autoimmune diabetes in a non-transgenic setting. We find that NOD.B10-*Idd2* mice are highly resistant to autoimmune diabetes. In addition, resistance alleles at the *Idd2* locus influence the germinal center response and MHC expression, both of which likely contribute to diabetes resistance in NOD.B10-*Idd2* mice.

2.3 Materials and methods

Mice

NOD/ShiLtJ (NOD, #001976), NOD.B6-Ptprc (NOD.CD45.2, #014149), NOD.Cg-*Rag1*^{tm1Mom} *Il2rg*^{tm1Wjl}/SzJ (NRG, # 007799) and NOD.129S7(B6)-*Rag1*^{tm1Mom}/J (NOD.Rag$^{-/-}$, #003729) mice were purchased from The Jackson Laboratory. NOD.*H2*^{k}-*Chr9L* congenic mice were used to generate the NOD.B10-*Idd2* (hereafter denoted as NOD.*Idd2*) congenic mice by outcrossing to NOD mice. Specifically, the NOD.*H2*^{k}-*Chr9L* congenic strain carries B10 alleles between the markers rs6385855 and rs13480186 (253). NOD.*H2*^{k}-*Chr9L* mice were crossed to NOD mice to generate NOD.*H2*^{k,g7}-*Chr9L*^{B10,NOD}. These mice, heterozygous for B10.BR and NOD alleles at both the MHC and *Chr9L* locus, were intercrossed; to generate pups bearing homozygous genotypes for H-2^{g7} and *Chr9L*^{B10}. B10 alleles at the *Chr9L* locus were genotyped using D9Mit328, D9Mit129 and D9Mit330 markers and the interval was validated by RNA-Seq detailed below. The NOD.*Idd2* strain is available at The Jackson Laboratory (#026624). To generate the NOD.*Idd2*.Rag$^{-/-}$ strain, NOD.*Idd2* mice were crossed to NOD.Rag$^{-/-}$ mice. All of the mouse strains were maintained at the Maisonneuve-Rosemont Hospital animal house facility. Seven to 12-week-old male and female mice were used for phenotypic analysis. No differences in immunological phenotypes were observed between the males and females (not shown), and the data were pooled. Sex of animals is specified in the figure legends. Diabetes incidence studies were carried out in female mice up to 30 weeks of age. The Maisonneuve-Rosemont Hospital ethics committee, overseen by the Canadian Council for Animal Protection, approved all of the experimental procedures.

Diabetes incidence study

Diabetes incidence was monitored daily in female mice for overt signs of diabetes (wet cage, hunched posture) and every 2 weeks for urine glucose level using Diastix (Bayer, Toronto, ON, Canada) starting before the age of 10 weeks. After two successive positive Diastix tests, overt diabetes was confirmed by blood glucose levels > 12 mmol/L. The mice were sacrificed within 1 week of detection of high blood glucose or when they reached > 30 weeks of age. At culling, tail DNA was collected to verify the genotype of the mouse. The pancreas was collected and conserved in formalin for at least 48h before being sent for paraffin inclusion.

Histology

Hematoxylin and eosin staining was performed on 6 μm pancreas sections from paraffin blocks, for 2 non-successive sections per slide with 2 slides per mouse. Slides were scored for infiltration as previously described (276), and according to the following scale: 0 = no infiltration, 1 = peri-insulitis, 2 = infiltration <50%, 3 = infiltration >50%, 4 = complete infiltration.

Glucose tolerance test

Eight-week-old mice were fasted for 14 hours overnight. Blood glucose was measured (Accu-Chek, Roche) at baseline and at 15, 30, 60, 120, and 240 minutes after intraperitoneal injection of 10% D-glucose (2 mg/kg; Sigma).

Immune cell isolation from pancreatic tissue

Mice were sacrificed and an incision was made in the abdomen. A clamp was placed on the small intestine, where the bile duct reaches the intestine. Approximately 3ml of collagenase P (Roche Diagnostics) solution (1 mg/ml in cold HBSS) was injected directly into the bile duct, using a 30g

needle. Once the pancreases were fully inflated, they were removed, and 2 ml of cold collagenase solution was added prior to a 20 min incubation at 37°C. The digestion was stopped by adding 15 ml of cold HBSS, vigorous mixing, followed by three washes in cold HBSS. The digested pancreatic tissue was then resuspended in 20 ml of HBSS with 10% FBS. The pancreatic islets were handpicked under a binocular microscope and dissociated by repeated passage using a fine gel-loading tip (Thermo Fisher Scientific, #LC1001). Cell suspensions were stained and analyzed by flow cytometry, as described below.

Generation of bone marrow chimeras

Prior to irradiation, the recipient mice were injected intraperitoneally with 1ml of PBS to avoid dehydration. Bone marrow cell suspensions were prepared from the tibia and femur of 8-12-week-old donor mice in sterile RPMI. The red blood cells were lysed using NH_4Cl and the bone marrow single cell suspension were prepared in sterile PBS. Seven to nine-week-old recipient mice were irradiated at 11Gy, using linac X-ray source. The same day, the mice were injected intravenously with $2x10^6$ bone marrow cells. Non-competitive chimeras received bone marrow cells from NOD or NOD.*Idd2* mice. Competitive chimeras received a 1:1 ratio of NOD.2 (expressing CD45.2 alleles) and NOD.*Idd2* bone marrow cells.

Cell injections into NRG mice

Spleens were passed through a 70-µm cell strainer. Cell suspensions were treated with NH_4Cl to lyse red blood cells and suspended in sterile PBS. For total spleen cell injections, each NRG mouse was injected intravenously with 20 x 10^6 spleen cells. For T cell transfer, T cells were isolated

from spleens by negative selection using biotin selection kits (EasySep, Stem Cell Technologies). Purity was > 90%. Each NRG mouse was injected intravenously with 10 x 10^6 purified T cells.

Flow cytometry

Spleen and pancreatic lymph nodes (pLN) were treated with collagenase (1 mg/ml in PBS, Type V from Clostridium histolyticum, Sigma-Aldrich) for 15 minutes at 37 °C to assay dendritic cell phenotypes. Peyer's patches, spleen and lymph nodes were pressed through a 70-µm cell strainer (Thermo Fisher Scientific). Spleen cell suspensions were treated with NH_4Cl to lyse red blood cells. Single-cell suspensions were stained with different combinations of the following antibodies; B220-Pacific Blue (RA3-6B2; BioLegend), CD4-PE (GK1.5; BioLegend), CD8-PE-Cy7 (H35-17.2; Thermo Fisher), CD11b-Pacific Blue (M1/70; BioLegend), CD11c-PE-Cy7 (N418; BioLegend), CD19-APC (6D5; BioLegend), CD21-APC (7E9; BioLegend), CD23-PE (B3B4; BioLegend), CD44-PE-Cy7 (IM7; BioLegend), CD45.1-FITC (A20.1; BioLegend), CD45.2-AlexaFluor700 (104; BioLegend), CD49b-Pacific Blue (DX5; BioLegend), CD62L-APC (MEL-14; Biolegend), CD69-APC/PE (H1.2F3; BioLegend), CD86-FITC (GL1; BioLegend), CD138-PE (281-2; BD Bioscience), CXCR4-PerCP-Cy5.5 (L276F12; BioLegend), FoxP3-FITC (FJK-16s; Thermo Fisher), FAS-biotin (Jo2; BD Bioscience), GL7-AlexaFluor647 (GL-7; eBioscience), H-2D^b-FITC (KH95; BD Bioscience), H-2K^d-FITC (SF1-1.1; BioLegend), I-A^d-AlexaFluor647 (39-10-08; BioLegend, cross-reacts to H-2^{g7}), IgD-Pacific Blue (11-26c.2a; BioLegend), IgM-PE-Cy7 (RMM1; BioLegend), insulin-Alexa647 (T56-706, BD), LIVE/DEAD™ Fixable Yellow Dead Cell Stain Kit (Thermo Fisher), Streptavidin-PE or -PE-Cy7 (BioLegend), TCRβ-FITC/PE (H57-597; BioLegend). The following reagents were obtained through the NIH Tetramer Core Facility: BV421-coupled PBS-57 mCD1d-tetramers, H2-D^b/gp33-41 biotinylated monomers.

Tetramers were generated using ExtrAvidin®-PE (Thermo Fisher Scientific). Intracellular staining was performed as recommended by the supplier. Data were collected on an LSRFortessaX20 (BD), and analyzed with FlowJo software (FlowJo LLC, BD).

Sheep red blood cell (SRBC) immunization

Eight to 12-week-old mice were injected intra-peritoneally with 10^9 SRBCs diluted in PBS (Innovative Research). Ten days after injection, the spleens were collected for flow cytometry analysis and analysis by microscopy.

Microscopy

Spleens were frozen in OCT over dry ice and 10 μm slices of tissues were prepared using a cryostat. Slides were washed three times for 5 minutes in PBS and fixed with 3.7% paraformaldehyde for 10 minutes. Slides were washed again three times in PBS, air dried and blocked for 30 minutes using a PBS solution containing 3% BSA. CD35-biotin (8C12, BD Bioscience) was added and incubated overnight at 4ºC. Slides were washed three time in PBS and all other antibodies (GL7-AlexaFluor647: GL-7, eBioscience; IgD-Pacific Blue, 11-26c.2a, Biolegend; Streptavidin-Alexafluor594, Biolegend) were added for 2 hours, at room temperature. Antibodies were washed in PBS. Diamond Antifade Mountant medium (Thermo Fisher) was added and slides were sealed with nail polish. Images were acquired using a fluorescent microscope (Axio Imager 2, ZEISS).

RNA-Seq

B cells and DCs were sorted from the spleen as $CD19^{+}CD45^{+}$ and $CD11c^{hi}B220^{-}$ single cells, respectively (purity > 98%). RNA was isolated using Trizol. Libraries were prepared using the KAPA RNA HyperPrep PolyA Single-end Read Kit. Libraries were sequenced using the Illumina NextSeq 500 in 2 sequencing runs. FASTQ files were trimmed for sequencing adapters and low quality 3' bases using Trimmomatic version 0.35 (277) and aligned to the reference mouse genome version GRCm38 (gene annotation from Gencode version M25, based on Ensembl 100) using STAR version 2.7.1a (278). Read counts were extracted directly from STAR at the gene level. BAM alignments from STAR were used to generate transcript level FPKM values were generated using RSEM (279). Missense mutations were detected using RNA-seq data in combination with the Freebayes tool (280). Their functional effect was then annotated using snpEff (281). Single point mutations found to be consistent across biological replicates within a given condition with at least 20X coverage were isolated with a base count euclidean distance > 0.5 across mouse strains. These mutations were leveraged to isolate the location of *Idd2* on Chromosome 9. DESeq2 (R; version 1.26) was then used to normalize gene read counts. Batch correction was added to the statistical model for differential expression to adjust for samples sorted on 2 separate days. Log-normalized FPKM values were batch corrected using the removeBatchEffect function from the limma R package (v 3.42.2) (282) and used as input for heatmap visualizations.

Lymphocytic choriomeningitis virus* (LCMV) *Armstrong infection

The LCMV Armstrong strain was kindly provided by Dr Alain Lamarre, INRS-IAF, Laval, QC, CA. The virus was replicated by infection of L929 cells, cultured in Minimum Essential Medium (MEM) containing 5% heat inactivated Nu serum (Corning), to obtain viral supernatant. The virus titer was determined using MC57G cells as previously described (283). Mice were infected with

$2x10^5$ PFU of LCMV Armstrong by i.p. injection. H-2Db/gp-33 tetramer staining was performed as previously described (284).

In vitro allogenic activation assay

T cells from skin draining lymph nodes of B10.BR ($H2^k$) mice were stained with CFSE (2μM). The cells were then co-cultured for 3 days with splenic B cells or DCs from NOD or NOD.*Idd2* mice, at a 1:1 ratio. At the end of the co-culture, activation and proliferation of $CD4^+$ and $CD8^+$ T cells were analyzed by flow cytometry.

Statistics

A Log-rank (Mantel-Cox) test was applied to data from the diabetes incidence study. Chi-square tests were applied to the pancreas histology scores. For the competitive bone marrow-chimeras experiment, a paired student T-test was applied. Otherwise, data were tested for significance using a nonparametric Mann-Whitney U test. The minimal significance threshold was set at 0.05 for all tests.

2.4 Results

B10 alleles at the *Idd2* locus confer diabetes resistance in NOD mice in a lymphoid cell-intrinsic manner.

To determine the impact of the *Idd2* locus on autoimmune diabetes, we monitored diabetes incidence in both the NOD and NOD.*Idd2* strains; the *Idd2* congenic interval is depicted in Figure 1A. In our cohort, nearly 90% of female NOD mice were diabetic at 30 weeks of age (Fig. 1B). In contrast, only one of 12 (8%) NOD.*Idd2* mice became hyperglycemic at 24 weeks of age, showing that the *Idd2* locus of B10 origin is sufficient to prevent or significantly delay diabetes onset (Fig. 1B). The degree of insulitis was also reduced in NOD.*Idd2* mice relative to NOD mice (Fig. 1C). Expectedly, as NOD mice had progressed to overt diabetes, they had fewer pancreatic islets than NOD.*Idd2* mice (Fig. 1D) (285). When comparing age-matched pre-diabetic NOD and NOD.*Idd2* mice, we also observed a lower degree of insulitis and a higher number of islets in NOD.*Idd2* relative to NOD mice (Fig.1E-F). Therefore, resistance alleles at the *Idd2* locus decrease the degree of insulitis and confer a significant delay in both the onset and incidence of diabetes.

Resistance to autoimmune diabetes can be hematopoietic-intrinsic and/or extrinsic (286, 287). Indeed, we have previously demonstrated that the NOD genetic background affects beta cell fragility, contributing to diabetes pathogenesis (288). Considering the difference in pancreatic islet numbers, even in young mice (Fig. 1F), we hypothesized that the *Idd2* locus might modulate islet cells independently of the autoimmune response. To study pancreatic islet cell function without the confounding factors of an ongoing autoimmune response, we generated a NOD.*Idd2*.Rag$^{-/-}$ strain. Specifically, Rag$^{-/-}$ mice lack all T and B lymphocytes (289), such that both NOD.Rag$^{-/-}$ and NOD.*Idd2*.Rag$^{-/-}$ mice do not show insulitis nor do they progress to overt diabetes. Pancreatic islet

numbers were similar between NOD.Rag$^{-/-}$ and NOD.*Idd2*.Rag$^{-/-}$ mice (Fig. 2A), and both strains had a comparable number of insulin-producing β cells (Fig. 2B). Finally, the response to a glucose tolerance test was also similar for both mouse strains (Fig. 2C). Together, these results suggest that the *Idd2* locus does not influence pancreatic islet number and β cell function.

Next, to determine if B10 alleles at the *Idd2* locus confer autoimmune diabetes resistance in a hematopoietic-intrinsic manner, we generated non-competitive bone marrow-chimeras. Lethally irradiated NOD.CD45.2 congenic mice received bone marrow from either NOD or NOD.*Idd2* mice, both of which bear the CD45.1 allele (Fig. 3A). The distinct CD45 alleles between donor and recipient mice allowed quantification of the effectiveness of the bone marrow reconstitution, which was above 90% for all recipients. Fifteen weeks post-reconstitution, we found that the degree of insulitis was lower in recipient mice of NOD.*Idd2* bone marrow when compared to those grafted with NOD bone marrow (Fig. 3B). In addition, at 20 weeks following engraftment, chimeras that received NOD bone marrow developed high incidence of diabetes while the recipient of NOD.*Idd2* bone marrow remained diabetes free (Fig. 3C). Similarly, NOD.*Idd2* spleen cells caused less insulitis than NOD spleen cells when adoptively transferred in lymphopenic NRG mice (Fig. 3D, E). Altogether, these data indicate that the lower degree of insulitis conferred by the *Idd2* locus is lymphoid cell-intrinsic.

T cell subsets and function are not affected in NOD.*Idd2* mice.

As T cells are necessary and sufficient to drive autoimmune diabetes in mice (166, 290), we first investigated if B10 alleles at the *Idd2* locus modulate T cell subset proportion. The proportion of CD4$^+$ T cells, CD8$^+$ T cells, NKT cells and Tregs was similar between NOD and NOD.*Idd2* mice

(Fig. 4A, B). In contrast to our previous study in the 3A9 TCR transgenic model (253), the proportion of immunoregulatory $CD4^{-}CD8^{-}$, double negative (DN) T cells was also comparable between both strains (Fig. 4A,B). This suggests that *Idd2* alleles likely influence the proportion of DN T cells specifically in a TCR transgenic setting. Notwithstanding the absence of difference in the proportion of T cell subsets between NOD and NOD.*Idd2* mice, we set out to determine if *Idd2* resistance alleles influenced the diabetogenic potential of T cells. As such, we performed adoptive T cell transfers from young NOD or NOD.*Idd2* mice into lymphopenic NRG mice and monitored diabetes incidence. Approximately 40% of NRG mice progressed to overt diabetes, irrespective of the origin of the donor T cells (Fig. 4C). Taken together, these results suggest that *Idd2* resistance alleles do not significantly influence T cell pathogenicity.

Genetic variants in the *Idd2* locus impact isotype switching in B cells.

In addition to T cells, B lymphocytes are key players in T1D pathogenesis (211, 244, 249, 266, 267). We therefore examined populations of B cells known to participate in the progression to diabetes (234, 291). Total ($CD19^{+}TCR\beta^{-}$), follicular ($CD21^{+}CD23^{low}$), marginal zone ($CD21^{-}CD23^{hi}$) and activated ($CD69^{+}$) B cells, as well as plasma cells ($B220^{-}CD138^{+}$) were present in similar proportion and numbers in both NOD and NOD.*Idd2* mice (Fig. 5A, B, Fig. S1A). Yet, the proportion of class switched $IgM^{-}IgD^{-}$ B cells was reduced in NOD.*Idd2* mice relative to NOD mice, in all lymphoid organs tested (Fig. 5C-E). This decrease in class switching resulted in a lower quantity of serum IgG, but not IgM, levels in NOD.*Idd2* mice relative to NOD mice (Fig 5F). The reduction of serum IgG in NOD.*Idd2* mice was not caused by a general reduction of B cells, as total and unswitched ($IgM^{+}IgD^{+}$) B cell numbers were not decreased in NOD.*Idd2* relative to NOD mice (Fig. 5E, Fig. S1A, B). B cell class switching primarily occurs in germinal centers

(GCs) (292), and ectopic GCs develop in the pancreas of NOD mice (234). We therefore quantified the GCs present directly in the pancreas of pre-diabetic NOD and NOD.*Idd2* mice. Relative to NOD mice, NOD.*Idd2* mice displayed a significantly lower proportion of GC B cells, defined by the co-expression of GL7 and FAS, within the pancreatic infiltrates (Fig. 5G, H). *Idd2* resistance alleles seems to impair immunoglobulin isotype class switching as well as germinal center formation, at least in the pancreas.

The reduction in GC B cells in NOD.*Idd2* mice is not limited to autoimmune reactions in pancreatic tissue.

The low number of GC observed in NOD.*Idd2* mice may simply result from the low level of immune infiltration, rather than a decreased ability to form GCs. To test this hypothesis, we quantified GC B cells in Peyer's patches of NOD and NOD.*Idd2* mice. GCs form spontaneously in Peyer's patches in response to the gut microbiota (293). As observed in the pancreatic infiltrates, a significantly lower proportion and absolute numbers of GC B cells were found in Peyer's patches from NOD.*Idd2* mice relative to NOD mice (Fig. 6A, B). This result suggests that the *Idd2* locus modulates spontaneous GC formation. To exclude the possibility that these differences are driven by variations in gut microbiota between the different strains, we generated non-competitive bone marrow chimeras, where NOD mice were reconstituted with bone marrow from either NOD or NOD.*Idd2* mice. NOD mice that received NOD.*Idd2* bone marrow still displayed a lower proportion of GC B cells in their Peyer's patches than mice that received NOD bone marrow (Fig. 6C). Similarly, GC B cells were significantly reduced in the spleen and pancreatic lymph nodes of NRG mice that received NOD.*Idd2* spleen cells compared to mice that received NOD spleen cells

(Fig. 6D). Therefore, with either NOD or NRG mice as hosts, immune cells bearing resistance alleles at the *Idd2* locus yield fewer GC B cells than those of NOD origin.

Spontaneous GC formation is clearly influenced by *Idd2* alleles. To determine whether this extended to induced GC formation, we immunized NOD and NOD.*Idd2* mice with SRBCs. The size of individual GCs (Fig. 6E) and the distribution of B cells in the light and dark zones based on CXCR4 and CD86 expression (Fig. 6F) were similar between NOD and NOD.*Idd2* mice. However, the proportion and numbers of GC B cells in the spleen of immunized mice was notably reduced in NOD.*Idd2* mice relative to NOD mice (Fig. 6G, H). Altogether, these data show that B10 alleles at the *Idd2* locus significantly impede both spontaneous and induced GC formation in NOD mice.

B10 alleles at the *Idd2* locus determines MHC expression.

Having established that B10 alleles at the *Idd2* locus did not influence the diabetogenic potential of T cells and instead appears to influence B cell responses, we compared the transcriptomic profile of B cells from NOD and NOD.*Idd2* mice. Out of the total 58 differentially expressed genes (Fig. 7A, Suppl Table 1, see (294)), 14 genes were encoded within the *Idd2* locus (Fig. 7B and Suppl Table 1, see (294)). Based on GO terms, only two of them were associated with immune functions, namely *Crtam* and *Hspa8*, with no obvious link to germinal center biology (Suppl Table 1, see (294)). Still, among the 44 differentially expressed genes outside of the *Idd2* locus, three encoded for MHC genes, namely H2-D1, H2-Q6 and H2-Q7 (Fig. 7A, C). This prompted us to examine the expression of MHC class I and class II molecules on immune cells from NOD and NOD.*Idd2* mice. NOD mice carry the H-2^{g7} MHC haplotype, composed of H-$2K^{d}$ and H-$2D^{b}$ MHC class I

and I-A^{g7} MHC class II molecules (132). A significant decrease in the expression of both MHC class I, H-2D^{b}, and class II, I-A^{g7}, was observed on B cells from NOD.*Idd2* mice compared to B cells from NOD mice, in both the spleen and pLN (Fig. 7D-F). The expression of H-2K^{d} was not affected (Fig. 7D). Moreover, the decrease in MHC class II, but not MHC class I, was specific to B cells. Indeed, every immune cell subset tested displayed reduced MHC class I H-2D^{b} expression (Fig. 7G), while conventional and plasmacytoid DCs showed similar levels of MHC class II expression in both strains (Fig. 7H). Transcriptomic analysis of cDCs from NOD and NOD.*Idd2* mice confirmed that H2-D and H-2Q mRNA levels are reduced in NOD.*Idd2* relative to NOD mice (Fig. S2A, B). Notably, competitive bone marrow chimeras indicate that the lower expression of MHC I and II on B cells is cell-intrinsic (Fig. 7I). These results suggest that B10 alleles within the *Idd2* locus globally modulate MHC class I H-2D expression and specifically influence MHC class II expression on B cells.

B10 alleles at the *Idd2* locus reduce the T cell activation potential of B cells and DCs.

MHC facilitates antigen presentation to T cells, leading to their activation. To assess if the reduction of H-2D^{b} and I-A^{g7} expression in NOD.*Idd2* mice results in a functional impact on T cell activation, we tested T cell activation in two different settings. First, we performed in vitro allogenic activation assays using total T cells from B10.BR mice (expressing H2^{k} haplotype) and B cells or DCs from NOD and NOD.*Idd2* mice. Both CD4^{+} and CD8^{+} T cell activation were reduced when B10.BR T cells were co-cultured with either B cells or cDCs from NOD.*Idd2* mice relative to NOD mice (Fig. 8A-C). Notably, the reduction in CD4^{+} T cell activation was more prominent in the B cell co-cultures (Fig. 8B, C), in line with the B cell-specific reduction of I-A expression (Fig. 7F, H). Secondly, to measure T cell activation in an antigen-specific manner, we

infected NOD and NOD.*Idd2* mice with the LCMV Armstrong virus. The LCMV gp33 immunodominant peptide is presented by H-2D^b, and the antigen-specific T cell response can be tracked using H2-D^b-gp33 tetramers. Using CD44 and CD62L as activation markers, we observed that while CD4$^+$ T cells were equally activated in infected mice from both strains, CD8$^+$ T cells showed a reduction of activation in NOD.*Idd2* mice (Fig. 8D, E). Compared to NOD mice, H2-D^b-gp33 specific CD8$^+$ T cells were virtually absent in NOD.*Idd2* mice (Fig. 8F, G), in line with the significant reduction of H2-D expression by antigen-presenting cells in NOD.*Idd2* mice (Fig. 7, Fig. S2). Together, these results demonstrates that genetic variants in the *Idd2* locus modulate MHC expression, significantly affecting T cell activation in vitro and in vivo.

2.5 Discussion

Over 30 *Idd* loci have been linked to autoimmune diabetes susceptibility in NOD mice (295), and the impact of many *Idd* loci on diabetes susceptibility has been validated using NOD congenic mice. Here, we generated NOD.*Idd2* congenic mice and validate that B10 alleles at the *Idd2* locus confer diabetes resistance. The diabetes resistance does not appear to be due to an increase in insulin-producing β cell mass or function, nor due to a decrease in T cell pathogenicity. Instead, this hematopoietic-intrinsic diabetes resistance affects germinal center formation and B cell isotype switching. In an attempt to identify candidate genes driving these phenotypes, we compared the B cell transcriptome from NOD and NOD.*Idd2* mice. This revealed an important variation in the expression of MHC molecules, which was confirmed by flow cytometry. While the decrease in MHC II expression appeared restricted to B cells, MHC I expression was more broadly observed in immune cells from NOD.*Idd2* mice relative to NOD mice. Altogether, we observed that the *Idd2* locus confers resistance to autoimmune diabetes, affects the humoral immune response in a hematopoietic-intrinsic manner, and results in impaired antigen-specific T cell activation likely through the reduction in MHC expression.

The impact of the *Idd2* locus on diabetes resistance has been previously investigated in NOD.NON-Thy-1^{a} congenic mice, which display NON alleles on chromosome 9 (166). These mice are protected from diabetes relative to NOD mice, although to lower levels than our NOD.*Idd2* mice (166). This suggests that B10.BR alleles confer stronger diabetes resistance than NON alleles. Alternatively, the difference in the degree of diabetes resistance between these two strains may be explained by the variation in size of the congenic intervals. Regardless, consistent with our findings, the diabetogenic potential of T cells from NOD.NON-Thy-1^{a} congenic mice

was not affected, as shown by T cell transfers in lymphopenic NOD mice (166). Unfortunately, upon further backcrossing, a recombination event occurred within the chromosome 9 locus of the NOD.NON-Thy-1^{a} congenic mice (296). The strain lost its resistance to diabetes, precluding further characterization of the traits conferring diabetes resistance (296).

We had also previously studied the *Idd2* locus in the context of the 3A9 TCR:insHEL NOD.*H2*^{k} transgenic model. Indeed, in this TCR transgenic model, immunoregulatory 3A9 TCR DN T cells are most abundant in 3A9 TCR transgenic mice bearing the B10.BR background relative to the NOD.*H2*^{k} counterpart (190, 254). A linkage analysis showed that the *Idd2* locus was linked to the proportion of 3A9 DN T cells, which prompted us to generate 3A9 TCR:insHEL NOD.*H2*^{k}*-Idd2* congenic mice (253). We found that B10.BR alleles at the *Idd2* locus was sufficient to increase the number of 3A9 DN T cells, decrease IgG autoantibody levels and reduce diabetes incidence in 3A9 TCR:insHEL NOD.*H2*^{k}*-Idd2* congenic mice (253). These results were in line with our previous data showing that transfer of 3A9 DN T cells in autoimmune diabetes-prone mice conferred diabetes resistance and reduced autoantibody levels, likely by eliminating activated B cells (190, 254). Altogether, these results suggested that low numbers of 3A9 DN T cells in autoimmune diabetes-prone mice were insufficient to control autoantibody production, thereby contributing to diabetes susceptibility.

TCR transgenes skew thymic differentiation and impose a more restricted T cell repertoire. As such, to determine whether the resistance alleles at the *Idd2* locus similarly affected diabetes onset and incidence in non-TCR transgenic NOD mice, we outcrossed the transgenes and the MHC locus to generate NOD.*Idd2* congenic mice. As for the TCR transgenic environment, we find that both

diabetes onset and incidence is reduced in NOD.*Idd2* relative to NOD mice. Moreover, the *Idd2* locus influences the formation of spontaneous GCs, in line with the reduced autoantibody levels observed in the transgenic setting (253). However, we could not confirm the role of *Idd2* on DN T cell proportion in non-TCR transgenic mice. This difference could be due to the fact that the genetic regulation of DN T cell proportion may be different in transgenic and non-transgenic animals. In addition, analysis of a locus on mouse chromosome 12, also linked to 3A9 DN T cell proportion, revealed that 3A9 DN T cell number, autoantibodies and diabetes resistance are not necessarily linked (297, 298). More studies are required to determine the role of non-TCR transgenic DN T cells in autoimmune regulation. Nonetheless, our results suggest that diabetes resistance alleles at the *Idd2* locus significantly impact antibody production.

Specifically, we find that resistance alleles at the *Idd2* locus not only impede autoimmune diabetes progression, but also limit antibody isotype switching, likely as a consequence of the reduced GC response (299). In NOD mice, ectopic GC are observed in the pancreatic tissue (234), and the number of GC B cells is reduced in NOD.*Idd2* congenic mice. The reduction in GC B cells in NOD.*Idd2* congenic mice relative to NOD mice was not restricted to the pancreas, as it was also observed in Peyer's patches, as well as in the spleen following immunization with SRBCs. Bone marrow chimeras and cell transfer experiments demonstrate that the difference in GC formation is caused by immune cell-intrinsic factors. Therefore, genetic variants within the *Idd2* locus have an immune cell-intrinsic impact on the humoral immune response.

The *Idd2* locus in the NOD.*Idd2* congenic mice spans a little over 12Mb. It encodes a large number of immune and non-immune genes that could contribute to the autoimmune diabetes-resistance

and GC formation. *Idd2* also links to metabolic changes inducing β cell apoptosis, and *Grik4*, a gene encoded in our interval, is a candidate gene (300). However, our data on the pancreatic function in NOD.*Idd2*.Rag$^{-/-}$ mice argues against a modulation of pancreatic function by B10 alleles in the *Idd2* locus. In addition, bone marrow chimeras and cell transfer experiments show that diabetes resistance and reduced GC numbers in NOD.*Idd2* mice are immune cell-intrinsic. Transcriptomic analysis of B cells from NOD and NOD.*Idd2* mice revealed 58 differentially expressed genes (DEG) genome-wide, 14 of which are located in the *Chr9* locus of B10 origin. Of those 14 genes, two are associated with immune functions, namely *Crtam* and *Hspa8*, but exert no defined role in GC B cells. In addition to the 14 DEGs from the *Idd2* locus, three of the 44 other DEGs are MHC genes, namely *H2-D1*, *H2-Q6* and *H2-Q7*; *H2-D1* and *H2-Q6* are also significantly differentially expressed in DCs from NOD.*Idd2* mice relative to NOD mice. We validated that H2-D protein expression was reduced in immune cells from NOD.*Idd2* mice when compared to NOD mice. The lower levels of MHC expression observed in NOD.*Idd2* mice could reflect a lower degree of inflammation relative to NOD mice. However, results from competitive bone marrow chimeras show that this is unlikely, as the level of H-2D expression is cell-intrinsic. Moreover, we find that H2-K expression was not affected, suggesting that this was not due to a global regulation of MHC genes. Furthermore, while the mRNA levels of the MHC class II molecules, H2-Aa and H2-Ab, were similar when comparing B cells from NOD and NOD.*Idd2* mice, the protein levels of I-A^{g7} were reduced in B cells from NOD.*Idd2* mice, and this phenotype was also cell-intrinsic. This suggests that the difference of expression for I-A^{g7} between the two strains is likely caused by post-transcriptional regulation. Additional studies are required to determine which genetic variant within the *Idd2* locus specifically modulate H-2D and I-A^{g7} MHC expression.

The reduction in MHC I and II expression on immune cells in NOD.*Idd2* congenic mice likely contributes to the decreased autoimmune diabetes incidence and the reduced number of GC B cells. Indeed, the MHC locus accounts for the majority of the genetic susceptibility to autoimmune diabetes (131). In NOD mice, presentation of autoantigens to T cells participates in the initiation of autoimmune diabetes (223, 226, 266, 268, 272, 301, 302). Modulation of MHC I expression on immune cells and MHC II expression specifically on B cells in NOD.*Idd2* mice is therefore likely to impact diabetes development. Moreover, interactions between $CD4^+$ T cells and B cells, in part through MHC II, are crucial for the induction and maintenance of GCs (303, 304). In addition to MHC genes, *Lta*, encoding for Lymphotoxin-α (LT-α), is downregulated in NOD.*Idd2* B cells when compared to NOD B cells. LT-α is highly expressed in B cells (305) and is essential for induction of germinal centers (240). The reduction of LT-α and MHC expression may therefore both contribute to the reduced GCs observed in NOD.*Idd2* mice.

Altogether, we find that the *Idd2* locus contributes to autoimmune diabetes susceptibility in NOD mice, impairs GCs, limits isotype switching and influences MHC expression. GCs can contribute to autoimmunity by facilitating the generation of high affinity autoantibodies, the proliferation of autoreactive B cells as well as epitope spreading (234, 306, 307). Notably, NOD mice have a high propensity to develop GCs (308), and ectopic GCs can be detected in the pancreas of NOD mice (234). It is thus likely that the lower levels of MHC, the reduced number of GCs, the decreased proportion of isotype switched B cells, and the substantial reduction in diabetes onset in NOD.*Idd2* mice relative to NOD mice are intricately linked. Overall, our findings show that *Idd2* locus confers diabetes resistance and influences the humoral immune response.

Acknowledgments

We thank Ianula Bahu and Catherine Mauger-Labelle for help in curating the mouse colonies, Dr. Alain Lamarre for the LCMV Armstrong strain and Martine Dupuis for assistance at the Flow Cytometry platform.

2.6 Figures

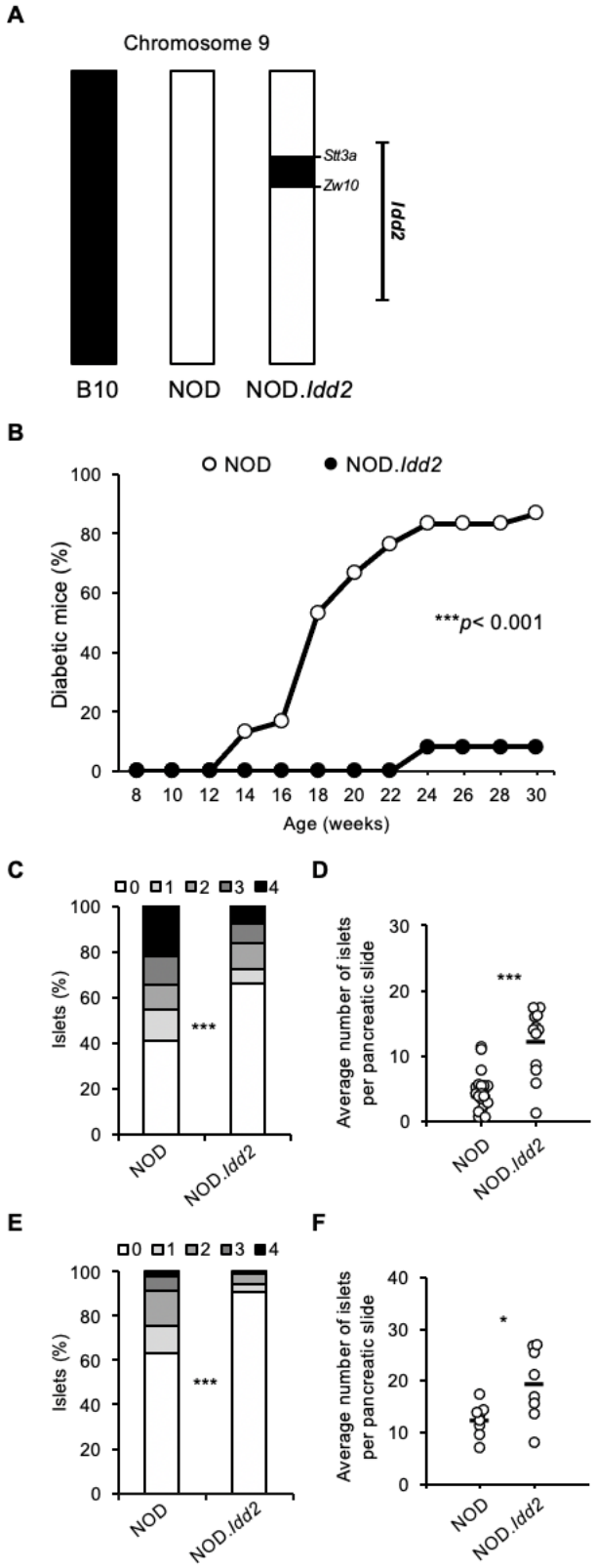

Figure 1. B10 alleles at the *Idd2* locus confer resistance to diabetes in NOD mice. **A)** Schematic representation of the chromosome 9 of B10, NOD and NOD.*Idd2* mice. Annotated genes represent the first and last genes of the locus of B10 origin. Identification of single nucleotide polymorphisms (SNPs) was conducted by paired-end RNA sequencing of NOD and NOD.*Idd2* cell samples. **B**) Diabetes incidence is shown for female NOD (n = 30) and NOD.*Idd2* (n = 12) mice. ***$P < 0.001$ according to a Log-rank (Mantel-Cox) test. **C**) The insulitis score is shown for mice included in the diabetes incidence study. **D)** Average number of pancreatic islets per slides of pancreas from NOD and NOD.*Idd2* mice from the diabetes incidence study. **E**) The insulitis score is shown for 7 to 11-week-old female mice. NOD, n = 8, NOD.*Idd2*, n = 8. **F)** Average number of pancreatic islets per slides of pancreas from young female NOD and NOD.*Idd2* mice. *$P < 0.05$, ***$P < 0.001$.

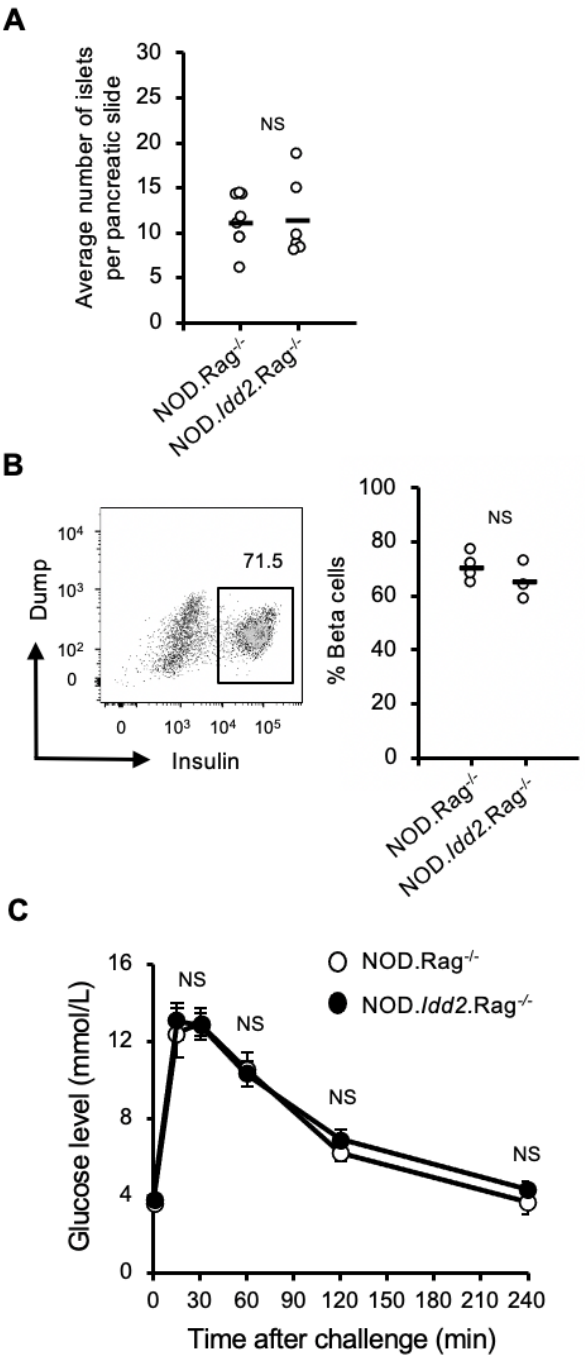

Figure 2. B10 alleles at the *Idd2* locus does not affect beta cell differentiation or function.

A) Average number of pancreatic islets per slides of pancreas from male NOD.Rag$^{-/-}$ and NOD.*Idd2*.Rag$^{-/-}$ mice. n = 6-7 per group. **B)** Representative flow cytometry plots of pancreatic islet cells from NOD.Rag$^{-/-}$ mice (left panel) and compilation of the percentage of insulin producing beta cells in pancreatic islets of male and female NOD.Rag$^{-/-}$ and NOD.*Idd2*.Rag$^{-/-}$ mice (right panel). n = 3-4 per group. **C)** Glucose tolerance test performed on 8 to 10-week old male NOD.Rag$^{-/-}$ (white dots) and NOD.*Idd2*.Rag$^{-/-}$ (black dots) mice. n = 6 per group. NS = non-significant.

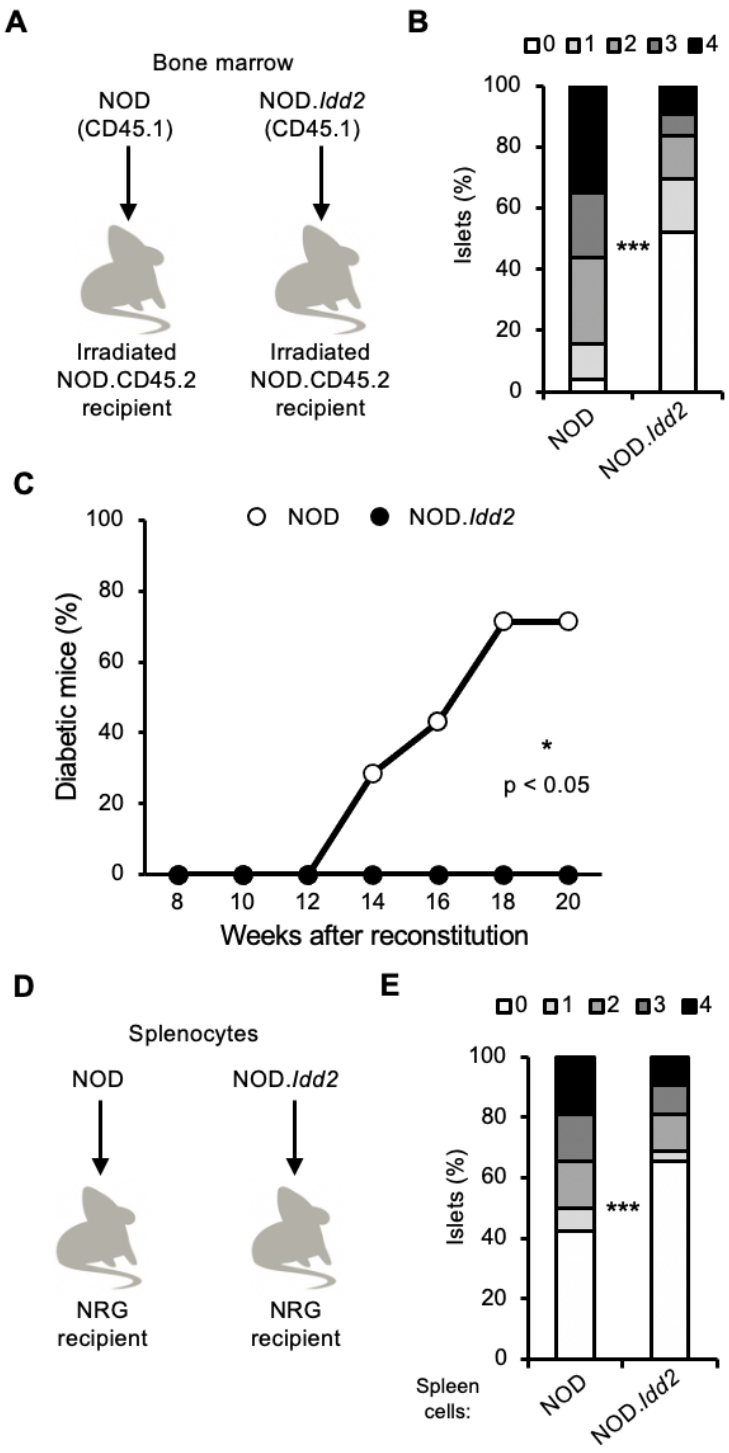

Figure 3. Resistance to insulitis and diabetes in NOD.*Idd2* mice is lymphoid cell-intrinsic.

A) Schematic depiction of bone marrow-chimera construction. **B)** The insulitis score of bone marrow chimera recipients is shown, 15 weeks post-reconstitution. Recipients of female NOD bone marrow, n = 6; recipients of female NOD.*Idd2* bone marrow, n = 14. **C)** Diabetes incidence is shown for female chimeras that received female NOD (n = 7) or NOD.*Idd2* (n = 6) bone marrow. **P* < 0.05 according to a Log-rank (Mantel-Cox) test. **D)** Schematic depiction of spleen cell transfers in female NRG recipients. **E)** The insulitis score of spleen cell recipients is shown, 15 weeks post-injection. n = 10 per group.

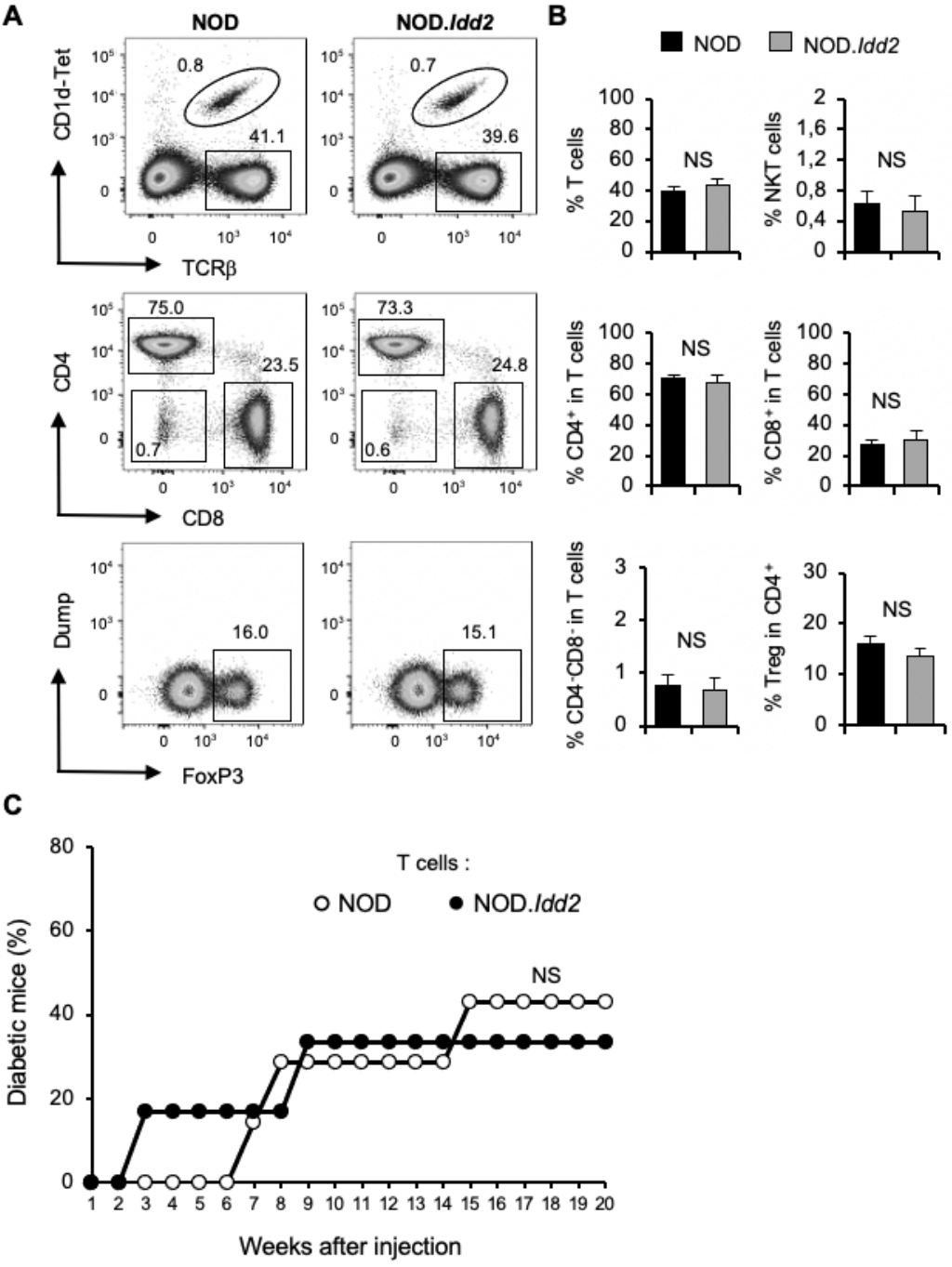

Figure 4. T cell diabetogenic potential is not affected in NOD.*Idd2* mice.
A) Representative flow cytometry plots of T cell subsets in the spleen of NOD and NOD.*Idd2* mice. **B)** Compilation of T cell subset proportion in the spleen of male NOD and NOD.*Idd2* mice. n > 3 per group. **C)** Diabetes incidence of female NRG mice injected with T cells from female NOD and NOD.*Idd2* mice. n = 6-7 per group. ns = non-significant.

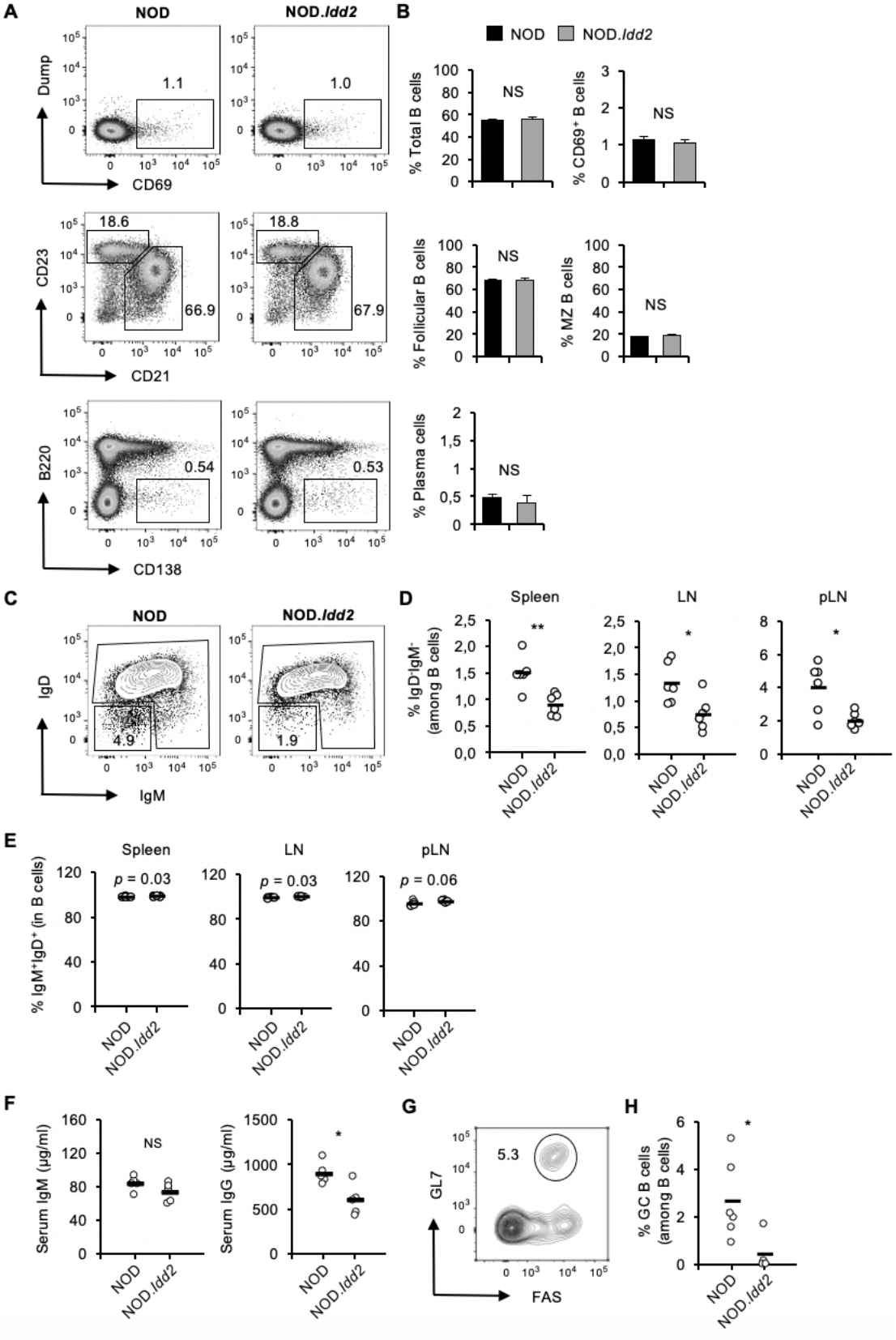
A
NOD
NOD.Idd2
Dump
CD69
1.1
1.0
CD23
CD21
18.6
66.9
18.8
67.9
B220
CD138
0.54
0.53
B
NOD
NOD.Idd2
% Total B cells
NS
% CD69+ B cells
NS
% Follicular B cells
NS
% MZ B cells
NS
% Plasma cells
NS
C
NOD
NOD.Idd2
IgD
IgM
4.9
1.9
D
Spleen
LN
pLN
% IgD-IgM- (among B cells)
**
*
*
NOD
NOD.Idd2
E
Spleen
LN
pLN
% IgM+IgD+ (in B cells)
p = 0.03
p = 0.03
p = 0.06
NOD
NOD.Idd2
F
Serum IgM (µg/ml)
NS
Serum IgG (µg/ml)
*
NOD
NOD.Idd2
G
GL7
FAS
5.3
H
% GC B cells (among B cells)
*
NOD
NOD.Idd2

Figure 5. B cell class switching and GC are affected in NOD.*Idd2* mice.
A) Representative flow cytometry plots of B cell subsets in the spleen of NOD and NOD.*Idd2* mice. **B)** Compilation of B cell subset proportion in the spleen of male NOD and NOD.*Idd2* mice. MZ = marginal zone. n > 3 per group. **C)** Representative flow cytometry plots of IgM and IgD expression by B cells from NOD and NOD.*Idd2* mice. **D)** Compilation of class switched B cell proportion in the spleen, LN and pLN of male NOD and NOD.*Idd2* mice. n = 6 per group. **E)** Compilation of unswitched B cell proportion in the spleen, LN and pLN of male NOD and NOD.*Idd2* mice. n = 6 per group. **F)** Total IgM and IgG concentration in the serum of male and female NOD and NOD.*Idd2* mice. n = 5 per group. **G)** Representative flow cytometry plots of FAS and GL7 expression in B cells from pancreatic islets of NOD mice. **H)** Compilation of GC B cell proportion from pancreatic islets of male and female NOD and NOD.*Idd2* mice. n = 4-6 per group. $*P < 0.05$, $**P < 0.01$, ns = non-significant. All mice used in these experiments were aged-matched (8-12 weeks old) and non-diabetic.

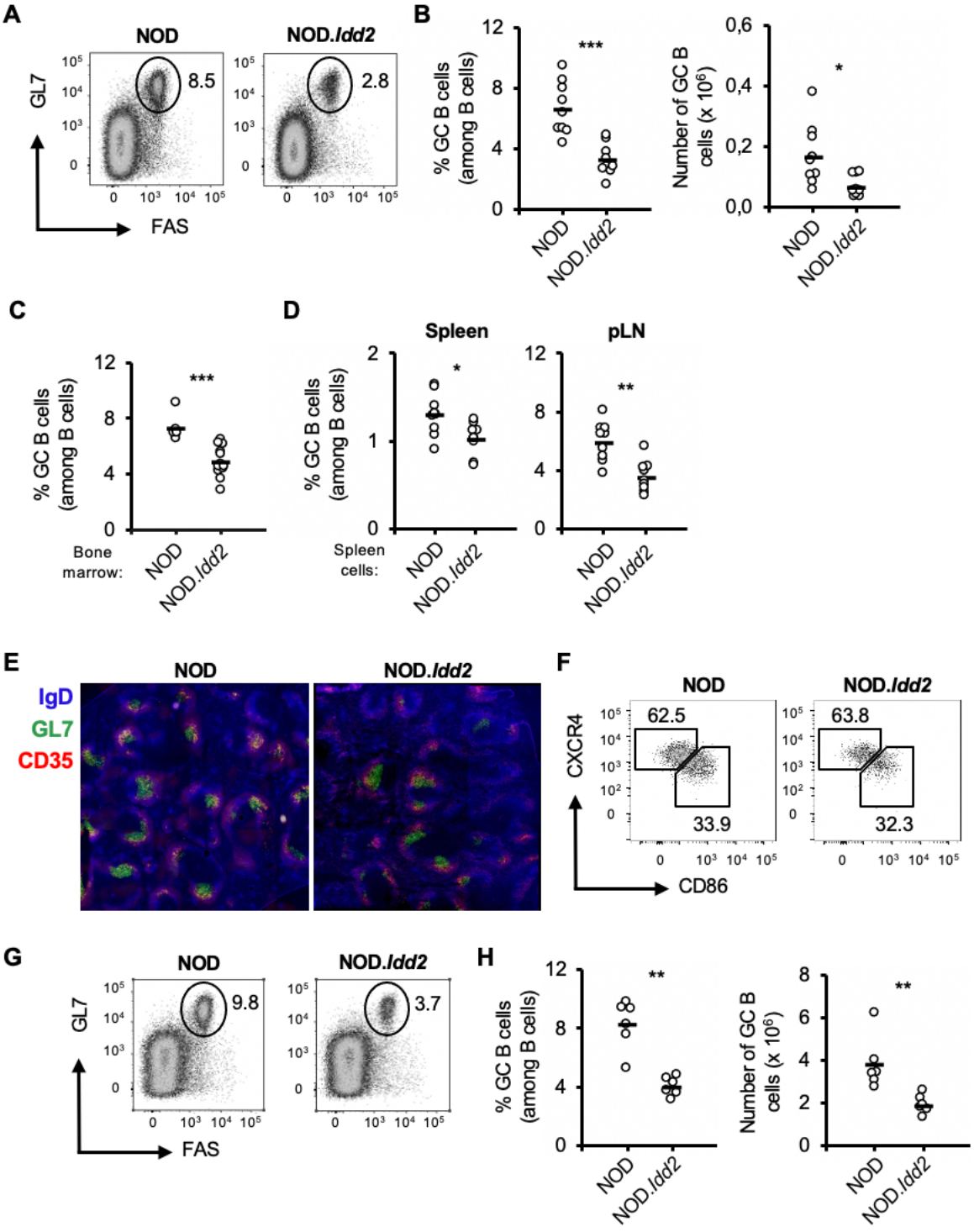
A
NOD
NOD.Idd2
GL7
FAS
8.5
2.8
B
% GC B cells (among B cells)
Number of GC B cells (x 10⁶)
***
*
NOD
NOD.Idd2
C
% GC B cells (among B cells)
***
Bone marrow:
NOD
NOD.Idd2
D
Spleen
pLN
% GC B cells (among B cells)
*
**
Spleen cells:
NOD
NOD.Idd2
E
NOD
NOD.Idd2
IgD
GL7
CD35
F
NOD
NOD.Idd2
CXCR4
CD86
62.5
33.9
63.8
32.3
G
NOD
NOD.Idd2
GL7
FAS
9.8
3.7
H
% GC B cells (among B cells)
Number of GC B cells (x 10⁶)
**
**
NOD
NOD.Idd2

Figure 6. Spontaneous and induced GC B cells are increased in NOD mice relative to NOD.*Idd2* mice.

A) Representative flow cytometry plots of GC B cells from Peyer's patches of NOD and NOD.*Idd2* mice. **B)** Compilation of GC B cell proportion (left panel) and absolute numbers (right panel) from Peyer's patches of male and female NOD and NOD.*Idd2* mice. n = 9 per group. **C)** Compilation of GC B cell proportion in Peyer's patches of non-competitive bone-marrow chimeras in NOD recipient mice. n = 5-12 per group. **D)** Compilation of GC B cell proportion in the spleen and pLN of female NRG mice injected with female NOD or NOD.*Idd2* spleen cells. **E)** Representative spleen immunohistochemistry of male NOD and NOD.*Idd2* mice immunized with SRBCs. **F, G)** Representative flow cytometry plots of (F) CD86 and CXCR4 expression on GC B cells and of (G) GL7 and FAS expression defining GC B cells of NOD and NOD.*Idd2* mice immunized with SRBCs. **H)** Compilation of GC B cell proportion (left panel) and absolute numbers (right panel) from the spleen of immunized male NOD and NOD.*Idd2* mice. n = 6 per group. $*P < 0.05$, $**P < 0.01$, $***P < 0.001$.

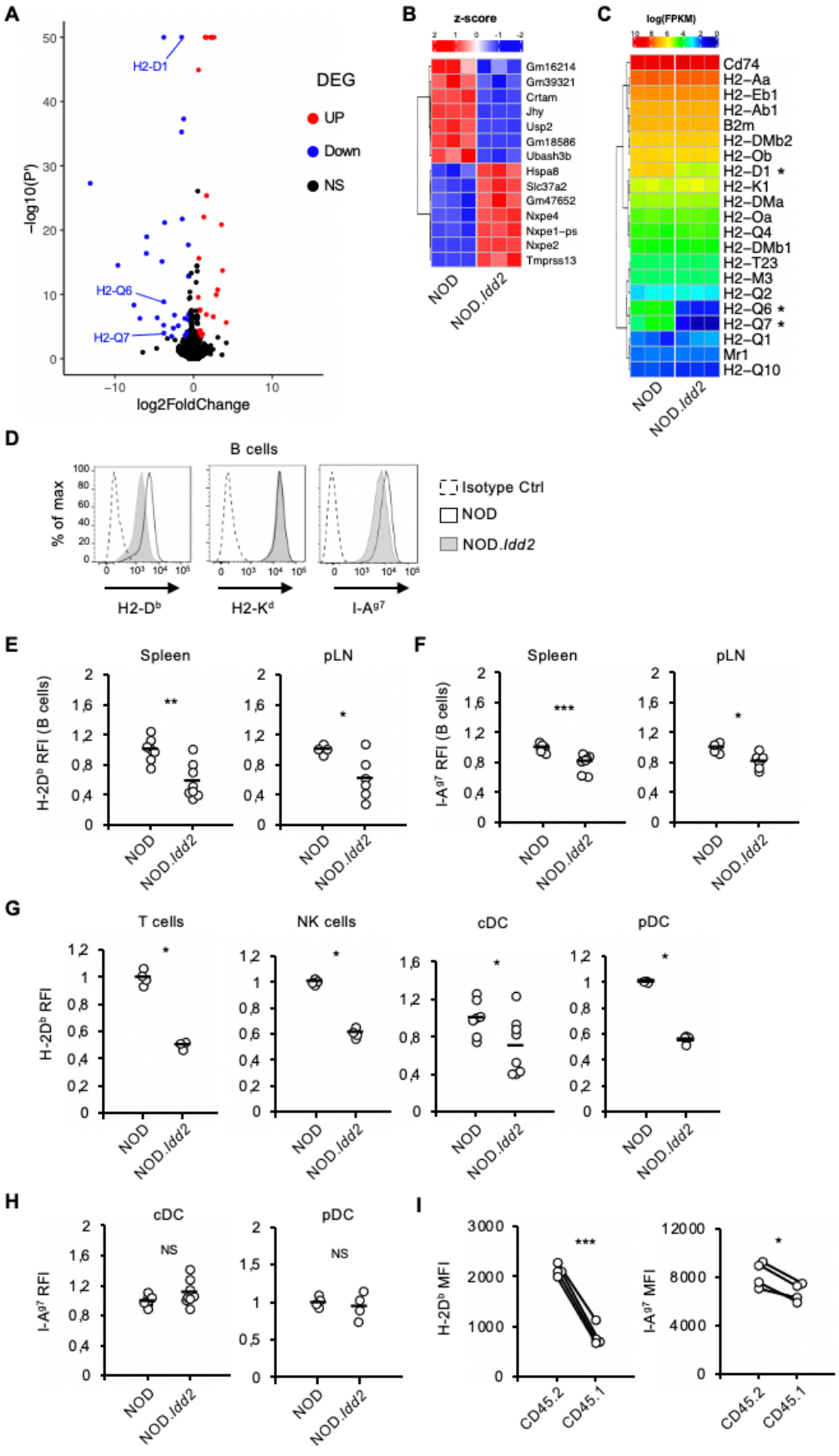
A
H2-D1
H2-Q6
H2-Q7
DEG
UP
Down
NS
−log10(P)
log2FoldChange
B
z-score
Gm16214
Gm39321
Crtam
Jhy
Usp2
Gm18586
Ubash3b
Hspa8
Slc37a2
Gm47652
Nxpe4
Nxpe1−ps
Nxpe2
Tmprss13
NOD
NOD.Idd2
C
log(FPKM)
Cd74
H2−Aa
H2−Eb1
H2−Ab1
B2m
H2−DMb2
H2−Ob
H2−D1 *
H2−K1
H2−DMa
H2−Oa
H2−Q4
H2−DMb1
H2−T23
H2−M3
H2−Q2
H2−Q6 *
H2−Q7 *
H2−Q1
Mr1
H2−Q10
NOD
NOD.Idd2
D
B cells
% of max
Isotype Ctrl
NOD
NOD.Idd2
H2-Db
H2-Kd
I-Ag7
E
Spleen
pLN
H-2Db RFI (B cells)
**
*
NOD
NOD.Idd2
F
Spleen
pLN
I-Ag7 RFI (B cells)
***
*
NOD
NOD.Idd2
G
T cells
NK cells
cDC
pDC
H-2Db RFI
*
NOD
NOD.Idd2
H
cDC
pDC
I-Ag7 RFI
NS
NOD
NOD.Idd2
I
H-2Db MFI
***
I-Ag7 MFI
*
CD45.2
CD45.1

Figure 7. Transcriptomic analysis of B cells reveals the impacts of the *Idd2* locus on MHC expression

A) Volcano Plots of Differentially Expressed Genes (DEG) from splenic B cells of female NOD and NOD.*Idd2* mice at FDR <0.05 and Fold Change > 1.5. Genes upregulated in B cells of NOD.*Idd2* mice are in red, downregulated in blue, and black if not significantly differentially expressed. **B)** Row-normalized (z-score) expression heatmap of the DEGs present in the locus of B10 origin of NOD.*Idd2* mice. Each row represents a gene and columns represent individual samples. Red represents a higher relative expression for a given gene, while blue denotes a lower relative expression. **C)** Log FPKM expression heatmap of genes implicated in antigenic presentation. Each row represents a gene and columns represent individual samples. Red represents a higher relative expression for a given gene, while blue denotes a lower relative expression. DEGs are marked with an asterisk. **D**) Representative flow cytometry plots of H-2D^{b}, H2-K^{d} and I-A^{g7} expression on B cells from NOD (black line) and NOD.*Idd2* (shaded line). Relative fluorescence intensity (RFI) of **E, G**) H-2D^{b} and **F, H**) I-A^{g7} expression on **E, F**) B cells and **G, H**) T cells, NK cells, conventional dendritic cells (cDC) and plasmacytoid dendritic cells (pDC) of male and female NOD and NOD.*Idd2* mice. RFI is based on the mean expression in NOD mice. n > 4 per group. **I)** H-2D^{b} and I-A^{g7} mean fluorescence intensity (MFI) of B cells from the spleen of female NOD and NOD.*Idd2* competitive bone-marrow chimeras in NOD recipient mice. *$P < 0.05$, **$P < 0.01$***$P < 0.001$, ns = non-significant.

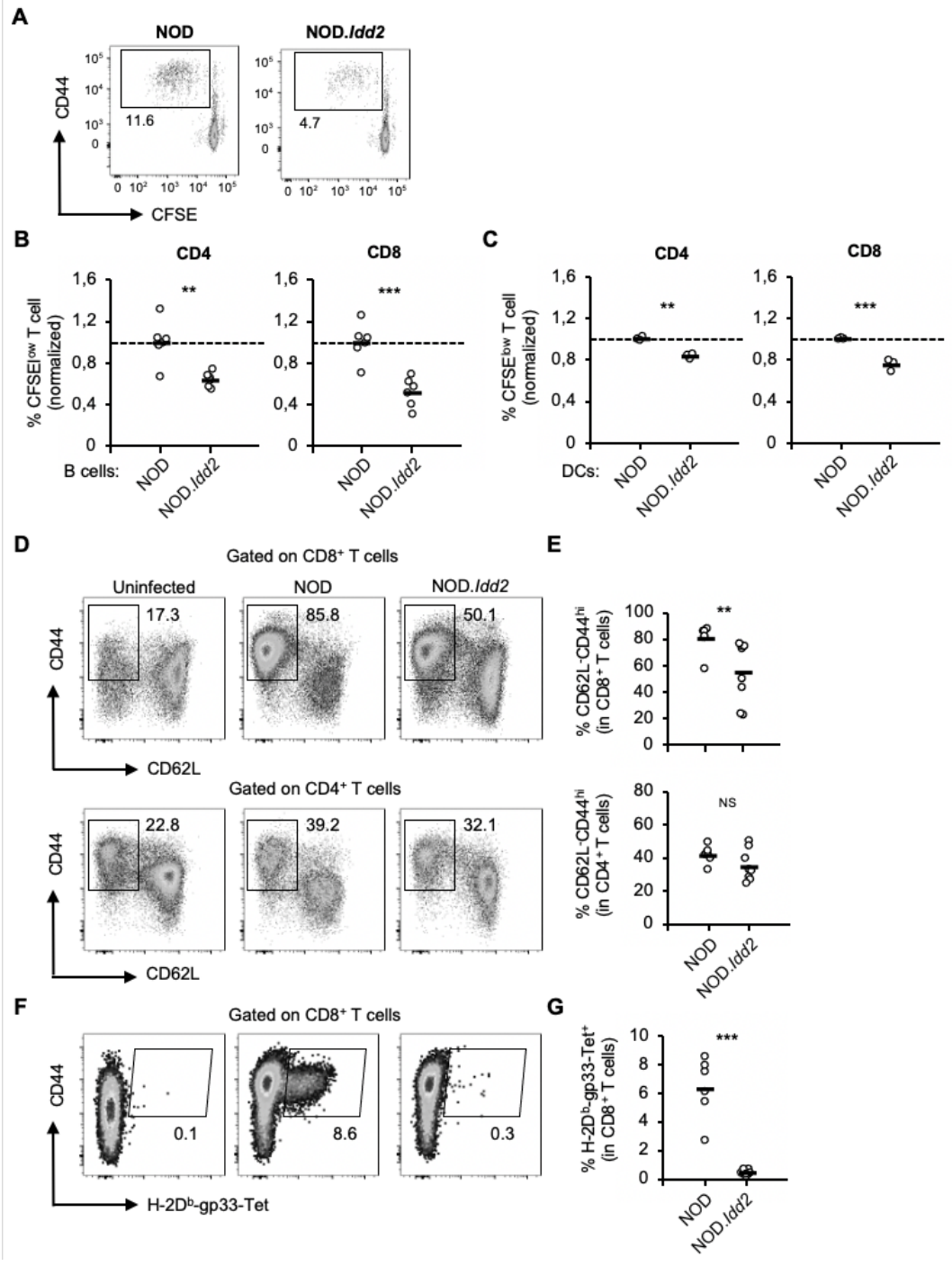
A
NOD
NOD.Idd2
CD44
CFSE
11.6
4.7
B
CD4
CD8
% CFSE^low T cell (normalized)
B cells:
NOD
NOD.Idd2
C
DCs:
D
Gated on CD8+ T cells
Uninfected
17.3
85.8
50.1
CD62L
Gated on CD4+ T cells
22.8
39.2
32.1
E
% CD62L-CD44^hi (in CD8+ T cells)
% CD62L-CD44^hi (in CD4+ T cells)
NS
F
0.1
8.6
0.3
H-2Db-gp33-Tet
G
% H-2Db-gp33-Tet+ (in CD8+ T cells)

Figure 8. Impact of the *Idd2* locus on T cell responses. A) Representative flow cytometry plots of CFSE labelled T cells from co-cultures with NOD and NOD.*Idd2* B cells. **B)** Percentage of $CFSE^{low}$ $CD4^+$ and $CD8^+$ T cells from co-cultures with NOD and NOD.*Idd2* B cells, normalized to the NOD co-cultures. **C)** Percentage of $CFSE^{low}$ $CD4^+$ and $CD8^+$ T cells from co-cultures with NOD and NOD.*Idd2* DCs, normalized to the NOD co-cultures. **D)** Representative flow cytometry plots of $CD4^+$ and $CD8^+$ T cells from LCMV infected mice and uninfected NOD mice. **E)** Compilation of $CD62L^-$ $CD44^{hi}$ cells from the spleen of infected male mice. **F)** Representative flow cytometry plots of $CD8^+$ T cells from LCMV infected mice and uninfected NOD mice. **G)** Compilation $H2D^b$-gp33 tetramers specific $CD8^+$ T cells from the spleen of infected male mice (n = 3-6). $*P < 0.05$, $**P < 0.01$$***P < 0.001$.

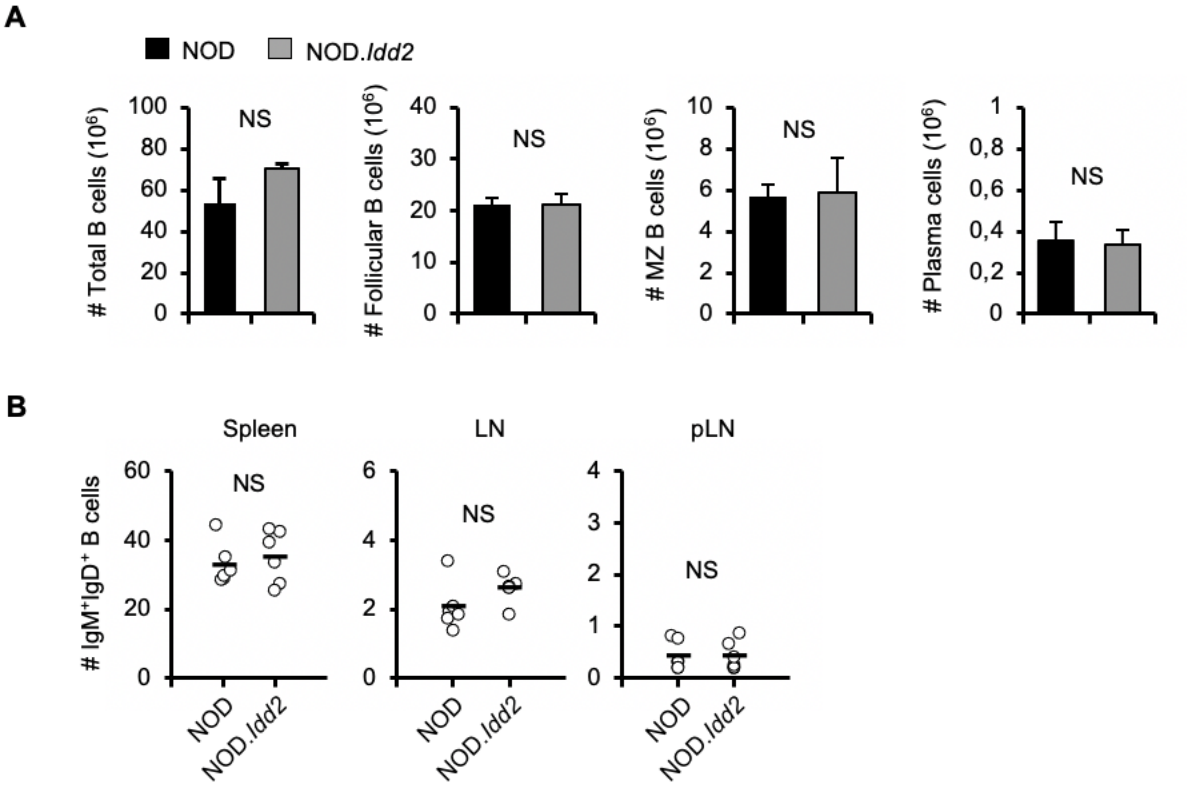

Figure S1. **Absolute numbers of B cell subsets. A)** Absolute number of total, follicular and marginal zone (MZ) B cells, and plasma cells, from the spleen of NOD and NOD.*Idd2* mice. n ≥ 3. **B)** Absolute number of unswitched B cells from the spleen, LN and pLN of NOD and NOD.*Idd2* mice. n = 5-6. NS = non-significant.

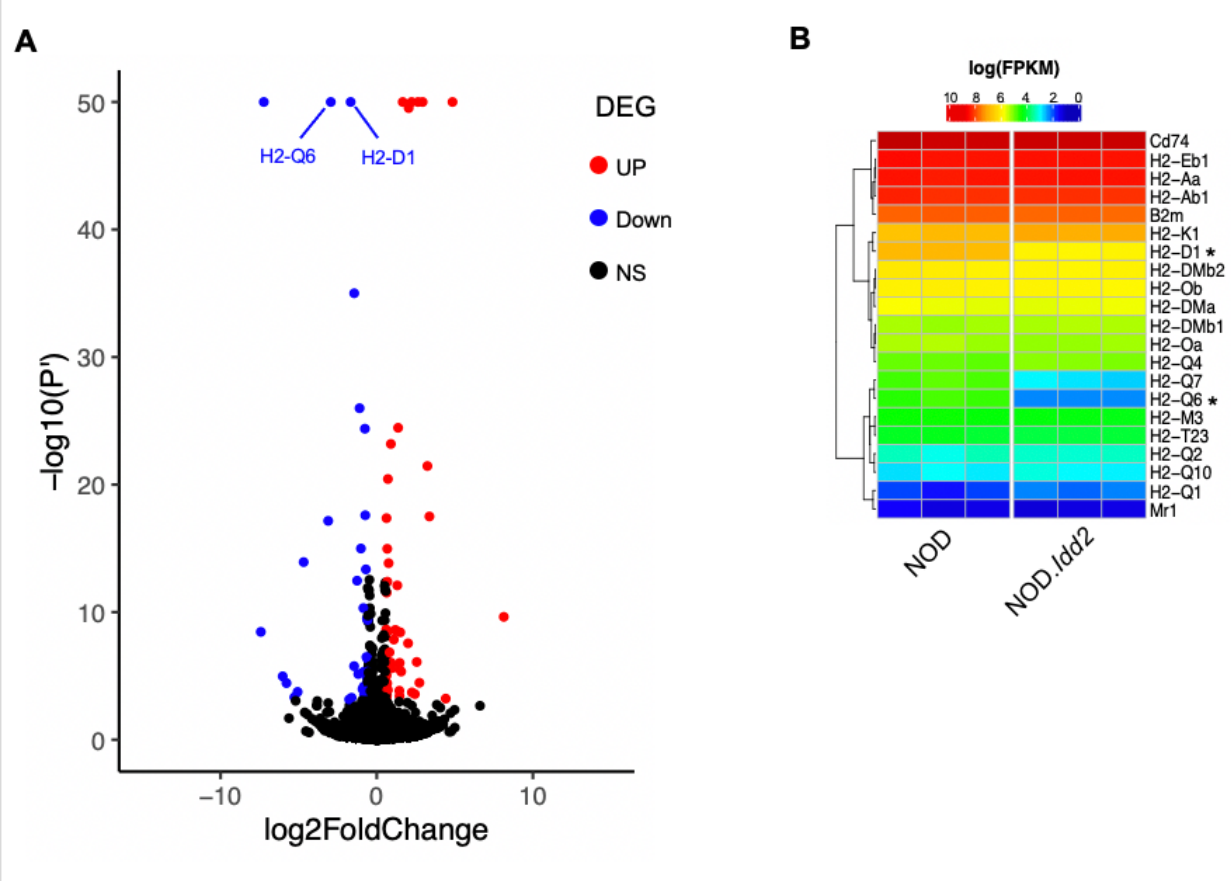

Figure S2. **Transcriptomic analysis of dendritic cells (DCs). A)** Volcano Plots of Differentially Expressed Genes (DEG) from splenic DCs of NOD and NOD.*Idd2* mice at FDR <0.05 and Fold Change > 1.5. Genes upregulated in DCs of NOD.*Idd2* mice are in red, downregulated in blue, and not significantly differentially expressed in black. **B)** Log FPKM expression heatmap of genes implicated in antigenic presentation. Each row represents a gene and columns represent individual samples. Red represents a higher relative expression for a given gene, while blue denotes a lower relative expression. DEGs are marked with an asterisk.

Preface to chapter 3

In the previous chapter, we have demonstrated that genetic variants in the *Idd2* locus impact autoimmune diabetes susceptibility and GC formation. Prior to the RNA-Seq analyses described in chapter 2, we rapidly aimed to identify candidate genes within the *Idd2* locus that could modulate GC formation. Among the few hundred candidate genes, our attention turned to *Pou2af1*, which encode the OCA-B protein. As mentioned in chapter 1, OCA-B is highly expressed in B cells and play multiple roles in B cell biology, such as promoting GC formation.

To investigate the cell-intrinsic role of OCA-B, we generated a new mouse model where *Pou2af1* can be disrupted in specific cell types. As we were generating this model, we obtained the RNA-Seq data suggesting that *Pou2af1* was just outside of the locus of interest in our congenic strain, and unlikely to contribute to the phenotypes observed in NOD.*Idd2* mice. Still, having generated this conditional *Pou2af1* mouse model, and seeing the growing body of literature describing a potential role for *Pou2af1* in T cells, we opted to exploit our model to determine how *Pou2af1* impacts T cell responses. In this chapter, we conclusively demonstrate that *Pou2af1* does not have a T cell-intrinsic role.

Chapter 3:

OCA-B does not act as a transcriptional co-activator in T cells

Running title: Extrinsic role for *Pou2af1* in T cells

Félix Lombard-Vadnais[1, 2], Julie Lacombe[3], Geneviève Chabot-Roy[1], Mathieu Ferron[3,4,5], Sylvie Lesage[1,6]

[1] Immunologie-oncologie, Centre de recherche de l'Hôpital Maisonneuve-Rosemont, Montréal, QC, H1T 2M4, Canada

[2] Department of Microbiology & Immunology, McGill University, Montreal, QC, H3A 0G4, Canada

[3] Maladies cardiovasculaires et métaboliques, Institut de recherches cliniques de Montréal, Montréal, QC, H2W 1R7, Canada

[4] Département de médecine, Université de Montréal, Montréal, QC, H3T 1J4, Canada

[5] Department of Experimental Medicine, McGill University, Montreal, QC, H3A 0G4, Canada

[6] Département de microbiologie, infectiologie et immunologie, Université de Montréal, Montréal, QC, H3T 1J4, Canada

*Correspondence: Sylvie Lesage, 514-252-3400 ext 4649, sylvie.lesage@umontreal.ca

Keywords: B cells / OCA-B / Pou2af1 / T cells / germinal centers/ Tfh

3.1 Abstract

Pou2af1 encodes for OCA-B, a coactivator of OCT-1/2 transcription factors, which plays a key role in B cell maturation. The function of OCA-B has also been studied in T cells, where T cells from *Pou2af1*$^{-/-}$ mice have impaired functions, such as cytokine production and T follicular helper (Tfh) differentiation. Arguably, some of these T cell phenotypes may result from impaired T-B interactions, secondary to the well-documented B cell defects in *Pou2af1*$^{-/-}$ mice. Yet, *Pou2af1* is actively transcribed in activated T cells, suggesting a T cell-intrinsic role. To isolate the T cell-intrinsic impact of *Pou2af1*, we generated *Pou2af1*$^{fl/fl}$ mice with specific genetic disruption of *Pou2af1* either in all hematopoietic cells or exclusively in T cells. While we confirm that *Pou2af1* is expressed in activated T cells, we surprisingly find that T cell cytokine production is not impaired in *Pou2af1*-deficient T cells. Moreover, *Pou2af1*-sufficient and -deficient T cells have comparable transcriptome profiles, arguing against a T cell-intrinsic role for *Pou2af1*. In line with these observations, we demonstrate that Tfh maturation is influenced by T cell-extrinsic deletion of *Pou2af1*, as observed both in competitive bone marrow chimeras and in *Pou2af1*$^{fl/fl}$ mice with specific deletion in B cells. Overall, this study provides strong evidence that *Pou2af1* does not act as a transcriptional coactivator in T cells, and conclusively demonstrates that loss of OCA-B in B cells indirectly impacts Tfh differentiation, clarifying the role of OCA-B in the immune system.

Keywords: B cells / OCA-B / Pou2af1 / T cells / germinal centers/ Tfh

3.2 Introduction

OCA-B (Oct-coactivator from B cells, also known as OBF-1 or BOB.1) is encoded by the *Pou2af1* gene and was first identified in B cell extracts on the basis of its ability to promote immunoglobulin (Ig) gene transcription (45). It is a transcriptional coactivator that interacts with the ubiquitously expressed OCT-1 and the B cell-specific OCT-2 transcription factors (44, 45). OCA-B expression is restricted to the hematopoietic system, with strong expression in the spleen, lymph nodes (LN), bone marrow and blood (44, 309).

The first *in vitro* studies of OCA-B function suggested that OCA-B was one of the main drivers of Ig gene transcription in B cells (44, 45). However, the generation of the B6.129S-*Pou2af1*$^{-/-}$ mouse, hereafter referred to as *Pou2af1*$^{-/-}$ mice, in which expression of OCA-B is disrupted in all cell types, revealed that OCA-B is dispensable for Ig transcription (74, 310). *Pou2af1* mRNA is detectable in B cells at all stages of maturation (311), and *Pou2af1* deficiency impairs many aspects of B cell biology including B cell development (46, 312-314), germinal center (GC) induction (74, 310, 315), IgG production (74, 310), B cell receptor signaling (316) and plasma cell differentiation (317). The target genes of OCA-B/OCT-1/2 complexes remain mostly unknown but candidate genes include *Spib* and *Bcl6* (75, 318), both of which contribute to GC B cell differentiation (319, 320), such that this could explain the reduced ability of *Pou2af1*$^{-/-}$ B cells to differentiate into GC B cells.

In addition to B cells, the function of OCA-B has been studied in T cells. Indeed, *Pou2af1* is transcribed in T cells following *in vitro* activation (321, 322). As OCT-1 is ubiquitously expressed,

OCA-B in T cells could act through OCT-1 coactivation. Notably, T follicular helper (Tfh) and T helper 17 (Th17) differentiation as well as $CD4^+$ T cell cytokine production are impaired in *Pou2af1*$^{-/-}$ mice (76, 321, 323). Still, due to the germline disruption of *Pou2af1* in these mice, one cannot conclude whether the T cell phenotypes are due to a cell-intrinsic loss of *Pou2af1* expression or are indirectly attributable to the loss of *Pou2af1* expression in other hematopoietic cells.

To determine the T cell-intrinsic roles for OCA-B, we generated mouse models in which we performed conditional deletion of *Pou2af1* specifically in hematopoietic cells or in T cells. Using these models, we provide strong evidence that *Pou2af1* does not impact T cell cytokine production or Th17 differentiation, and does not act as a transcriptional coactivator in T cells. Rather, we demonstrate that *Pou2af1* regulates Tfh differentiation in a T cell-extrinsic manner, specifically via *Pou2af1*-expressing B cells.

3.3 Results

Generation of a *Pou2af1*$^{fl/fl}$ mouse for cell-specific *Pou2af1* deletion

In order to generate a mouse strain with cell-specific disruption of the *Pou2af1* gene, we obtained *Pou2af1*$^{+/LacZ}$ mice (*Pou2af1*$^{tm1a(KOMP)Wtsi}$) from the KOMP Repository (324). In this mouse strain, the *Pou2af1* locus has been targeted to generate a *knockout-first* allele which can be converted to a conditional (Fl, floxed) allele through FLP-mediated recombination (Supplementary figure 1**a**). Proper targeting of the locus was confirmed through 5' and 3' long range PCR performed on genomic DNA isolated from mouse tails (Supplementary figure 1**b**). Genotyping PCR using internal primers also confirmed the generation of *Pou2af1*$^{+/LacZ}$ mice (Supplementary figure 1**c**). These animals were next crossed with ACTBFLPe transgenic mice, which expressed the FLPe recombinase gene under the direction of the human ACTB promoter (325), to excise the LacZ and Neomycin (Neo) cassettes. The resulting ACTBFLPe.*Pou2af1*$^{+/fl}$ mice were then crossed with C57BL/6J mice to isolate the floxed allele from the ACTBFLPe transgene and proper recombination at the *Pou2af1* locus was confirmed in the progeny of these mice using specific genotyping PCR (Supplementary figure 1**d**). *Pou2af1*$^{+/fl}$ mice were intercrossed to obtain *Pou2af1*$^{fl/fl}$ mice.

To disrupt the *Pou2af1* gene in all hematopoietic cells, *Pou2af1*$^{fl/fl}$ mice were crossed to Vav-Cre^{+} mice (326, 327). Complete absence of *Pou2af1* mRNA expression was confirmed by RT-qPCR on spleen cells from Vav-Cre^{+} and Vav-Cre^{-} littermates (deletion > 99%) (Supplementary figure 1**e-f**). As for *Pou2af1*$^{-/-}$ mice (74, 76, 312), B cell proportion and numbers were reduced in the spleen, Peyer's patches (PP) and mesenteric LNs (mLNs) of Vav-Cre^{+}.*Pou2af1*$^{fl/fl}$ mice relative to Vav-Cre^{-} littermates (Figure 1**a, b**). Similar to *Pou2af1*$^{-/-}$ mice (76), Vav-Cre^{+}.*Pou2af1*$^{fl/fl}$ mice

also showed a reduction of GC B cells (GL-7^{+}FAS^{+}) in both PP and mLNs relative to littermate control mice (Figure 1**c, d**). In addition, most of the remaining GL-7^{+}FAS^{+} GC B cells in Vav-Cre^{+}.*Pou2af1*$^{fl/fl}$ mice expressed a CD86^{+}CXCR4^{Low} phenotype (Figure 1**e, f**). The low number of GC B cells in Vav-Cre^{+}.*Pou2af1*$^{fl/fl}$ mice are thus skewed towards a phenotype associated with light zone B cells, suggesting that GC B cell differentiation is perturbed in the absence of OCA-B.

***Pou2af1* is expressed in T cells**

Before investigating the effect of a T cell-specific deletion of *Pou2af1*, we validated that OCA-B was expressed in T cells. With the anti-OCA-B 6F10 monoclonal antibody yielding non-specific binding (Supplementary figure 2**a, b**), we quantified *Pou2af1* transcription by measuring mRNA levels in *Pou2af1*-sufficient mice. *Pou2af1* mRNA was expectedly abundant in total splenocytes, whereas mRNA levels were barely detectable in T cells (Figure 2**a**). As previously reported (328), *in vitro* activation of T cells induced a small but significant increase in *Pou2af1* mRNA levels (Figure 2**a**). These data show that OCA-B is expressed at low levels in total T cells and its expression can be induced upon activation. OCA-B expression was specific, as *Pou2af1* mRNA was undetectable in both unactivated and activated T cells isolated from either Vav-Cre^{+}.*Pou2af1*$^{fl/fl}$ or CD4-Cre^{+}.*Pou2af1*$^{fl/fl}$ mice (Figure 2**a**). Note that CD4-Cre is expressed in the early CD4^{+}CD8^{+}thymic differentiation stage, such that genetic deletion is transmitted to all daughter cells, therefore resulting in targeted gene deletion in both CD4^{+} and CD8^{+} T cells (Supplementary figure 2**c, d**) (329). As previously reported for *Pou2af1*$^{-/-}$ mice (76, 310, 314), deletion of *Pou2af1* in both Vav-Cre^{+}.*Pou2af1*$^{fl/fl}$ and CD4-Cre^{+}.*Pou2af1*$^{fl/fl}$ mice did not affect CD4^{+} and CD8^{+} T cell numbers in secondary lymphoid organs (Supplementary figure 2**e, f**). Taken

together, these data show that *Pou2af1* deletion is efficient in both Vav-Cre^{+}.*Pou2af1*$^{fl/fl}$ and CD4-Cre^{+}.*Pou2af1*$^{fl/fl}$ mice. Indeed, B cell phenotypes in Vav-Cre^{+}.*Pou2af1*$^{fl/fl}$ mice recapitulate those observed in *Pou2af1*$^{-/-}$ mice, demonstrating that *Pou2af1* is efficiently deleted in this model. In addition, *Pou2af1* mRNA is undetectable in T cells from both Vav-Cre^{+}.*Pou2af1*$^{fl/fl}$ and CD4-Cre^{+}.*Pou2af1*$^{fl/fl}$ mice. More importantly, these data confirm that OCA-B is expressed, all be it at low levels, in T cells.

Pou2af1 is dispensable for previously reported T cell phenotypes

We next sought to investigate whether T cell phenotypes previously reported in *Pou2af1*$^{-/-}$ mice were T cell-intrinsic or extrinsic. One of the reported T cell phenotypes in *Pou2af1*$^{-/-}$ mice is impaired cytokine production (321). Specifically, IL-2 cytokine production was quantified in CD4^{+} T cells that had been stimulated with anti-CD3 and anti-CD28 antibodies, rested for 8 days, and restimulated with anti-CD3 and anti-CD28 antibodies for 6 hours. Under these conditions, IL-2 cytokine production by CD4^{+} T cells from *Pou2af1*$^{-/-}$ mice was shown to be significantly decreased when compared to B6 mice (321). Here, we quantified IL-2, TNF-α and IFN-γ cytokine production in CD4^{+} T cells from CD4-Cre^{+}.*Pou2af1*$^{fl/fl}$ relative to Cre^{-}.*Pou2af1*$^{fl/fl}$ littermate controls, using a similar CD4^{+} T cell activation protocol, with an 8 day rest period prior to a 6h restimulation with anti-CD3 and anti-CD28 antibodies. We found that *Pou2af1*-sufficient and -deficient CD4^{+} T cells both produced similar levels of IL-2, TNF-α and IFN-γ (Figure 2**b, c**), suggesting that *Pou2af1* plays a cell-extrinsic role in facilitating CD4^{+} T cell cytokine production. To validate the cell-extrinsic role of *Pou2af1*, we also assessed IL-2, TNF-α and IFN-γ cytokine production in CD4^{+} T cells from Vav-Cre^{+}.*Pou2af1*$^{fl/fl}$ relative to Cre^{-}.*Pou2af1*$^{fl/fl}$ littermate controls. In this model, with the deletion of *Pou2af1* in all hematopoietic cells, we expected that

CD4$^+$ T cell cytokine production would be impaired in *Pou2af1*-deficient T cells, similar to what had been observed in *Pou2af1*$^{-/-}$ mice (321). However, IL-2, TNF-α and IFN-γ cytokine production was similar in CD4$^+$ T cells from Vav-Cre$^+$.*Pou2af1*$^{fl/fl}$ and Cre$^-$.*Pou2af1*$^{fl/fl}$ mice (Figure 2**d**). This was observed through a wide range of anti-CD3 concentration, in the presence or absence of co-stimulation (Figure 2**e, f**). These results thus contrast with previous findings (321) and suggest that *Pou2af1* does not impact CD4$^+$ T cell cytokine production neither directly, nor indirectly.

Due to the discrepancy between the CD4$^+$ T cell cytokine production of *Pou2af1*$^{-/-}$ mice and of our newly generated *Pou2af1*$^{fl/fl}$ mice, we considered potential differences in the genetic make-up of the strains. The same exons, namely 2, 3 and 4, are targeted in both models ((310) and Supplementary figure 1). The main difference is genetic background. *Pou2af1* gene targeting in the *Pou2af1*$^{-/-}$ mice was initially performed in 129S embryonic stem cells and the resulting mice were kept on a mixed B6 and 129S genetic background (310). In contrast, gene targeting in the *Pou2af1*$^{fl/fl}$ mice described here was performed directly on C57BL/6N-A^{tm1Brd} background and *Pou2af1*$^{fl/fl}$ mice were maintained by backcrossing to B6 mice. As the level of CD4$^+$ T cell cytokine production from *Pou2af1*$^{-/-}$ mice on a mixed genetic background was compared to that of CD4$^+$ T cells from B6 mice (321), we questioned whether genetic variants from the 129S background could explain the difference in phenotype. We quantified IL-2 cytokine production in CD4$^+$ T cell from B6 and 129S mice and found that IL-2 production was significantly reduced in CD4$^+$ T cell from 129S relative to B6 mice (Figure 2**g, h**). Next, we acquired *Pou2af1*$^{-/-}$ mice with a mixed genetic background and tested IL-2 production from CD4$^+$ T cells. When compared among littermates (i.e. with similar mixed genetic background), IL-2 production was not affected by the *Pou2af1* genotype (Figure 2**i**). Altogether, these data suggest that genetic variants from the 129S

background in *Pou2af1*$^{-/-}$ mice likely affect CD4^{+} T cell cytokine production and that *Pou2af1* expression is dispensable for optimal cytokine production by CD4^{+} T cells.

The observation that potential 129S carryover genes could affect T cell phenotypes prompted us to revisit the impact of *Pou2af1* on Th17 differentiation (323) and memory CD4^{+} T cells (321). When subjected to Th17 differentiation conditions, T cells from Vav-Cre^{+}.*Pou2af1*$^{fl/fl}$ and Vav-Cre^{-}.*Pou2af1*$^{fl/fl}$ littermates showed similar levels of RORγt induction and IL-17 production, demonstrating that Th17 differentiation is not affected by the genetic deletion of *Pou2af1* (Figure 3**a-c**). Th17 differentiation and IL-17 production was also similar for CD4^{+} T cells from *Pou2af1*$^{-/-}$ mice and the littermate controls (Figure 3**d, e**). CD4^{+} T cells with a memory phenotype can be distinguished from naïve cells based on a CD62L^{Lo}CD44^{Hi}CD45RB^{Lo} phenotype. The absence of CD25 expression also discriminates memory CD4^{+} T cells from early effector T cells (330). No difference in the percentage or number of CD4^{+} T cells with a memory phenotype was observed in the spleen, bone marrow and LN for both Vav- and CD4-Cre^{+}.*Pou2af1*$^{fl/fl}$ mice relative to their littermate controls (Figure 3**f, g** and Supplementary figure 3). Altogether, these results argue against an effect of *Pou2af1* on Th17 differentiation and CD4^{+} T cell memory phenotype.

T cell-extrinsic impact of *Pou2af1* deletion on Tfh and GC development

Pou2af1$^{-/-}$ mice also display a strong reduction of Tfh in PP at steady state, relative to wild type (WT) mice (76). In contrast to the other T cell traits investigated above, we find a clear reduction in the percentage and number of Tfh in both the PP and mLN of Vav-Cre^{+}.*Pou2af1*$^{fl/fl}$ mice (Figure 4**a, b** and Supplementary figure 4**a, e**). *Pou2af1* expression in hematopoietic cells is therefore necessary for optimal Tfh differentiation. Interestingly, while Tfh are considerably reduced in

Vav-Cre^{+}.*Pou2af1*$^{fl/fl}$ mice, early Tfh (CXCR5^{Low}PD-1^{Low}) are present in similar proportions in PP and mLN (Figure 4**c** and Supplementary figure 4**b**) and are increased numbers in PP (Supplementary figure 4**f**), relative to Cre^{-} littermate controls. When gated on total CD4^{+} T cells expressing CXCR5 and PD-1, to include both early and mature Tfh, we observe a severe decrease in the expression level of CXCR5 and PD-1 (Figure 4**d**). These data suggest that Tfh differentiation is blocked at the early Tfh maturation stage in Vav-Cre^{+}.*Pou2af1*$^{fl/fl}$ mice.

To determine if *Pou2af1* plays a T cell-intrinsic role in Tfh differentiation, we studied Tfh differentiation in PP and mLN from CD4-Cre^{+}.*Pou2af1*$^{fl/fl}$ mice. In contrast to *Pou2af1*$^{-/-}$ mice and Vav-Cre^{+}.*Pou2af1*$^{fl/fl}$ mice, the proportion and number of Tfh and of early Tfh was not affected by the specific deletion of *Pou2af1* in T cells from both PP and mLN (Figure 4**e-g** and Supplementary figure 4**a, b, g, h**). In addition, specific disruption of *Pou2af1* in T cells did not affect the percentage and number of GC B cells in PP and in mLN (Figure 4**h** and Supplementary figure 4**c, i**). The GC B cell bias towards a light zone phenotype observed in the Vav-Cre^{+}.*Pou2af1*$^{fl/fl}$ mice (Figure 1**e, f**) was also not observed in CD4-Cre^{+}.*Pou2af1*$^{fl/fl}$ mice (Figure 4**i** and Supplementary figure 4**d**). These results suggest that T cell-intrinsic expression of *Pou2af1* is not necessary for the development of both Tfh and GCs.

As *Pou2af1* mRNA levels are low in naïve T cells and induced upon activation (Figure 2**a**), we reasoned that Tfh differentiation in CD4-Cre^{+}.*Pou2af1*$^{fl/fl}$ mice may only be impaired upon immunization rather than steady state conditions. To test this possibility, we immunized Vav- and CD4-Cre^{+}.*Pou2af1*$^{fl/fl}$ mice as well as Cre^{-}.*Pou2af1*$^{fl/fl}$ littermate controls with sheep red blood cells, as they induce robust GC formation in the spleen (331). Ten days post-immunization, we

quantified GC B cells and Tfh in the spleen of these mice. Expectedly, the proportion of PD-1^{+}CXCR5^{+} Tfh (Figure 4**j, k**) and GL-7^{+}FAS^{+} GC B cells (Figure 4**l**) were low in Vav-Cre^{+}.*Pou2af1*$^{fl/fl}$ mice. However, both CD4-Cre^{+}.*Pou2af1*$^{fl/fl}$ and littermate controls had similar levels of Tfh and GC B cells in the spleens (Figure 4**j-l**). Consistent with our data in the PPs and mLNs at steady state, we observed a reduction of PD-1 and CXCR5 RFI in Tfh from Vav-Cre^{+}.*Pou2af1*$^{fl/fl}$ mice relative to both CD4-Cre^{+}.*Pou2af1*$^{fl/fl}$ mice and littermate controls (Supplementary figure 5**a**). Altogether, these results strongly point to a T cell-extrinsic role of *Pou2af1* in regulating Tfh differentiation in *Pou2af1*$^{-/-}$ mice.

OCA-B is not an active transcriptional coactivator in T cells

As we observed no T cell-intrinsic phenotypes in the absence of *Pou2af1*, we sought to investigate whether the increase in *Pou2af1* mRNA in activated T cells has an impact on the T cell transcriptome. OCA-B associates with the OCT-1 and OCT-2 transcription factors to regulate transcription of their target genes (44, 45). As OCT-1 is expressed in both CD4^{+} and CD8^{+} T cells (332), OCA-B may act as a transcriptional cofactor in activated T cells. To identify the potential consequence of *Pou2af1* induction on the T cell transcriptome, we sorted naïve CD4^{+} and CD8^{+} T cells from the spleen of CD4-Cre^{-}.*Pou2af1*$^{fl/fl}$, CD4-Cre^{+}.*Pou2af1*$^{fl/+}$ and CD4-Cre^{+}.*Pou2af1*$^{fl/fl}$ littermates. Sorted cells were stimulated *in vitro* with anti-CD3 and anti-CD28 for 48h hours, RNA was isolated and subjected to RNA-Seq analysis. Principal component analysis (PCA) applied to the 500 most differentially expressed genes did not segregate T cells on the basis of their genotype (Figure 5**a**), suggesting an absence of transcriptomic regulation by *Pou2af1*. *Pou2af1* mRNA expression was significantly decreased in T cells from CD4-Cre^{+}.*Pou2af1*$^{fl/fl}$ mice relative to T cells from CD4-Cre^{-}.*Pou2af1*$^{fl/fl}$ mice, confirming that *Pou2af1* mRNA is expressed in activated

CD4$^+$ and CD8$^+$ T cells (Figure 5**b** and Supplementary figure 6**a**). Apart from *Pou2af1*, only four genes were significantly differentially expressed when comparing CD4$^+$ or CD8$^+$ cells from CD4-Cre$^-$.*Pou2af1*$^{fl/fl}$ and CD4-Cre$^+$.*Pou2af1*$^{fl/fl}$ littermates (Figure 5**b** and Supplementary figure 6**a**). Among those four genes, only two were observed in both CD4$^+$ and CD8$^+$ T cells: *Rps3a1* and *Tpm3-rs7*. Of note, these two genes were also differentially expressed in T cells from CD4-Cre$^+$.*Pou2af1*$^{fl/+}$ heterozygous mice when compared to CD4-Cre$^-$.*Pou2af1*$^{fl/fl}$ mice (Figure 5**b**), suggesting that the expression of the CD4-Cre transgene may be responsible for these differences, rather than an effect of the *Pou2af1* deletion. Together, these data demonstrate that, although *Pou2af1* is expressed in T cells following *in vitro* stimulation, it does not act as an important coactivator of transcription.

***Pou2af1* expression in B cells is necessary for adequate Tfh maturation**

Notwithstanding the absence of a T cell-intrinsic role for *Pou2af1*, our data point to a T cell-extrinsic role in Tfh differentiation. To specifically test if the Tfh maturation block observed in Vav-Cre$^+$.*Pou2af1*$^{fl/fl}$ mice is caused by defective crosstalk between T cells and *Pou2af1*$^{-/-}$ hematopoietic cells *in vivo*, we generated competitive bone marrow chimeras. B6.SJL (CD45.1) and Vav-Cre$^+$.*Pou2af1*$^{fl/fl}$ (CD45.2) bone marrow were mixed at 1:1 ratio and injected in lethally irradiated B6 x B6.SJL F1 (CD45.1 and CD45.2 co-dominant expression) (Supplementary figure 6**b**). Expectedly, WT B cells (CD45.1) showed a growth advantage over *Pou2af1*-deficient B cells differentiated from Vav-Cre$^+$.*Pou2af1*$^{fl/fl}$ (CD45.2) bone marrow (Figure 5**c, d**). In contrast, and consistent with our observations in both Vav- and CD4-Cre$^+$.*Pou2af1*$^{fl/fl}$ mice (Supplementary figure 2**e, f**), T cells from WT and Vav-Cre$^+$.*Pou2af1*$^{fl/fl}$ precursors were present in equal proportions (Figure 5**c, d**), confirming an absence of competitive disadvantage for *Pou2af1*

targeted T cells. We also observed a severe reduction of GC B cells of Vav-Cre^{+}.*Pou2af1*$^{fl/fl}$ origin (Supplementary figure 6**c, d**), confirming the B cell-intrinsic defect of GC induction in the absence of *Pou2af1*. As opposed to the observations made in Vav-Cre^{+}.*Pou2af1*$^{fl/fl}$ mice, CD4^{+} T cells were able to fully mature into Tfh in the spleen, PP and mLN of the chimeras, regardless of their genotype (Figure 5**e, f**). This is likely due to the presence of a sufficient number of OCA-B expressing B cells in this competitive bone marrow chimera setting (Figure 5**c**), suggesting a T cell extrinsic role for OCA-B in Tfh differentiation. These results are consistent with a previous report also demonstrating a T cell-extrinsic role for OCA-B in Tfh development and function using mixed bone marrow chimeras (333).

Next, to determine if loss of OCA-B in B cells is sufficient to impede Tfh differentiation, we crossed *Pou2af1*$^{fl/fl}$ mice to CD19-Cre^{+} mice to disrupt *Pou2af1* specifically in B cells. The percentage of B cells were reduced in the lymphoid organs of CD19-Cre^{+}.*Pou2af1*$^{fl/fl}$ mice, in line with effective *Pou2af1* disruption (Figure 5**g**). Compared to CD19-Cre^{-} littermates, CD19-Cre^{+}.*Pou2af1*$^{fl/fl}$ mice showed a significant reduction in Tfh and a reduced expression of CXCR5 and PD-1 on CD4^{+} T cells from the PP and mLN (Figure 5**h-j**). These results show that specific loss of OCA-B expression in B cells is sufficient to impair Tfh differentiation. Altogether, our data conclusively demonstrate that *Pou2af1* plays a T cell-extrinsic role in Tfh differentiation.

3.4 Discussion

The levels of expression of *Pou2af1* are clearly more prominent in B cells than in T cells. The Immunological Genome Project database shows that *Pou2af1* mRNA is detectable in all B cell stages, from B cell precursors to plasma cells (311). Multiple transcriptomic and proteomic databases also show that, among immune cell types, *Pou2af1* expression is undetectable in non-B cells, in both mice and humans (305, 309, 311). Still, we and others report that *Pou2af1* expression can be induced in T cells (322, 328)(and this manuscript), and the biological impact of *Pou2af1* in T cells has been investigated for more than two decades (322, 334). By generating a new mouse strain in which *Pou2af1* can be conditionally deleted, we provide evidence that, as opposed to previous reports (321, 323, 335), *Pou2af1* is dispensable for $CD4^+$ T cell cytokine production, Th17 differentiation and does not affect the T cell pool. Using an unbiased approach to determine the impact of *Pou2af1* in regulating the transcriptional profile of $CD4^+$ and $CD8^+$ T cells, we find that *Pou2af1* does not act as an effective transcriptional coactivator in activated T cells. We also report that *Pou2af1* indirectly promotes the differentiation of $CD4^+$ T cells into mature Tfh, via *Pou2af1*-expressing B cells.

As mentioned, $CD4^+$ T cells isolated from B6.129S-*Pou2af1*$^{-/-}$ show defects in cytokine production, immunological memory as well as in Th17 and Tfh differentiation (76, 321, 323). Moreover, *Pou2af1* mRNA is induced in activated T cells (321, 322). With this growing literature on the role of OCA-B in T cells, we expected to find that T cell specific deletion of *Pou2af1* expression would alter T cell functions. With the two mouse models that specifically target deletion in either all hematopoietic cells or in all T cells, we set out to determine the T cell specific role of OCA-B in transcriptional regulation. Instead, we were taken aback and noted that T cell

specific deletion of *Pou2af1* expression does not influence T cell phenotypes and does not significantly affect the T cell transcriptome. We provide evidence to suggest that the difference between our results and that of others appear to stem from the differences in genetic background; whereas our floxed model was generated on the C57BL/6N-A^{tm1Brd} background, the B6.129S-*Pou2af1*$^{-/-}$ model is held on a mixed B6 and 129S genetic background. Notably, we find that cytokine production in T cells from 129S mice is reduced relative to that of B6 mice. These observations are in line with previous reports demonstrating that carryover genes influence the phenotype of knock-out and congenic mice (336, 337).

Notwithstanding the lack of impact of *Pou2af1* in various T cell phenotypes, hematopoietic deletion of *Pou2af1* expression resulted in a significant decrease in Tfh. Characterization of mature Tfh in CD4-Cre^{+}.*Pou2af1*$^{fl/fl}$ mice and in competitive bone marrow experiments confirmed a T cell-extrinsic role of *Pou2af1* in Tfh differentiation. Notably, the proportion and absolute numbers of early Tfh cells were unaffected in Vav-Cre^{+}.*Pou2af1*$^{fl/fl}$ mice whereas late Tfh were significantly reduced, suggesting that lack of OCA-B predominantly affects the transition from early Tfh to late Tfh. This is not surprising considering that early Tfh differentiation is highly dependent on DCs (78), which do not express *Pou2af1*. IL-6 and IL-21 produced by DCs during priming of CD4^{+} T cells induce changes in chemokine receptors expression, resulting in migration of early Tfh to the B cell follicle border (77). At this step, early Tfh express low levels of BCL6, CXCR5 and PD-1 and require additional signals to further differentiate into mature Tfh (338). At the T-B border, B cells provide crucial signals to developing Tfh, such as ICOS-L, antigens, and cytokines (77, 339). As B cells express high levels of OCA-B, *Pou2af1* disruption strongly affects their differentiation and functions (46, 312, 315)(and this manuscript). The reduction of total B cells and GC B cells

in *Pou2af1*$^{-/-}$ and Vav-Cre^{+}.*Pou2af1*$^{fl/fl}$ mice likely impairs crosstalk between B cells and early Tfh, thereby limiting early Tfh maturation. Using CD19-Cre mice to specifically disrupt *Pou2af1* in B cells, we show that crosstalk between B cells and early Tfh requires OCA-B expression in B cells to promote efficient Tfh maturation. This crosstalk might be impaired in OCA-B-deficient mice through reduced expression of ICOSL, highly expressed by GC B cells (94), or by impaired cytokine production by B cells. Indeed, OCA-B promotes IL-6 production in activated B cells during infection, and B cell-derived IL-6 can induce Tfh development (333). CXCR5^{+}PD-1^{+} CD4^{+} T cells from *Pou2af1*$^{-/-}$ mice also display lower BCL6 levels relative to B6 mice (76). As such, it was suggested that *Pou2af1* directly promotes Tfh differentiation by regulating BCL6 (76). However, considering that *Pou2af1* indirectly regulates Tfh differentiation, the reduction of BCL6 expression in Tfh from *Pou2af1*$^{-/-}$ mice is most likely caused by the maturation block at the early Tfh stage, which express lower BCL6 levels than mature Tfh (338).

It is interesting to note that *Pou2af1*$^{-/-}$ mice show a severe reduction in serum IgG, IgA and IgE, while IgM is not affected (74, 310, 314). This feature of the *Pou2af1*$^{-/-}$ mouse does not seem to be attributed to a B cell-intrinsic class switching defect, as *Pou2af1*$^{-/-}$ B cells are able to class switch *in vitro* as efficiently as WT B cells (310). Since Tfh directly promote B cell class switching from IgM to other isotypes (98, 340), the lack of mature Tfh indirectly caused by *Pou2af1* deletion in B cells may explain the reduction of IgG, IgA and IgE in the *Pou2af1*$^{-/-}$ mouse. Alternatively, a B cell-intrinsic role of OCA-B in plasma cell differentiation may also contribute to the reduction of isotype switched serum antibody levels (317).

Although *Pou2af1* expression is induced in T cells following activation, we did not identify any T cell intrinsic function. By comparing the mRNA transcriptome of activated T cells isolated from CD4-Cre^{-}.*Pou2af1*$^{fl/fl}$ and CD4-Cre^{+}.*Pou2af1*$^{fl/fl}$ mice, we further show that OCA-B does not seem to exhibit significant transcriptional activity in T cells. The functional impact, if any, of the low *Pou2af1* mRNA expression levels in activated T cells remains to be determined.

In conclusion, this study shows that *Pou2af1* is dispensable for most of the T cell-associated phenotypes previously identified in the *Pou2af1*$^{-/-}$ mouse, with the exception of the T cell-extrinsic effect on Tfh differentiation; *Pou2af1* expression in B cells promotes maturation of early Tfh into Tfh *in vivo*. Overall, this study clarifies the role of OCA-B in the immune system, by conclusively demonstrating that *Pou2af1* does not act as a coactivator of transcription in T cells, and therefore does not bear T cell-intrinsic activities. Furthermore, we demonstrate that OCA-B expression in B cells facilitates Tfh differentiation, explaining the T cell-extrinsic role of *Pou2af1*.

3.5 Methods

Mice

B6 mice (#000664, Jax labs, Bar Harbor, United States) were crossed to B6.SJL mice (#002014, Jax labs) to generate F1 mice (B6.1.2), with co-dominant expression of CD45.1 and CD45.2 on all hematopoietic cells, were used as bone marrow chimera recipients. *Pou2af1*$^{+/LacZ}$ mice (*Pou2af1*$^{tm1a(KOMP)Wtsi}$) were obtained from the KOMP Repository (#049152-UCD, Davis, United States) (324), for which embryonic stem cells were of C57BL/6N-A^{tm1Brd} background. Proper targeting of the locus was confirmed by 5' and 3' long range PCR performed on genomic DNA isolated from mouse tails using a combination of two primers located respectively inside and outside the targeting construct. Genotyping PCR using internal primers also confirmed the generation of *Pou2af1*$^{+/LacZ}$ mice. The genotyping primers are: P1, 5'-TACAGAGAGACTAGACACGGTCTGC-3'; P2, 5'-AGAAGGCCTCGTTACACTCCTATGC-3'; P3, 5'-GAGATGGCGCAACGCAATTAATG-3'; P4, 5'-GATGAGGACTCTGGGTTCAGAGAGG-3'; P5, 5'-GGGATCTCATGCTGGAGTTCTTCG-3'. These mice were crossed with ACTBFLPe Tg mice (#005703, Jax labs) to excise the LacZ and Neo cassettes and generate *Pou2af1*$^{+/fl}$ mice (*Pou2af1*^{tm1c}; see Supplementary figure 1) in which exon 2, 3 and 4 are flanked by loxP sites. The ACTBFLPe transgene was removed by subsequent breeding to B6 mice. *Pou2af1*$^{+/fl}$ mice were intercrossed to generate *Pou2af1*$^{fl/fl}$ mice. Vav-Cre^{+}.*Pou2af1*$^{fl/fl}$, CD4-Cre^{+}.*Pou2af1*$^{fl/fl}$ and CD19-Cre^{+}.*Pou2af1*$^{fl/fl}$ mice (#008610 and #022071, #006785, Jax labs) were generated by crossing Cre^{+}.*Pou2af1*$^{fl/+}$ mice to *Pou2af1*$^{fl/fl}$, to avoid germline deletion (341). ROSA-YFP mice (#007903, Jax labs) were crossed to CD4-Cre^{+} mice to validate genetic deletion in T cells. 129S and *Pou2af1*$^{-/-}$ mice (#002448, #007596, Jax labs) were used to test the influence of the genetic background on the phenotypes. Genotype of all transgenic

mice was verified by PCR. Transgenic positive and negative littermates were used in every experiment. Male and female mice were used in this study and no phenotypic difference was observed based on sex. All of the mouse strains were maintained at the Maisonneuve-Rosemont Hospital animal facility (Montreal, Canada). The Maisonneuve-Rosemont Hospital ethics committee, overseen by the Canadian Council for Animal Protection, approved the experimental procedures.

Generation of bone marrow chimeras

Prior to irradiation, recipient mice were injected intraperitoneally with 1 mL of PBS to avoid dehydration. Bone marrow cell suspensions were prepared from the tibia and femur of 10-week-old mice in sterile RPMI. The red blood cells were lysed using NH_4Cl and the bone marrow single cell suspension were prepared in sterile PBS. A 1:1 bone marrow ratio was confirmed by flow cytometry (with anti-CD45.1 and anti-CD45.2 antibodies) prior to injection. Eight-week-old recipient mice were irradiated at 11Gy, using linac X-ray source and, subsequently, injected intravenously with $2x10^6$ bone marrow cells.

Sheep red blood cell immunization

Mice were injected intra-peritoneally with $5x10^8$ sheep red blood cells (Innovative Research, Novi, United States) diluted in PBS. Ten days after injection, the spleens were collected for flow cytometry analysis.

Flow cytometry and cell sorting

Spleen, bone marrow, PP and LNs were pressed through a 70-µm cell strainer (Thermo Fisher Scientific, Waltham, United States). Spleen cell suspensions were treated with NH_4Cl to lyse red blood cells. Single-cell suspensions were stained for 30 minutes at 4°C with different combinations of antibodies listed as target (clone): From BioLegend (San Diego, United States), B220 (RA3-6B2), CD4 (GK1.5), CD8a (53-6.7), CD19 (6D5), CD25 (PC61.5.3), CD44 (IM7), CD45.1 (A20), CD45.2 (104), CD45RB (C363-16A), CD62L (MEL-14), CD69 (H1.2F3), CD86 (GL-1), CXCR4 (L276F12), CXCR5 (L138D7), GL-7 (GL7), IFN-γ (XMG1.2), IL-2 (JES6-5H4), PD-1 (RMP1-30), TCRβ (H57-597), TNF-α (MP6-XT22); From BD Biosciences (New Jersey, United States), CD95 (Jo2); From Thermo Fisher, CD8b (H35-17.2), FoxP3 (FJK-16s), IL-17 (eBio1787), RORγt (B2D); From Santa Cruz Biotechnology (Dallas, United States), OCA-B (6F10). Biotin-labelled antibodies were revealed with fluorescently-coupled streptavidins from BioLegend. Viable cells were stained using LIVE/DEAD™ Fixable Yellow Dead Cell Stain Kit (Thermo Fisher). Before staining with 6F10 antibodies, cells were fixed and permeabilized using BD Cytofix/Cytoperm™ kit, as published (321). Cells were stained in 100µl of buffer plus 7.5µl of PE-conjugated 6F10 antibodies (321). For transcription factor staining, cells were treated with FOXP3 Transcription Factor Staining Buffer Set (Thermo Fischer). Data were collected on an LSRFortessaX20 (BD Biosciences), and analyzed with FlowJo software (BD Biosciences). For cell sorting, spleen cell suspensions were stained with antibodies against TCRβ and B220, in sterile conditions. T cells were sorted on a FACS Aria II (BD Biosciences) as $TCR\beta^{+}B220^{-}$ single cells (purity > 99%).

In vitro T cell stimulation

As described in Shakya *et al.*(321), *in vitro* T cell stimulation was performed in flat bottom 96 well plates (Sarstedt, Nümbrecht, Germany) coated with anti-CD3 (either 1 µg mL^{-1} or graded

concentrations as indicated, 145-2C11) and anti-CD28 (10 μg mL^{-1}, 37.51) antibodies in PBS overnight at 4°C. Plates were washed in serum-containing media prior to adding the cells. For primary stimulation, spleen cells ($5x10^5$ mL^{-1}) were stimulated for 2 days in complete RPMI-1640 medium. In some experiments, cells were analyzed after primary stimulation. Otherwise, cells were rested for 8 days, in complete RPMI-1640 medium with IL-2 (30 U mL^{-1}). For secondary stimulation, rested cells were activated for 6 hours with plate bound anti-CD3 and anti-CD28 antibodies, at 1 and 10 μg mL^{-1} respectively, in the presence of Brefeldin A (10 μg mL^{-1}). Cells were then harvested and stained with antibodies prior to analysis by flow cytometry.

RT-qPCR

5-10 x 10^6 sorted T cells were stored in Trizol while the remaining T cells (2.5-5 x 10^5) were activated *in vitro* for 2 days using anti-CD3 and anti-CD28 antibodies. RNA extraction for all samples was conducted as indicated by the manufacturer (Trizol, Thermo Fisher Scientific). Mouse *Pou2af1* mRNA levels were measured using primers targeting exons 4 and 5 of *Pou2af1* (Pou2af1-F: 5'-CCTGCCTTGACATGGAGGTT-3' and Pou2af1-R: 5'-AGTGCTTCTTGGCGTGACAT-3'), *Gapdh* (Gapdh-F:5'-TCAACGGCACAGTCAAGG-3' and Gapdh-R: 5'-ACTCCACGACATACTCAGC-3') and *Actb* (Actb-F:5'-GAAATCGTGCGTGACATCAAAG-3' and Actb-R: 5'-TGTAGTTTCATGGATGCCACAG-3') mRNA levels were used as loading controls and ddCT variations calculated in all cases.

Th17 differentiation

To differentiate T cells into either Th0 or Th17 profiles, LN cells were activated with plate bound anti-CD3 (2 μg mL^{-1}) and anti-CD28 (2 μg mL^{-1}) antibodies. While Th0 differentiation proceeded

in the absence of cytokines, Th17 was induced in the presence of 2 ng mL^{-1} rhTGF-β1 and 25 ng mL^{-1} rmIL-6 (both cytokines from Miltenyi Biotec, Bergisch Gladbach, Germany), as described in Yosef *et al*. (323). Cells were cultured for 3 days prior to analysis. T cell supernatants were collected at the end of the 3-day culture. Quantification of IL-17A in the media was performed by ELISA as indicated by the manufacturer (Mouse Il-17 Quantikine ELISA Kit, R&D Systems, Minneapolis, United States). For quantifying IL-2 and IL-17A production by flow cytometry, cells were incubated with phorbol 12-myristate 13-acetate (50 ng mL^{-1}), ionomycin (500 ng mL^{-1}) and Brefeldin A (10 μg mL^{-1}) for 4h prior to staining.

RNA sequencing

Naïve $CD4^+$ and $CD8^+$ T cells were sorted from the spleen as $CD19^-TCR\beta^+CD4^+CD62L^+$ and $CD19^-TCR\beta^+CD8^+CD62L^+$ single cells, respectively (purity > 96%). T cells were activated *in vitro* for two days using anti-CD3 and anti-CD28 antibodies. RNA was isolated using Trizol and sent to the IRIC genomic platform for processing. Libraries were prepared using the KAPA mRNA stranded Hyperprep Kit. Libraries were sequenced using the Illumina NextSeq 500 FASTQ files were trimmed for sequencing adapters and low quality 3' bases using Trimmomatic version 0.35 (277) and aligned to the reference mouse genome version GRCm38 (gene annotation from Gencode version M25, based on Ensembl 100) using STAR version 2.7.1a (278). Read counts were extracted directly from STAR at the gene level. DESeq2 (R; version 1.26) was then used to normalize gene read counts. Batch correction was added to the statistical model for differential expression to adjust for samples sorted on 2 separate days. Log normalized counts were batch corrected using the removeBatchEffect function from the limma R package (v 3.42.2) (282) and

used as input for PCA and heatmap visualizations. The raw RNAseq data files have been uploaded into the GEO database (accession number: GSE171544).

Statistical analyses

Data were tested for significance using a nonparametric Mann-Whitney *U*-test or a one-way ANOVA, where appropriate. Numbers of animal used per group are indicated in the figure legends. The minimal significance threshold was set at 0.05 for all tests.

Acknowledgments: We thank Dr Frédéric Picard, Dr Heather Melichar and Dr Nathalie Labrecque for a critical review of the manuscript and all laboratory members for helpful discussions. We are grateful for Martine Dupuis from the flow cytometry facility as well as all animal house staff for technical support. We also thank Dr Patrick Gendron from the IRIC platform, and Dr Adam-Nicolas Pelletier from RPM Bioinfo Solutions for expert bioinformatics analyses.

Funding: This work was supported by a grant from the Natural Sciences and Engineering Research Council of Canada (2019-05047). F.L.-V. hold scholarships from the Fondation de l'Hôpital Maisonneuve-Rosemont, the Cole Foundation, and the Fonds de Recherche Quebec Santé. MF holds a Canada Research Chair in Bone and Energy Metabolism. S.L. is a Research Scholars Emeritus awardee from the Fonds de Recherche Quebec Santé.

Conflict of interest: The authors declare that they have no conflicts of interest.

Data availability: The raw RNAseq data files have been uploaded into the GEO database (accession number: GSE171544).

Author contributions: F.L.-V. designed and conducted most of the experiments, prepared the figures, and wrote the manuscript. J.L. generated and validated the *Pou2af1*$^{fl/fl}$ mouse and designed *Pou2af1* RT-qPCR primers. G.C.-R. performed the flow cytometry analysis of CD4-Cre^{+}.ROSA-YFP^{+} mice. M.F. contributed to the generation of the *Pou2af1*$^{fl/fl}$ mouse and to revisions of the manuscript. S.L. supervised the study, wrote and revised the manuscript.

3.6 References

1. Luo Y, Fujii H, Gerster T, Roeder RG. A novel B cell-derived coactivator potentiates the activation of immunoglobulin promoters by octamer-binding transcription factors. *Cell* 1992; **71**: 231-241.
2. Strubin M, Newell JW, Matthias P. OBF-1, a novel B cell-specific coactivator that stimulates immunoglobulin promoter activity through association with octamer-binding proteins. *Cell* 1995; **80**: 497-506.
3. Uhlen M, Fagerberg L, Hallstrom BM*, et al.* Proteomics. Tissue-based map of the human proteome. *Science* 2015; **347**: 1260419.
4. Schubart DB, Rolink A, Kosco-Vilbois MH, Botteri F, Matthias P. B-cell-specific coactivator OBF-1/OCA-B/Bob1 required for immune response and germinal centre formation. *Nature* 1996; **383**: 538-542.
5. Kim U, Qin XF, Gong S*, et al.* The B-cell-specific transcription coactivator OCA-B/OBF-1/Bob-1 is essential for normal production of immunoglobulin isotypes. *Nature* 1996; **383**: 542-547.
6. Heng TS, Painter MW, Immunological Genome Project C. The Immunological Genome Project: networks of gene expression in immune cells. *Nat Immunol* 2008; **9**: 1091-1094.
7. Hess J, Nielsen PJ, Fischer KD, Bujard H, Wirth T. The B lymphocyte-specific coactivator BOB.1/OBF.1 is required at multiple stages of B-cell development. *Mol Cell Biol* 2001; **21**: 1531-1539.
8. Teitell MA. OCA-B regulation of B-cell development and function. *Trends Immunol* 2003; **24**: 546-553.
9. Samardzic T, Marinkovic D, Nielsen PJ, Nitschke L, Wirth T. BOB.1/OBF.1 deficiency affects marginal-zone B-cell compartment. *Mol Cell Biol* 2002; **22**: 8320-8331.
10. Nielsen PJ, Georgiev O, Lorenz B, Schaffner W. B lymphocytes are impaired in mice lacking the transcriptional co-activator Bob1/OCA-B/OBF1. *Eur J Immunol* 1996; **26**: 3214-3218.
11. Qin XF, Reichlin A, Luo Y, Roeder RG, Nussenzweig MC. OCA-B integrates B cell antigen receptor-, CD40L- and IL 4-mediated signals for the germinal center pathway of B cell development. *EMBO J* 1998; **17**: 5066-5075.
12. Siegel R, Kim U, Patke A*, et al.* Nontranscriptional regulation of SYK by the coactivator OCA-B is required at multiple stages of B cell development. *Cell* 2006; **125**: 761-774.
13. Corcoran LM, Hasbold J, Dietrich W*, et al.* Differential requirement for OBF-1 during antibody-secreting cell differentiation. *J Exp Med* 2005; **201**: 1385-1396.
14. Bartholdy B, Du Roure C, Bordon A, Emslie D, Corcoran LM, Matthias P. The Ets factor Spi-B is a direct critical target of the coactivator OBF-1. *Proc Natl Acad Sci U S A* 2006; **103**: 11665-11670.
15. Chu CS, Hellmuth JC, Singh R*, et al.* Unique Immune Cell Coactivators Specify Locus Control Region Function and Cell Stage. *Mol Cell* 2020; **80**: 845-861 e810.
16. Su GH, Chen HM, Muthusamy N*, et al.* Defective B cell receptor-mediated responses in mice lacking the Ets protein, Spi-B. *EMBO J* 1997; **16**: 7118-7129.
17. Basso K, Dalla-Favera R. BCL6: master regulator of the germinal center reaction and key oncogene in B cell lymphomagenesis. *Adv Immunol* 2010; **105**: 193-210.
18. Shakya A, Goren A, Shalek A*, et al.* Oct1 and OCA-B are selectively required for CD4 memory T cell function. *J Exp Med* 2015; **212**: 2115-2131.

19. Sauter P, Matthias P. The B cell-specific coactivator OBF-1 (OCA-B, Bob-1) is inducible in T cells and its expression is dispensable for IL-2 gene induction. *Immunobiology* 1997; **198**: 207-216.
20. Stauss D, Brunner C, Berberich-Siebelt F, Hopken UE, Lipp M, Muller G. The transcriptional coactivator Bob1 promotes the development of follicular T helper cells via Bcl6. *EMBO J* 2016; **35**: 881-898.
21. Yosef N, Shalek AK, Gaublomme JT*, et al.* Dynamic regulatory network controlling TH17 cell differentiation. *Nature* 2013; **496**: 461-468.
22. Skarnes WC, Rosen B, West AP*, et al.* A conditional knockout resource for the genome-wide study of mouse gene function. *Nature* 2011; **474**: 337-342.
23. Rodriguez CI, Buchholz F, Galloway J*, et al.* High-efficiency deleter mice show that FLPe is an alternative to Cre-loxP. *Nat Genet* 2000; **25**: 139-140.
24. Ogilvy S, Metcalf D, Gibson L, Bath ML, Harris AW, Adams JM. Promoter elements of vav drive transgene expression in vivo throughout the hematopoietic compartment. *Blood* 1999; **94**: 1855-1863.
25. Georgiades P, Ogilvy S, Duval H*, et al.* VavCre transgenic mice: a tool for mutagenesis in hematopoietic and endothelial lineages. *Genesis* 2002; **34**: 251-256.
26. Mueller K, Quandt J, Marienfeld RB*, et al.* Octamer-dependent transcription in T cells is mediated by NFAT and NF-*κ*B. *Nucleic Acids Res* 2013; **41**: 2138-2154.
27. Wolfer A, Bakker T, Wilson A*, et al.* Inactivation of Notch 1 in immature thymocytes does not perturb CD4 or CD8T cell development. *Nat Immunol* 2001; **2**: 235-241.
28. Moulton VR, Bushar ND, Leeser DB, Patke DS, Farber DL. Divergent generation of heterogeneous memory CD4 T cells. *J Immunol* 2006; **177**: 869-876.
29. McAllister EJ, Apgar JR, Leung CR, Rickert RC, Jellusova J. New Methods To Analyze B Cell Immune Responses to Thymus-Dependent Antigen Sheep Red Blood Cells. *J Immunol* 2017; **199**: 2998-3003.
30. Hwang SS, Kim LK, Lee GR, Flavell RA. Role of OCT-1 and partner proteins in T cell differentiation. *Biochim Biophys Acta* 2016; **1859**: 825-831.
31. Karnowski A, Chevrier S, Belz GT*, et al.* B and T cells collaborate in antiviral responses via IL-6, IL-21, and transcriptional activator and coactivator, Oct2 and OBF-1. *J Exp Med* 2012; **209**: 2049-2064.
32. Schaum N, Karkanias J, Neff NF*, et al.* Single-cell transcriptomics of 20 mouse organs creates a Tabula Muris. *Nature* 2018; **562**: 367-372.
33. Zwilling S, Dieckmann A, Pfisterer P, Angel P, Wirth T. Inducible expression and phosphorylation of coactivator BOB.1/OBF.1 in T cells. *Science* 1997; **277**: 221-225.
34. Brunner C, Sindrilaru A, Girkontaite I, Fischer KD, Sunderkotter C, Wirth T. BOB.1/OBF.1 controls the balance of TH1 and TH2 immune responses. *EMBO J* 2007; **26**: 3191-3202.
35. Hogenbirk MA, Heideman MR, Velds A*, et al.* Differential programming of B cells in AID deficient mice. *PLoS One* 2013; **8**: e69815.
36. Chisolm DA, Cheng W, Colburn SA*, et al.* Defining Genetic Variation in Widely Used Congenic and Backcrossed Mouse Models Reveals Varied Regulation of Genes Important for Immune Responses. *Immunity* 2019; **51**: 155-168 e155.
37. Goenka R, Barnett LG, Silver JS*, et al.* Cutting edge: dendritic cell-restricted antigen presentation initiates the follicular helper T cell program but cannot complete ultimate effector differentiation. *J Immunol* 2011; **187**: 1091-1095.

38. Crotty S. T follicular helper cell differentiation, function, and roles in disease. *Immunity* 2014; **41**: 529-542.
39. Trub M, Barr TA, Morrison VL*, et al.* Heterogeneity of Phenotype and Function Reflects the Multistage Development of T Follicular Helper Cells. *Front Immunol* 2017; **8**: 489.
40. Weinstein JS, Bertino SA, Hernandez SG*, et al.* B cells in T follicular helper cell development and function: separable roles in delivery of ICOS ligand and antigen. *J Immunol* 2014; **192**: 3166-3179.
41. Liu D, Xu H, Shih C*, et al.* T-B-cell entanglement and ICOSL-driven feed-forward regulation of germinal centre reaction. *Nature* 2015; **517**: 214-218.
42. Reinhardt RL, Liang HE, Locksley RM. Cytokine-secreting follicular T cells shape the antibody repertoire. *Nat Immunol* 2009; **10**: 385-393.
43. Weinstein JS, Hernandez SG, Craft J. T cells that promote B-Cell maturation in systemic autoimmunity. *Immunol Rev* 2012; **247**: 160-171.
44. Siegemund S, Shepherd J, Xiao C, Sauer K. hCD2-iCre and Vav-iCre mediated gene recombination patterns in murine hematopoietic cells. *PLoS One* 2015; **10**: e0124661.
45. Bolger AM, Lohse M, Usadel B. Trimmomatic: a flexible trimmer for Illumina sequence data. *Bioinformatics* 2014; **30**: 2114-2120.
46. Dobin A, Davis CA, Schlesinger F*, et al.* STAR: ultrafast universal RNA-seq aligner. *Bioinformatics* 2013; **29**: 15-21.
47. Ritchie ME, Phipson B, Wu D*, et al.* limma powers differential expression analyses for RNA-sequencing and microarray studies. *Nucleic Acids Res* 2015; **43**: e47.

3.7 Figures

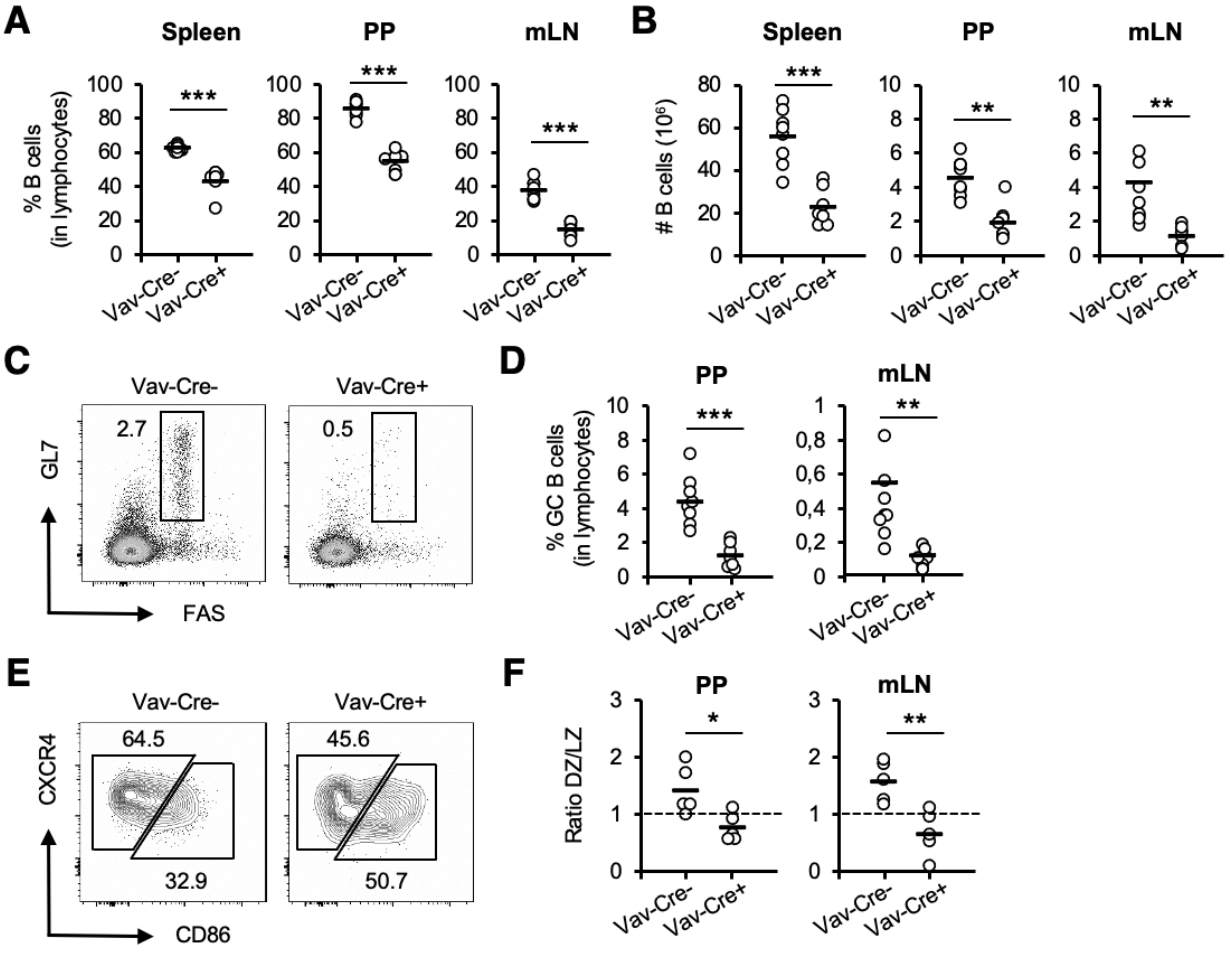

Figure 1. **B cell phenotypes following hematopoietic cell-specific deletion of *Pou2af1*.**
(a) Percentage and **(b)** number of B cells in the spleen, PP and mLN of Vav-Cre^{-}.*Pou2af1*$^{fl/fl}$ and Vav-Cre^{+}.*Pou2af1*$^{fl/fl}$ mice (n = 8, collected in six independent experiments). **(c)** Representative flow cytometry profiles of GL-7 and FAS expression on total B cells gated as B220^{+} cells from the mLN of Vav-Cre^{-}.*Pou2af1*$^{fl/fl}$ and Vav-Cre^{+}.*Pou2af1*$^{fl/fl}$ littermate controls. The gate selects for GL-7^{+}FAS^{+} GC B cells. **(d)** Percentage of GC B cells from the PP and mLN of Vav-Cre^{-}.*Pou2af1*$^{fl/fl}$ and Vav-Cre^{+}.*Pou2af1*$^{fl/fl}$ littermate controls (n = 8, collected in six independent experiments). **(e)** Representative flow cytometry profiles of CXCR4 and CD86 expression by GC B cells from the mLN of Vav-Cre^{-}.*Pou2af1*$^{fl/fl}$ and Vav-Cre^{+}.*Pou2af1*$^{fl/fl}$ littermate controls. **(f)** Ratio of dark zone (CXCR4^{Hi}CD86^{-}) over light zone (CXCR4^{Low}CD86^{+}) GC B cells from the PP and mLN of Vav-Cre^{-}.*Pou2af1*$^{fl/fl}$ and Vav-Cre^{+} (n = 8, collected in six independent experiments).
Data information: Mann Whitney *U*-test, *P*-values * < 0.05; ** < 0.01; *** < 0.001.

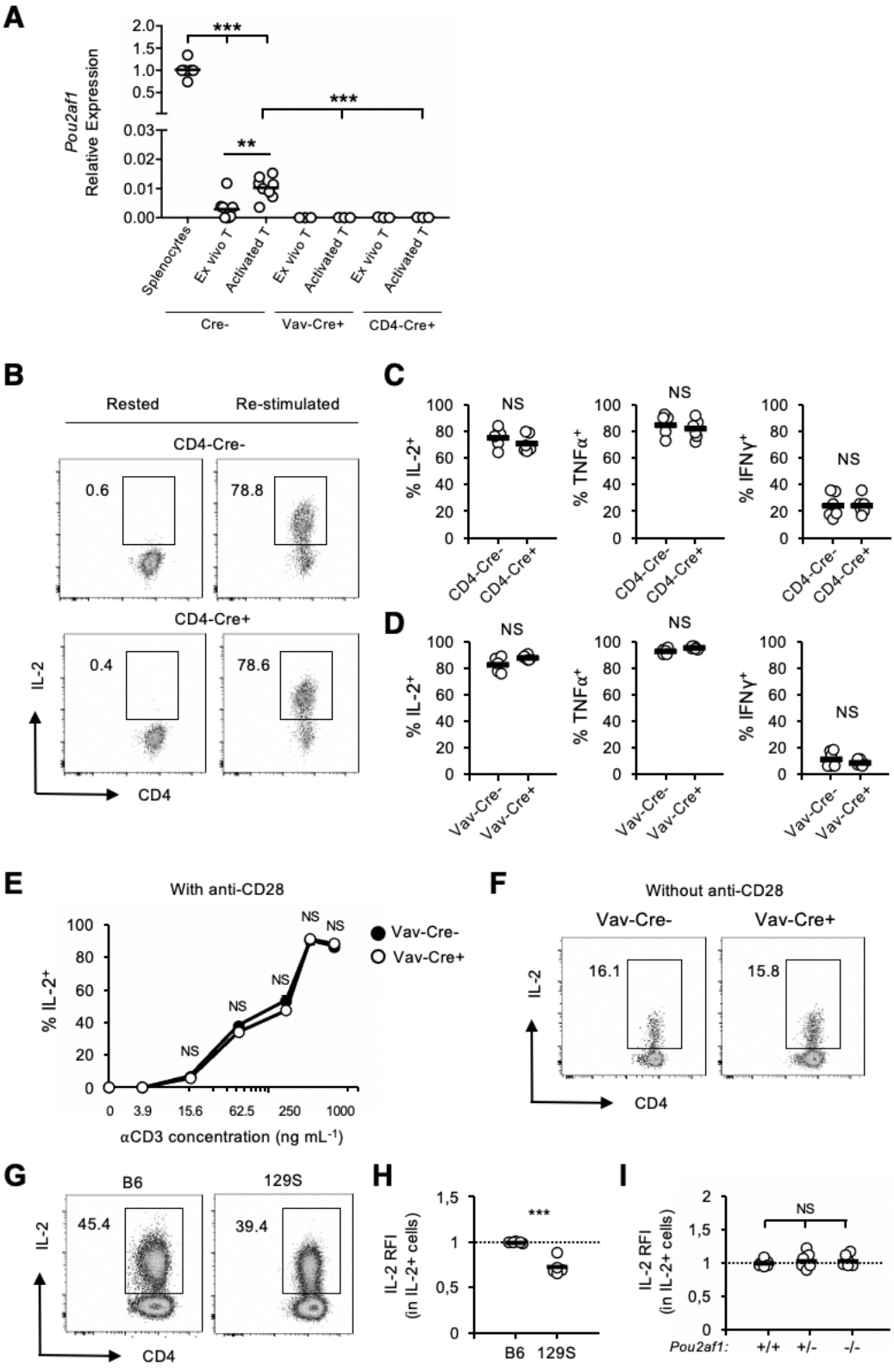
A
Pou2af1 Relative Expression
***
**
***
Splenocytes
Ex vivo T
Activated T
Cre-
Vav-Cre+
CD4-Cre+
B
Rested
Re-stimulated
CD4-Cre-
0.6
78.8
CD4-Cre+
0.4
78.6
IL-2
CD4
C
% IL-2+
% TNFα+
% IFNγ+
NS
CD4-Cre-
CD4-Cre+
D
Vav-Cre-
Vav-Cre+
E
With anti-CD28
Vav-Cre-
Vav-Cre+
αCD3 concentration (ng mL-1)
F
Without anti-CD28
16.1
15.8
G
B6
129S
45.4
39.4
H
IL-2 RFI (in IL-2+ cells)
I
Pou2af1:
+/+
+/-
-/-

Figure 2. ***Pou2af1* is expressed in activated T cells but does not affect T cell cytokine production.**
(a) *Pou2af1* relative mRNA expression in spleen cells as well as in unactivated and activated T cells from *Pou2af1*$^{fl/fl}$ (Cre-), Vav-Cre^{+}.*Pou2af1*$^{fl/fl}$ (Vav-Cre+) and CD4-Cre^{+}.*Pou2af1*$^{fl/fl}$ (CD4-Cre+) mice (n = 3-8, collected in three to four independent experiments), measured by RT-qPCR. *Actb* was used as control. **(b)** Representative flow cytometry profiles of IL-2 expression by rested and re-stimulated CD4^{+} T cells from the spleens of CD4-Cre^{-}.*Pou2af1*$^{fl/fl}$ and CD4-Cre^{+}.*Pou2af1*$^{fl/fl}$ mice. **(c, d)** Percentage of IL-2-, TNFα- and IFNγ-producing CD4^{+} T cells after re-stimulation of T cells from **(c)** CD4-Cre^{-}.*Pou2af1*$^{fl/fl}$ and CD4-Cre^{+}.*Pou2af1*$^{fl/fl}$ mice and **(d)** Vav-Cre^{-}.*Pou2af1*$^{fl/fl}$ and Vav-Cre^{+}.*Pou2af1*$^{fl/fl}$ mice (n = 6, collected in three independent experiments). **(e)** Percentage of IL-2-producing CD4^{+} T cells after re-stimulation of T cells from Vav-Cre^{-}.*Pou2af1*$^{fl/fl}$ and Vav-Cre^{+}.*Pou2af1*$^{fl/fl}$ at the indicated anti-CD3 concentrations in the presence of anti-CD28 (n = 3, collected in two independent experiments). **(f)** Representative flow cytometry profiles of IL-2 expression by re-stimulated CD4^{+} T cells from Vav-Cre^{-}.*Pou2af1*$^{fl/fl}$ and Vav-Cre^{+}.*Pou2af1*$^{fl/fl}$ mice, in absence of anti-CD28 antibodies. Representative of two experiments. **(g)** Representative flow cytometry profiles of IL-2 expression by re-stimulated CD4^{+} T cells from the spleens of B6 and 129S mice. **(h)** IL-2 relative fluorescence intensity (RFI) of IL-2-producing CD4^{+} T cells after re-stimulation of T cells from B6 and 129S mice (n = 6, collected in three independent experiments). **(i)** IL-2 RFI of IL-2-producing CD4^{+} T cells after re-stimulation of T cells from B6.129S-*Pou2af1*$^{-/-}$ littermates carrying *Pou2af1* +/+, +/- and -/- genotypes (n = 6, collected in three independent experiments). NS, non-significant, *P*-value > 0.05, ***, *P*-value < 0.001.

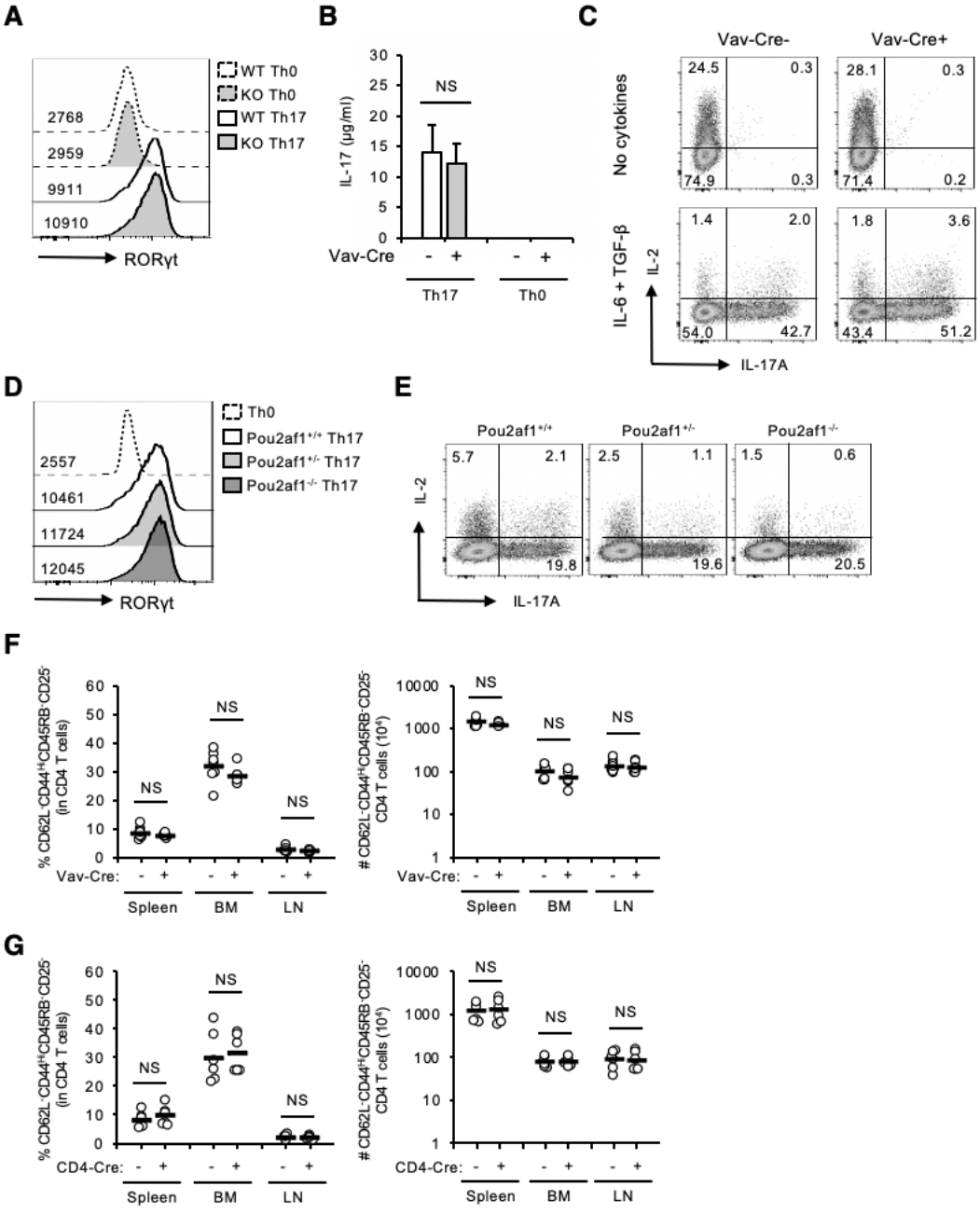
A
WT Th0
KO Th0
WT Th17
KO Th17
2768
2959
9911
10910
RORγt
B
IL-17 (μg/ml)
NS
Vav-Cre
Th17
Th0
C
Vav-Cre-
Vav-Cre+
No cytokines
IL-6 + TGF-β
IL-2
IL-17A
24.5
0.3
74.9
0.3
28.1
0.3
71.4
0.2
1.4
2.0
54.0
42.7
1.8
3.6
43.4
51.2
D
Th0
Pou2af1+/+ Th17
Pou2af1+/- Th17
Pou2af1-/- Th17
2557
10461
11724
12045
RORγt
E
Pou2af1+/+
Pou2af1+/-
Pou2af1-/-
IL-2
IL-17A
5.7
2.1
19.8
2.5
1.1
19.6
1.5
0.6
20.5
F
% CD62L-CD44hiCD45RB-CD25- (in CD4 T cells)
# CD62L-CD44hiCD45RB-CD25- CD4 T cells (10⁴)
NS
Vav-Cre:
Spleen
BM
LN
G
% CD62L-CD44hiCD45RB-CD25- (in CD4 T cells)
# CD62L-CD44hiCD45RB-CD25- CD4 T cells (10⁴)
NS
CD4-Cre:
Spleen
BM
LN

Figure 3. ***Pou2af1* does not affect Th17 differentiation and CD4$^+$ T cell memory phenotype.** **(a)** Representative flow cytometry profiles of RORγt expression by CD4$^+$ T cells from the spleen of Vav-Cre$^-$.*Pou2af1*$^{fl/fl}$ and Vav-Cre$^+$.*Pou2af1*$^{fl/fl}$ mice under Th0 and Th17 differentiation conditions. MFI are indicated for each population. **(b)** IL-17A concentration in the supernatants of T cell cultures from Vav-Cre$^-$.*Pou2af1*$^{fl/fl}$ and Vav-Cre$^+$.*Pou2af1*$^{fl/fl}$ mice under Th0 and Th17 differentiation conditions, measured by ELISA (n = 3, collected in three independent experiments). **(c)** Representative flow cytometry profiles of IL-2 and IL-17A expression by CD4$^+$ T cells from Vav-Cre$^-$.*Pou2af1*$^{fl/fl}$ and Vav-Cre$^+$.*Pou2af1*$^{fl/fl}$ mice under Th0 and Th17 differentiation conditions. **(d)** Representative flow cytometry profiles of RORγt expression by CD4$^+$ T cells from *Pou2af1*$^{-/-}$ mice and control littermates under Th0 and Th17 differentiation conditions. MFI of RORγt are indicated for each population. **(e)** Representative flow cytometry profiles of IL-2 and IL-17A expression by CD4$^+$ T cells from the same mice as in **(d)** under Th17 differentiation conditions. **(f, g)** Percentage (left panels) and absolute numbers (right panels) of CD62L$^-$ CD44^{Hi}CD45RB$^-$CD25$^-$ CD4$^+$ T cells from the spleen, bone marrow (BM) and of pool of axial, brachial and inguinal LN of (**f**) Vav-Cre$^-$.*Pou2af1*$^{fl/fl}$ and Vav-Cre$^+$.*Pou2af1*$^{fl/fl}$ mice and **(g)** CD4-Cre$^-$.*Pou2af1*$^{fl/fl}$ and CD4-Cre$^+$.*Pou2af1*$^{fl/fl}$ mice (n = 6, collected in three independent experiments). Data information: Mann Whitney *U*-test, NS, non-significant, *P*-value > 0.05.

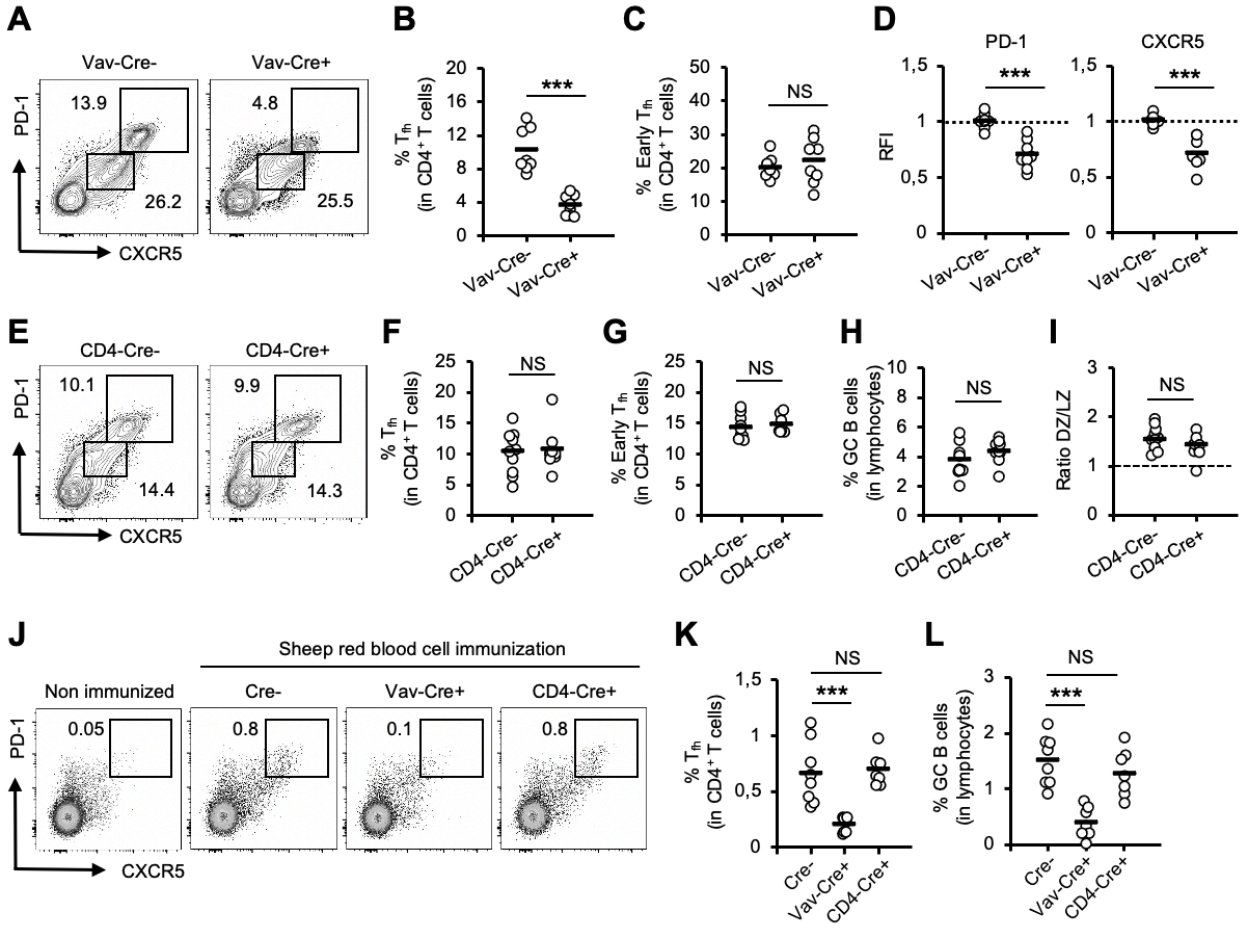

Figure 4. **OCA-B expression in non-T cells is necessary for Tfh maturation. (a)** Representative flow cytometry profiles of CXCR5 and PD-1 expression on $CD4^+$ T cells from the PP of Vav-Cre^-.*Pou2af1*$^{fl/fl}$ and Vav-Cre^+.*Pou2af1*$^{fl/fl}$ mice. **(b, c)** Percentage of Tfh ($CXCR5^{Hi}PD\text{-}1^{Hi}$) and early Tfh ($CXCR5^{Low}PD\text{-}1^{Low}$) in the PP of Vav-$Cre^-$.*Pou2af1*$^{fl/fl}$ and Vav-Cre^+.*Pou2af1*$^{fl/fl}$ mice (n = 8, collected in three independent experiments). **(d)** PD-1 and CXCR5 relative fluorescence intensity (RFI) on $CXCR5^+PD\text{-}1^+$ $CD4^+$ T cells from the PP of Vav-Cre^-.*Pou2af1*$^{fl/fl}$ and Vav-Cre^+.*Pou2af1*$^{fl/fl}$ mice (n = 8, collected in three independent experiments). **(e)** Representative flow cytometry profiles of CXCR5 and PD-1 expression on $CD4^+$ T cells from the PP of CD4-Cre^-.*Pou2af1*$^{fl/fl}$ and CD4-Cre^+.*Pou2af1*$^{fl/fl}$ mice. **(f, g)** Percentage of Tfh and early Tfh in the PP of CD4-Cre^-.*Pou2af1*$^{fl/fl}$ and CD4-Cre^+.*Pou2af1*$^{fl/fl}$ mice (n = 10, collected in three independent experiments). **(h)** Percentage of GC B cells in the PP of CD4-Cre^-.*Pou2af1*$^{fl/fl}$ and CD4-Cre^+.*Pou2af1*$^{fl/fl}$ mice (n = 10, collected in three independent experiments). **(i)** Ratio of dark zone ($CXCR4^{Hi}CD86^-$) over light zone ($CXCR4^{Low}CD86^+$) GC B cells from the PP of CD4-Cre^-.*Pou2af1*$^{fl/fl}$ and CD4-Cre^+.*Pou2af1*$^{fl/fl}$ mice (n = 10, collected in three independent experiments). **(j)** Representative flow cytometry profiles of Tfh ($CXCR5^{Hi}PD\text{-}1^{Hi}$) from the spleen of immunized Cre^-.*Pou2af1*$^{fl/fl}$, Vav-Cre^+.*Pou2af1*$^{fl/fl}$ and CD4-Cre^+.*Pou2af1*$^{fl/fl}$ mice. **(k)** Percentage of Tfh cells in the spleen of the same groups of mice listed in **(j)** (n > 5, collected in four independent experiments)**. (l)** Percentage of GL-7^+FAS^+ GC B cells in the spleen, assessed by flow cytometry, of the same groups of mice listed in **(j)** (n > 5, collected in four independent experiments). Data information: Mann Whitney *U*-test for figures (**b-d, f-i)**. One-way ANOVA for figures **(k-l)**, NS, non-significant *P*-value > 0.05; *P*-values ** < 0.01; *** < 0.001.

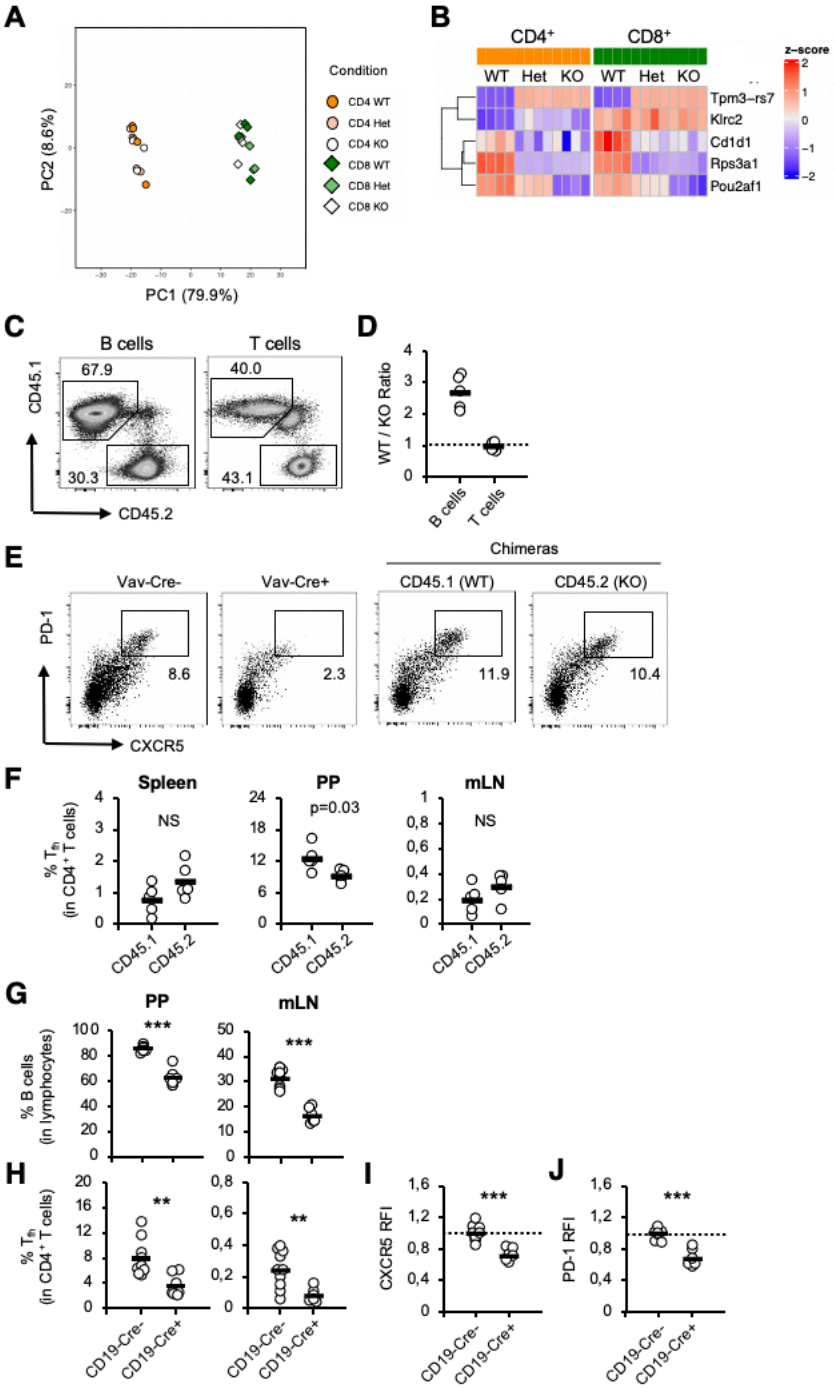
A
PC2 (8.6%)
PC1 (79.9%)
Condition
CD4 WT
CD4 Het
CD4 KO
CD8 WT
CD8 Het
CD8 KO
B
CD4+
CD8+
WT Het KO WT Het KO
z-score
Tpm3–rs7
Klrc2
Cd1d1
Rps3a1
Pou2af1
C
B cells
T cells
CD45.1
67.9
30.3
40.0
43.1
CD45.2
D
WT / KO Ratio
B cells
T cells
E
Chimeras
Vav-Cre-
Vav-Cre+
CD45.1 (WT)
CD45.2 (KO)
PD-1
8.6
2.3
11.9
10.4
CXCR5
F
Spleen
PP
mLN
% Tfh (in CD4+ T cells)
NS
p=0.03
NS
CD45.1
CD45.2
G
PP
mLN
% B cells (in lymphocytes)
***
***
H
% Tfh (in CD4+ T cells)
**
**
CD19-Cre-
CD19-Cre+
I
CXCR5 RFI
***
J
PD-1 RFI
***

Figure 5. **OCA-B is not an active transcriptional coactivator in CD4$^+$ and CD8$^+$ T cells and is required in B cells to facilitate Tfh differentiation.**
(a) Principal Component Analysis of top 500 most variable genes from CD4$^+$ and CD8$^+$ T cell RNA-Seq samples from the spleen of CD4-Cre$^-$.*Pou2af1*$^{fl/fl}$ (WT), CD4-Cre$^+$.*Pou2af1*$^{fl/+}$ (Het) and CD4-Cre$^+$.*Pou2af1*$^{fl/fl}$ (KO) mice. **(b)** Row-normalized (z-score) expression heatmap of selected DEGs, where each row represents a gene and columns represent individual samples. Red represents a higher relative expression for a given gene, while blue denotes a lower relative expression. Column annotation tracks represent sample cell type and genotype. **(c)** Representative flow cytometry profiles of CD45.1 and CD45.2 expression on B (left panel) and T (right panel) cells from the spleen of the chimeras. **(d)** Ratio of CD45.1$^+$ (WT genotype) over CD45.2$^+$ (KO genotype) cells in the spleen of the chimeras (n = 5, collected in two independent experiments). **(e)** Representative flow cytometry profiles of Tfh from the PP of Vav-Cre$^-$.*Pou2af1*$^{fl/fl}$, Vav-Cre$^+$.*Pou2af1*$^{fl/fl}$ and the bone marrow competitive chimeras, for which the profiles are separated based on CD45.1$^+$ and CD45.2$^+$ expression. **(f)** Percentage of Tfh in the spleen, PP and mLN of the chimeras, gated based on the expression of CD45.1 (B6.SJL) and CD45.2 (Vav-Cre$^+$.*Pou2af1*$^{fl/fl}$) to identify the origin and, thus the genotype, of the donor cells (n = 5, collected in two independent experiments). **(g)** Percentage of B cells in the PP and mLN of CD19-Cre$^-$.*Pou2af1*$^{fl/fl}$ and CD19-Cre$^+$.*Pou2af1*$^{fl/fl}$ mice, **(h)** percentage of Tfh in the PP and mLN of CD19-Cre$^-$.*Pou2af1*$^{fl/fl}$ and CD19-Cre$^+$.*Pou2af1*$^{fl/fl}$ mice, and **(i-j)** CXCR5 and PD-1 RFI on CXCR5$^+$PD-1$^+$ CD4$^+$ T cells from the PP of CD19-Cre$^-$.*Pou2af1*$^{fl/fl}$ and CD19-Cre$^+$.*Pou2af1*$^{fl/fl}$ mice (n = 7-10, collected in five independent experiments). Data information: Mann Whitney *U*-test, NS, non-significant, *P*-value > 0.05; *P*-values ** < 0.01; *** < 0.001.

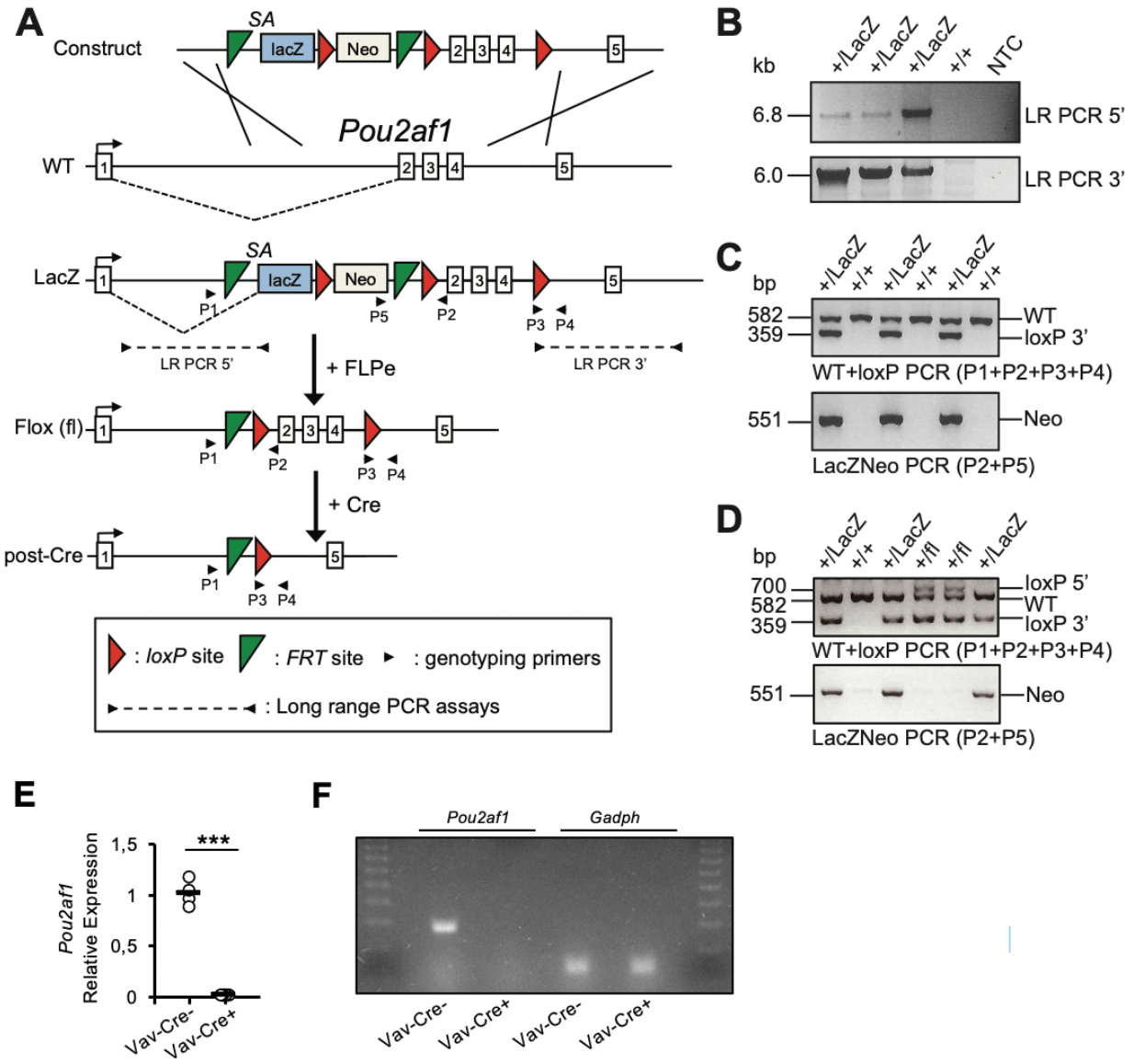

Supplementary figure 1. **Generation of a *Pou2af1*$^{fl/fl}$ mouse for cell specific deletion of *Pou2af1***. (**a**) Targeting strategy used to generate Pou2af1$^{+/LacZ}$ and Pou2af1$^{+/fl}$ mice. The position of the primers and long-range PCR assays used for genotyping are indicated. *SA:* splice acceptor site located in front of the lacZ cassette. (**b**) Long range PCR on mouse tail DNA confirming the proper targeting of the *Pou2af1* locus. (**c**) Genotyping PCR demonstrating the generation of *Pou2af1*$^{+/LacZ}$ mice. (**d**) Genotyping PCR demonstrating the generation of *Pou2af1*$^{+/fl}$ mice following breeding with *ACTBFLPe* mice. (**e**) *Pou2af1* relative expression in splenocytes from Vav-Cre^{-}.*Pou2af1*$^{fl/fl}$ and Vav-Cre^{+}.*Pou2af1*$^{fl/fl}$ mice (n = 4), measured by RT-qPCR. *Gapdh* mRNA levels were used as loading control. (**f**) *Pou2af1* and *Gadph* RT-qPCR products were migrated on agarose gel for mice of the indicated genotypes. ***, $P < 0.001$.

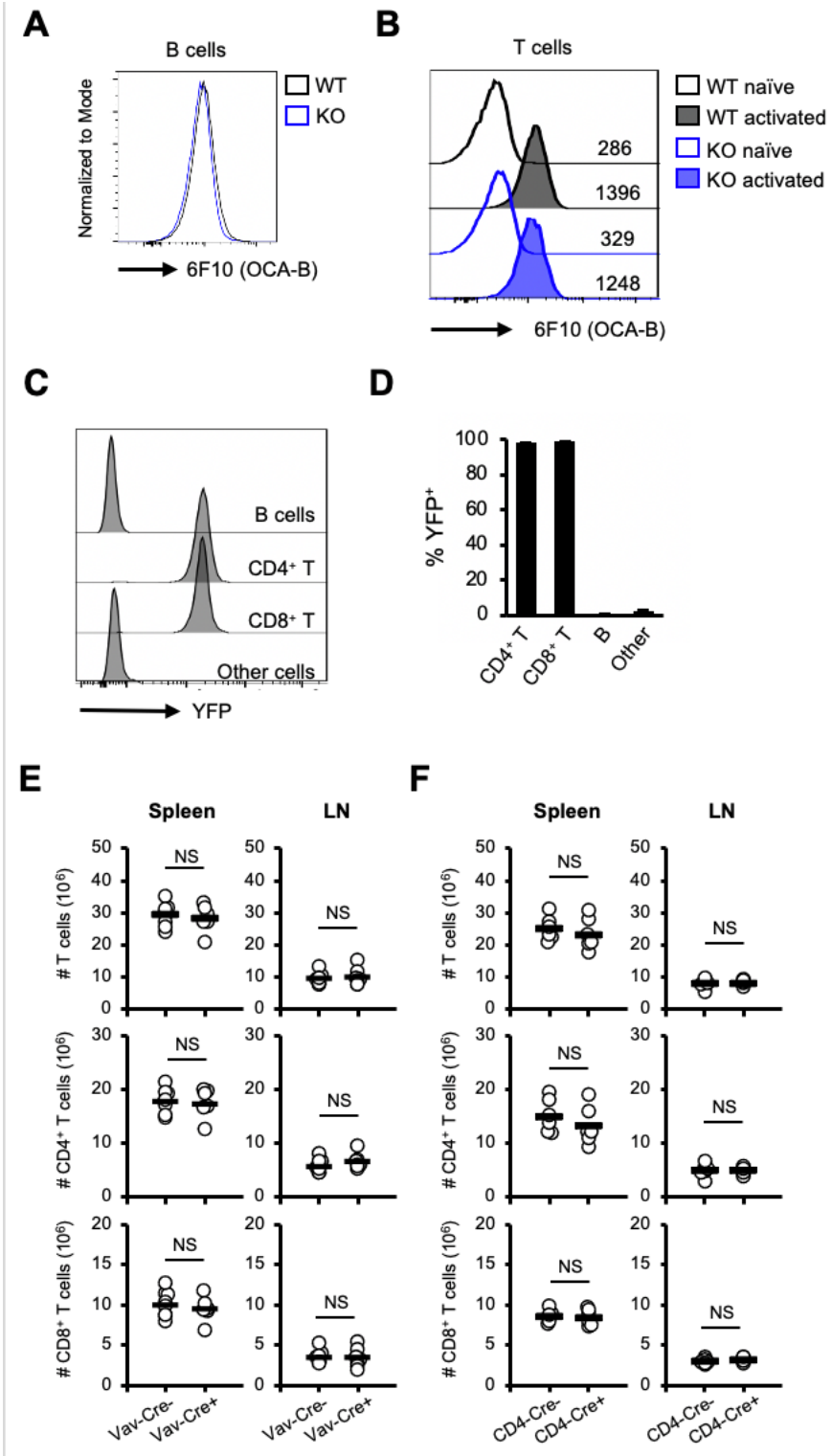

Supplementary figure 2. **Validation of tools to the study of OCA-B expression and function in T cells. (a)** Representative flow cytometry profiles of 6F10 staining on B cells from Vav-Cre^{-}.*Pou2af1*$^{fl/fl}$ and Vav-Cre^{+}.*Pou2af1*$^{fl/fl}$ mice. **(b)** Representative flow cytometry profiles of 6F10 staining on naïve and activated T cells from Vav-Cre^{-}.*Pou2af1*$^{fl/fl}$ and Vav-Cre^{+}.*Pou2af1*$^{fl/fl}$ mice. MFI are indicated for each population. **(c)** Representative flow cytometry profiles of YFP expression on cells from the spleen of CD4-Cre^{+}.ROSA-YFP^{+} mice. **(d)** Percentage of YFP^{+} cells from the spleen of CD4-Cre^{+}.ROSA-YFP^{+} mice (n = 3). **(e)** Numbers of total, CD4^{+} and CD8^{+} T cells from the spleen and a pool of inguinal, axial and brachial LN of Vav-Cre^{-}.*Pou2af1*$^{fl/fl}$ and Vav-Cre^{+}.*Pou2af1*$^{fl/fl}$ mice (n = 6 per group), and **(f)** CD4-Cre^{-}.*Pou2af1*$^{fl/fl}$ and CD4-Cre^{+}.*Pou2af1*$^{fl/fl}$ mice (n = 6). NS, non-significant, $P > 0.05$

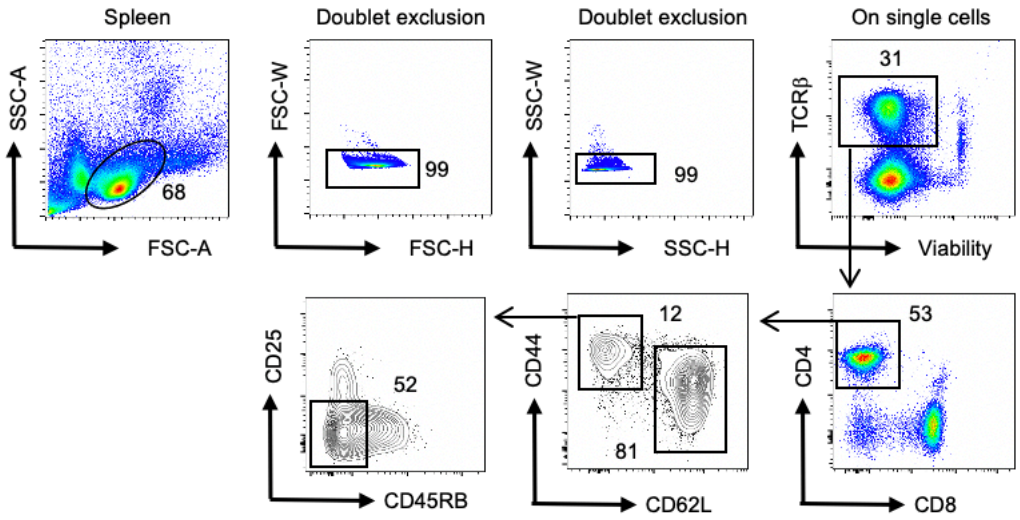

Supplementary figure 3. **Gating strategy for the analysis of CD4^{+} T cells with a memory phenotype.** Representative flow cytometry profiles of cells from the spleen of Vav-Cre^{-} .*Pou2af1*$^{fl/fl}$ mice.

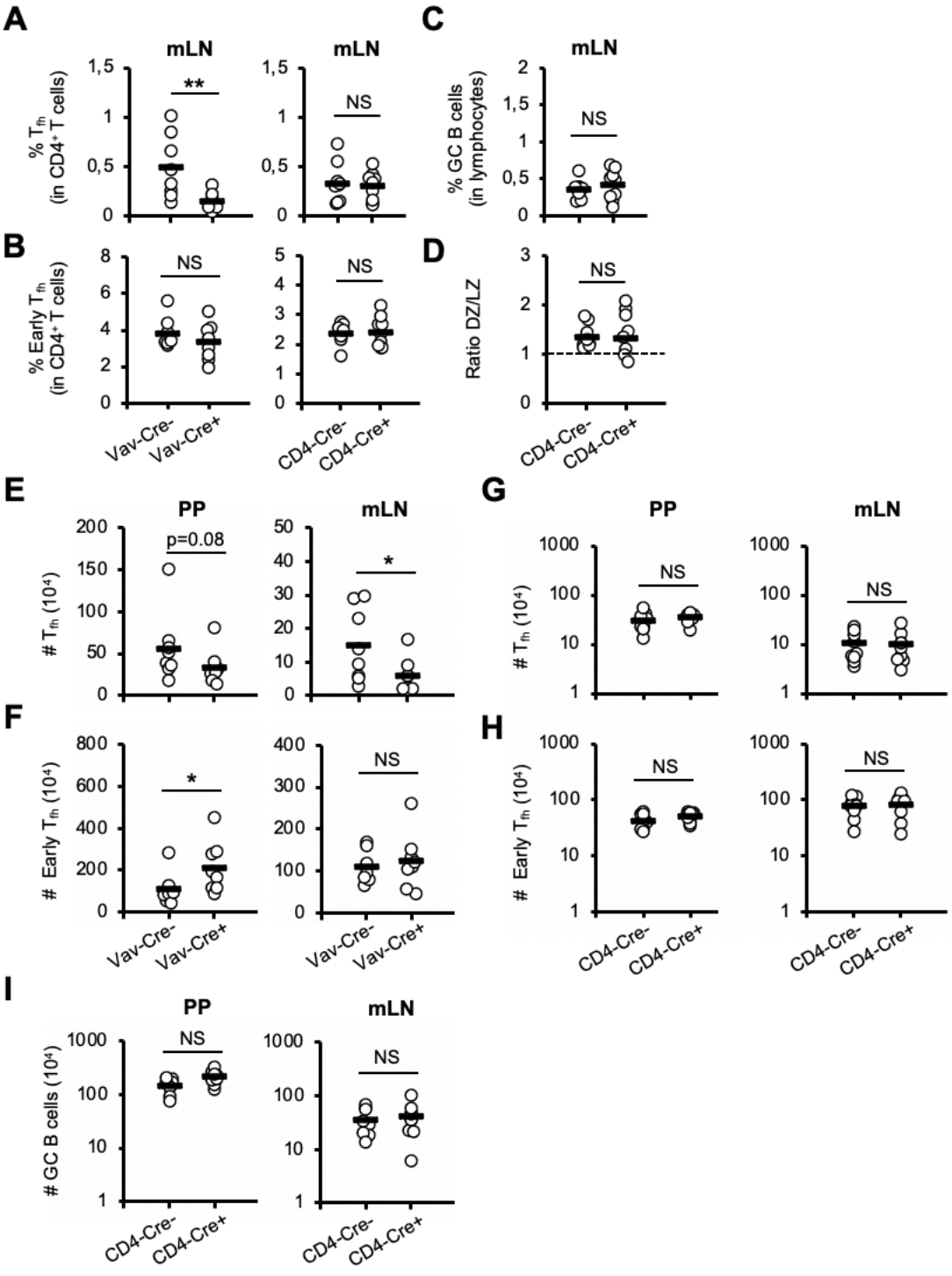
A
mLN
mLN
% Tfh (in CD4+ T cells)
1,5
1
0,5
0
**
NS
C
mLN
% GC B cells (in lymphocytes)
2
1,5
1
0,5
0
NS
B
% Early Tfh (in CD4+ T cells)
8
6
4
2
0
5
4
3
2
1
0
NS
NS
Vav-Cre-
Vav-Cre+
CD4-Cre-
CD4-Cre+
D
Ratio DZ/LZ
3
2
1
0
NS
CD4-Cre-
CD4-Cre+
E
PP
mLN
Tfh (10⁴)
200
150
100
50
0
50
40
30
20
10
0
p=0.08
*
F
Early Tfh (10⁴)
800
600
400
200
0
400
300
200
100
0
*
NS
Vav-Cre-
Vav-Cre+
Vav-Cre-
Vav-Cre+
G
PP
mLN
Tfh (10⁴)
1000
100
10
1
1000
100
10
1
NS
NS
H
Early Tfh (10⁴)
1000
100
10
1
1000
100
10
1
NS
NS
CD4-Cre-
CD4-Cre+
CD4-Cre-
CD4-Cre+
I
PP
mLN
GC B cells (10⁴)
1000
100
10
1
1000
100
10
1
NS
NS
CD4-Cre-
CD4-Cre+
CD4-Cre-
CD4-Cre+

Supplementary figure 4. **Hematopoietic cell-specific but not T cell-specific *Pou2af1* deletion limits Tfh maturation. (a, b)** Percentage of **(a)** Tfh ($CXCR5^{Hi}PD\text{-}1^{Hi}$) and **(b)** early Tfh ($CXCR5^{Low}PD\text{-}1^{Low}$) in the mLN of Vav-$Cre^{-}$.*Pou2af1*$^{fl/fl}$, Vav-$Cre^{+}$.*Pou2af1*$^{fl/fl}$ mice, CD4-Cre^{-}.*Pou2af1*$^{fl/fl}$ and CD4-Cre^{+}.*Pou2af1*$^{fl/fl}$ mice (n = 8-10). **(c)** Percentage of GC B cells in the mLN of CD4-Cre^{-}.*Pou2af1*$^{fl/fl}$ and CD4-Cre^{+}.*Pou2af1*$^{fl/fl}$ mice (n = 10). **(d)** Ratio of dark zone ($CXCR4^{Hi}CD86^{-}$) over light zone ($CXCR4^{Low}CD86^{+}$) GC B cells from the mLN of CD4-Cre^{-}.*Pou2af1*$^{fl/fl}$ and CD4-Cre^{+}.*Pou2af1*$^{fl/fl}$ mice (n = 10 per group). **(e, f)** Absolute numbers of Tfh and early Tfh cells from the PP and mLN of Vav-Cre^{-}.*Pou2af1*$^{fl/fl}$ and Vav-Cre^{+}.*Pou2af1*$^{fl/fl}$ (n = 8 per group). **(g, h)** Absolute numbers of Tfh and early Tfh cells from the PP and mLN of CD4-Cre^{-}.*Pou2af1*$^{fl/fl}$ and CD4-Cre^{+}.*Pou2af1*$^{fl/fl}$ mice (n = 10). **(i)** Absolute numbers of GC B cells from the PP and mLN of CD4-Cre^{-}.*Pou2af1*$^{fl/fl}$ and CD4-Cre^{+}.*Pou2af1*$^{fl/fl}$ mice (n = 10). NS, non-significant, $P > 0.05$; *, $P < 0.05$

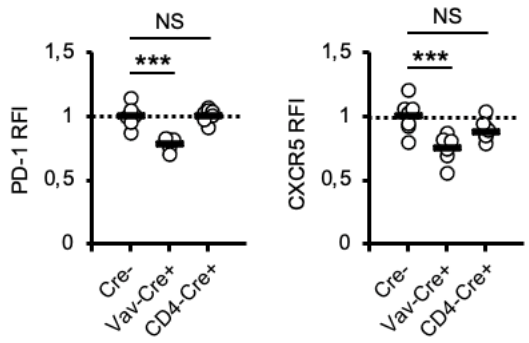

Supplementary figure 5. ***Pou2af1*** **deletion impacts Tfh maturation and GC formation in a T cell-extrinsic manner.** PD-1 and CXCR5 RFI on $CXCR5^{+}PD\text{-}1^{+}$ $CD4^{+}$ T cells from the spleen of the same groups of mice listed in Figure 4J (n = 6-8).

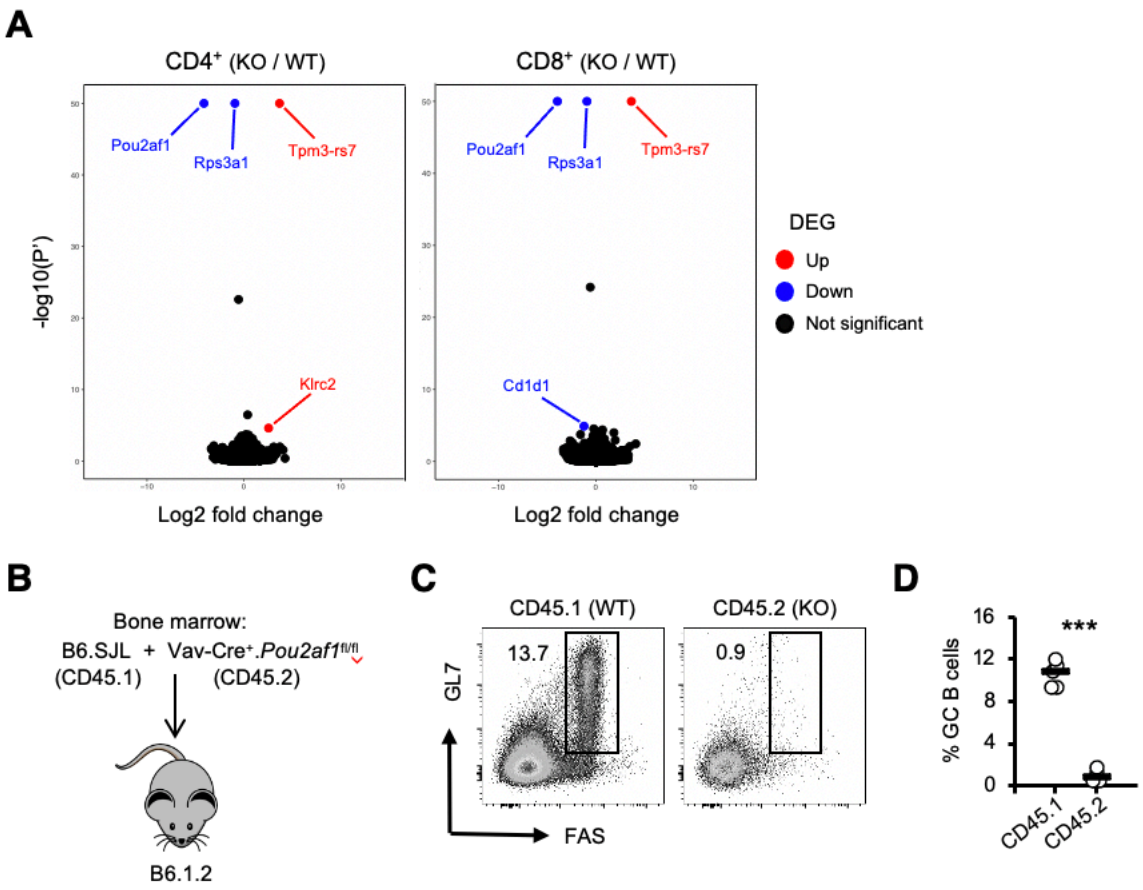

Supplementary figure 6. **OCA-B is not an active transcriptional coactivator in CD4$^+$ and CD8$^+$ T cells. (a)** Volcano Plots of Differentially Expressed Genes (DEG) from CD4$^+$ (left) and CD8$^+$ (right) T cells of CD4-Cre$^-$.*Pou2af1*$^{fl/fl}$ and CD4-Cre$^+$.*Pou2af1*$^{fl/fl}$ mice at FDR <0.05 and Fold Change > 1.5. Genes upregulated in the KO are in red, downregulated in blue, and black if not significantly differentially expressed. **(b)** Schematic representation of the competitive bone marrow chimeras. **(c)** Representative flow cytometry profiles of GL7$^+$FAS$^+$ GC cells in B220$^+$ B cells from the PP of the chimeras. **(d)** Percentage of GC B cells in the PP of the chimeras (n = 5). Data information: Mann Whitney *U*-test, ***, $P < 0.001$.

Preface to chapter 4

In the previous chapters, we have shown that GC responses are influenced by polymorphism in the *Idd2* locus, and have dissected the cell-intrinsic roles of *Pou2af1* in GCs. These two studies focused on the interplay between B and T cells in secondary lymphoid organs, such as the spleen and lymph nodes, in relationship with GCs. Although less studied, the thymus also contains a population of B cells. Notably, thymic B cells are suggested to play important roles in T cell development, mostly through the elimination of autoreactive CD4SP thymocytes (342, 343).

Interestingly, interactions between thymocytes and thymic B cells promotes intrathymic B cell class-switching in B6 mice (113). This process is AID-dependent, a gene essential to GC responses. Class-switched thymic B cells are also present in human thymus (344, 345). Of interest, class-switching of thymic B cells has been suggested to play a role in the selection process of thymocytes by thymic B cells (113). Still, this hypothesis has not been directly tested.

In this chapter, we used multiple genetically diverse mouse strains, transgenic and KO mice to investigate the role of thymic B cell class-switching on T cell selection and its impact on T cell tolerance and autoimmunity.

Chapter 4

AID expression by thymic B cells promotes T cell tolerance and limits autoimmunity

Félix Lombard-Vadnais[1,2], Geneviève Chabot-Roy[1], Astrid Zahn[3], Javier M Di Noia[2,3,4,5], Heather Melichar[1,4,*], Sylvie Lesage[1,6,*]

*co-corresponding

Running title: Thymic B cell class-switching promotes T cell tolerance

[1] Immunologie-oncologie, Centre de recherche de l'hôpital Maisonneuve-Rosemont, Montréal, QC, H1T 2M4, Canada

[2] Department of Microbiology & Immunology, McGill University, Montreal, QC, H3A 0G4, Canada

[3] Unité de recherche en biologie moléculaire des cellules B, Institut de recherches cliniques de Montréal, Montréal, QC, H2W 1R7

[4] Département de médecine, Université de Montréal, Montréal, QC, H3T 1J4, Canada

[5] Department of Experimental Medicine, McGill University, Montreal, QC, H3A 0G4, Canada

[6] Département de microbiologie, infectiologie et immunologie, Université de Montréal, Montréal, QC, H3T 1J4, Canada

*Correspondence: Sylvie Lesage, 514-252-3400 ext 4649, sylvie.lesage@umontreal.ca

4.1 Abstract

Elimination of self-reactive T cells in the thymus is critical for the establishment of T cell tolerance. A growing body of evidence suggests a role for thymic B cells in the elimination of self-reactive thymocytes. To specifically address the role of thymic B cells in central tolerance, we investigated the phenotype of thymic B cells in various mouse strains, including non-obese diabetic (NOD) mice, a mouse model of autoimmune diabetes. We noted that isotype switching of NOD thymic B cells is reduced as compared to other, autoimmune-resistant, mouse strains. To determine the impact of B cell isotype switching on thymocyte selection and tolerance, we generated NOD.AID$^{-/-}$ mice. Diabetes incidence was enhanced in these mice. Moreover, we observed reduced clonal deletion, resulting in an increase in self-reactive CD4^{+} T cells in NOD.AID$^{-/-}$ mice relative to NOD controls. Together, this study reveals a novel role for AID in thymic B cells in the promotion of T cell tolerance.

4.2 Introduction

Developing T cells undergo a series of selection processes in the thymus to yield a functional repertoire of T cells able to recognize antigens in the context of major histocompatibility complex (MHC) molecules, while ensuring tolerance to self-antigens (3, 27, 346). Selection of thymocytes is mediated by various antigen presenting cells (APCs), such as thymic epithelial cells (TECs), conventional dendritic cells (cDCs) and plasmacytoid dendritic cells (pDCs) (27). In addition, human and mouse thymi also harbor a small population of B cells (347, 348). Although B cells are not considered efficient phagocytes, they take advantage of their antigen receptor (B cell receptor, BCR) to efficiently capture antigens from the environment and present peptides from these proteins via MHC II molecules (57, 349). Thymic B cells express high levels of MHC II as well as co-stimulatory molecules and contribute to thymocyte education in some settings (8). Negative selection is the processes by which thymocytes bearing T cell receptors (TCR) with high affinity to self-peptide MHC complexes are purged via apoptosis (17, 350). Notably, in antigen receptor transgenic mice with monoclonal T and B cell repertoires, thymic B cells can promote the elimination of self-reactive CD4 single positive (SP) thymocytes (8, 30, 112). Still, the factors contributing to thymic B cell-mediated negative selection are incompletely understood.

A recent study suggests that thymic B cells that have undergone class switch recombination (CSR) to change BCR isotype may promote central T cell tolerance (113). It was shown that CSR can occur directly in the thymus and is dependent on thymocyte-derived signals (113). IgG^+ and IgA^+ thymic B cells were shown to express activation-induced cytidine deaminase (AID). Importantly, the BCR repertoire of isotype switched thymic B cells appears to be skewed towards self-antigens (113). This finding led to the hypothesis that self-reactive isotype switched thymic B cells may facilitate negative selection of self-reactive thymocytes. Yet, whether isotype switched thymic B cells directly induce negative selection of autoreactive thymocytes has not been assessed. More importantly, due to the redundancy in both central and peripheral tolerance processes for preventing autoimmune diseases, it is not clear whether elimination of self-reactive thymocytes by isotype switched thymic B cells has a functional impact on the development of autoimmunity.

Type 1 diabetes (T1D) is an autoimmune disease characterized by the destruction of insulin-producing pancreatic β cells (351). The non-obese diabetic (NOD) mouse strain is autoimmune-

prone (352) and spontaneously develops autoimmune diabetes characteristic of human disease (123, 133, 137). T cells are necessary and sufficient for autoimmune diabetes onset and progression (166, 353, 354), and it has been suggested that defects in central T cell tolerance in NOD mice contribute to the development of autoimmune diabetes (12, 233, 355-358). Intriguingly, the defects in central tolerance correlate with abnormal B cell development in the thymus of NOD mice (359). Still, the contribution of thymic B cells to T cell tolerance in NOD mice is unknown.

To investigate the potential contributions of thymic B cells to T cell tolerance and autoimmunity, we phenotyped B cells from the thymus of various mouse strains, including NOD mice. As compared to genetically divergent mouse strains, we observe that NOD thymic B cell CSR is inefficient. Interestingly, this trait correlates with reduced tolerance of thymocytes towards self-antigens. We also show that disruption of AID impairs negative selection of CD4SP thymocytes and favors the development of autoimmunity. Our data reveal a new role for AID in the thymus in T cell tolerance. Moreover, we demonstrate that thymic B cell expression of AID, by promoting negative selection of self-reactive thymocytes, has a functional consequence on autoimmune disease susceptibility.

4.3 Results

Reduction of co-stimulation and CSR in NOD thymic B cells

To investigate the potential role for thymic B cells in impaired T cell tolerance in NOD mice, we analyzed the phenotype of thymic B cells from 7- to 10-week-old non-diabetic B6 and NOD mice (Fig. S1A). As compared to splenic B cells, thymic B cells from both strains expressed higher levels of MHC II molecules (Fig. 1A, B). In contrast, while a higher percentage of thymic B cells from B6 mice express CD80 relative to B cells isolated from the spleen (Fig. 1C, D) (8), thymic B cells from NOD mice expressed lower levels of this co-stimulatory molecule as compared to their B6 counterparts (Fig. 1C, D). This low level of CD80 expression in the NOD thymus is specific to thymic B cells, as other thymic APCs express levels of CD80 that are comparable to those observed in B6 mice (Fig. S1B, C). This reveals that thymic B cells in NOD mice have a distinct phenotype relative to other thymic APCs.

CD80 expression on APCs is typically induced following activation (360, 361). The low expression of these co-stimulatory molecules on thymic B cells in NOD mice suggest that they may not be effectively activated. This is not due to defects in their response to stimuli; thymic B cells from NOD mice efficiently upregulate the expression of co-stimulatory molecules and activation markers following *in vitro* activation with LPS or anti-CD40 (Fig. S1D). Therefore, the reduced expression of CD80 on thymic B cells from NOD mice relative to B6 mice suggests that the NOD thymic environment provides less B cell activation signals *in vivo*. Activation of thymic B cells can also lead to the expression of AID and, consequently, to CSR (113). In line with the low level of CD80 expression, a lower percentage of $IgM^{-}IgD^{-}$ isotype switched thymic B cells was observed in NOD mice relative to B6 mice (Fig. 1E, F). To determine if the relatively higher level of thymic B cell CSR is a specific feature of the B6 strain (113), we analyzed thymic B cells from multiple genetically divergent mouse strains: the common C3H, A/J and NZO strains as well as the more recently wild-derived PWK and CAST inbred strains (Fig. S1E). Isotype switched $IgM^{-}IgD^{-}$ thymic B cells were observed in the thymus of all tested strains (Fig. 1G), with most of those cells expressing an IgG or IgA BCR (Fig. 1H). Among these genetically divergent mouse strains, the NOD mouse, the only strain spontaneously developing autoimmunity, displays the lowest percentage of isotype switched thymic B cells (Fig. 1G). Altogether, these data suggest that thymic B cells in NOD mice express lower levels of co-stimulatory molecules and exhibit less CSR than the other mouse strains tested.

The NOD thymic B cell traits correlate with reduced T cell tolerance to self-antigens

It has been recently suggested that isotype switched thymic B cells may promote central T cell tolerance (113). Using the genetically divergent mouse strains, we determined that the percentage of isotype switched thymic B cells varies tremendously (Fig. 1G). We took advantage of this variability to assess whether the percentage of isotype switched thymic B cells correlated with thymic phenotypes. Interestingly, we found that the percentage of $IgM^{-}IgD^{-}$ thymic B cells correlated with the percentage of $CD69^{+}$ CD4SP thymocytes (Fig 2A). Notably, CD69 expression is induced following TCR stimulation, during positive and negative selection (362). In contrast to CD4SP thymocytes, no correlation between isotype switched B cells and CD69 upregulation was observed for CD8SP thymocytes (Fig. 2B). These results suggest that isotype switched thymic B

cells, which express high levels of MHC II, may participate in thymic selection of CD4SP thymocytes.

We observed a greater percentage and number of CD4SP, but not of CD8SP, thymocytes in NOD mice as compared to B6 mice (Fig. 2C, S1F), suggesting a potential defect in negative selection of CD4SP thymocytes in NOD mice. In addition, among these CD4SP thymocytes, the percentage of active caspase-3^+ cells, a marker of cells undergoing clonal deletion (363), was reduced in NOD mice (Fig. 2D). These results suggest that negative selection of CD4SP thymocytes is less effective in NOD mice. As a result, CD4SP thymocytes from NOD mice should exhibit enhanced self-reactivity. To assess the level of self-reactivity of CD4SP thymocytes from B6 and NOD mice, we performed an *in vitro* proliferation assay of CD4SP thymocytes on activated splenic B cells (Fig. 2E). Specifically, splenic B cells from both strains were activated using αCD40 antibodies and used as a source of APCs and self-antigens. *In vitro* activation induced high levels of CD80 on B cells from both strains (Fig. S1G). CFSE labelled CD4SP thymocytes were co-cultured for three days with activated B cells from the respective strains. At the end of the co-culture, CD4SP thymocyte proliferation and activation was quantified by flow cytometry. While proliferation of CD4SP thymocytes in the B6 co-culture was minimal, those from NOD mice proliferated significantly more (Fig. 2F, G). This increase in $CFSE^{lo}$ cells was not caused by more rapid proliferation of NOD thymocytes, as CD4SP cells from B6 and NOD mice had a similar proliferation index (Fig. 2H). Altogether, these results demonstrate that the low percentage of CSR in thymic B cells in NOD mice correlates with a decrease in the induction of negative selection at the CD4SP stage and a corresponding increase in self-reactive CD4SP thymocytes in NOD relative to B6 mice.

Loss of AID in thymic B cells promotes the development of autoimmune diabetes

To study the impact of AID expression in thymic B cell on the development of autoimmunity, we generated a NOD.$AID^{-/-}$ strain. As expected, NOD.$AID^{-/-}$ mice completely lack CSR in thymic B cells (Fig. 3A). Genetic deletion of AID does not impact thymic B cell expression of MHC II, CD80, or CD69 (Fig. S2A), allowing us to assess the impact of AID independent of variations in the expression of costimulatory molecules. There was also no significant difference in the abundance of B cells in the thymus of NOD.$AID^{+/+}$ and NOD.$AID^{-/-}$ mice (Fig. S2B). First, to test

the impact of B cell CSR on the development of autoimmunity, we performed a diabetes incidence study. Compared to NOD.AID$^{+/+}$ littermates, diabetes onset was accelerated and diabetes incidence was higher in NOD.AID$^{-/-}$ mice (Fig. 3B). In addition to the increased diabetes incidence, NOD.AID$^{-/-}$ mice exhibited an enlargement of the spleen and pancreatic lymph nodes, but not of skin-draining lymph nodes (Fig 3C, D and S2C), similar to previous reports (364). Secondary lymphoid tissue enlargement was thus more pronounced in organs where diabetogenic T cells are primed by self-antigens (365, 366). In the spleen and pancreatic lymph nodes, we also observed an increase in the percentage and number of activated CD4^{+} T cells, as detected by both the increase in expression of CD69 and an increase in CD62L^{lo}CD44^{hi} CD4^{+} T cells (Fig. 3E, F, S2D, E). No increase in activated T cells was observed in skin-draining lymph nodes (Fig. 3E, F S2D). The T cell activation phenotype is specific to CD4^{+} T cells, as no difference in the percentage of activated CD8^{+} T cells was observed between NOD.AID$^{+/+}$ and NOD.AID$^{-/-}$ mice in any of the organs tested (Fig. 3G). Together, these data suggest that a lack of AID expression increases diabetes incidence in NOD mice and is associated with an increase in activated CD4^{+} T cells, but not CD8^{+} T cells, in the spleen and pancreatic lymph nodes, where priming of islet antigen-specific T cells takes place (365, 366).

AID expression impacts multiple aspects of B cell biology including antibody production and germinal center formation (367, 368). It is therefore possible that the increased diabetes onset in AID$^{-/-}$ NOD mice (Fig. 3B) is a consequence of altered B cell function in the periphery rather than an impact on the diabetogenic potential of T cells. To test this possibility, we used lymphopenic NOD.Rag$^{-/-}$ mice, which lack all T and B lymphocytes and therefore do not progress to diabetes (289). Adoptive transfer of T cells into NOD.Rag$^{-/-}$ mice induces autoimmune diabetes (289). When compared to recipients of total peripheral T cells from NOD.AID$^{+/+}$ mice, recipients of T cells from NOD.AID$^{-/-}$ mice showed accelerated diabetes onset (Fig. 4A), indicating that a lack of AID impacts T cell diabetogenicity. This result also suggests that the increased diabetes onset observed in NOD.AID$^{-/-}$ mice (Fig. 3B) is, at least in part, T cell-mediated.

Peripheral T cell tolerance mechanisms potentially contribute to the diabetogenic potential of T cells in NOD.AID$^{-/-}$ mice. To determine if loss of AID in thymic B cells alters the diabetogenic potential of thymocytes, we transferred thymocytes from NOD.AID$^{+/+}$ and NOD.AID$^{-/-}$ mice into NOD.Rag$^{-/-}$ recipients. We collected pancreas 10 weeks post-transfer and quantified insulitis (Fig.

4B). Recipients of thymocytes from NOD.AID$^{-/-}$ mice showed comparably more insulitis than the recipients of thymocytes from AID$^{+/+}$ mice (Fig. 4C). Consistent with the increase of activated CD4^{+} T cells in NOD.AID$^{-/-}$ mice (Fig. 3E, F), an increase of activated CD4^{+} T cells was observed in the spleen and pancreatic lymph nodes of mice receiving thymocytes from NOD.AID$^{-/-}$ mice (Fig. 4D). Once again, activation of CD8^{+} T cells was not affected (Fig. 4E). Altogether, our results suggest that self-reactive thymocytes are not effectively eliminated in mice lacking AID expression, and that AID-expressing thymic B cells likely mediate negative selection of self-reactive thymocytes. Moreover, these self-reactive thymocytes can cause significant lesions in the pancreas.

AID deletion impairs negative selection of CD4SP thymocytes

We next aimed to determine whether negative selection of thymocytes was impaired in the absence of AID. As a measure of negative selection, we quantified the percentage of thymocytes from NOD.AID$^{+/+}$ and NOD.AID$^{-/-}$ mice expressing active caspase-3 (Fig. S3A). A lower percentage of CD4SP thymocytes from NOD.AID$^{-/-}$ mice expressed active caspase-3 than NOD.AID$^{+/+}$ littermates (Fig. 5A, B). In contrast, no significant difference was observed in DP and CD8SP thymocytes (Fig. 5A, B). In addition to active caspase-3, we quantified HELIOS expression. HELIOS is induced in self-reactive CD4SP thymocytes following strong TCR signals, and can be used as a marker of negative selection (369). Notably, as CD4^{+}FOXP3^{+} regulatory T cells (Tregs) also express HELIOS, Tregs were excluded from the analysis (Fig. 5C). As for active caspase-3, we found a significant reduction of HELIOS^{+}FOXP3^{-} CD4SP thymocytes in NOD.AID$^{-/-}$ mice relative to NOD.AID$^{+/+}$ littermates (Fig. 5C, D). These results are consistent with impaired negative selection of self-reactive CD4SP thymocytes in NOD.AID$^{-/-}$ mice.

The decrease in negative selection of thymocytes in NOD.AID$^{-/-}$ mice could be due to a reduction of interactions with thymic B cells or by an impaired capacity of thymic B cells to induce TCR signaling. To test if interactions between thymic B cells and thymocytes are affected by AID deletion, we quantified interactions using flow cytometry. Co-expression of B220 and CD19 was used to identify thymic B cells interacting with double positive (DP), CD4SP and CD8SP thymocyte subsets (Fig. 5E, S3B). Expectedly, doublets were larger in size, as defined by the FSC/SSC profile (Fig S3B). Thymic B cells preferentially interacted with CD4SP thymocytes (Fig.

5E, F). Interestingly, a significant reduction of doublets was observed between thymic B cells and CD4SP thymocytes from NOD.AID$^{-/-}$ mice as compared to cells from NOD.AID$^{+/+}$ mice (Fig. 5F), suggesting that AID expression by thymic B cells promotes interactions with CD4SP thymocytes.

In the absence of AID, there are fewer interactions between thymic B cells and CD4SP thymocytes, and fewer CD4SP thymocytes expressing negative selection markers. Thymocytes from these NOD.AID$^{-/-}$ mice also promote insulitis. This suggest that there may be an accumulation of self-reactive CD4SP thymocytes in NOD.AID$^{-/-}$ mice. To test this hypothesis, we quantified tolerance of CD4SP thymocytes to self-antigens in NOD.AID$^{+/+}$ and NOD.AID$^{-/-}$ mice as before (Fig. 2E). Relative to CD4SP thymocytes from NOD.AID$^{+/+}$ mice, a greater percentage of CD4SP thymocytes from NOD.AID$^{-/-}$ mice was activated and proliferated in response to activated B cells isolated from NOD.CD45.2 mice (Fig. 5G-I). An absence of AID thus leads to an accumulation of autoreactive CD4SP thymocytes, and a reduction of tolerance to self-antigens. Together, these results suggest that AID expression by thymic B cells promotes negative selection of self-reactive thymocytes and improves T cell tolerance.

AID expression in B cells promotes clonal deletion of self-reactive thymocytes

The efficacy of antigen-specific negative selection is difficult to quantify in a non-transgenic setting, where thymocytes express a polyclonal TCR repertoire. To determine the extent to which AID impacts negative selection of CD4SP thymocytes in a setting distinct from NOD.AID$^{-/-}$ mice, we turned to an MHC class-II restricted TCR transgenic mouse model. In 3A9 TCR transgenic mice, most thymocytes express the MHC II (I-A^{k}) restricted 3A9 TCR specific for a peptide from the hen egg lysozyme (HEL) protein. In the absence of HEL, thymocytes complete their differentiation into CD4SP thymocytes (Fig. 6 A, B, 3A9 TCR^{+} HEL^{-} AID$^{+/+}$). When the HEL transgene driven by the rat insulin promoter is also expressed, soluble HEL is detected in circulation as well as in the thymus (12, 370). In these TCR:HEL double transgenic mice, most CD4SP thymocytes are eliminated by negative selection (Fig. 6A, B, 3A9 TCR^{+} HEL^{+} AID$^{+/+}$) (233). We crossed the TCR:HEL double transgenic mice onto the AID$^{-/-}$ background to quantify clonal deletion of self-reactive CD4SP thymocytes in the absence of AID expression by thymic B cells. In the absence of HEL, AID disruption did not impact the differentiation of 3A9TCR^{+}

CD4SP thymocytes (Fig. 6A, B, 3A9 TCR^+ HEL^- $AID^{-/-}$), suggesting that the AID-deficiency does not impact positive selection of thymocytes. In contrast, in the presence of HEL (Fig. 6A, B, 3A9 TCR^+ HEL^+ $AID^{-/-}$), an ~ 20% increase of self-reactive 3A9TCR^+ CD4SP thymocytes was observed in the thymus of $AID^{-/-}$ mice as compared to $AID^{+/+}$ controls, indicating a significant reduction in clonal deletion (Fig. 6A, B). In addition, interactions between thymic B cells and CD4SP thymocytes, which were very rare in the absence of the cognate antigen, were increased in mice expressing HEL (Fig. 6C). Interestingly, 3A9TCR^+ CD4SP thymocytes that were interacting with thymic B cells *in vivo* showed significantly lower expression of the 3A9TCR than CD4SP thymocytes that were not interacting with B cells (Fig. 6D). This observation supports the notion that thymic B cells can induce TCR signaling in CD4SP thymocytes in an antigen-specific manner, as TCR downregulation is a consequence of strong TCR signaling during thymocyte selection (371). Overall, these results suggest that AID expression in polyclonal thymic B cells can have a significant impact on negative selection of thymocytes.

Deletion of AID in B6 mice limits negative selection and induces insulitis

The impact of AID expression by thymic B cells on diabetes and insulitis was studied in NOD mice, which are prone to pancreatic autoimmunity. To test the impact of AID expression in thymic B cells in mice that do not spontaneously develop autoimmunity, we compared negative selection and insulitis in B6.$AID^{+/+}$ and B6.$AID^{-/-}$ mice. As previously observed in NOD.$AID^{-/-}$ mice (Fig. 5A, B), CD4SP thymocytes from B6.$AID^{-/-}$ mice showed a significant reduction in active caspase-3 expression relative to littermate controls (Fig. 7A), suggesting a reduction of negative selection. Again, no difference was observed for CD8SP thymocytes (Fig. 7A). While young B6.$AID^{+/+}$ and B6.$AID^{-/-}$ mice are free of immune infiltration in pancreatic islets, older B6.$AID^{-/-}$ mice display detectable levels of insulitis (Fig. 7B), consistent with previously reported insulitis in aged BALB/c.$AID^{-/-}$ mice (372). In addition, $CD4^+$ T cells were detected in the immune infiltrate in those mice, confirming their presence in the insulitic lesions (Fig. 7C). Together, these results confirm that the enhanced autoimmunity caused by inhibition of AID expression by thymic B cells in NOD.$AID^{-/-}$ mice may also impact T cell tolerance in autoimmune-resistant mice.

4.4 Discussion

In the last few years, thymic B cells have emerged as important mediators of thymic selection (373, 374). Still, the role of thymic B cells in the prevention of T cell-mediated autoimmunity is unclear. In this study, we identified B cell-specific phenotypes in the thymic APC pool of NOD mice, a common mouse model for autoimmune diabetes and other autoimmune syndromes (122, 137, 352). In addition to a B cell-specific deficit of co-stimulation, NOD thymic B cells do not switch to secondary isotypes as efficiently as in other mouse strains, a trait that correlates with a reduction of CD4SP thymocyte tolerance to self-antigens. To investigate a potential impact of AID expression by thymic B cell on T cell tolerance and autoimmunity, we generated NOD.AID$^{-/-}$ mice. As compared to NOD.AID$^{+/+}$ littermates, diabetes was more penetrant in NOD.AID$^{-/-}$ mice, and its onset was accelerated. Adoptive transfer of peripheral T cells and thymocytes revealed an impact of AID expression on T cell diabetogenicity, consistent with a role for thymic AID expression on thymocyte selection. Negative selection of CD4SP thymocytes was impaired in NOD.AID$^{-/-}$ mice. Using an antigen-specific model of clonal deletion, our data show that AID augments negative selection of CD4SP thymocytes. Lastly, we find that deletion of AID in the diabetes-resistant B6 strain resulted in a reduction of CD4SP thymocyte apoptosis and low-level insulitis. Together, these results identify a novel role for AID expression by thymic B cells in T cell selection and in the control of autoimmunity.

Previous studies suggested that thymic B cells can directly mediate negative selection of self-reactive CD4SP thymocytes (8, 30, 112). Because of the difficulty of studying negative selection in mice with a polyclonal T cell and B cell repertoire, most studies have used mice with expression of TCR and BCR transgenes to investigate the role of thymic B cells in the elimination of autoreactive CD4SP thymocytes (30, 112). For example, thymic B cells express the transcription factor AIRE, enabling expression of tissue-restricted antigens (30). Although AIRE expression is lower in thymic B cells than in mTECs, its expression is sufficient to drive the negative selection of TCR transgenic CD4SP thymocytes specific for a self-antigen expressed via the AIRE promotor (30). Similarly, in a BCR and TCR transgenic mouse model, directing BCR specificity towards the same antigen as transgenic thymocytes enabled thymic B cells to support deletion of the TCR transgenic thymocytes (8). Although these studies show that thymic B cells can induce negative selection of thymocytes when either TCR or BCR specificities are fixed, they do not allow

quantification of the impact of thymic B cells on negative selection of thymocytes in polyclonal settings. We show that AID expression promotes negative selection of thymocytes by thymic B cells, even in non-transgenic settings.

The absence of AID does not influence expression of MHC or selected costimulatory molecules on thymic B cells. This suggests that AID expression in thymic B cells facilitates negative selection of CD4SP thymocytes via other means. AID promotes intra-thymic CSR, leading to expression of IgG or IgA BCRs (113). We demonstrate that the presence of isotype switched B cells in the thymus is common across mouse strains. This has also been observed in humans (345, 375) and other animals (376), suggesting an important role of thymic B cell CSR in T cell development. One hypothesis for the role of isotype-switched B cells in the thymus is that they promote tolerance towards the different immunoglobulin isotypes (377). While possible for certain isotypes, the scarcity of thymic B cells expressing some specific isotypes, such as IgG1, IgG3 (30) and IgE (359) suggests that this may not be true for all of them. Furthermore, the increase in insulitis caused by AID disruption in this study suggests an impact on tolerance that is broader than specifically against immunoglobulin antigens. Analysis of the BCR repertoire of thymic B cells revealed enrichment of self-reactive clones in isotype-switched B cells (113). Indeed, the thymic environment appears to favor enrichment for self-reactive thymic B cells relative to the periphery (8). Analysis of B cell specificities in human thymi also reveal an enrichment for self-reactive B cells, especially against peptide antigens, including insulin-reactive B cells (345). Self-reactive thymic B cells may more effectively capture self-antigens through their isotype-switched high affinity BCRs, allowing enhanced presentation of self-antigens to thymocytes, resulting in greater negative selection. Of interest, among thymic B cells, the frequency of B cells bearing an insulin-specific BCR is reduced in NOD mice relative to B6 mice (359). This suggests that the reduction in self-reactive B cells in the thymus of NOD mice may explain, to some degree, the impaired tolerance of CD4SP thymocytes to self-antigens. While the specific factors promoting the accumulation of self-reactive B cells in the thymus are largely unknown, our results suggest that AID expression in thymic B cells enhances their potential to induce negative selection of thymocytes. This may be due, at least in part, to the fact that AID promotes modification of the BCR through CSR and somatic hypermutation, resulting in modulation of BCR signaling and antigen specificity (84, 108, 378-380).

As mentioned above, thymic B cells are thought to induce negative selection of self-reactive CD4SP thymocytes. Negative selection at the CD4SP stage is estimated to take place at a rate of more than $1.6x10^5$ cells per hour in mice, accounting for almost 25% of all clonal deletion (6). Although there are many APCs in the thymus, we find that thymic B cells play a non-redundant role in negative selection of self-reactive thymocytes. Using a TCR transgenic system in conjunction with cognate antigen expression in the thymus, we demonstrate that the absence of AID results in an increase in self-reactive CD4SP thymocytes. Of note, this experiment was performed in mice with non-transgenic BCRs, where the B cell repertoire is highly polyclonal. The modest impact on negative selection observed is therefore likely caused by the scarcity of HEL-specific B cells in these mice. Interestingly, the non-redundant role of AID expression in thymic B cells in negative selection is limited to CD4SP thymocytes. Considering that thymic B cells are primarily located in the thymic medulla, it is not surprising that they have a limited impact on DP thymocytes. However, thymic B cells express both MHC I and MHC II. The reason why isotype switched thymic B cells specifically induce negative selection of CD4SP thymocyte, and not CD8SP thymocytes, is unclear. Still, our results are consistent with previous reports demonstrating a modulation of CD4SP thymocyte differentiation in B cell-deficient mice, with no overt impact on CD8SP thymocytes (30).

Various central and peripheral tolerance mechanisms are in place to limit autoimmune diseases. If thymic B cells play a truly non-redundant role in central tolerance, the increase in the number of self-reactive CD4SP thymocytes in AID-deficient mice should increase autoimmune disease susceptibility. Indeed, AID disruption increases autoimmune diabetes incidence. This observation is consistent with a previous report showing that AID deficiency accelerates diabetes onset in NOD mice (364), although thymic B cells were not specifically studied. While another group observed a reduction of diabetes onset in AID-deficient NOD mice, likely caused by an expansion of regulatory B cells (381), the diabetogenicity of T cells in AID-deficient NOD mice was increased compared to AID-sufficient NOD mice, consistent with our data and a role for AID expression in thymic B cells in the elimination of pathogenic T cells. We also show that disruption of AID increases insulitis in diabetes-prone (NOD) and diabetes-resistant (B6) mice. As the nature of the antigens presented by thymic B cells is unknown, it is unclear if antigen presentation by thymic B cells prevents autoimmunity against specific antigens and organs. Interestingly, BALB/c.AID$^{-/-}$

mice display $CD4^+$ T cell-mediated infiltration of multiple organs (stomach, liver, lungs salivary glands and pancreas), consistent with a role for thymic B cells in the elimination of a broad range of self-reactive CD4SP thymocytes. However, this multi-organ immune infiltration may also have been caused by a potential, at the time unknown, mutation in the *Lag3* gene of the BALB/c.$AID^{-/-}$ mice (382). We have previously reported that B6.$AID^{-/-}$ mice have a reduced lifespan compared to WT littermates (383), but the cause for this remains unknown. It is tempting to speculate that enhanced autoimmunity caused by loss of AID expression in thymic B cells may contribute to this reduced lifespan. More work is needed to understand the complete impact of loss of AID expression in thymic B cells in B6 mice.

Mutations in *AID* have been detected in patients with hyper-IgM syndrome (384). Strikingly, a large portion of those patients present some auto-immune or inflammatory disorders (385, 386). Those include T-cell mediated diseases, such as T1D, Crohn's disease and non-infectious uveitis (385, 386). However, as participation of peripheral B cells has also been reported in those pathologies, we cannot confirm that the increased autoimmunity in AID-deficient patients is due to defects in thymic B cell-mediated T cell tolerance. Nevertheless, we have shown that the increased diabetes onset in NOD.$AID^{-/-}$ mice is, at least in part, T cell-mediated. Furthermore, thymocyte transfers confirm a role for AID expression specifically by thymic B cells in modulating the T cell repertoire, likely through the promotion of negative selection of CD4SP thymocytes.

In conclusion, this study reveals a non-redundant role for AID expression in thymic B cells in the induction of $CD4^+$ T cell tolerance. Previous studies suggest that isotype-switched thymic B cells have a greater propensity to express a self-reactive BCR, which may facilitate presentation of self-antigens to thymocytes. Additional studies are required to determine the peptide repertoire presented by isotype-switched thymic B cells, and how this can be manipulated to prevent autoimmune diseases.

4.5 Materials and methods

Mice

A/j (#000646), C57BL/B6 (B6, #000664), CAST/EiJ (CAST, #000928), C3H/HeJ (C3H, #000659), NOD/ShiLtJ (NOD, #001976), NZO/HILtJ (NZO, #002105) and PWK/PhJ (PWK. #003715) mice were obtained from Jackson Laboratory (Bar Harbor, United States). B6.AID$^{-/-}$ mice were generously shared by Dr Tasuku Honjo (Kyoto University, Japan). 3A9 TCR transgenic and rat insulin promoter-driven HEL transgenic mice (ripHEL) on the B10.BR background have been previously described (233). To generate NOD.AID$^{-/-}$ mice, B6.AID$^{-/-}$ mice were backcrossed to NOD mice for 10 generations. At each generation, mice were genotyped and AID$^{+/-}$ mice were used for backcrossing to NOD. At the 10th generation, NOD.AID$^{+/-}$ mice were intercrossed to yield NOD.AID$^{-/-}$ as well as NOD.AID$^{+/-}$ and NOD.AID$^{+/+}$ littermates for controls.

The genotype of all transgenic mice was verified by PCR. Transgene positive and negative littermates were used in every experiment where applicable. All mice used for experiments were aged between 8-12 weeks, unless indicated otherwise. For phenotyping experiments, both male and female mice were used. For experiments assessing diabetes onset and insulitis, only female mice were used. Mice were age matched for every experiment. All of the mouse strains were maintained at the Maisonneuve-Rosemont Hospital animal facility. The Maisonneuve-Rosemont Hospital ethics committee, overseen by the Canadian Council for Animal Protection, approved the experimental procedures.

Cell isolation

Thymus, spleen and LNs were pressed through a 70-µm cell strainer (Thermo Fisher Scientific, Waltham, United States). Spleen cell suspensions were treated with NH_4Cl to lyse red blood cells.

For TEC analysis, thymi were processed and digested as previously described (387). Briefly, thymi were cut in small pieces and pipetted up and down to release thymocytes. The remaining tissues was digested with papain (0.25 mg/ml), collagenase D (0.25 mg/ml) and DNAse (0.1 mg/ml) for 15 minutes at 37 °C in complete RPMI.

Flow cytometry

Single-cell suspensions were stained for 30 minutes at 4°C with different combinations of the following antibodies targeting (the antibody clone is in parentheses): B220 (RA3-6B2), CD3 (145-2C11), CD4 (GK1.5), CD5 (53-7.3), CD8a (53-6.7), CD11b (M1/70), CD11c (N418), CD19 (6D5), CD44 (IM7), CD45.1 (A20), CD45.2 (104), CD62L (MEL-14), CD69 (H1.2F3), CD80 (16-10A1), CD326/EpCAM (G8.8), I-A^d (39-10-8, cross-react to I-A^{g7}), IA/IE (M5/114.15.2), IgA (RMA-1), IgD (11-26c.2a), IgG1 (RMG1-1), IgG2b (RMG2-1), IgM (RMM1), and TCRβ (H57-597) from BioLegend (San Diego, United States); Active Caspase-3 (C92-605) from BD Biosciences (Franklin Lakes, United States); CD8b (H35-17.2), FOXP3 (FJK-16s), and HELIOS (22F6) from Thermo Fisher Scientific (Waltham, United States). Homemade 1G12 antibodies were used to stain for the 3A9TCR (388). Biotin-labelled antibodies were revealed with fluorescently-coupled streptavidin from BioLegend. Dead cells were stained using LIVE/DEAD™ Fixable Yellow Dead Cell Stain Kit (Thermo Fisher Scientific). For caspase staining, cells were treated with Cytofix/Cytoperm Fixation kit (BD Biosciences) as directed by the manufacturer. The FOXP3 Transcription Factor Staining Buffer Set (eBioscience) was used for transcription factor staining as directed by the manufacturer. Data were collected on an LSRFortessaX20 (BD) and analyzed with FlowJo software (BD Biosciences). B cells were gated as $CD19^+B220^+$ cells. TECs, cDC1, cDC2 and pDC were gated as $EpCAM^+CD45^-$, $CD11c^{hi}CD8\alpha^+CD11b^-$, $CD11c^{hi}CD8^-$

$CD11b^+$, and $CD11c^{low}B220^+$, respectively. CD4SP, CD8SP and post-selection DP were gated as $TCR\beta^+CD5^+CD4^+CD8^-$, $TCR\beta^+CD5^+CD4^-CD8^+$, and $TC\beta^+CD5^+CD4^+CD8^+$, respectively.

In vitro activation of thymic B cells

Total thymic cells were incubated for 72h in 96 well plates (flat bottom, 1 x 10^6 cells per well), in the presence of LPS (25µg/ml) or anti-CD40 antibodies (10µg/ml). Unstimulated controls were stained directly after mouse sacrifice.

In vitro co-culture

Splenic B cells were positively selected with a magnetic bead isolation kit (STEMCELL technologies, Vancouver, Canada) and anti-CD19 antibodies. B cells were cultured *in vitro* for 3 days with anti-CD40 antibodies (10µg/ml). Activation was confirmed by staining for expression of CD80/CD86 (Fig. S1G). CD4SP thymocytes were negatively selected with a magnetic bead isolation kit (STEMCELL technologies) and anti-CD8 and anti-CD19 antibodies. Isolated CD4SP thymocytes were stained with CFSE (Sigma, Saint-Louis, United States) (final concentration of 2 µM). Activated B cells and CFSE-stained CD4SP thymocytes were co-cultured at a 1:1 ratio ($2x10^5$ cells of each per well) in round bottom 96 well plates. Proliferation and activation of thymocytes was assessed by flow cytometry after 72h of co-culture. The proliferation index was measured using FlowJo software.

Diabetes incidence

Diabetes incidence was monitored daily in female mice for overt signs of diabetes (wet cage, hunched posture) and every 2 weeks for urine glucose levels using Diastix (Bayer, Toronto,

Canada) starting before the age of 10 weeks. After a positive Diastix test, overt diabetes was confirmed by blood glucose levels > 12 mmol/L, measured using Accu-Chek strips (Roche, Basel, Switzerland). The mice were sacrificed within 1 week of detection of high blood glucose or when they reached > 34 weeks of age. The pancreas was collected and conserved in formalin for at least 48h before paraffin embedding.

Histology

Hematoxylin and eosin staining was performed on 6 µm pancreas sections from paraffin blocks, for 2 non-successive sections per slide with 2 slides per mouse. Slides were scored for infiltration as previously described (276), and according to the following scale: 0 = no infiltration, 1 = peri-insulitis, 2 = infiltration <50%, 3 = infiltration >50%, 4 = complete infiltration.

Fluorescence microscopy

Pancreas were frozen in OCT (Thermo Fischer Scientific) over dry ice, and 10 µm slices of tissues were prepared using a cryostat. Slides were washed for 5 minutes in PBS (Wisent Bio, Saint-Jean-Baptiste, Canada) three times and fixed with 3.7% paraformaldehyde (Sigma) for 10 minutes. Slides were washed again in PBS three times, permeabilized, and blocked for 60 minutes using TritonX100 (0.1%) and BSA (3% in PBS). Antibodies (FITC-labelled anti-CD4, PE-labelled anti-CD45, Alexa Fluor 647-labelled anti-insulin) were added and incubated for 2 hours at room temperature then washed in PBS three times. Mounting medium containing DAPI (Abcam, Cambridge, United Kingdom) was added, and slides were sealed with nail polish. Images were acquired using a fluorescent microscope (Axio Imager 2, ZEISS).

Statistical analyses

Data were tested for significance using a nonparametric Mann-Whitney U test, a one-way ANOVA or a paired t-Test. A Log-Rank (Mantel Cox) test was used for the incidence studies. Numbers of animals used per group are indicated in the figure legends. The minimal significance threshold was set at 0.05 for all tests. NS, non-significant $P > 0.05$; *, $P < 0.05$ **, $P < 0.01$; ***, $P < 0.001$.

4.6 References

1. Labrecque N, Baldwin T, Lesage S. Molecular and genetic parameters defining T-cell clonal selection. Immunol Cell Biol. 2011;89(1):16-26.
2. Klein L, Kyewski B, Allen PM, Hogquist KA. Positive and negative selection of the T cell repertoire: what thymocytes see (and don't see). Nat Rev Immunol. 2014;14(6):377-91.
3. Sebzda E, Mariathasan S, Ohteki T, Jones R, Bachmann MF, Ohashi PS. Selection of the T cell repertoire. Annu Rev Immunol. 1999;17:829-74.
4. Miyama-Inaba M, Kuma S, Inaba K, Ogata H, Iwai H, Yasumizu R, et al. Unusual phenotype of B cells in the thymus of normal mice. J Exp Med. 1988;168(2):811-6.
5. Isaacson PG, Norton AJ, Addis BJ. The human thymus contains a novel population of B lymphocytes. Lancet. 1987;2(8574):1488-91.
6. Chen X, Jensen PE. The role of B lymphocytes as antigen-presenting cells. Arch Immunol Ther Exp (Warsz). 2008;56(2):77-83.
7. Yuseff MI, Pierobon P, Reversat A, Lennon-Dumenil AM. How B cells capture, process and present antigens: a crucial role for cell polarity. Nat Rev Immunol. 2013;13(7):475-86.
8. Perera J, Meng L, Meng F, Huang H. Autoreactive thymic B cells are efficient antigen-presenting cells of cognate self-antigens for T cell negative selection. Proc Natl Acad Sci U S A. 2013;110(42):17011-6.
9. Palmer E. Negative selection--clearing out the bad apples from the T-cell repertoire. Nat Rev Immunol. 2003;3(5):383-91.
10. Ramsdell F, Fowlkes BJ. Clonal deletion versus clonal anergy: the role of the thymus in inducing self tolerance. Science. 1990;248(4961):1342-8.
11. Frommer F, Waisman A. B cells participate in thymic negative selection of murine auto-reactive CD4+ T cells. PLoS One. 2010;5(10):e15372.
12. Yamano T, Nedjic J, Hinterberger M, Steinert M, Koser S, Pinto S, et al. Thymic B Cells Are Licensed to Present Self Antigens for Central T Cell Tolerance Induction. Immunity. 2015;42(6):1048-61.
13. Perera J, Zheng Z, Li S, Gudjonson H, Kalinina O, Benichou JIC, et al. Self-Antigen-Driven Thymic B Cell Class Switching Promotes T Cell Central Tolerance. Cell Rep. 2016;17(2):387-98.
14. Atkinson MA, Eisenbarth GS, Michels AW. Type 1 diabetes. Lancet. 2014;383(9911):69-82.
15. Aubin AM, Lombard-Vadnais F, Collin R, Aliesky HA, McLachlan SM, Lesage S. The NOD Mouse Beyond Autoimmune Diabetes. Front Immunol. 2022;13:874769.
16. Chen YG, Mathews CE, Driver JP. The Role of NOD Mice in Type 1 Diabetes Research: Lessons from the Past and Recommendations for the Future. Front Endocrinol (Lausanne). 2018;9:51.
17. Thayer TC, Wilson SB, Mathews CE. Use of nonobese diabetic mice to understand human type 1 diabetes. Endocrinol Metab Clin North Am. 2010;39(3):541-61.
18. Lehuen A, Diana J, Zaccone P, Cooke A. Immune cell crosstalk in type 1 diabetes. Nat Rev Immunol. 2010;10(7):501-13.

19. Christianson SW, Shultz LD, Leiter EH. Adoptive transfer of diabetes into immunodeficient NOD-scid/scid mice. Relative contributions of CD4+ and CD8+ T-cells from diabetic versus prediabetic NOD.NON-Thy-1a donors. Diabetes. 1993;42(1):44-55.
20. Yagi H, Matsumoto M, Kunimoto K, Kawaguchi J, Makino S, Harada M. Analysis of the roles of CD4+ and CD8+ T cells in autoimmune diabetes of NOD mice using transfer to NOD athymic nude mice. Eur J Immunol. 1992;22(9):2387-93.
21. Roep BO. The role of T-cells in the pathogenesis of Type 1 diabetes: from cause to cure. Diabetologia. 2003;46(3):305-21.
22. Lesage S, Hartley SB, Akkaraju S, Wilson J, Townsend M, Goodnow CC. Failure to censor forbidden clones of CD4 T cells in autoimmune diabetes. J Exp Med. 2002;196(9):1175-88.
23. Liston A, Lesage S, Gray DH, O'Reilly LA, Strasser A, Fahrer AM, et al. Generalized resistance to thymic deletion in the NOD mouse; a polygenic trait characterized by defective induction of Bim. Immunity. 2004;21(6):817-30.
24. Thomas-Vaslin V, Damotte D, Coltey M, Le Douarin NM, Coutinho A, Salaun J. Abnormal T cell selection on nod thymic epithelium is sufficient to induce autoimmune manifestations in C57BL/6 athymic nude mice. Proc Natl Acad Sci U S A. 1997;94(9):4598-603.
25. Kishimoto H, Sprent J. A defect in central tolerance in NOD mice. Nat Immunol. 2001;2(11):1025-31.
26. Zucchelli S, Holler P, Yamagata T, Roy M, Benoist C, Mathis D. Defective central tolerance induction in NOD mice: genomics and genetics. Immunity. 2005;22(3):385-96.
27. Dong M, Audiger C, Adegoke A, Lebel ME, Valbon SF, Anderson CC, et al. CD5 levels reveal distinct basal T-cell receptor signals in T cells from non-obese diabetic mice. Immunol Cell Biol. 2021;99(6):656-67.
28. Pinto AI, Smith J, Kissack MR, Hogg KG, Green EA. Thymic B Cell-Mediated Attack of Thymic Stroma Precedes Type 1 Diabetes Development. Front Immunol. 2018;9:1281.
29. Evans DE, Munks MW, Purkerson JM, Parker DC. Resting B lymphocytes as APC for naive T lymphocytes: dependence on CD40 ligand/CD40. J Immunol. 2000;164(2):688-97.
30. Van Gool SW, Vandenberghe P, de Boer M, Ceuppens JL. CD80, CD86 and CD40 provide accessory signals in a multiple-step T-cell activation model. Immunol Rev. 1996;153:47-83.
31. Brandle D, Muller S, Muller C, Hengartner H, Pircher H. Regulation of RAG-1 and CD69 expression in the thymus during positive and negative selection. Eur J Immunol. 1994;24(1):145-51.
32. Breed ER, Watanabe M, Hogquist KA. Measuring Thymic Clonal Deletion at the Population Level. J Immunol. 2019;202(11):3226-33.
33. Tan Q, Tai N, Li Y, Pearson J, Pennetti S, Zhou Z, et al. Activation-induced cytidine deaminase deficiency accelerates autoimmune diabetes in NOD mice. JCI Insight. 2018;3(1).
34. Gagnerault MC, Luan JJ, Lotton C, Lepault F. Pancreatic lymph nodes are required for priming of beta cell reactive T cells in NOD mice. J Exp Med. 2002;196(3):369-77.
35. Wan X, Vomund AN, Peterson OJ, Chervonsky AV, Lichti CF, Unanue ER. The MHC-II peptidome of pancreatic islets identifies key features of autoimmune peptides. Nat Immunol. 2020;21(4):455-63.
36. Honjo T, Muramatsu M, Fagarasan S. AID: how does it aid antibody diversity? Immunity. 2004;20(6):659-68.

37. Zaheen A, Boulianne B, Parsa JY, Ramachandran S, Gommerman JL, Martin A. AID constrains germinal center size by rendering B cells susceptible to apoptosis. Blood. 2009;114(3):547-54.
38. Soderstrom I, Bergman ML, Colucci F, Lejon K, Bergqvist I, Holmberg D. Establishment and characterization of RAG-2 deficient non-obese diabetic mice. Scand J Immunol. 1996;43(5):525-30.
39. Daley SR, Hu DY, Goodnow CC. Helios marks strongly autoreactive CD4+ T cells in two major waves of thymic deletion distinguished by induction of PD-1 or NF-kappaB. J Exp Med. 2013;210(2):269-85.
40. Akkaraju S, Ho WY, Leong D, Canaan K, Davis MM, Goodnow CC. A range of CD4 T cell tolerance: partial inactivation to organ-specific antigen allows nondestructive thyroiditis or insulitis. Immunity. 1997;7(2):255-71.
41. Mariathasan S, Bachmann MF, Bouchard D, Ohteki T, Ohashi PS. Degree of TCR internalization and Ca2+ flux correlates with thymocyte selection. J Immunol. 1998;161(11):6030-7.
42. Hase K, Takahashi D, Ebisawa M, Kawano S, Itoh K, Ohno H. Activation-induced cytidine deaminase deficiency causes organ-specific autoimmune disease. PLoS One. 2008;3(8):e3033.
43. Perera J, Huang H. The development and function of thymic B cells. Cell Mol Life Sci. 2015;72(14):2657-63.
44. Castaneda J, Hidalgo Y, Sauma D, Rosemblatt M, Bono MR, Nunez S. The Multifaceted Roles of B Cells in the Thymus: From Immune Tolerance to Autoimmunity. Front Immunol. 2021;12:766698.
45. Pearson JA, Wong FS, Wen L. The importance of the Non Obese Diabetic (NOD) mouse model in autoimmune diabetes. J Autoimmun. 2016;66:76-88.
46. Spencer J, Choy M, Hussell T, Papadaki L, Kington JP, Isaacson PG. Properties of human thymic B cells. Immunology. 1992;75(4):596-600.
47. Rother MB, Schreurs MW, Kroek R, Bartol SJ, van Dongen JJ, van Zelm MC. The Human Thymus Is Enriched for Autoreactive B Cells. J Immunol. 2016;197(2):441-8.
48. Butler JE, Sun J, Weber P, Ford SP, Rehakova Z, Sinkora J, et al. Antibody repertoire development in fetal and neonatal piglets. IV. Switch recombination, primarily in fetal thymus, occurs independent of environmental antigen and is only weakly associated with repertoire diversification. J Immunol. 2001;167(6):3239-49.
49. Haba S, Nisonoff A. IgE-secreting cells in the thymus: correlation with induction of tolerance to IgE. Proc Natl Acad Sci U S A. 1992;89(11):5185-7.
50. Feng Y, Seija N, Di Noia JM, Martin A. AID in Antibody Diversification: There and Back Again. Trends Immunol. 2020;41(7):586-600.
51. Wakabayashi C, Adachi T, Wienands J, Tsubata T. A distinct signaling pathway used by the IgG-containing B cell antigen receptor. Science. 2002;298(5602):2392-5.
52. Liu W, Meckel T, Tolar P, Sohn HW, Pierce SK. Intrinsic properties of immunoglobulin IgG1 isotype-switched B cell receptors promote microclustering and the initiation of signaling. Immunity. 2010;32(6):778-89.
53. Martin SW, Goodnow CC. Burst-enhancing role of the IgG membrane tail as a molecular determinant of memory. Nat Immunol. 2002;3(2):182-8.

54. Torres M, Casadevall A. The immunoglobulin constant region contributes to affinity and specificity. Trends Immunol. 2008;29(2):91-7.
55. Stritesky GL, Xing Y, Erickson JR, Kalekar LA, Wang X, Mueller DL, et al. Murine thymic selection quantified using a unique method to capture deleted T cells. Proc Natl Acad Sci U S A. 2013;110(12):4679-84.
56. Ratiu JJ, Racine JJ, Hasham MG, Wang Q, Branca JA, Chapman HD, et al. Genetic and Small Molecule Disruption of the AID/RAD51 Axis Similarly Protects Nonobese Diabetic Mice from Type 1 Diabetes through Expansion of Regulatory B Lymphocytes. J Immunol. 2017;198(11):4255-67.
57. Okazaki T, Okazaki IM, Wang J, Sugiura D, Nakaki F, Yoshida T, et al. PD-1 and LAG-3 inhibitory co-receptors act synergistically to prevent autoimmunity in mice. J Exp Med. 2011;208(2):395-407.
58. Safavi S, Larouche A, Zahn A, Patenaude AM, Domanska D, Dionne K, et al. The uracil-DNA glycosylase UNG protects the fitness of normal and cancer B cells expressing AID. NAR Cancer. 2020;2(3):zcaa019.
59. Revy P, Muto T, Levy Y, Geissmann F, Plebani A, Sanal O, et al. Activation-induced cytidine deaminase (AID) deficiency causes the autosomal recessive form of the Hyper-IgM syndrome (HIGM2). Cell. 2000;102(5):565-75.
60. Quartier P, Bustamante J, Sanal O, Plebani A, Debre M, Deville A, et al. Clinical, immunologic and genetic analysis of 29 patients with autosomal recessive hyper-IgM syndrome due to Activation-Induced Cytidine Deaminase deficiency. Clin Immunol. 2004;110(1):22-9.
61. Durandy A, Cantaert T, Kracker S, Meffre E. Potential roles of activation-induced cytidine deaminase in promotion or prevention of autoimmunity in humans. Autoimmunity. 2013;46(2):148-56.
62. Lebel ME, Coutelier M, Galipeau M, Kleinman CL, Moon JJ, Melichar HJ. Differential expression of tissue-restricted antigens among mTEC is associated with distinct autoreactive T cell fates. Nat Commun. 2020;11(1):3734.
63. Van Parijs L, Peterson DA, Abbas AK. The Fas/Fas ligand pathway and Bcl-2 regulate T cell responses to model self and foreign antigens. Immunity. 1998;8(2):265-74.
64. Hillhouse EE, Collin R, Chabot-Roy G, Guyon MJ, Tessier N, Boulay M, et al. Nearby Construction Impedes the Progression to Overt Autoimmune Diabetes in NOD Mice. J Diabetes Res. 2013;2013:620313.

4.7 Figures

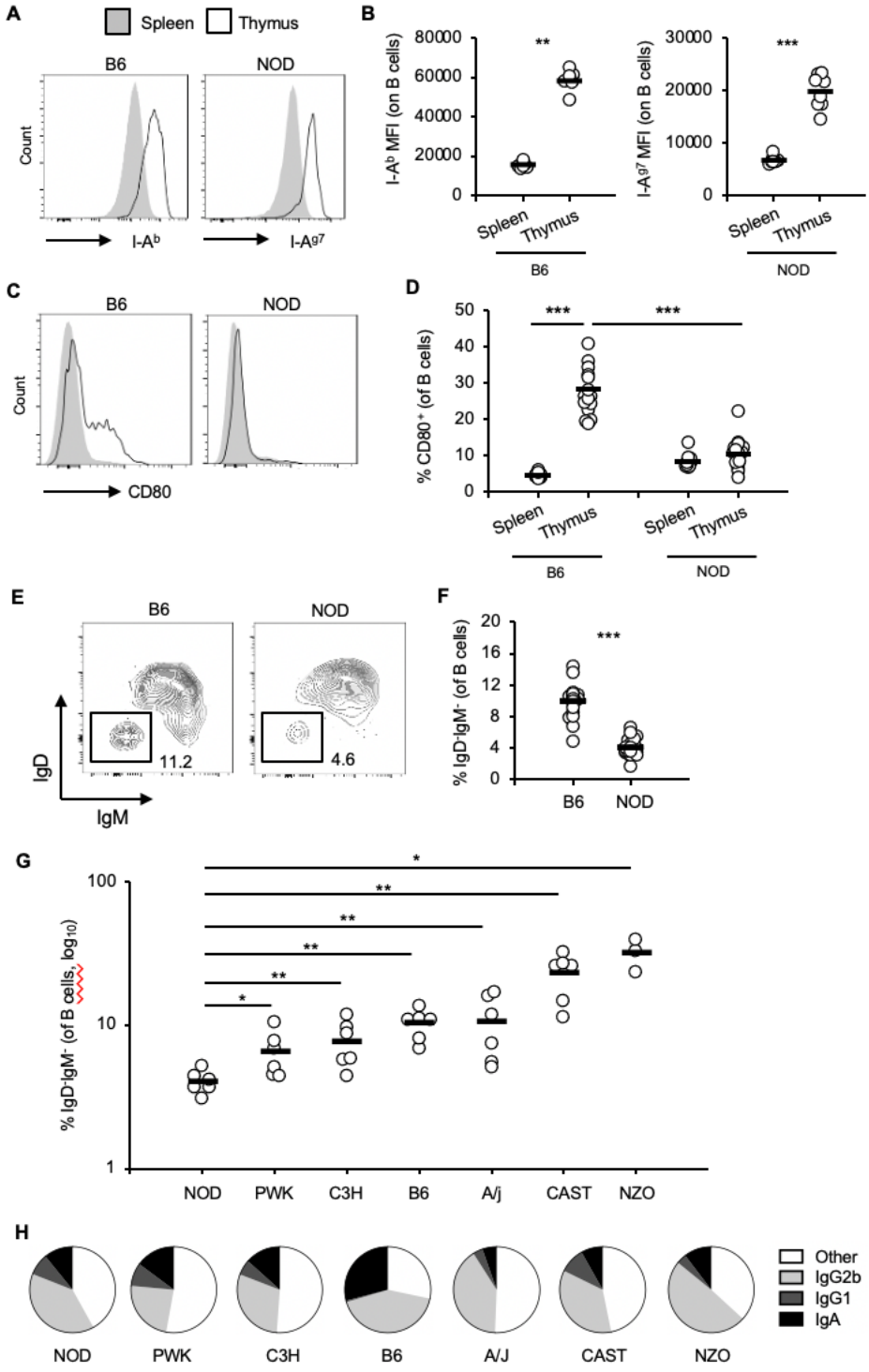
A
Spleen
Thymus
B6
NOD
Count
I-Ab
I-Ag7
B
I-Ab MFI (on B cells)
I-Ag7 MFI (on B cells)
Spleen
Thymus
B6
NOD
C
CD80
D
% CD80+ (of B cells)
E
11.2
4.6
IgD
IgM
F
% IgD-IgM- (of B cells)
G
% IgD-IgM- (of B cells, log10)
NOD
PWK
C3H
B6
A/j
CAST
NZO
H
Other
IgG2b
IgG1
IgA

Figure 1. **Unique characteristics of thymic B cells from NOD mice. (A)** Representative flow cytometry profiles and **(B)** quantification of MHC II by B cells from the spleen and the thymus of B6 and NOD mice (n = 7-8), measured by mean fluorescence intensity (MFI). **(C)** Representative flow cytometry profiles of CD80 on splenic and thymic B cells ($CD19^+B220^+$) from B6 and NOD mice. **(D)** Compilation of the percentage of $CD80^+$ B cells from the spleen and thymus of B6 and NOD mice (n > 14). **(E)** Representative flow cytometry profile of IgM and IgD on thymic B cells from B6 and NOD mice. **(F)** Compilation of the percentage of IgM^-IgD^- thymic B cells from B6 and NOD mice (n > 16). **(G)** Compilation of the percentage of IgM^-IgD^- thymic B cells from genetically divergent mouse strains (n ≥ 3). **(H)** Distribution of isotypes expressed by IgM^-IgD^- thymic B cells from the same mice as in **(F)**. "Other" refers to B cells with a $IgD^-IgM^-IgA^-IgG1^-IgG2b^-$ phenotype.

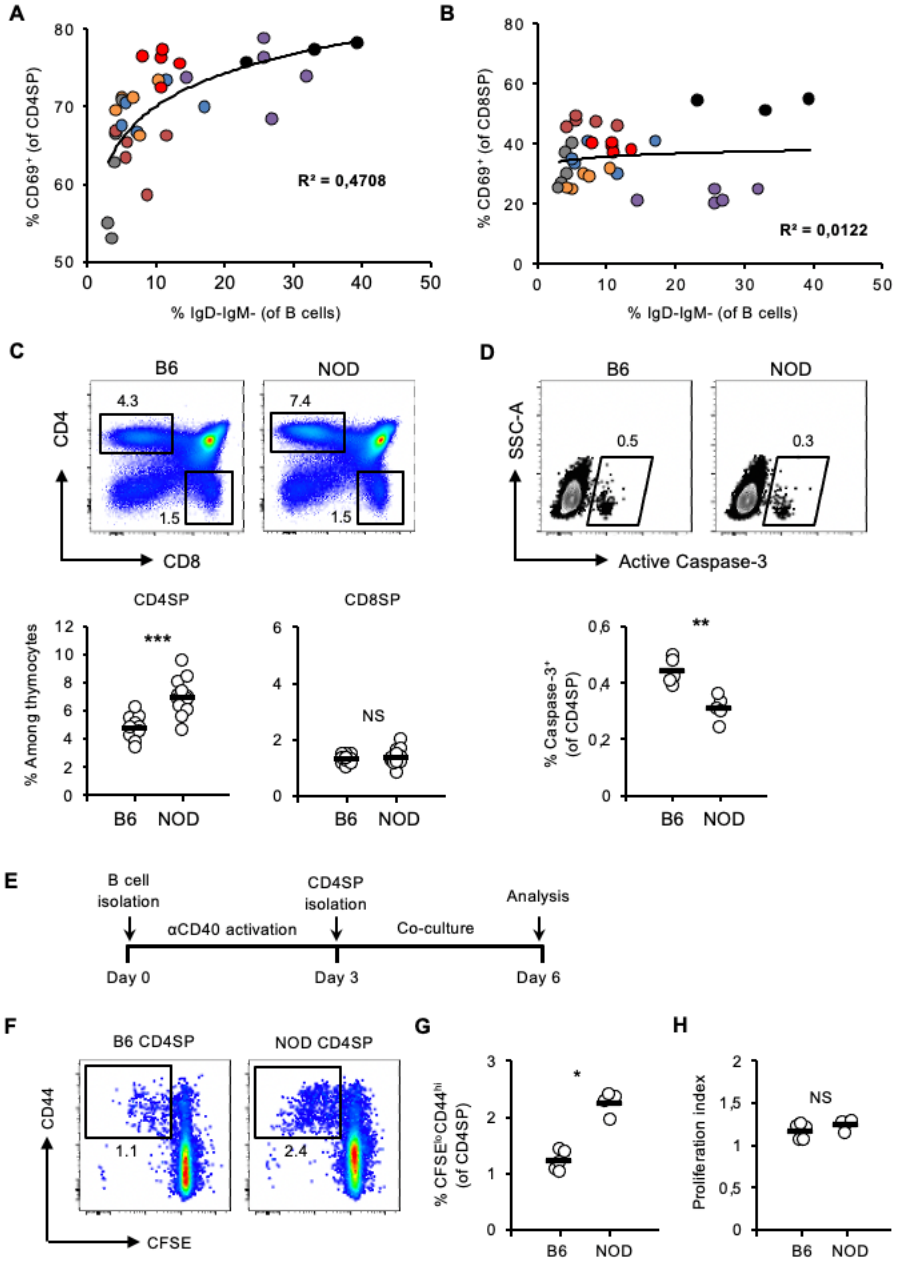
A
% CD69+ (of CD4SP)
% IgD-IgM- (of B cells)
R² = 0,4708
B
% CD69+ (of CD8SP)
% IgD-IgM- (of B cells)
R² = 0,0122
C
B6
NOD
CD4
CD8
4.3
1.5
7.4
1.5
CD4SP
CD8SP
% Among thymocytes
***
NS
B6
NOD
D
B6
NOD
SSC-A
Active Caspase-3
0.5
0.3
% Caspase-3+ (of CD4SP)
**
B6
NOD
E
B cell isolation
αCD40 activation
CD4SP isolation
Co-culture
Analysis
Day 0
Day 3
Day 6
F
B6 CD4SP
NOD CD4SP
CD44
CFSE
1.1
2.4
G
% CFSEloCD44hi (of CD4SP)
*
B6
NOD
H
Proliferation index
NS
B6
NOD

Figure 2. **NOD thymic B cell traits correlate with reduced T cell tolerance to self-antigens.** Correlation between the percentage of isotype-switched thymic B cells and the expression of CD69 on **(A)** CD4SP and **(B)** CD8SP thymocytes from the same mice as in Fig. 1F. **(C)** Representative flow cytometry profile (top panel) and compilation (bottom panel) of CD4SP and CD8SP subsets in the thymus of B6 and NOD mice (n = 10-11). **(D)** Representative flow cytometry profile (top panel) and percentage (bottom panel) of active caspase-3^+ CD4SP thymocytes from B6 and NOD mice (n = 5). **(E)** Schematic of the *in vitro* co-culture assay used in F-H. **(F)** Representative flow cytometry profile of CFSE and CD44 expression on CD4SP thymocytes from the co-cultures. **(G)** Compilation of the percentage of $CFSE^{lo}CD44^{hi}$ cells in thymocytes from the co-cultures (n = 4-5). **(H)** Proliferation index of the thymocytes at the end of the co-cultures (n = 4-5).

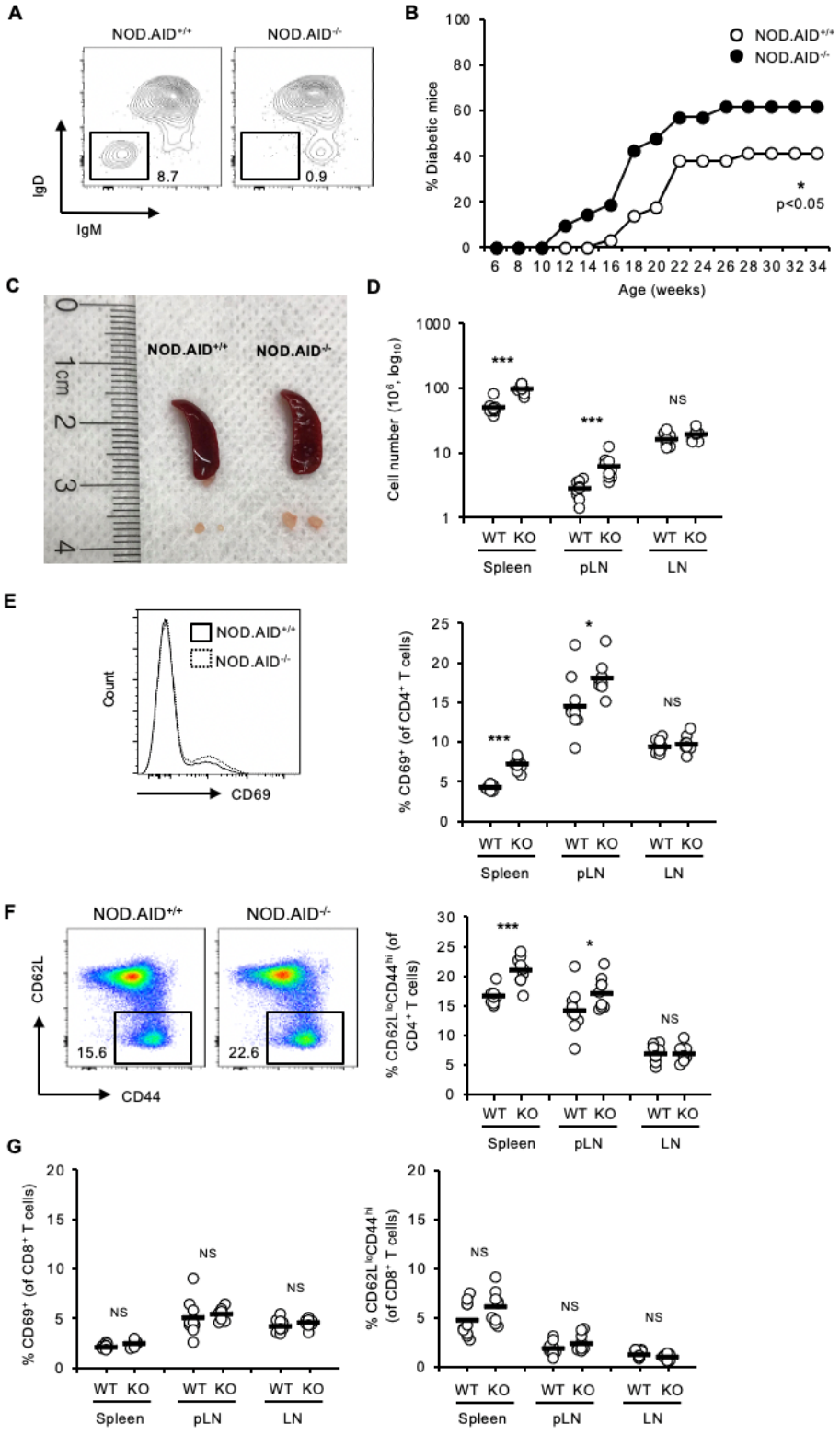
A
NOD.AID+/+
NOD.AID-/-
IgD
IgM
8.7
0.9
B
NOD.AID+/+
NOD.AID-/-
% Diabetic mice
Age (weeks)
*
p<0.05
C
NOD.AID+/+
NOD.AID-/-
D
Cell number (10^6, log10)
***
NS
WT KO
Spleen
pLN
LN
E
NOD.AID+/+
NOD.AID-/-
Count
CD69
% CD69+ (of CD4+ T cells)
F
NOD.AID+/+
NOD.AID-/-
CD62L
CD44
15.6
22.6
% CD62L^loCD44^hi (of CD4+ T cells)
G
% CD69+ (of CD8+ T cells)
% CD62L^loCD44^hi (of CD8+ T cells)

Figure 3. **AID deficiency promotes the development of autoimmune diabetes. (A)** Representative flow cytometry profile of IgM and IgD expression on thymic B cells from NOD.AID$^{+/+}$ and NOD.AID$^{-/-}$ mice. **(B)** Diabetes incidence of female NOD.AID$^{+/+}$ (n = 29) and NOD.AID$^{-/-}$ (n = 21) mice. **(C)** Image of representative spleens and pancreatic lymph nodes from non-diabetic NOD.AID$^{+/+}$ and NOD.AID$^{-/-}$ mice. **(D)** Absolute numbers of cells in the spleen, pancreatic and skin draining lymph nodes from non-diabetic NOD.AID$^{+/+}$ and NOD.AID$^{-/-}$ mice (n = 9-10). **(E)** Representative flow cytometry profile of splenic CD4^{+} T cells (left panel) and compilation of the percentage (right panel) of CD69^{+} CD4^{+} T cells from the spleen, pancreatic lymph nodes, and skin draining lymph nodes of non-diabetic NOD.AID$^{+/+}$ and NOD.AID$^{-/-}$ mice (n = 9-10). **(F)** Representative flow cytometry profile of splenic CD4^{+} T cells (left panel) and compilation of percentage (right panel) of CD62L^{lo}CD44^{hi} CD4^{+} T cells from the spleen, pancreatic lymph nodes and skin draining lymph nodes of non-diabetic NOD.AID$^{+/+}$ and NOD.AID$^{-/-}$ mice (n = 9-10). **(G)** Compilation of the percentage of CD69^{+} (left panel) and CD62L^{lo}CD44^{hi} (right panel) CD8^{+} T cells from the spleen, pancreatic lymph nodes and skin draining lymph nodes of non-diabetic NOD.AID$^{+/+}$ and NOD.AID$^{-/-}$ mice (n = 9-10).

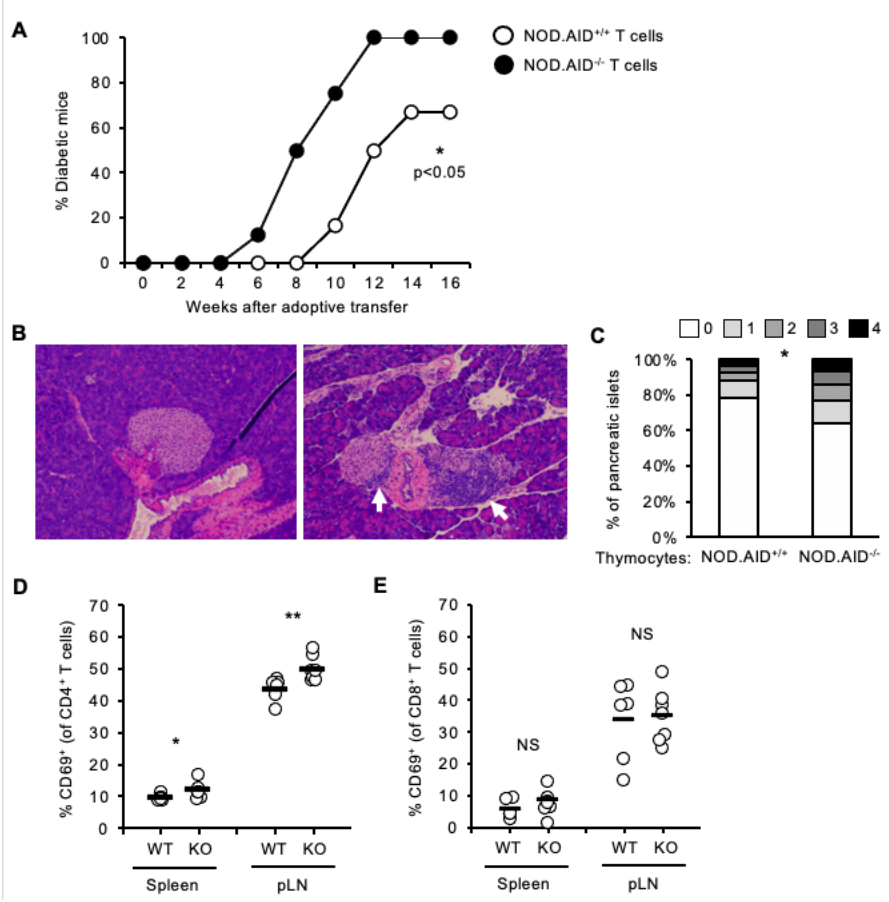

Figure 4. **AID deletion impacts T cell diabetogenicity and enhances insulitis. (A)** Diabetes incidence of female NOD.Rag$^{-/-}$ mice that received 6-8 x 10^6 total splenic T cells from age-matched non-diabetic female NOD.AID$^{+/+}$ and NOD.AID$^{-/-}$ mice (n = 6-8). **(B)** Representative images of an intact (left) and infiltrated (right) islet from the pancreas of a NOD.Rag$^{-/-}$ mouse, 10 weeks after injection of 22 x 10^6 total NOD.AID$^{-/-}$ thymocytes. **(C)** Insulitis score for female NOD.Rag$^{-/-}$ mice 10 weeks post-injection of 22 x 10^6 total thymocytes from adult female NOD.AID$^{+/+}$ or NOD.AID$^{-/-}$ mice (n = 6-7). Scale: 0 = no infiltration, 1 = peri-insulitis, 2 = infiltration <50%, 3 = infiltration >50%, 4 = complete infiltration. Compilation of the percentage of CD69$^+$ CD4$^+$ **(D)** and CD8$^+$ **(E)** T cells at the time of sacrifice of the mice described in **(C)** (n =6-7).

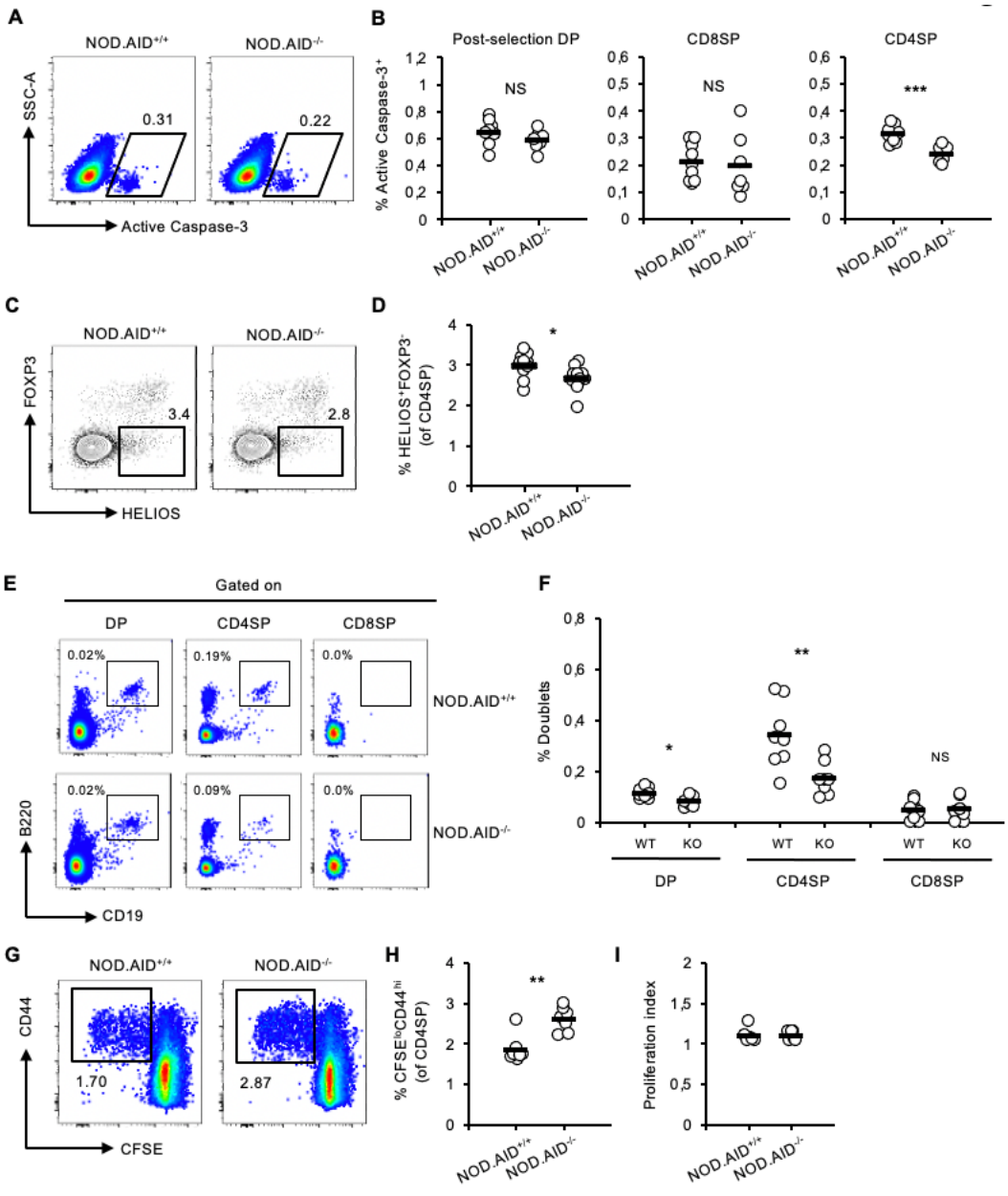
A
NOD.AID+/+
NOD.AID-/-
SSC-A
0.31
0.22
Active Caspase-3
B
Post-selection DP
CD8SP
CD4SP
% Active Caspase-3+
NS
NS
***
NOD.AID+/+
NOD.AID-/-
C
NOD.AID+/+
NOD.AID-/-
FOXP3
3.4
2.8
HELIOS
D
% HELIOS+FOXP3- (of CD4SP)
*
NOD.AID+/+
NOD.AID-/-
E
Gated on
DP
CD4SP
CD8SP
0.02%
0.19%
0.0%
NOD.AID+/+
0.02%
0.09%
0.0%
NOD.AID-/-
B220
CD19
F
% Doublets
*
**
NS
WT
KO
DP
CD4SP
CD8SP
G
NOD.AID+/+
NOD.AID-/-
CD44
1.70
2.87
CFSE
H
% CFSEloCD44hi (of CD4SP)
**
NOD.AID+/+
NOD.AID-/-
I
Proliferation index
NOD.AID+/+
NOD.AID-/-

Figure 5. **AID deletion impairs negative selection of CD4SP thymocytes. (A)** Representative flow cytometry profiles of CD4SP thymocytes and **(B)** compilation of the percentage of active caspase-3^+ DP, CD4SP and CD8SP thymocytes from NOD.$AID^{+/+}$ and NOD.$AID^{-/-}$ mice (n = 8-10). **(C)** Representative flow cytometry profiles and **(D)** compilation of the percentage of $HELIOS^+$ CD4SP thymocytes from NOD.$AID^{+/+}$ and NOD.$AID^{-/-}$ mice (n = 9-13). **(E)** Representative flow cytometry profiles of ex vivo DP, CD4SP and CD8SP thymocytes conjugated with thymic B cells from NOD.$AID^{+/+}$ and NOD.$AID^{-/-}$ mice. **(F)** Compilation of the percentage of DP, CD4SP and CD8SP conjugated to thymic B cells from NOD.$AID^{+/+}$ and NOD.$AID^{-/-}$ mice, adjusted to the percentage of total B cells in the thymus of each mouse (n = 8-9). **(G)** Representative flow cytometry profiles of CFSE and CD44 expression of CD4SP thymocytes from co-cultures with activated splenic B cells from NOD.$AID^{+/+}$ and NOD.$AID^{-/-}$ mice. **(H)** Compilation of the percentage of $CFSE^{lo}CD44^{hi}$ cells in thymocytes from the co-cultures (n = 7). **(I)** Proliferation index of the thymocytes at the end of the co-cultures (n = 7).

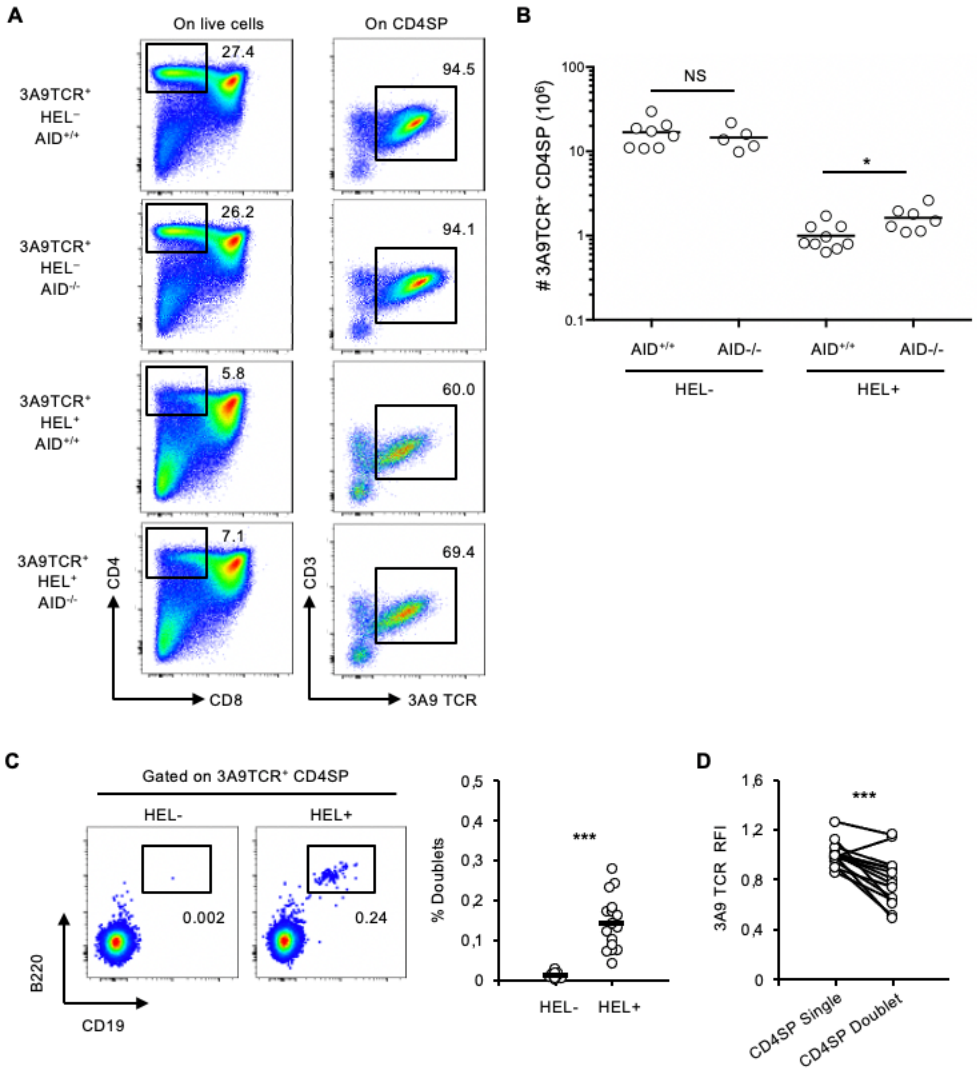
A
On live cells
On CD4SP
3A9TCR+ HEL− AID+/+
3A9TCR+ HEL− AID-/-
3A9TCR+ HEL+ AID+/+
3A9TCR+ HEL+ AID-/-
27.4
94.5
26.2
94.1
5.8
60.0
7.1
69.4
CD4
CD8
CD3
3A9 TCR
B
3A9TCR+ CD4SP (10^6)
NS
*
AID+/+
AID-/-
AID+/+
AID-/-
HEL-
HEL+
C
Gated on 3A9TCR+ CD4SP
HEL-
HEL+
0.002
0.24
B220
CD19
% Doublets
***
HEL-
HEL+
D
3A9 TCR RFI
***
CD4SP Single
CD4SP Doublet

Figure 6. **AID expression promotes clonal deletion of self-reactive thymocytes. (A)** Representative flow cytometry profiles of 3A9 TCR-transgenic CD4SP thymocytes from single transgenic (HEL^-) and double transgenic (HEL^+) B10.BR mice. **(B)** Compilation of the number of 3A9 TCR^+ CD4SP thymocytes in the same mice presented in (A) (n = 5-9). **(C)** Representative flow cytometry profiles (left panel) and compilation (right panel) of conjugates between 3A9 TCR^+ CD4SP thymocytes and thymic B cells in HEL^- and HEL^+ transgenic B10.BR mice. **(D)** RFI (Relative fluorescence intensity) of the 3A9 TCR on the surface of 3A9 TCR^+ CD4SP thymocytes, conjugated or not with thymic B cells (n = 16). RFI were calculated by normalizing to the average of the 3A9 TCR MFI on CD4SP single cells for each experiment.

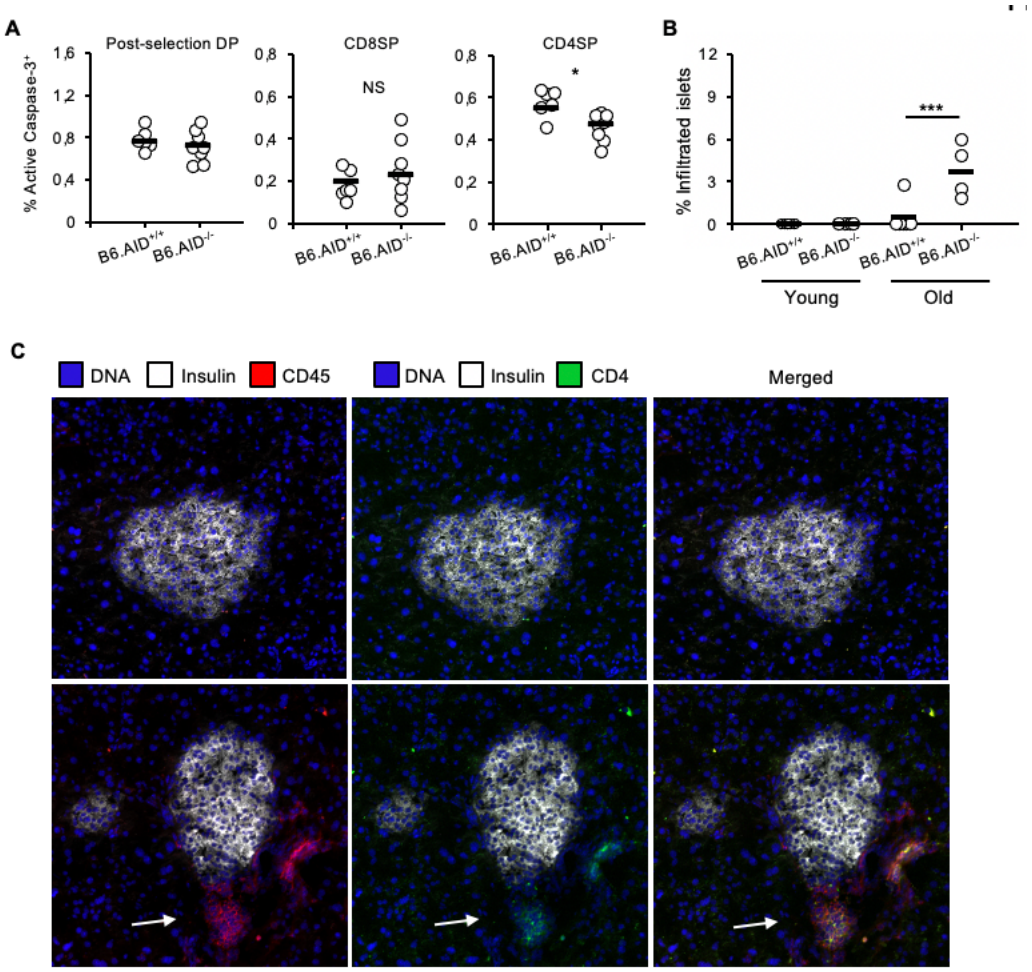

Figure 7. **Deletion of AID in B6 mice limits apoptosis of CD4SP thymocytes and induces insulitis. (A)** Compilation of the percentage of active caspase-3^{+} post-selection DP, CD8SP and CD4SP thymocytes from B6.$AID^{+/+}$ and B6.$AID^{-/-}$ mice (n =6-8). **(B)** Compilation of the percentage of infiltrated pancreatic islets in 2-month-old and 12-month-old B6.$AID^{+/+}$ and B6.$AID^{-/-}$ mice (n = 4-6). **(C)** Representative fluorescence microscopy image of pancreatic islets from a 12-month-old B6.$AID^{-/-}$ mouse, with (bottom panels) and without (top panels) peri-insulitis (magnification 10X).

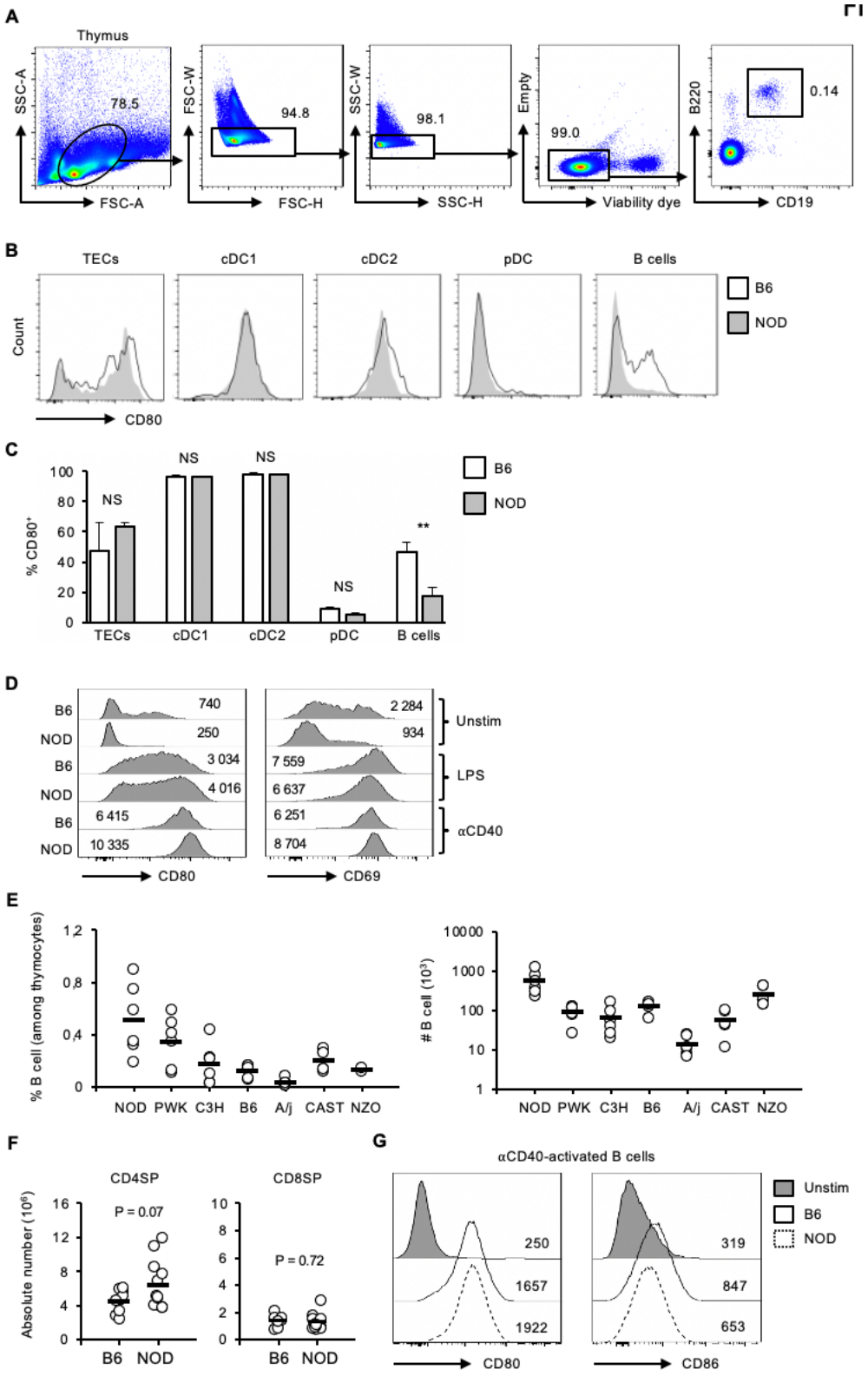
A
Thymus
SSC-A
78.5
FSC-A
FSC-W
94.8
FSC-H
SSC-W
98.1
SSC-H
Empty
99.0
Viability dye
B220
0.14
CD19
B
TECs
cDC1
cDC2
pDC
B cells
Count
CD80
B6
NOD
C
% CD80+
NS
NS
NS
**
NS
TECs
cDC1
cDC2
pDC
B cells
B6
NOD
D
B6
NOD
740
250
3 034
4 016
6 415
10 335
2 284
934
7 559
6 637
6 251
8 704
Unstim
LPS
αCD40
CD80
CD69
E
% B cell (among thymocytes)
NOD PWK C3H B6 A/j CAST NZO
B cell (10³)
NOD PWK C3H B6 A/j CAST NZO
F
CD4SP
CD8SP
Absolute number (10⁶)
P = 0.07
P = 0.72
B6 NOD
B6 NOD
G
αCD40-activated B cells
250
1657
1922
319
847
653
Unstim
B6
NOD
CD80
CD86

Figure S1. **Characterization of thymic APCs in NOD mice. (A)** Gating strategy for the analysis of thymic B cells. **(B)** Representative flow cytometry profiles of CD80 expression on thymic APC subsets, from B6 and NOD mice. **(C)** Compilation of the percentage of $CD80^+$ thymic APCs from B6 and NOD mice (n = 3). **(D)** Representative flow cytometry profiles of thymic B cells from B6 and NOD mice, unstimulated or stimulated with LPS or anti-CD40 antibodies for 72h. MFI is indicated. **(E)** Compilation of the percentage and number of thymic B cells in various mouse strains (n = 3-6). **(F)** Compilation of absolute numbers of CD4SP and CD8SP thymocytes in B6 and NOD mice (n = 10-11). **(G)** Representative cytometry profiles of CD80 and CD86 expression on CD40-activated splenic B cells and unstimulated controls (from B6), from B6 and NOD mice. MFI is indicated.

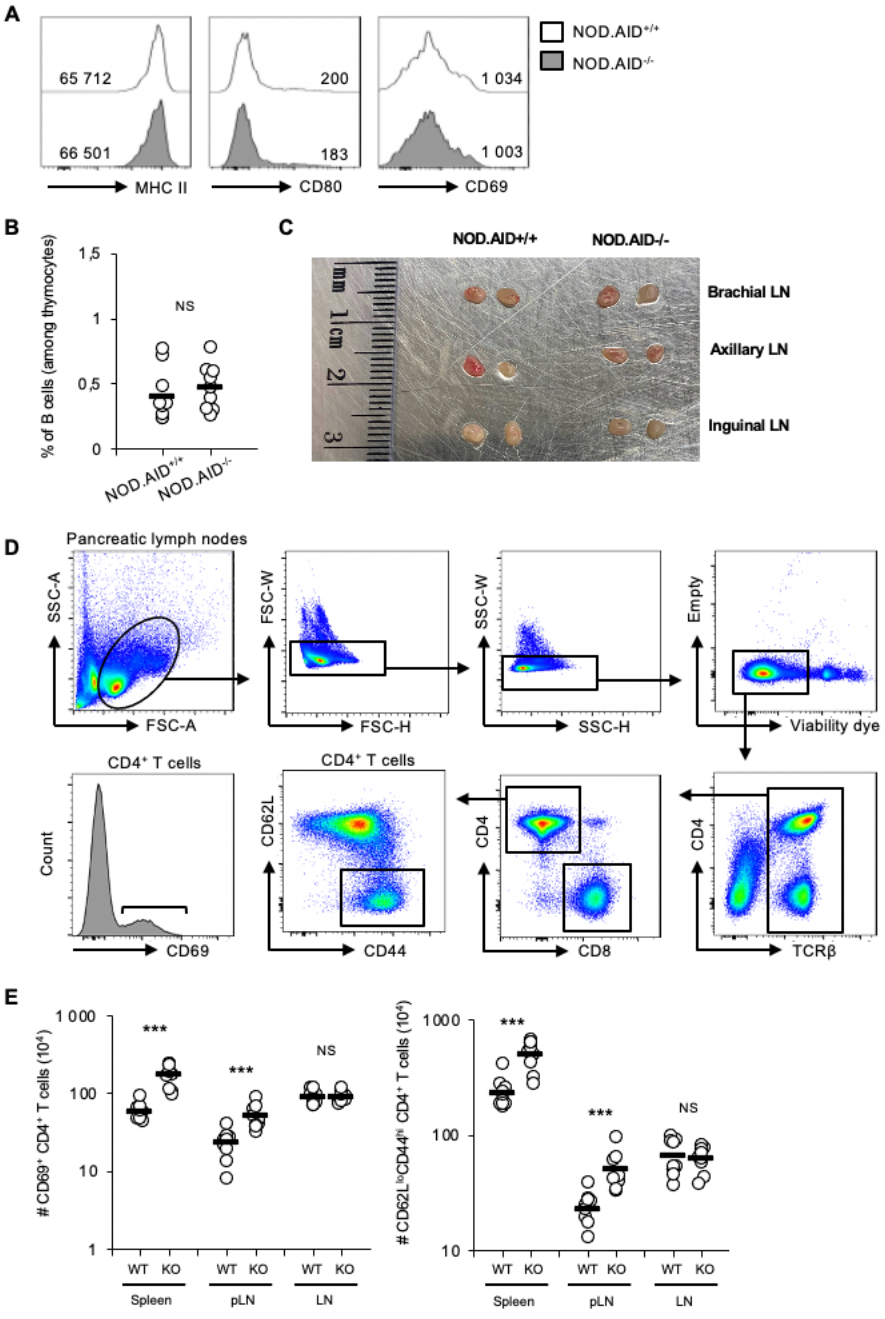
A
65 712
66 501
200
183
1 034
1 003
NOD.AID+/+
NOD.AID-/-
MHC II
CD80
CD69
B
% of B cells (among thymocytes)
NS
NOD.AID+/+
NOD.AID-/-
C
NOD.AID+/+
NOD.AID-/-
Brachial LN
Axillary LN
Inguinal LN
D
Pancreatic lymph nodes
SSC-A
FSC-A
FSC-W
FSC-H
SSC-W
SSC-H
Empty
Viability dye
CD4+ T cells
Count
CD69
CD4+ T cells
CD62L
CD44
CD4
CD8
CD4
TCRβ
E
CD69+ CD4+ T cells (10⁴)
CD62L^lo CD44^hi CD4+ T cells (10⁴)
***
NS
WT KO
Spleen
pLN
LN

Figure S2. **Characterization of B and T cells in NOD.AID$^{-/-}$ mice. (A)** Representative cytometry profiles of MHC II, CD80 and CD69 expression on thymic B cells from NOD.AID$^{+/+}$ and NOD.AID$^{-/-}$ mice; MFI is indicated. **(B)** Compilation of the percentage of B cells in the thymus of NOD.AID$^{+/+}$ and NOD.AID$^{-/-}$ mice (n = 8-9). **(C)** Image of representative skin draining lymph nodes from non-diabetic NOD.AID$^{+/+}$ and NOD.AID$^{-/-}$ mice. **(D)** Gating strategy for the analysis of quantification of activated CD4^{+} and CD8^{+} T cells. **(E)** Absolute numbers of CD69^{+} and CD62L^{-}CD44^{hi} CD4^{+} T cells from the spleen, pancreatic lymph nodes and skin draining lymph nodes of NOD.AID$^{+/+}$ and NOD.AID$^{-/-}$ mice (n = 9-10).

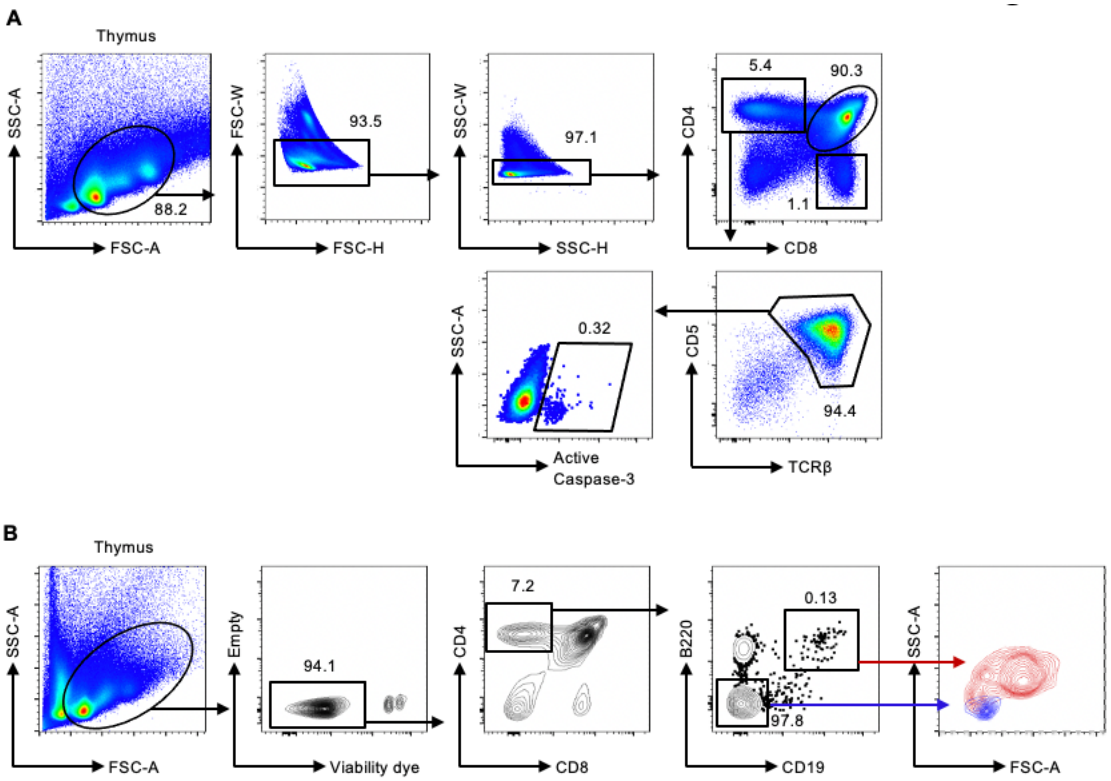

Figure S3. **Analysis of thymocytes and thymic B cells by flow cytometry**. Gating strategies for **(A)** the expression of active caspase-3 in thymocytes and **(B)** quantification of thymocytes conjugated with thymic B cells.

Chapter 5:

Discussion

The pathogenesis of T1D has been studied for several decades. While many factors favoring or limiting the development of this autoimmune disease have been identified, we still do not completely understand why, in some susceptible individuals, a breach of tolerance against pancreatic cells occurs. In chapters 2-4, we have investigated genetic and cellular factors that influence the interplay between T and B cells, and how this crosstalk influences the development of autoimmune diabetes, the mouse equivalent of T1D.

5.1 The *Idd2* locus confers prominent resistance to autoimmune diabetes

In chapter 2, we have investigated the importance of genetic variants in the *Idd2* locus in autoimmune diabetes susceptibility. To do so, we generated a congenic strain (NOD.*Idd2*), which share >99% of its genetic background with the NOD strain, except for a locus on chromosome 9 (coinciding with part of the *Idd2* locus) of B10 origin. Compared to NOD mice, NOD.*Idd2* mice were highly protected from autoimmune diabetes, with very low diabetes onset and significantly lower insulitis levels. Using bone marrow-chimeras and by performing adoptive cell transfers, we showed that the diabetes protection conferred by the *Idd2* locus is mediated by immune cells rather than modulation of pancreatic function. Phenotyping of immune cell subsets in NOD.*Idd2* mice revealed a reduction of B cell class-switching and GC formation. This finding was generalized to spontaneous GC in the pancreas and secondary lymphoid organs, as well as GC formation following immunization. Transcriptomic analysis of splenic B cells from NOD and NOD.*Idd2*

mice revealed a signature for antigen presentation, with a reduction of expression of specific MHC molecules (H2-D1, H2-Q6, H2-Q7) on B cells from NOD.*Idd2* mice. Flow cytometry analysis confirmed a reduction of H2-D expression on all immune cells of NOD.*Idd2* mice and revealed a B cell-specific reduction of MHC II molecules. To test the functional impact of this reduction of MHC expression on T cell activation, we performed allogenic in vitro activation assays and LCMV infections. In both cases, the reduction of MHC expression in NOD.*Idd2* mice resulted in a reduction of T cell activation and priming, demonstrating the indirect impact of the *Idd2* locus on T cell responses.

The MHC locus (*Idd1* in mice, *IDDM1* in humans) represents the most important genetic locus in the control of T1D susceptibility (131). It is therefore highly likely that the reduction of MHC expression in NOD.*Idd2* mice and the resulting impact on T cell responses play a major role in the diabetes protection of the congenic strain. While the reduction of MHC II expression is specific to B cells, MHC I expression is reduced on all immune cells tested, meaning that all APC types express lower levels of H2-D. Is it therefore unclear if the reduction of activation of $CD8^+$ T cells in the LCMV infected mice or the reduction of diabetes onset is mediated, at least in part, by B cells. Indeed, those phenotypes could also be caused by the reduction of MHC I expression on DCs, which are known to be efficient APCs for the priming of $CD8^+$ T cells.

To address the specific contribution of B cells, we performed adoptive cell transfer into lymphopenic NOD mice. Unfortunately, when transferred together with T cells from NOD mice, B cells from NOD.*Idd2* mice did not survive (data not shown). The reduced level of MHC I expression of B cells from NOD.*Idd2* mice could contribute to loss of these B cells in the recipient

mice. Indeed, as part of their immunosurveillance mechanisms, NK cells effectively target and eliminate cells that express low levels of MHC (389). To circumvent this issue, it would be interesting to acquire B cell-deficient NOD mice. MuMt$^{-/-}$ mice, which bear a mutation in the gene encoding for the heavy chain of IgM, completely lack mature B cells. When crossed to NOD mice, this results in B cell-deficient NOD mice that present with low incidence of diabetes (211). These mice could be used as bone marrow-chimeras recipients to generate mice with B cells from NOD.*Idd2* mice and other APCs from NOD mice (see figure 6 below). As T cells and NK cells would develop in environments containing cells of NOD.*Idd2* origin (with low H2-D expression), these cells may become tolerant, therefore inhibiting the killing of NOD.*Idd2* cells. Diabetes incidence could then be compared between chimeras with all APC types from NOD mice and chimeras with B cells from NOD.*Idd2* mice and a mix of other APC types from both NOD and NOD.*Idd2* mice. This model is not perfect, as some other APCs would also be of NOD.*Idd2* origin (Fig. 6). The contribution of these NOD.*Idd2*-derived APCs could be reduced by lowering the % of NOD.*Idd2* stem cells injected in the chimeras, as long as the homeostatic proliferation of the resulting B cells would allow sufficient reconstitution of the B cell pool in the chimeras.

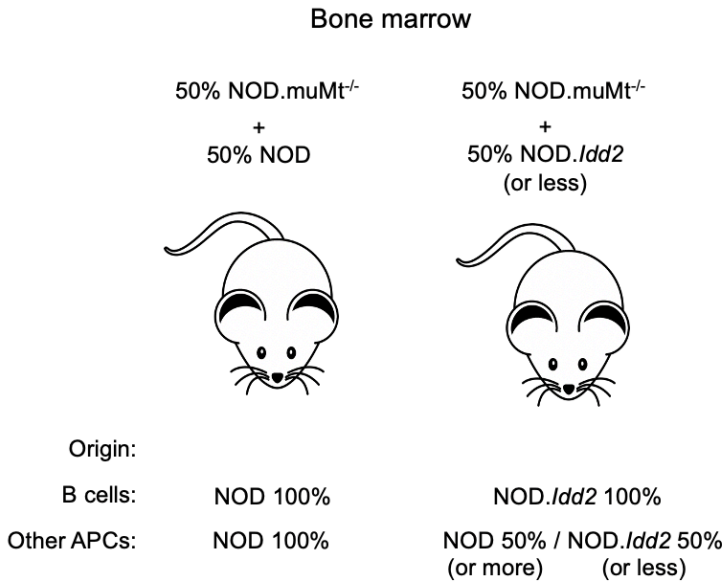

Figure 1: Schematic representation of bone marrow-chimeras for the study of the contribution of NOD.*Idd2* B cells in the diabetes protection of NOD.*Idd2* mice.

Another unresolved element regarding the implication of the *Idd2* locus in the regulation of MHC expression is the identification of the genetic variant (or variants) inside the locus that control MHC expression. Notably, as H2-D1 and I-A seem to be regulated at different levels (transcriptional regulation of H2-D1 and post-transcriptional regulation for I-A), it is likely that regulation of expression of these molecules is independent. With our RNA-seq analysis, we have identified 14 DEGs in the *Idd2* locus of our congenic mouse. Those include *Crtam, Hspa8, Usp2, Jhy, Tmprss13, Ubash3b, Nxpe1/2/4* and other genes with yet unknown functions. With only *Crtam* and *Hspa8* having an identified role in the immune system, there is no clear candidate gene for the regulation of MHC expression. For this reason, each gene should be tested, starting with the genes with a known function. Since our RNA-seq was performed on a heterogeneous

population of cells (total splenic B cells), it is possible that some genes expressed only in some rare B cells subsets in the spleen (such as B1 B cells) may have been missed. An alternative approach would have been to perform single-cell RNAseq, to obtain a better view of the heterogeneity in the B cell populations. Furthermore, we have focused our analysis on protein-coding genes, but genes coding for lncRNA or miRNA could also be responsible for the phenotypes observed in our congenic mice.

To test the impact of each gene on MHC expression, we could use cell lines and perform knock outs or knock down of each gene, one by one. These techniques are easier to perform in vitro in immortalized cells, rather than on primary cells. As the regulation of I-A expression was B cell-specific in our study, it suggests that modulation of this specific MHC molecule by a variant of the *Idd2* locus requires other factor(s) uniquely present in B cells. We would therefore use cell lines of B cell origin to increase our chances of recapitulating the phenotype observed in NOD.*Idd2* mice. Knocking out a gene, to completely eliminate its expression, can be done via CRISPR-Cas9 technology. In contrast, genetic knock down only partially reduces the expression of a gene. These can be done using shRNAs, which either eliminate its mRNA target or inhibit its translation (390). Efficient knock out or knock down can be confirmed by RT-qPCR. Once reduced expression of our target gene is confirmed, the impact on MHC expression can be assessed by flow cytometry. These experiments would be performed in multiple different cell lines, as most cell lines display large amounts of mutations that could potentially influence the effect of the Knock out/down. It is however not impossible that non-protein coding genes, such as small interfering RNAs, are responsible for the modulation of MHC expression in the NOD.*Idd2* strain. In that case, we would not observe any phenotype with the inhibition of any of the 14 genes identified in our transcriptomic analysis. If we identify a gene that significantly impact MHC expression in vitro,

these observations should be confirmed in vivo. By transducing shRNAs, knock down can be performed in primary murine hematopoietic stem cells (HSCs). These transduced HSCs can then be transferred into lethally irradiated mice to generate chimeras with immune cells expressing low levels of the target gene (391). MHC expression on immune cells would then be quantified and compared to cells from chimeras that received HSCs transduced with empty viral vectors.

In addition to the reduction of MHC expression, genetic variants in the *Idd2* locus also modulate formation of GCs. Since spontaneous GCs can be observed in the pancreas and secondary lymphoid organs of NOD mice, GCs have been suggested to participate in the pathology of T1D (231, 392). The implication of GCs in T1D have, however, never been directly assessed. It is still unknown if GCs directly participate in the pathology or if they are simple bystanders, resulting from the ongoing inflammation. It would be interesting to address this long-lasting unresolved question.

We have tried inhibiting GC formation in pre-diabetic NOD mice by repeated injections of the BCL6 inhibitor 79-6 (393). Unfortunately, GC formation was not significantly reduced in vivo (data not shown), likely because the dosage was insufficient. Long-term inhibition of BCL6 in vivo using pharmacologic inhibitors will likely result in toxicity. Therefore, a more targeted approach, using genetic inhibition of GC formation would be more appropriate to effectively inhibit GC in NOD mice. Two transcriptional regulators, BCL6 and OCA-B, could be disrupted to inhibit GC formation. However BCL6 play important roles outside of the GC, in both B and T cells (394), complicating the eventual interpretation of BCL6 disruption. Similarly, OCA-B plays multiple roles in B cell biology, inside and outside the GCs. An alternative strategy would be to

disrupt the function of FDCs, central players in GCs. FDCs express high levels of CD21 (complement receptor 2, *Cr2*), which is used to present complement bound antigens to B cells in the light zone of GCs (395). In *Cr2*$^{-/-}$ mice, the size and number of GCs are severely reduced (396). However, in addition to its high expression of FDCs, CD21 is also expressed on follicular B cells. To specifically target FDCs, bone marrow-chimeras could be generated. Since FDCs are not derived from HSC, reconstitution of lethally irradiated CD21$^{-/-}$ mice with WT bone marrow would result in specific deletion of CD21 on FDCs, with normal expression on B cells. This experimental design is feasible, as a similar approach was used to study FDC-specific traits (397). Notably, applying this system in mice carrying the NOD genetic background would inform us of the implication of GCs in the pathology of autoimmune diabetes.

Lastly, it would be interesting to test the effect of the NOD derived alleles at the *Idd2* locus on a non-diabetes prone mouse strain, i.e. to generate a B6.*NOD-Idd2* mouse as a corollary to the NOD.*B6-Idd2* mouse. Indeed, except for the *Idd1* locus which confers 100% diabetes protection, the *Idd2* locus is, to date, the locus conferring the strongest diabetes protection on the NOD background. Most non-MHC loci only confer modest protection against insulitis and autoimmune diabetes, with *Idd3* and *Idd5* conferring the strongest protection after *Idd2* (137). Around 30% of female NOD.*Idd3* mice (145) and 50% of female NOD.*Idd5* mice (398) develop autoimmune diabetes, which is higher than the 10% of female NOD.*Idd2* mice (chapter 2). It would therefore be interesting to know if inserted NOD alleles at *Idd2* locus in B6 mice would be sufficient to induce diabetes onset or insulitis. As B6.*Idd1* mice (B6 mice bearing the NOD MHC, H-2^{g7}) and other mice congenic for various *Idds* do not progress to diabetes and only show mild peri-insulitis (142), it is unlikely that B6.*Idd2* mice would progress to diabetes. However, a combination of

NOD alleles at both the *Idd1* and *Idd2* loci could be sufficient to promote diabetes onset, such that B6.*NOD-Idd1/Idd2* double congenic mice may progress to overt diabetes. To do so, B6 and NOD mice would be crossed, followed by > 10 backcross to B6 mice. By genotyping the *Idd2* locus at each generation and only using mice that retain the *Idd2* locus of NOD origin, we would obtain B6.*Idd2* mice. These mice would then be cross to B6.*Idd1* mice to generate the double congenic strain. If these congenic mice develop autoimmune diabetes, they would represent the first non-transgenic mouse model of B6 origin to spontaneously progress to autoimmune diabetes. This model would indicate that NOD alleles at *Idd1* and *Idd2* are sufficient to break immune tolerance to pancreatic self-antigens and could be used to further dissect out key cellular and molecular mechanisms driving the autoimmune response.

5.2 Cell intrinsic role of OCA-B in B cells but not in T cells

Concurrent to our investigations in NOD.*Idd2* mice, in chapter 3, we investigated the cell-intrinsic role of the transcriptional co-activator OCA-B. *Pou2af1*, encoding for OCA-B, is present on the chromosome 9 of the mouse, inside the initially identified *Idd2* locus (144). We have focused on this particular gene for multiple reasons, such as its high expression in B cells and its important role for the formation of GCs and IgG production (74), which were both reduced in our congenic NOD.*Idd2* mice. Therefore, *Pou2af1* represented the most obvious candidate gene of our locus. However, our transcriptomic analysis of NOD and NOD.*Idd2* B cells did not detect differential expression of *Pou2af1* (Chapter 2) and revealed that *Pou2af1* is situated outside of our locus of interest. These observations make it unlikely that genetic variants in *Pou2af1* are responsible for the diabetes protection of the NOD.*Idd2* mice.

Interestingly, concurrent with our ongoing work, a study demonstrated that disruption of OCA-B in NOD mice significantly inhibited diabetes onset (399). This observation suggested that, while *Pou2af1* was no longer a candidate gene in our chromosome 9 locus, *Pou2af1* may still have important roles in the development autoimmune diabetes. Since the mechanism behind the participation of OCA-B in diabetes susceptibility remained unknown, we took advantage of our newly generated *Pou2af1*^{flox} mouse to study the cell-intrinsic role of OCA-B. OCA-B is highly expressed in B cells and multiple roles for this transcriptional co-activator have been identified in B cells (46). OCA-B expression is also induced in T cells after activation (Chapter 3). Since T cells and B cells play central roles in T1D and autoimmune diabetes, OCA-B could participate in T1D pathogenesis through modulation of T cell and/or B cell function. Studies of OCA-B in T

cells have all been performed using the *Pou2af1*$^{-/-}$ mouse, a mouse with mixed genetic background (B6 and 129S) and a germline mutation in the *Pou2af1* gene that completely disrupt OCA-B expression. The germline mutation does not allow to specifically investigate the T and B cell specific role of OCA-B. With the growing evidence that OCA-B can be expressed in both T and B cells, we decided to investigate the cell-intrinsic role of OCA-B in T cells.

We generated a mouse model using the Cre/Lox technology, allowing for cell-specific disruption of *Pou2af1* in vivo. While we confirmed induction of *Pou2af1* expression in T cells after activation, we showed that OCA-B deletion does not explain most of the previously identified phenotypes (IL-2 production and Th17 differentiation). Rather, these traits can be explained by the mixed genetic background of the *Pou2af*1$^{-/-}$ mice, which were compared to B6 mice instead of B6x129 littermates during the initial studies (321, 323). The only phenotype that we recapitulated was the impaired Tfh development in *Pou2af1*$^{-/-}$ mice. However, the defect of Tfh maturation was not caused by loss of OCA-B in T cells, as shown in CD4Cre^{+}-OCA-B$^{fl/flx}$ mice and confirmed in competitive bone marrow chimeras. Rather, specific disruption of *Pou2af1* in B cells impairs the differentiation of T cells into mature Tfh. Finally, we show that disruption of *Pou2af1* has minimal (if any) impact on the T cell transcriptome, confirming that OCA-B is not an active transcriptional co-activator in T cells, contrary to previous beliefs. The only transcriptional changes observed in samples from CD4Cre^{+}-OCA-B$^{fl/fl}$ mice, relative to CD4Cre^{-}-OCA-B$^{fl/fl}$ mice, were also observed in samples from CD4Cre^{+}-OCA-B$^{+/fl}$ (i.e., heterozygous) mice. This suggests that expression of the CD4-Cre may be responsible for these changes in gene expression. To test this hypothesis, analysis of the transcriptome of cells from CD4Cre^{+}-OCA-B$^{+/+}$ and CD4Cre^{-}-OCA-B$^{+/+}$ could be performed. As expression of some Cre have been reported to impact immune cell functions (400),

it would be interesting to test the impact of the CD4Cre in the context of our study, by comparing CD4Cre^{-}-OCA-B$^{+/+}$ and CD4Cre^{+}-OCA-B$^{+/+}$ mice. Similarly, the potential impact of the insertion of loxP sequences could be investigated by comparing Cre^{-}OCA-B$^{fl/fl}$ mice to B6 (WT) mice. However, it is unlikely that an impact of the CD4Cre or loxP sequences would change the conclusion of our study, as no significant differences have been observed between CD4Cre^{-}-OCA-B$^{fl/fl}$ and CD4Cre^{+}-OCA-B$^{fl/fl}$ mice.

With this new discovery, it strongly suggests that the diabetes protection of NOD.OCA-B$^{-/-}$ mice is caused by depletion of OCA-B in B cells, rather than in T cells. Depletion of OCA-B impacts B cell development, germinal center formation, antibody production, BCR signaling and plasma cell differentiation (46). All of these phenotypes, with the possible exception of antibody production, could impact diabetes development in mice. Similarly to the proposed experiment described above, defining the implication of germinal centers in the pathology of T1D will help uncover the role of OCA-B in this disease.

Our work also contributed to better understanding the role of OCA-B in the crosstalk between T and B cells. Using bone marrow-chimeras, we have shown that the initial differentiation of CD4^{+} T cells in early Tfh is not affected by the lack of OCA-B, a step mostly dependent on DCs (77). Rather, the block in Tfh development seems to take place at the transition from early Tfh (CXCR5^{low}PD-1^{low}) to mature Tfh (CXCR5^{hi}PD-1^{hi}). Consistent with the requirement of B cell-specific expression of OCA-B for Tfh maturation (chapter 3), this transition is highly dependent on B cell-derived signals (77). To complement the results from our bone marrow-chimeras experiments, additional approaches could be used to confirm the specific block in Tfh maturation

in absence of OCA-B. For instance, naïve $CD4^+$ T cells, early Tfh and mature Tfh from immunized WT mice could be injected into immunized OCA-B-sufficient and deficient mice. The injected cells could then be tracked after multiple days in order to assess their maturation profile. We expect that naïve T cells will differentiate into early Tfh in both OCA-B-sufficient and deficient recipients, and reach a mature Tfh phenotype in OCA-B-sufficient mice. Similarly, a greater proportion of early Tfh injected should acquire a mature Tfh in OCA-B-sufficient mice. Lastly, the injection of mature Tfh would inform us on the impact of OCA-B deficiency on the stability and maintenance of the cells.

Our data point to a role for OCA-B in B cells to facilitate the early Tfh to mature Tfh transition. Various experimental approaches could be used to define the OCA-B-driven factors that allow the proper crosstalk between early Tfh and B cells. For example, fluorescence microscopy would allow to position early Tfh and B cell interactions. Notably, Tfh and B cell interactions initially take place at the border of the B cell follicles (77). As B cells are greatly affected by OCA-B deficiency, it is possible that B cell follicles display abnormalities in absence of OCA-B, which may impair the crosstalk between B cells and Tfh. Live imaging of lymph nodes from immunized OCA-B-sufficient and deficient mice could also be used to track the movement of early Tfh, as well at the length of interactions with B cells at the border of the follicles (401). Such experiment would indicate if the crosstalk between B and T cells is quantitatively diminished (reduction of interactions) or qualitatively diminished (signals from B cells are not sufficient to promote the maturation).

In addition to imaging, one could investigate the molecular factors that may explain the low number of mature Tfh in OCA-B-deficient mice. Indeed, the impact of the loss of OCA-B expression on follicular and germinal center B cells has yet to be fully elucidated. As such, it would be interesting to investigate the expression of molecules known to be involved in the interactions between B cells and Tfh. Among these, ICOSL and CD40 are relevant candidates. ICOS is expressed on early Tfh and its interaction with ICOSL on B cells promotes maturation into Tfh (77). Similarly, CD40 (on B cells) and CD40L (on T cells) are key molecules in the crosstalk between Tfh and GC B cells. While CD40-CD40L interactions mainly provide signals to the B cells, deficiency in CD40 or CD40L indirectly reduces Tfh number through its impact on B cells (402). Reduction of expression of ICOSL or CD40 on follicular B cells in OCA-B-deficient mice could therefore explain the impaired differentiation of Tfh. In addition to surface proteins, cytokines may also be important factors in this defective crosstalk. B cells can produce different pro-and anti-inflammatory cytokines, such as IL-4, IL-6, IL-12, IFNγ and IL-10 (403, 404). This raises the possibility that differential cytokine production by WT and OCA-B$^{-/-}$ B cells may impact maturation of early Tfh. Alternatively, RNA sequencing of B cells could be performed to obtain a more complete picture of the different molecular pathways potentially explaining the impaired crosstalk.

Lastly, it remains unknown why OCA-B is an active transcriptional co-activator specifically in B cells, even though its expression is induced in activated T cells. Indeed, OCA-B and its co-factors are suggested to promote the regulation of BCL6 (76), thereby allowing GC B cell differentiation. As BCL6 expression is also crucial for Tfh differentiation, regulation of BCL6 by OCA-B in CD4^{+} T cells would result in a cell-intrinsic role for OCA-B in Tfh differentiation.

However, we find no T cell-intrinsic role for OCA-B in Tfh differentiation. This suggests that B cell-specific co-factors or other transcription factors are required for OCA-B to modulate BCL6 expression. To that effect, a recent report demonstrated that OCA-B binds OCT2 and MEF2B, two B cell-specific transcription factors, and that cooperation between these three factors promote regulation of the BCL6 promoter in B cells (75).

Beyond GC formation, OCA-B mediates several other functions such as B cell development, BCR signaling, IgG production and plasma cell differentiation (46). As such, it is unlikely that regulation of BCL6 is the only target of OCA-B and its co-factors. It would therefore be interesting to define all B cell-specific OCA-B co-factors, as well as to compare them to T cell-specific OCA-B co-factors, if any. To identify OCA-B binding partners, BioID (405) and co-immunoprecipitation (Co-IP) assays could be performed using naïve T cells (no expression of OCA-B), activated T cells (low expression of OCA-B), naïve B cells (medium expression of OCA-B) and GC B cells (high expression of OCA-B). Identification of OCA-B binding partners would open the door to new studies on the molecular mechanisms behind the function of OCA-B. Furthermore, identification of OCA-B binding partners only present in B cells would help understand why this transcriptional co-activator possesses cell-specific functions.

5.3 AID expression by thymic B cells promotes T cell tolerance

Having identified that genetic variants in the *Idd2* locus affect GC formation and cellular crosstalk in secondary lymphoid organs, we next turned our attention to T and B cell interactions in the thymus. Specifically, in chapter 4, we investigated the role of thymic B cells in negative selection. While characterizing thymic APCs in NOD mice, we identified B cell-specific phenotypes. In addition to a reduction of expression of co-stimulatory molecules, NOD thymic B cells do not CS to secondary isotypes as efficiently as in other mouse strains. These B cell traits correlate with a reduction of CD4SP thymocyte apoptosis and impaired tolerance towards autoantigens. To investigate the potential impact of thymic B cell CS on T cell tolerance and autoimmunity development, we generated NOD.AID$^{-/-}$ mice, in which B cell CS and SHM are completely abrogated. Compared to AID$^{+/+}$ littermates, AID$^{-/-}$ mice developed increased and accelerated diabetes onset, with an accumulation of activated CD4^{+} T cells in spleen and pancreatic lymph nodes. Adoptive transfers of peripheral T cells and thymocytes revealed an impact of AID expression on the T cell repertoire, consistent with a role for thymic B cell CS/SHM on thymocyte selection. Lastly, negative selection of CD4SP thymocytes was impaired in AID$^{-/-}$ NOD and B6 mice, a finding confirmed using an antigen-specific model of clonal deletion. Together, these results identify a novel role for AID expression by thymic B cells in the modulation of the T cell repertoire and the control of autoimmunity.

Of note, it is important to point out that the diabetes incidence of NOD.AID$^{+/+}$ mice in this chapter is substantially lower than that of NOD mice in chapter 2 (41% vs 80%). This difference is likely explained by the method used to generate the NOD.AID$^{-/-}$ strain, which was generated by backcrossing of B6.AID$^{-/-}$ mice to NOD mice. While 10 backcrosses to NOD mice were performed (which is standard procedure in the field), it is possible that contaminating DNA from B6 origin

remains in our colony, resulting in a lower diabetes incidence. It is however important to note that WT mice (NOD.AID$^{+/+}$ mice) used as controls were littermates to the analyzed NOD.AID$^{-/-}$ mice, greatly reducing the potential impact of contaminating B6 DNA in our studies. It would be possible to test the presence of contaminating DNA by DNA or RNA sequencing, as done for the NOD.*Idd2* mouse in chapter 2.

AID initiates two main processes in human and mice: CS and SHM (84, 406). While both impact the BCR, CS affects the constant region and SHM affects the variable region of the receptor (406). By directly modifying the BCR locus, CS recombination minimally removes the DNA segment encoding for IgM and IgD, thereby converting IgM^{+}IgD^{+} B cells into IgM^{-}IgD^{-} B cells. Depending on the switch recombination site, the CS B cells will express IgG, IgA or IgE isotypes. Each antibody isotype exhibits specific characteristics. IgGs have the longest serum half-life and dominate in secondary infections. In contrast, IgA are mostly present at mucosal surfaces and in secretions and IgE are particularly implicated in allergies and in controlling worm infections through a strong binding of the Fc-receptor FcεRI (103). As a membrane-bound receptor, BCR isotypes also impact B cell functions. The main differences between IgM/IgD, IgG, IgA and IgE BCRs are found at the cytoplasmic tail of the receptor, where IgM/IgD have considerably shorter cytoplasmic tail than other BCR types and each have distinct amino acid composition (103, 407). Those differences affect B cell signaling, leading to distinct activation threshold (107, 408), intracellular Ca^{2+} mobilization (108, 378) and response to antigen encounter (379). In addition, IgG BCRs allow for stronger traction force against antigens than IgM BCRs (409), which could directly impact BCR-dependent antigen capture in the thymus. BCR isotype has also been suggested to modulate antigen specificity and binding affinity, independently of the variable region (380, 410). In the thymus, IgG and IgA are the dominant istotypes found in CS B cells (our

manuscript) (113). Our results suggest that switching from IgM to either IgG or IgA may enable thymic B cells to participate in negative selection of CD4SP thymocytes more efficiently. Although not investigated, it is tempting to suggest that negative selection of CD4SP thymocytes by CS thymic B cells may be facilitated due to isotype specific BCR signaling and/or antigen uptake.

SHM induces point mutations in the variable region of the BCR, at a rate of 10^{-3}/basepair/generation (411). Combined with selection of B cells with advantageous mutations, usually in GCs, SHM leads to affinity maturation of the BCR for antigens (84). While we focused on CS thymic B cells, B cells with mutated BCRs have been detected in the thymus of mice and humans (113, 412), suggesting the presence of ongoing SHM in thymic B cells. GCs can be detected in the thymus of some mice and humans (413, 414) and are sufficient to drive affinity maturation in some cases (415). However, presence of intrathymic GCs is rather rare. The mechanism that would allow for affinity maturation of thymic B cell is therefore still unknown. It is, however, noteworthy that extrafollicular affinity maturation has been reported. SHM and affinity maturation have been detected outside of GCs in infection and autoimmunity models (416-419). SHM and affinity maturation can be observed in $Lta^{-/-}$ mice, which lack the ability to form GCs (420), clearly demonstrating that those processes can take place independently of GCs. AID expression by thymic B cells may therefore lead to SHM and affinity maturation for self-antigens in situ, even in the absence of thymic GCs. In our study, we have not determined whether the impact of AID expression by thymic B cell on the T cell repertoire are caused by CS and/or SHM. It is interesting to note that class-switched ($IgM^{-}IgD^{-}$) thymic B cells are enriched in self-reactive clones relative to unswitched ($IgM^{+}IgD^{+}$) thymic B cells (113), suggesting that CS may be accompanied by affinity maturation towards self-antigens.

To dissect the implication of CS and SHM in thymic B cell functions, multiple experiments could be performed. First, the presence of SHM in thymic B cells should be confirmed. To do so, thymic B cells from BCR transgenic mice could be isolated for amplification and sequencing of the BCR sequences through single cell PCRs. Mutations would then be detectable by comparing the different sequences with the original BCR sequence. As thymic B cell CS is suggested to be driven by self-antigens (113), the presence of the cognate antigen of the transgenic BCR may be required for SHM to take place. To test that, SW_{HEL} mice, in which B cell express a HEL-specific BCR, could be crossed to our ins:HEL transgenic mice, leading to the presence of HEL in the thymus, as well as HEL-specific thymic B cells. Of note, compared to other BCR transgenic B cells, such as the HEL-specific MD4 B cells, B cells from SW_{HEL} mice can CS to the different isotypes and perform SHM (421).

Once confirmed, the importance of CS vs SHM in thymic B cell function could be dissected using different KO mice. As mentioned before, $AID^{-/-}$ B cells are deficient in CS and SHM. In contrast, $UNG^{-/-}$ B cells are deficient in CS but retain the ability to perform SHM. $AID^{-/-}$ and $UNG^{-/-}$ mice can therefore be used to dissect the contribution of CS and SHM in different settings (422). By comparing negative selection of CD4SP thymocytes in WT, $AID^{-/-}$ and $UNG^{-/-}$ mice, we could assess if CS and/or SHM is the main factor that promotes selection of thymocytes by thymic B cells.

In addition to SHM, affinity maturation can also be studied in BCR transgenic mice. The SW_{HEL} transgenic mouse system can be used to measure the affinity of the transgenic BCR (423). In the context of immunization or infection with pathogens expressing HEL^{3X}, the affinity of the SW_{HEL} mouse B cells towards HEL can be measured by incubating the cells with low concentration of fluorescent HEL^{3X} and measuring the binding through flow cytometry (see figure 7 below)

(421). As we are interested in measuring affinity maturation of thymic B cells towards self-antigens, we could use the same system as mentioned above: insHEL-SW_{HEL} double transgenic mice. The resulting mice would bear HEL-specific B cells as well as soluble HEL in the thymus. By flow cytometry, we could determine if thymic B cell proceed to affinity maturation toward self-antigens. As negative controls, $AID^{-/-}$ mice or mice lacking expression of HEL would allow to set up the threshold for presence or absence of affinity maturation.

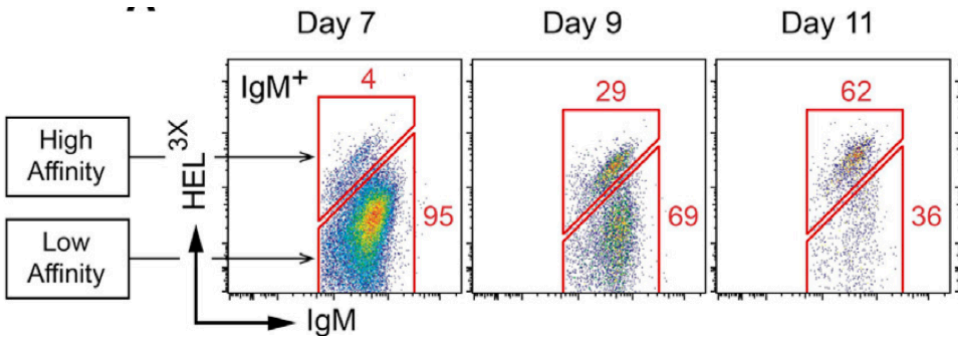

Figure 2: Flow cytometry analysis of the affinity of SW_{HEL} B cells to HEL. Analysis of the affinity of IgM^+ B cells towards HEL^{3X}, 7, 9, and 11 days after immunization with HEL. Source: Adapted from (421).

Clonal deletion of self-reactive thymocytes is a central process in the establishment of T cell tolerance. We have shown here that deletion of AID expression impairs negative selection of CD4SP thymocytes, without affecting the CD8SP population. Of note, B cell-deficient mice also show a specific impact on CD4SP but not CD8SP thymocytes (30). The specific impact of thymic B cells on CD4SP thymocytes may be caused by preferential interactions between thymic B cells and CD4SP thymocytes, as observed in our study. As thymic B cells express both MHC I and MHC II molecules, the impact of thymic B cells specifically on CD4SP thymocytes is still not

fully understood. A potential factor is the expression of CD40L by CD4SP thymocytes (30). CD40/CD40L signaling is essential for thymic B cell survival and licensing (30, 424). The lack of CD40L expression on CD8SP thymocyte may therefore limit their crosstalk with thymic B cells, inhibiting their selection by this specific type of thymic APC. Of note, in addition to induction of negative selection, strong TCR signaling by CD4SP thymocytes can also lead to differentiation into Tregs. As Tregs are important mediators of T cell tolerance in the periphery, an impact on Treg development could also be responsible for the increased diabetes onset observed in NOD.AID$^{-/-}$ mice. However, no difference in. FOXP3^{+} Tregs proportions or numbers were observed in NOD.AID$^{-/-}$ mice relative to NOD.AID$^{+/+}$ mice, in the thymus or in secondary lymphoid organs (data not shown).

One major missing piece to the complex puzzle of thymocyte selection is the relative contribution of thymic B cells to negative selection. Indeed, in addition to thymic B cells, mTECs, cDCs and pDCs are also present in the thymic medulla and each APC subset participate in the negative selection of thymocytes. It is unclear if antigen presentation by each subset possess unique or redundant roles in the elimination of self-reactive thymocytes. Reaggregated thymic organ cultures have been used to assess the contribution of each thymic APC types (425), and demonstrated that among bone marrow-derived APCs, cDCs are the most efficient at negatively selecting thymocytes, with a minor contribution of thymic B cells (425). However, these experiments were performed using transgenic thymocytes (OT-II) and soluble antigen (OVA) was added to the culture media. While interesting, these experiments do not take into consideration the unique features of some thymic APCs, such as the expression of tissue-restricted antigens by mTECs and thymic B cells, as well as the capacity of different thymic APCs to capture antigens present in limiting concentrations. As DCs and B cells acquire antigens through different

mechanisms (phagocytosis vs BCR-mediated internalization), it is possible that the repertoire of peptides presented by different thymic APC types is qualitatively distinct.

To investigate the nature of the peptidome presented by distinct thymic APCs, a possible approach would be to isolate the different cell types from the mouse thymus and elute the peptides present on MHC II molecules. The different peptides could then be identified through mass spectrometry. This strategy has successfully identified a variety of autoantigens presented by B cells in the context of autoimmune diabetes (366). Characterizing the repertoire of antigens presented by thymic B cells would greatly increase our understanding of their role in the establishment of T cell tolerance and could identify a unique role in the elimination of self-reactive T cells.

Chapter 6:

Conclusion

T1D is a complex autoimmune disease and its development in susceptible individuals is caused by a variety of genetic and environmental factors. Even before T1D onset, immune cells participate in autoimmune reactions that specifically target beta cells in the pancreas. During this pre-diabetic phase, T and B lymphocytes interact together in various lymphoid and non-lymphoid organs, which contribute to the development of T1D.

By investigating T and B cells in different lymphoid organs, we have explored the contribution of their interactions in the pathogenesis of autoimmune diabetes in NOD mice, a mouse model of T1D. Using a variety of congenic, transgenic and KO mice, we have demonstrated the complex nature of the crosstalk between these two populations of lymphocytes. We showed that *Idd2* is a key diabetes-susceptibility locus, which influences MHC-mediated interactions between B and T cells in the periphery, affecting the priming of pathogenic T cells and controlling diabetes development. In addition, NOD-derived genetic variants from this same locus favors GC formation. OCA-B was one of the early candidate genes identified in our study. However, further analyses suggest that OCA-B is not differentially expressed and unlikely to explain the variations in GC formation between NOD and NOD.*Idd2* mice. Concurrently, we demonstrated that OCA-B acts as a transcriptional co-activator specifically in B cells, but impacts T cell functions through the regulation of the crosstalk between B and T lymphocytes. Finally, analysis of the small population of thymic B cells in various genetically distinct mice revealed a deficiency of B cell

CS in NOD mice. We then showed that this trait, which correlates with an impaired tolerance to self-antigens in NOD thymocytes, has a significant impact on diabetes development, as inhibition of CS in thymic B cells increases insulitis. Our study defines a novel role for AID expression in the development of T cells and for the prevention of autoimmune diseases.

The sum of our findings highlights the complexity of the role of B cells in shaping T cell-mediated responses in the context of autoimmune diabetes. While interactions in the periphery, such as in secondary lymphoid organs and in the pancreas, promote pathogenic T cell responses that lead to beta cell destruction, interactions in the thymus favors the elimination of pathogenic T cells. T and B cells therefore share an intricate connection, starting from the development of T cells, where thymic B cells shape the T cell repertoire. Once in the periphery, the impact of B cells on mature T cells changes to favor autoimmune responses. Cognate interactions between the two cell types favor the activation of self-reactive T cells and the differentiation of these cells into helper T cell subsets, such as Tfh.

Current B cell-targeting therapies for the treatment of T1D show only modest efficacy. The reasons for these limited results include the heterogeneity of B cell phenotypes and functions. The studies performed here highlight the complexity of the role of B cells in the context of T cell-mediated autoimmune disease. It is therefore critical to understand and consider the multi-faceted role of T and B cells when developing immunotherapies targeting those populations.

References

1. Shah DK, Zuniga-Pflucker JC. An overview of the intrathymic intricacies of T cell development. J Immunol. 2014;192(9):4017-23.
2. Hu Z, Lancaster JN, Ehrlich LI. The Contribution of Chemokines and Migration to the Induction of Central Tolerance in the Thymus. Front Immunol. 2015;6:398.
3. Labrecque N, Baldwin T, Lesage S. Molecular and genetic parameters defining T-cell clonal selection. Immunol Cell Biol. 2011;89(1):16-26.
4. Moran AE, Holzapfel KL, Xing Y, Cunningham NR, Maltzman JS, Punt J, et al. T cell receptor signal strength in Treg and iNKT cell development demonstrated by a novel fluorescent reporter mouse. J Exp Med. 2011;208(6):1279-89.
5. McDonald BD, Bunker JJ, Ishizuka IE, Jabri B, Bendelac A. Elevated T cell receptor signaling identifies a thymic precursor to the TCRalphabeta(+)CD4(-)CD8beta(-) intraepithelial lymphocyte lineage. Immunity. 2014;41(2):219-29.
6. Stritesky GL, Xing Y, Erickson JR, Kalekar LA, Wang X, Mueller DL, et al. Murine thymic selection quantified using a unique method to capture deleted T cells. Proc Natl Acad Sci U S A. 2013;110(12):4679-84.
7. Gordon J, Manley NR. Mechanisms of thymus organogenesis and morphogenesis. Development. 2011;138(18):3865-78.
8. Perera J, Meng L, Meng F, Huang H. Autoreactive thymic B cells are efficient antigen-presenting cells of cognate self-antigens for T cell negative selection. Proc Natl Acad Sci U S A. 2013;110(42):17011-6.
9. Weinreich MA, Hogquist KA. Thymic emigration: when and how T cells leave home. J Immunol. 2008;181(4):2265-70.
10. James KD, Cosway EJ, Lucas B, White AJ, Parnell SM, Carvalho-Gaspar M, et al. Endothelial cells act as gatekeepers for LTbetaR-dependent thymocyte emigration. J Exp Med. 2018;215(12):2984-93.
11. Nikolich-Zugich J, Slifka MK, Messaoudi I. The many important facets of T-cell repertoire diversity. Nat Rev Immunol. 2004;4(2):123-32.
12. Liston A, Lesage S, Gray DH, O'Reilly LA, Strasser A, Fahrer AM, et al. Generalized resistance to thymic deletion in the NOD mouse; a polygenic trait characterized by defective induction of Bim. Immunity. 2004;21(6):817-30.
13. Cosway E, Anderson G, Garside P, Prendergast C. The thymus and rheumatology: should we care? Curr Opin Rheumatol. 2016;28(2):189-95.
14. Vafiadis P, Bennett ST, Todd JA, Nadeau J, Grabs R, Goodyer CG, et al. Insulin expression in human thymus is modulated by INS VNTR alleles at the IDDM2 locus. Nat Genet. 1997;15(3):289-92.
15. Gabrielsen IS, Amundsen SS, Helgeland H, Flam ST, Hatinoor N, Holm K, et al. Genetic risk variants for autoimmune diseases that influence gene expression in thymus. Hum Mol Genet. 2016;25(14):3117-24.
16. van Meerwijk JP, Marguerat S, Lees RK, Germain RN, Fowlkes BJ, MacDonald HR. Quantitative impact of thymic clonal deletion on the T cell repertoire. J Exp Med. 1997;185(3):377-83.

17. Palmer E. Negative selection--clearing out the bad apples from the T-cell repertoire. Nat Rev Immunol. 2003;3(5):383-91.
18. Alam SM, Travers PJ, Wung JL, Nasholds W, Redpath S, Jameson SC, et al. T-cell-receptor affinity and thymocyte positive selection. Nature. 1996;381(6583):616-20.
19. McKeithan TW. Kinetic proofreading in T-cell receptor signal transduction. Proc Natl Acad Sci U S A. 1995;92(11):5042-6.
20. Alberola-Ila J, Forbush KA, Seger R, Krebs EG, Perlmutter RM. Selective requirement for MAP kinase activation in thymocyte differentiation. Nature. 1995;373(6515):620-3.
21. Calnan BJ, Szychowski S, Chan FK, Cado D, Winoto A. A role for the orphan steroid receptor Nur77 in apoptosis accompanying antigen-induced negative selection. Immunity. 1995;3(3):273-82.
22. Page DM, Kane LP, Allison JP, Hedrick SM. Two signals are required for negative selection of CD4+CD8+ thymocytes. J Immunol. 1993;151(4):1868-80.
23. Kishimoto H, Sprent J. Several different cell surface molecules control negative selection of medullary thymocytes. J Exp Med. 1999;190(1):65-73.
24. McCarron MJ, Irla M, Serge A, Soudja SM, Marie JC. Transforming Growth Factor-beta signaling in alphabeta thymocytes promotes negative selection. Nat Commun. 2019;10(1):5690.
25. Watanabe M, Lu Y, Breen M, Hodes RJ. B7-CD28 co-stimulation modulates central tolerance via thymic clonal deletion and Treg generation through distinct mechanisms. Nat Commun. 2020;11(1):6264.
26. Sakaguchi S, Yamaguchi T, Nomura T, Ono M. Regulatory T cells and immune tolerance. Cell. 2008;133(5):775-87.
27. Klein L, Kyewski B, Allen PM, Hogquist KA. Positive and negative selection of the T cell repertoire: what thymocytes see (and don't see). Nat Rev Immunol. 2014;14(6):377-91.
28. Takaba H, Takayanagi H. The Mechanisms of T Cell Selection in the Thymus. Trends Immunol. 2017;38(11):805-16.
29. Takaba H, Morishita Y, Tomofuji Y, Danks L, Nitta T, Komatsu N, et al. Fezf2 Orchestrates a Thymic Program of Self-Antigen Expression for Immune Tolerance. Cell. 2015;163(4):975-87.
30. Yamano T, Nedjic J, Hinterberger M, Steinert M, Koser S, Pinto S, et al. Thymic B Cells Are Licensed to Present Self Antigens for Central T Cell Tolerance Induction. Immunity. 2015;42(6):1048-61.
31. Blackburn CC, Manley NR. Developing a new paradigm for thymus organogenesis. Nat Rev Immunol. 2004;4(4):278-89.
32. Kondo M, Weissman IL, Akashi K. Identification of clonogenic common lymphoid progenitors in mouse bone marrow. Cell. 1997;91(5):661-72.
33. Harly C, Cam M, Kaye J, Bhandoola A. Development and differentiation of early innate lymphoid progenitors. J Exp Med. 2018;215(1):249-62.
34. Manz MG, Traver D, Miyamoto T, Weissman IL, Akashi K. Dendritic cell potentials of early lymphoid and myeloid progenitors. Blood. 2001;97(11):3333-41.
35. Hardy RR, Hayakawa K. B cell development pathways. Annu Rev Immunol. 2001;19:595-621.
36. Decker JM. B Cell Development. Immunology. p. https://www2.nau.edu/~fpm/immunology/Exams/Bcelldevelopment-401.html#generation.

37. Pelanda R, Torres RM. Central B-cell tolerance: where selection begins. Cold Spring Harb Perspect Biol. 2012;4(4):a007146.
38. Melchers F. Checkpoints that control B cell development. J Clin Invest. 2015;125(6):2203-10.
39. Carotta S, Nutt SL. Losing B cell identity. Bioessays. 2008;30(3):203-7.
40. Nutt SL, Heavey B, Rolink AG, Busslinger M. Commitment to the B-lymphoid lineage depends on the transcription factor Pax5. Nature. 1999;401(6753):556-62.
41. Bain G, Robanus Maandag EC, te Riele HP, Feeney AJ, Sheehy A, Schlissel M, et al. Both E12 and E47 allow commitment to the B cell lineage. Immunity. 1997;6(2):145-54.
42. Lin H, Grosschedl R. Failure of B-cell differentiation in mice lacking the transcription factor EBF. Nature. 1995;376(6537):263-7.
43. Wang H, Jain S, Li P, Lin JX, Oh J, Qi C, et al. Transcription factors IRF8 and PU.1 are required for follicular B cell development and BCL6-driven germinal center responses. Proc Natl Acad Sci U S A. 2019;116(19):9511-20.
44. Strubin M, Newell JW, Matthias P. OBF-1, a novel B cell-specific coactivator that stimulates immunoglobulin promoter activity through association with octamer-binding proteins. Cell. 1995;80(3):497-506.
45. Luo Y, Fujii H, Gerster T, Roeder RG. A novel B cell-derived coactivator potentiates the activation of immunoglobulin promoters by octamer-binding transcription factors. Cell. 1992;71(2):231-41.
46. Teitell MA. OCA-B regulation of B-cell development and function. Trends Immunol. 2003;24(10):546-53.
47. Jankovic M, Nussenzweig MC. OcaB regulates transitional B cell selection. Int Immunol. 2003;15(9):1099-104.
48. de Andres B, Gonzalo P, Minguet S, Martinez-Marin JA, Soro PG, Marcos MA, et al. The first 3 days of B-cell development in the mouse embryo. Blood. 2002;100(12):4074-81.
49. Gathings WE, Lawton AR, Cooper MD. Immunofluorescent studies of the development of pre-B cells, B lymphocytes and immunoglobulin isotype diversity in humans. Eur J Immunol. 1977;7(11):804-10.
50. Montecino-Rodriguez E, Dorshkind K. B-1 B cell development in the fetus and adult. Immunity. 2012;36(1):13-21.
51. Baumgarth N. A Hard(y) Look at B-1 Cell Development and Function. J Immunol. 2017;199(10):3387-94.
52. Akashi K, Richie LI, Miyamoto T, Carr WH, Weissman IL. B lymphopoiesis in the thymus. J Immunol. 2000;164(10):5221-6.
53. Reiser H, Stadecker MJ. Costimulatory B7 molecules in the pathogenesis of infectious and autoimmune diseases. N Engl J Med. 1996;335(18):1369-77.
54. Silverman GJ, Goodyear CS. Confounding B-cell defences: lessons from a staphylococcal superantigen. Nat Rev Immunol. 2006;6(6):465-75.
55. Elgueta R, Benson MJ, de Vries VC, Wasiuk A, Guo Y, Noelle RJ. Molecular mechanism and function of CD40/CD40L engagement in the immune system. Immunol Rev. 2009;229(1):152-72.
56. Browne EP. Regulation of B-cell responses by Toll-like receptors. Immunology. 2012;136(4):370-9.

57. Chen X, Jensen PE. The role of B lymphocytes as antigen-presenting cells. Arch Immunol Ther Exp (Warsz). 2008;56(2):77-83.
58. Pape KA, Catron DM, Itano AA, Jenkins MK. The humoral immune response is initiated in lymph nodes by B cells that acquire soluble antigen directly in the follicles. Immunity. 2007;26(4):491-502.
59. Knight AM. B-cell acquisition of antigen: Sensing the surface. Eur J Immunol. 2015;45(6):1600-4.
60. Batista FD, Harwood NE. The who, how and where of antigen presentation to B cells. Nat Rev Immunol. 2009;9(1):15-27.
61. Byersdorfer CA, Dipaolo RJ, Petzold SJ, Unanue ER. Following immunization antigen becomes concentrated in a limited number of APCs including B cells. J Immunol. 2004;173(11):6627-34.
62. Szakal AK, Holmes KL, Tew JG. Transport of immune complexes from the subcapsular sinus to lymph node follicles on the surface of nonphagocytic cells, including cells with dendritic morphology. J Immunol. 1983;131(4):1714-27.
63. Bergtold A, Desai DD, Gavhane A, Clynes R. Cell surface recycling of internalized antigen permits dendritic cell priming of B cells. Immunity. 2005;23(5):503-14.
64. Kranich J, Krautler NJ. How Follicular Dendritic Cells Shape the B-Cell Antigenome. Front Immunol. 2016;7:225.
65. Heesters BA, Myers RC, Carroll MC. Follicular dendritic cells: dynamic antigen libraries. Nat Rev Immunol. 2014;14(7):495-504.
66. Vidard L, Kovacsovics-Bankowski M, Kraeft SK, Chen LB, Benacerraf B, Rock KL. Analysis of MHC class II presentation of particulate antigens of B lymphocytes. J Immunol. 1996;156(8):2809-18.
67. Simitsek PD, Campbell DG, Lanzavecchia A, Fairweather N, Watts C. Modulation of antigen processing by bound antibodies can boost or suppress class II major histocompatibility complex presentation of different T cell determinants. J Exp Med. 1995;181(6):1957-63.
68. Schneider SC, Sercarz EE. Antigen processing differences among APC. Hum Immunol. 1997;54(2):148-58.
69. Victora GD, Nussenzweig MC. Germinal centers. Annu Rev Immunol. 2012;30:429-57.
70. Shinall SM, Gonzalez-Fernandez M, Noelle RJ, Waldschmidt TJ. Identification of murine germinal center B cell subsets defined by the expression of surface isotypes and differentiation antigens. J Immunol. 2000;164(11):5729-38.
71. Stoler-Barak L, Biram A, Davidzohn N, Addadi Y, Golani O, Shulman Z. B cell dissemination patterns during the germinal center reaction revealed by whole-organ imaging. J Exp Med. 2019;216(11):2515-30.
72. Ye BH, Cattoretti G, Shen Q, Zhang J, Hawe N, de Waard R, et al. The BCL-6 proto-oncogene controls germinal-centre formation and Th2-type inflammation. Nat Genet. 1997;16(2):161-70.
73. Choi J, Diao H, Faliti CE, Truong J, Rossi M, Belanger S, et al. Bcl-6 is the nexus transcription factor of T follicular helper cells via repressor-of-repressor circuits. Nat Immunol. 2020;21(7):777-89.

74. Schubart DB, Rolink A, Kosco-Vilbois MH, Botteri F, Matthias P. B-cell-specific coactivator OBF-1/OCA-B/Bob1 required for immune response and germinal centre formation. Nature. 1996;383(6600):538-42.
75. Chu CS, Hellmuth JC, Singh R, Ying HY, Skrabanek L, Teater MR, et al. Unique Immune Cell Coactivators Specify Locus Control Region Function and Cell Stage. Mol Cell. 2020;80(5):845-61 e10.
76. Stauss D, Brunner C, Berberich-Siebelt F, Hopken UE, Lipp M, Muller G. The transcriptional coactivator Bob1 promotes the development of follicular T helper cells via Bcl6. EMBO J. 2016;35(8):881-98.
77. Crotty S. T follicular helper cell differentiation, function, and roles in disease. Immunity. 2014;41(4):529-42.
78. Goenka R, Barnett LG, Silver JS, O'Neill PJ, Hunter CA, Cancro MP, et al. Cutting edge: dendritic cell-restricted antigen presentation initiates the follicular helper T cell program but cannot complete ultimate effector differentiation. J Immunol. 2011;187(3):1091-5.
79. Choi YS, Eto D, Yang JA, Lao C, Crotty S. Cutting edge: STAT1 is required for IL-6-mediated Bcl6 induction for early follicular helper cell differentiation. J Immunol. 2013;190(7):3049-53.
80. Choi YS, Kageyama R, Eto D, Escobar TC, Johnston RJ, Monticelli L, et al. ICOS receptor instructs T follicular helper cell versus effector cell differentiation via induction of the transcriptional repressor Bcl6. Immunity. 2011;34(6):932-46.
81. Roco JA, Mesin L, Binder SC, Nefzger C, Gonzalez-Figueroa P, Canete PF, et al. Class-Switch Recombination Occurs Infrequently in Germinal Centers. Immunity. 2019;51(2):337-50 e7.
82. Allen CD, Okada T, Cyster JG. Germinal-center organization and cellular dynamics. Immunity. 2007;27(2):190-202.
83. Odegard VH, Schatz DG. Targeting of somatic hypermutation. Nat Rev Immunol. 2006;6(8):573-83.
84. Feng Y, Seija N, Di Noia JM, Martin A. AID in Antibody Diversification: There and Back Again. Trends Immunol. 2020;41(7):586-600.
85. Hwang JK, Alt FW, Yeap LS. Related Mechanisms of Antibody Somatic Hypermutation and Class Switch Recombination. Microbiol Spectr. 2015;3(1):MDNA3-0037-2014.
86. McKean D, Huppi K, Bell M, Staudt L, Gerhard W, Weigert M. Generation of antibody diversity in the immune response of BALB/c mice to influenza virus hemagglutinin. Proc Natl Acad Sci U S A. 1984;81(10):3180-4.
87. Lee BO, Moyron-Quiroz J, Rangel-Moreno J, Kusser KL, Hartson L, Sprague F, et al. CD40, but not CD154, expression on B cells is necessary for optimal primary B cell responses. J Immunol. 2003;171(11):5707-17.
88. Kawabe T, Naka T, Yoshida K, Tanaka T, Fujiwara H, Suematsu S, et al. The immune responses in CD40-deficient mice: impaired immunoglobulin class switching and germinal center formation. Immunity. 1994;1(3):167-78.
89. Papa I, Vinuesa CG. Synaptic Interactions in Germinal Centers. Front Immunol. 2018;9:1858.

90. Luo W, Weisel F, Shlomchik MJ. B Cell Receptor and CD40 Signaling Are Rewired for Synergistic Induction of the c-Myc Transcription Factor in Germinal Center B Cells. Immunity. 2018;48(2):313-26 e5.
91. Koike T, Harada K, Horiuchi S, Kitamura D. The quantity of CD40 signaling determines the differentiation of B cells into functionally distinct memory cell subsets. Elife. 2019;8.
92. Dong C, Temann UA, Flavell RA. Cutting edge: critical role of inducible costimulator in germinal center reactions. J Immunol. 2001;166(6):3659-62.
93. Bossaller L, Burger J, Draeger R, Grimbacher B, Knoth R, Plebani A, et al. ICOS deficiency is associated with a severe reduction of CXCR5+CD4 germinal center Th cells. J Immunol. 2006;177(7):4927-32.
94. Liu D, Xu H, Shih C, Wan Z, Ma X, Ma W, et al. T-B-cell entanglement and ICOSL-driven feed-forward regulation of germinal centre reaction. Nature. 2015;517(7533):214-8.
95. Tangye SG, Ma CS. Regulation of the germinal center and humoral immunity by interleukin-21. J Exp Med. 2020;217(1).
96. Vajdy M, Kosco-Vilbois MH, Kopf M, Kohler G, Lycke N. Impaired mucosal immune responses in interleukin 4-targeted mice. J Exp Med. 1995;181(1):41-53.
97. King IL, Mohrs M. IL-4-producing CD4+ T cells in reactive lymph nodes during helminth infection are T follicular helper cells. J Exp Med. 2009;206(5):1001-7.
98. Reinhardt RL, Liang HE, Locksley RM. Cytokine-secreting follicular T cells shape the antibody repertoire. Nat Immunol. 2009;10(4):385-93.
99. Murray PD, McKenzie DT, Swain SL, Kagnoff MF. Interleukin 5 and interleukin 4 produced by Peyer's patch T cells selectively enhance immunoglobulin A expression. J Immunol. 1987;139(8):2669-74.
100. Meli AP, Fontes G, Leung Soo C, King IL. T Follicular Helper Cell-Derived IL-4 Is Required for IgE Production during Intestinal Helminth Infection. J Immunol. 2017;199(1):244-52.
101. Xu Z, Zan H, Pone EJ, Mai T, Casali P. Immunoglobulin class-switch DNA recombination: induction, targeting and beyond. Nat Rev Immunol. 2012;12(7):517-31.
102. Stavnezer J, Kang J. The surprising discovery that TGF beta specifically induces the IgA class switch. J Immunol. 2009;182(1):5-7.
103. Schroeder HW, Jr., Cavacini L. Structure and function of immunoglobulins. J Allergy Clin Immunol. 2010;125(2 Suppl 2):S41-52.
104. Gutzeit C, Chen K, Cerutti A. The enigmatic function of IgD: some answers at last. Eur J Immunol. 2018;48(7):1101-13.
105. Nimmerjahn F, Ravetch JV. Fcgamma receptors as regulators of immune responses. Nat Rev Immunol. 2008;8(1):34-47.
106. Palmeira P, Quinello C, Silveira-Lessa AL, Zago CA, Carneiro-Sampaio M. IgG placental transfer in healthy and pathological pregnancies. Clin Dev Immunol. 2012;2012:985646.
107. Wan Z, Chen X, Chen H, Ji Q, Chen Y, Wang J, et al. The activation of IgM- or isotype-switched IgG- and IgE-BCR exhibits distinct mechanical force sensitivity and threshold. Elife. 2015;4.
108. Wakabayashi C, Adachi T, Wienands J, Tsubata T. A distinct signaling pathway used by the IgG-containing B cell antigen receptor. Science. 2002;298(5602):2392-5.
109. Corthesy B. Roundtrip ticket for secretory IgA: role in mucosal homeostasis? J Immunol. 2007;178(1):27-32.

110. Kelly BT, Grayson MH. Immunoglobulin E, what is it good for? Ann Allergy Asthma Immunol. 2016;116(3):183-7.
111. Kehry MR, Yamashita LC. Low-affinity IgE receptor (CD23) function on mouse B cells: role in IgE-dependent antigen focusing. Proc Natl Acad Sci U S A. 1989;86(19):7556-60.
112. Frommer F, Waisman A. B cells participate in thymic negative selection of murine auto-reactive CD4+ T cells. PLoS One. 2010;5(10):e15372.
113. Perera J, Zheng Z, Li S, Gudjonson H, Kalinina O, Benichou JIC, et al. Self-Antigen-Driven Thymic B Cell Class Switching Promotes T Cell Central Tolerance. Cell Rep. 2016;17(2):387-98.
114. DiMeglio LA, Evans-Molina C, Oram RA. Type 1 diabetes. Lancet. 2018;391(10138):2449-62.
115. Nally LM, Sherr JL, Van Name MA, Patel AD, Tamborlane WV. Pharmacologic treatment options for type 1 diabetes: what's new? Expert Rev Clin Pharmacol. 2019;12(5):471-9.
116. Katsarou A, Gudbjornsdottir S, Rawshani A, Dabelea D, Bonifacio E, Anderson BJ, et al. Type 1 diabetes mellitus. Nat Rev Dis Primers. 2017;3:17016.
117. Karvonen M, Viik-Kajander M, Moltchanova E, Libman I, LaPorte R, Tuomilehto J. Incidence of childhood type 1 diabetes worldwide. Diabetes Mondiale (DiaMond) Project Group. Diabetes Care. 2000;23(10):1516-26.
118. Fox DA, Islam N, Sutherland J, Reimer K, Amed S. Type 1 diabetes incidence and prevalence trends in a cohort of Canadian children and youth. Pediatr Diabetes. 2018;19(3):501-5.
119. Abela AG, Fava S. Why is the Incidence of Type 1 Diabetes Increasing? Curr Diabetes Rev. 2021;17(8):e030521193110.
120. Makino S, Kunimoto K, Muraoka Y, Mizushima Y, Katagiri K, Tochino Y. Breeding of a non-obese, diabetic strain of mice. Jikken Dobutsu. 1980;29(1):1-13.
121. Mullen Y. Development of the Nonobese Diabetic Mouse and Contribution of Animal Models for Understanding Type 1 Diabetes. Pancreas. 2017;46(4):455-66.
122. Pearson JA, Wong FS, Wen L. The importance of the Non Obese Diabetic (NOD) mouse model in autoimmune diabetes. J Autoimmun. 2016;66:76-88.
123. Lehuen A, Diana J, Zaccone P, Cooke A. Immune cell crosstalk in type 1 diabetes. Nat Rev Immunol. 2010;10(7):501-13.
124. Anderson MS, Bluestone JA. The NOD mouse: a model of immune dysregulation. Annu Rev Immunol. 2005;23:447-85.
125. Drescher KM, Kono K, Bopegamage S, Carson SD, Tracy S. Coxsackievirus B3 infection and type 1 diabetes development in NOD mice: insulitis determines susceptibility of pancreatic islets to virus infection. Virology. 2004;329(2):381-94.
126. Steck AK, Rewers MJ. Genetics of type 1 diabetes. Clin Chem. 2011;57(2):176-85.
127. Redondo MJ, Jeffrey J, Fain PR, Eisenbarth GS, Orban T. Concordance for islet autoimmunity among monozygotic twins. N Engl J Med. 2008;359(26):2849-50.
128. Pociot F. Type 1 diabetes genome-wide association studies: not to be lost in translation. Clin Transl Immunology. 2017;6(12):e162.
129. Wakeland EK. Hunting autoimmune disease genes in NOD: early steps on a long road to somewhere important (hopefully). J Immunol. 2014;193(1):3-6.

130. Driver JP, Chen YG, Mathews CE. Comparative genetics: synergizing human and NOD mouse studies for identifying genetic causation of type 1 diabetes. Rev Diabet Stud. 2012;9(4):169-87.
131. Noble JA, Valdes AM, Cook M, Klitz W, Thomson G, Erlich HA. The role of HLA class II genes in insulin-dependent diabetes mellitus: molecular analysis of 180 Caucasian, multiplex families. Am J Hum Genet. 1996;59(5):1134-48.
132. Hattori M, Buse JB, Jackson RA, Glimcher L, Dorf ME, Minami M, et al. The NOD mouse: recessive diabetogenic gene in the major histocompatibility complex. Science. 1986;231(4739):733-5.
133. Thayer TC, Wilson SB, Mathews CE. Use of nonobese diabetic mice to understand human type 1 diabetes. Endocrinol Metab Clin North Am. 2010;39(3):541-61.
134. Nejentsev S, Howson JM, Walker NM, Szeszko J, Field SF, Stevens HE, et al. Localization of type 1 diabetes susceptibility to the MHC class I genes HLA-B and HLA-A. Nature. 2007;450(7171):887-92.
135. Valdes AM, Thomson G, Type 1 Diabetes Genetics C. Several loci in the HLA class III region are associated with T1D risk after adjusting for DRB1-DQB1. Diabetes Obes Metab. 2009;11 Suppl 1:46-52.
136. Morran MP, Vonberg A, Khadra A, Pietropaolo M. Immunogenetics of type 1 diabetes mellitus. Mol Aspects Med. 2015;42:42-60.
137. Chen YG, Mathews CE, Driver JP. The Role of NOD Mice in Type 1 Diabetes Research: Lessons from the Past and Recommendations for the Future. Front Endocrinol (Lausanne). 2018;9:51.
138. Stratmann T, Apostolopoulos V, Mallet-Designe V, Corper AL, Scott CA, Wilson IA, et al. The I-Ag7 MHC class II molecule linked to murine diabetes is a promiscuous peptide binder. J Immunol. 2000;165(6):3214-25.
139. Stadinski BD, Zhang L, Crawford F, Marrack P, Eisenbarth GS, Kappler JW. Diabetogenic T cells recognize insulin bound to IAg7 in an unexpected, weakly binding register. Proc Natl Acad Sci U S A. 2010;107(24):10978-83.
140. Kanagawa O, Martin SM, Vaupel BA, Carrasco-Marin E, Unanue ER. Autoreactivity of T cells from nonobese diabetic mice: an I-Ag7-dependent reaction. Proc Natl Acad Sci U S A. 1998;95(4):1721-4.
141. Lund T, O'Reilly L, Hutchings P, Kanagawa O, Simpson E, Gravely R, et al. Prevention of insulin-dependent diabetes mellitus in non-obese diabetic mice by transgenes encoding modified I-A beta-chain or normal I-E alpha-chain. Nature. 1990;345(6277):727-9.
142. Yui MA, Muralidharan K, Moreno-Altamirano B, Perrin G, Chestnut K, Wakeland EK. Production of congenic mouse strains carrying NOD-derived diabetogenic genetic intervals: an approach for the genetic dissection of complex traits. Mamm Genome. 1996;7(5):331-4.
143. Prochazka M, Serreze DV, Frankel WN, Leiter EH. NOR/Lt mice: MHC-matched diabetes-resistant control strain for NOD mice. Diabetes. 1992;41(1):98-106.
144. Prochazka M, Leiter EH, Serreze DV, Coleman DL. Three recessive loci required for insulin-dependent diabetes in nonobese diabetic mice. Science. 1987;237(4812):286-9.
145. Wicker LS, Todd JA, Prins JB, Podolin PL, Renjilian RJ, Peterson LB. Resistance alleles at two non-major histocompatibility complex-linked insulin-dependent diabetes loci on

chromosome 3, Idd3 and Idd10, protect nonobese diabetic mice from diabetes. J Exp Med. 1994;180(5):1705-13.
146. Podolin PL, Wilusz MB, Cubbon RM, Pajvani U, Lord CJ, Todd JA, et al. Differential glycosylation of interleukin 2, the molecular basis for the NOD Idd3 type 1 diabetes gene? Cytokine. 2000;12(5):477-82.
147. Kamanaka M, Rainbow D, Schuster-Gossler K, Eynon EE, Chervonsky AV, Wicker LS, et al. Amino acid polymorphisms altering the glycosylation of IL-2 do not protect from type 1 diabetes in the NOD mouse. Proc Natl Acad Sci U S A. 2009;106(27):11236-40.
148. Yamanouchi J, Rainbow D, Serra P, Howlett S, Hunter K, Garner VE, et al. Interleukin-2 gene variation impairs regulatory T cell function and causes autoimmunity. Nat Genet. 2007;39(3):329-37.
149. Schuster C, Jonas F, Zhao F, Kissler S. Peripherally induced regulatory T cells contribute to the control of autoimmune diabetes in the NOD mouse model. Eur J Immunol. 2018;48(7):1211-6.
150. Petzold C, Riewaldt J, Watts D, Sparwasser T, Schallenberg S, Kretschmer K. Foxp3(+) regulatory T cells in mouse models of type 1 diabetes. J Diabetes Res. 2013;2013:940710.
151. Bennett ST, Lucassen AM, Gough SC, Powell EE, Undlien DE, Pritchard LE, et al. Susceptibility to human type 1 diabetes at IDDM2 is determined by tandem repeat variation at the insulin gene minisatellite locus. Nat Genet. 1995;9(3):284-92.
152. Kennedy GC, German MS, Rutter WJ. The minisatellite in the diabetes susceptibility locus IDDM2 regulates insulin transcription. Nat Genet. 1995;9(3):293-8.
153. Lowe CE, Cooper JD, Brusko T, Walker NM, Smyth DJ, Bailey R, et al. Large-scale genetic fine mapping and genotype-phenotype associations implicate polymorphism in the IL2RA region in type 1 diabetes. Nat Genet. 2007;39(9):1074-82.
154. Garg G, Tyler JR, Yang JH, Cutler AJ, Downes K, Pekalski M, et al. Type 1 diabetes-associated IL2RA variation lowers IL-2 signaling and contributes to diminished CD4+CD25+ regulatory T cell function. J Immunol. 2012;188(9):4644-53.
155. Chinen T, Kannan AK, Levine AG, Fan X, Klein U, Zheng Y, et al. An essential role for the IL-2 receptor in Treg cell function. Nat Immunol. 2016;17(11):1322-33.
156. Ross SH, Cantrell DA. Signaling and Function of Interleukin-2 in T Lymphocytes. Annu Rev Immunol. 2018;36:411-33.
157. Bottini N, Vang T, Cucca F, Mustelin T. Role of PTPN22 in type 1 diabetes and other autoimmune diseases. Semin Immunol. 2006;18(4):207-13.
158. Armitage LH, Wallet MA, Mathews CE. Influence of PTPN22 Allotypes on Innate and Adaptive Immune Function in Health and Disease. Front Immunol. 2021;12:636618.
159. Burn GL, Cornish GH, Potrzebowska K, Samuelsson M, Griffie J, Minoughan S, et al. Superresolution imaging of the cytoplasmic phosphatase PTPN22 links integrin-mediated T cell adhesion with autoimmunity. Sci Signal. 2016;9(448):ra99.
160. Wu J, Katrekar A, Honigberg LA, Smith AM, Conn MT, Tang J, et al. Identification of substrates of human protein-tyrosine phosphatase PTPN22. J Biol Chem. 2006;281(16):11002-10.
161. Bottini N, Musumeci L, Alonso A, Rahmouni S, Nika K, Rostamkhani M, et al. A functional variant of lymphoid tyrosine phosphatase is associated with type I diabetes. Nat Genet. 2004;36(4):337-8.

162. Smyth D, Cooper JD, Collins JE, Heward JM, Franklyn JA, Howson JM, et al. Replication of an association between the lymphoid tyrosine phosphatase locus (LYP/PTPN22) with type 1 diabetes, and evidence for its role as a general autoimmunity locus. Diabetes. 2004;53(11):3020-3.
163. Lin X, Pelletier S, Gingras S, Rigaud S, Maine CJ, Marquardt K, et al. CRISPR-Cas9-Mediated Modification of the NOD Mouse Genome With Ptpn22R619W Mutation Increases Autoimmune Diabetes. Diabetes. 2016;65(8):2134-8.
164. Bottazzo GF, Dean BM, McNally JM, MacKay EH, Swift PG, Gamble DR. In situ characterization of autoimmune phenomena and expression of HLA molecules in the pancreas in diabetic insulitis. N Engl J Med. 1985;313(6):353-60.
165. Prochazka M, Gaskins HR, Shultz LD, Leiter EH. The nonobese diabetic scid mouse: model for spontaneous thymomagenesis associated with immunodeficiency. Proc Natl Acad Sci U S A. 1992;89(8):3290-4.
166. Christianson SW, Shultz LD, Leiter EH. Adoptive transfer of diabetes into immunodeficient NOD-scid/scid mice. Relative contributions of CD4+ and CD8+ T-cells from diabetic versus prediabetic NOD.NON-Thy-1a donors. Diabetes. 1993;42(1):44-55.
167. Tsai S, Shameli A, Santamaria P. CD8+ T cells in type 1 diabetes. Adv Immunol. 2008;100:79-124.
168. Suk K, Kim S, Kim YH, Kim KA, Chang I, Yagita H, et al. IFN-gamma/TNF-alpha synergism as the final effector in autoimmune diabetes: a key role for STAT1/IFN regulatory factor-1 pathway in pancreatic beta cell death. J Immunol. 2001;166(7):4481-9.
169. Chatenoud L, Thervet E, Primo J, Bach JF. Anti-CD3 antibody induces long-term remission of overt autoimmunity in nonobese diabetic mice. Proc Natl Acad Sci U S A. 1994;91(1):123-7.
170. Chatenoud L. Immune therapy for type 1 diabetes mellitus-what is unique about anti-CD3 antibodies? Nat Rev Endocrinol. 2010;6(3):149-57.
171. Keymeulen B, Walter M, Mathieu C, Kaufman L, Gorus F, Hilbrands R, et al. Four-year metabolic outcome of a randomised controlled CD3-antibody trial in recent-onset type 1 diabetic patients depends on their age and baseline residual beta cell mass. Diabetologia. 2010;53(4):614-23.
172. Gaglia J, Kissler S. Anti-CD3 Antibody for the Prevention of Type 1 Diabetes: A Story of Perseverance. Biochemistry. 2019;58(40):4107-11.
173. Burrack AL, Martinov T, Fife BT. T Cell-Mediated Beta Cell Destruction: Autoimmunity and Alloimmunity in the Context of Type 1 Diabetes. Front Endocrinol (Lausanne). 2017;8:343.
174. von Scholten BJ, Kreiner FF, Gough SCL, von Herrath M. Current and future therapies for type 1 diabetes. Diabetologia. 2021;64(5):1037-48.
175. Visperas A, Vignali DA. Are Regulatory T Cells Defective in Type 1 Diabetes and Can We Fix Them? J Immunol. 2016;197(10):3762-70.
176. Tritt M, Sgouroudis E, d'Hennezel E, Albanese A, Piccirillo CA. Functional waning of naturally occurring CD4+ regulatory T-cells contributes to the onset of autoimmune diabetes. Diabetes. 2008;57(1):113-23.
177. Feuerer M, Jiang W, Holler PD, Satpathy A, Campbell C, Bogue M, et al. Enhanced thymic selection of FoxP3+ regulatory T cells in the NOD mouse model of autoimmune diabetes. Proc Natl Acad Sci U S A. 2007;104(46):18181-6.

178. D'Alise AM, Auyeung V, Feuerer M, Nishio J, Fontenot J, Benoist C, et al. The defect in T-cell regulation in NOD mice is an effect on the T-cell effectors. Proc Natl Acad Sci U S A. 2008;105(50):19857-62.
179. Godoy GJ, Paira DA, Olivera C, Breser ML, Sanchez LR, Motrich RD, et al. Differences in T regulatory cells between mouse strains frequently used in immunological research: Treg cell quantities and subpopulations in NOD, B6 and BALB/c mice. Immunol Lett. 2020;223:17-25.
180. Tang Q, Adams JY, Penaranda C, Melli K, Piaggio E, Sgouroudis E, et al. Central role of defective interleukin-2 production in the triggering of islet autoimmune destruction. Immunity. 2008;28(5):687-97.
181. Grinberg-Bleyer Y, Baeyens A, You S, Elhage R, Fourcade G, Gregoire S, et al. IL-2 reverses established type 1 diabetes in NOD mice by a local effect on pancreatic regulatory T cells. J Exp Med. 2010;207(9):1871-8.
182. Spangler JB, Moraga I, Mendoza JL, Garcia KC. Insights into cytokine-receptor interactions from cytokine engineering. Annu Rev Immunol. 2015;33:139-67.
183. Tahvildari M, Dana R. Low-Dose IL-2 Therapy in Transplantation, Autoimmunity, and Inflammatory Diseases. J Immunol. 2019;203(11):2749-55.
184. Viisanen T, Gazali AM, Ihantola EL, Ekman I, Nanto-Salonen K, Veijola R, et al. FOXP3+ Regulatory T Cell Compartment Is Altered in Children With Newly Diagnosed Type 1 Diabetes but Not in Autoantibody-Positive at-Risk Children. Front Immunol. 2019;10:19.
185. Brusko T, Wasserfall C, McGrail K, Schatz R, Viener HL, Schatz D, et al. No alterations in the frequency of FOXP3+ regulatory T-cells in type 1 diabetes. Diabetes. 2007;56(3):604-12.
186. Vecchione A, Di Fonte R, Gerosa J, Jofra T, Cicalese MP, Napoleone V, et al. Reduced PD-1 expression on circulating follicular and conventional FOXP3(+) Treg cells in children with new onset type 1 diabetes and autoantibody-positive at-risk children. Clin Immunol. 2020;211:108319.
187. Bluestone JA, Buckner JH, Fitch M, Gitelman SE, Gupta S, Hellerstein MK, et al. Type 1 diabetes immunotherapy using polyclonal regulatory T cells. Sci Transl Med. 2015;7(315):315ra189.
188. Zhang Q, Lu W, Liang CL, Chen Y, Liu H, Qiu F, et al. Chimeric Antigen Receptor (CAR) Treg: A Promising Approach to Inducing Immunological Tolerance. Front Immunol. 2018;9:2359.
189. Hillhouse EE, Delisle JS, Lesage S. Immunoregulatory CD4(-)CD8(-) T cells as a potential therapeutic tool for transplantation, autoimmunity, and cancer. Front Immunol. 2013;4:6.
190. Dugas V, Beauchamp C, Chabot-Roy G, Hillhouse EE, Lesage S. Implication of the CD47 pathway in autoimmune diabetes. J Autoimmun. 2010;35(1):23-32.
191. Duncan B, Nazarov-Stoica C, Surls J, Kehl M, Bona C, Casares S, et al. Double negative (CD3+ 4- 8-) TCR alphabeta splenic cells from young NOD mice provide long-lasting protection against type 1 diabetes. PLoS One. 2010;5(7):e11427.
192. Ford MS, Chen W, Wong S, Li C, Vanama R, Elford AR, et al. Peptide-activated double-negative T cells can prevent autoimmune type-1 diabetes development. Eur J Immunol. 2007;37(8):2234-41.
193. Dugas V, Liston A, Hillhouse EE, Collin R, Chabot-Roy G, Pelletier AN, et al. Idd13 is involved in determining immunoregulatory DN T-cell number in NOD mice. Genes Immun. 2014;15(2):82-7.

194. Purcell AW, Sechi S, DiLorenzo TP. The Evolving Landscape of Autoantigen Discovery and Characterization in Type 1 Diabetes. Diabetes. 2019;68(5):879-86.
195. Roep BO, Peakman M. Antigen targets of type 1 diabetes autoimmunity. Cold Spring Harb Perspect Med. 2012;2(4):a007781.
196. Chaparro RJ, Dilorenzo TP. An update on the use of NOD mice to study autoimmune (Type 1) diabetes. Expert Rev Clin Immunol. 2010;6(6):939-55.
197. Nakayama M. Insulin as a key autoantigen in the development of type 1 diabetes. Diabetes Metab Res Rev. 2011;27(8):773-7.
198. Weiss M, Steiner DF, Philipson LH. Insulin Biosynthesis, Secretion, Structure, and Structure-Activity Relationships. In: Feingold KR, Anawalt B, Boyce A, Chrousos G, de Herder WW, Dhatariya K, et al., editors. Endotext. South Dartmouth (MA)2000.
199. Daniel D, Gill RG, Schloot N, Wegmann D. Epitope specificity, cytokine production profile and diabetogenic activity of insulin-specific T cell clones isolated from NOD mice. Eur J Immunol. 1995;25(4):1056-62.
200. Nakayama M, Abiru N, Moriyama H, Babaya N, Liu E, Miao D, et al. Prime role for an insulin epitope in the development of type 1 diabetes in NOD mice. Nature. 2005;435(7039):220-3.
201. Mohan JF, Levisetti MG, Calderon B, Herzog JW, Petzold SJ, Unanue ER. Unique autoreactive T cells recognize insulin peptides generated within the islets of Langerhans in autoimmune diabetes. Nat Immunol. 2010;11(4):350-4.
202. Wan X, Zinselmeyer BH, Zakharov PN, Vomund AN, Taniguchi R, Santambrogio L, et al. Pancreatic islets communicate with lymphoid tissues via exocytosis of insulin peptides. Nature. 2018.
203. Delong T, Wiles TA, Baker RL, Bradley B, Barbour G, Reisdorph R, et al. Pathogenic CD4 T cells in type 1 diabetes recognize epitopes formed by peptide fusion. Science. 2016;351(6274):711-4.
204. Baker RL, Jamison BL, Haskins K. Hybrid insulin peptides are neo-epitopes for CD4 T cells in autoimmune diabetes. Curr Opin Endocrinol Diabetes Obes. 2019;26(4):195-200.
205. Zhang ZJ, Davidson L, Eisenbarth G, Weiner HL. Suppression of diabetes in nonobese diabetic mice by oral administration of porcine insulin. Proc Natl Acad Sci U S A. 1991;88(22):10252-6.
206. Shoda LK, Young DL, Ramanujan S, Whiting CC, Atkinson MA, Bluestone JA, et al. A comprehensive review of interventions in the NOD mouse and implications for translation. Immunity. 2005;23(2):115-26.
207. Wherrett DK, Bundy B, Becker DJ, DiMeglio LA, Gitelman SE, Goland R, et al. Antigen-based therapy with glutamic acid decarboxylase (GAD) vaccine in patients with recent-onset type 1 diabetes: a randomised double-blind trial. Lancet. 2011;378(9788):319-27.
208. Skyler JS, Krischer JP, Wolfsdorf J, Cowie C, Palmer JP, Greenbaum C, et al. Effects of oral insulin in relatives of patients with type 1 diabetes: The Diabetes Prevention Trial--Type 1. Diabetes Care. 2005;28(5):1068-76.
209. Willcox A, Richardson SJ, Bone AJ, Foulis AK, Morgan NG. Analysis of islet inflammation in human type 1 diabetes. Clin Exp Immunol. 2009;155(2):173-81.

210. Magnuson AM, Thurber GM, Kohler RH, Weissleder R, Mathis D, Benoist C. Population dynamics of islet-infiltrating cells in autoimmune diabetes. Proc Natl Acad Sci U S A. 2015;112(5):1511-6.
211. Serreze DV, Chapman HD, Varnum DS, Hanson MS, Reifsnyder PC, Richard SD, et al. B lymphocytes are essential for the initiation of T cell-mediated autoimmune diabetes: analysis of a new "speed congenic" stock of NOD.Ig mu null mice. J Exp Med. 1996;184(5):2049-53.
212. Regnell SE, Lernmark A. Early prediction of autoimmune (type 1) diabetes. Diabetologia. 2017;60(8):1370-81.
213. Jacobsen LM, Haller MJ, Schatz DA. Understanding Pre-Type 1 Diabetes: The Key to Prevention. Front Endocrinol (Lausanne). 2018;9:70.
214. Mehers KL, Gillespie KM. The genetic basis for type 1 diabetes. Br Med Bull. 2008;88(1):115-29.
215. Achenbach P, Warncke K, Reiter J, Naserke HE, Williams AJ, Bingley PJ, et al. Stratification of type 1 diabetes risk on the basis of islet autoantibody characteristics. Diabetes. 2004;53(2):384-92.
216. Roll U, Christie MR, Fuchtenbusch M, Payton MA, Hawkes CJ, Ziegler AG. Perinatal autoimmunity in offspring of diabetic parents. The German Multicenter BABY-DIAB study: detection of humoral immune responses to islet antigens in early childhood. Diabetes. 1996;45(7):967-73.
217. Diana J, Simoni Y, Furio L, Beaudoin L, Agerberth B, Barrat F, et al. Crosstalk between neutrophils, B-1a cells and plasmacytoid dendritic cells initiates autoimmune diabetes. Nat Med. 2013;19(1):65-73.
218. Greeley SA, Katsumata M, Yu L, Eisenbarth GS, Moore DJ, Goodarzi H, et al. Elimination of maternally transmitted autoantibodies prevents diabetes in nonobese diabetic mice. Nat Med. 2002;8(4):399-402.
219. von Herrath M, Bach JF. Juvenile autoimmune diabetes: a pathogenic role for maternal antibodies? Nat Med. 2002;8(4):331-3.
220. Martin S, Wolf-Eichbaum D, Duinkerken G, Scherbaum WA, Kolb H, Noordzij JG, et al. Development of type 1 diabetes despite severe hereditary B-cell deficiency. N Engl J Med. 2001;345(14):1036-40.
221. Koczwara K, Bonifacio E, Ziegler AG. Transmission of maternal islet antibodies and risk of autoimmune diabetes in offspring of mothers with type 1 diabetes. Diabetes. 2004;53(1):1-4.
222. Wong FS, Wen L, Tang M, Ramanathan M, Visintin I, Daugherty J, et al. Investigation of the role of B-cells in type 1 diabetes in the NOD mouse. Diabetes. 2004;53(10):2581-7.
223. Serreze DV, Fleming SA, Chapman HD, Richard SD, Leiter EH, Tisch RM. B lymphocytes are critical antigen-presenting cells for the initiation of T cell-mediated autoimmune diabetes in nonobese diabetic mice. J Immunol. 1998;161(8):3912-8.
224. Noorchashm H, Lieu YK, Noorchashm N, Rostami SY, Greeley SA, Schlachterman A, et al. I-Ag7-mediated antigen presentation by B lymphocytes is critical in overcoming a checkpoint in T cell tolerance to islet beta cells of nonobese diabetic mice. J Immunol. 1999;163(2):743-50.
225. Felton JL, Maseda D, Bonami RH, Hulbert C, Thomas JW. Anti-Insulin B Cells Are Poised for Antigen Presentation in Type 1 Diabetes. J Immunol. 2018;201(3):861-73.
226. Marino E, Tan B, Binge L, Mackay CR, Grey ST. B-cell cross-presentation of autologous antigen precipitates diabetes. Diabetes. 2012;61(11):2893-905.

227. Lu J, Liu J, Li L, Lan Y, Liang Y. Cytokines in type 1 diabetes: mechanisms of action and immunotherapeutic targets. Clin Transl Immunology. 2020;9(3):e1122.
228. El-Mokhtar MA, Elsherbiny NM, Sayed D, Raafat DM, Askar E, Hussein A, et al. Altered Regulatory B Cell Subsets in Children with Type 1 Diabetes Mellitus. J Immunol Res. 2020;2020:8935694.
229. Jagannathan M, McDonnell M, Liang Y, Hasturk H, Hetzel J, Rubin D, et al. Toll-like receptors regulate B cell cytokine production in patients with diabetes. Diabetologia. 2010;53(7):1461-71.
230. Silveira PA, Chapman HD, Stolp J, Johnson E, Cox SL, Hunter K, et al. Genes within the Idd5 and Idd9/11 diabetes susceptibility loci affect the pathogenic activity of B cells in nonobese diabetic mice. J Immunol. 2006;177(10):7033-41.
231. Luzina IG, Atamas SP, Storrer CE, daSilva LC, Kelsoe G, Papadimitriou JC, et al. Spontaneous formation of germinal centers in autoimmune mice. J Leukoc Biol. 2001;70(4):578-84.
232. Karnell JL, Mahmoud TI, Herbst R, Ettinger R. Discerning the kinetics of autoimmune manifestations in a model of Sjogren's syndrome. Mol Immunol. 2014;62(2):277-82.
233. Lesage S, Hartley SB, Akkaraju S, Wilson J, Townsend M, Goodnow CC. Failure to censor forbidden clones of CD4 T cells in autoimmune diabetes. J Exp Med. 2002;196(9):1175-88.
234. Astorri E, Bombardieri M, Gabba S, Peakman M, Pozzilli P, Pitzalis C. Evolution of ectopic lymphoid neogenesis and in situ autoantibody production in autoimmune nonobese diabetic mice: cellular and molecular characterization of tertiary lymphoid structures in pancreatic islets. J Immunol. 2010;185(6):3359-68.
235. McGuire HM, Vogelzang A, Hill N, Flodstrom-Tullberg M, Sprent J, King C. Loss of parity between IL-2 and IL-21 in the NOD Idd3 locus. Proc Natl Acad Sci U S A. 2009;106(46):19438-43.
236. Sutherland AP, Van Belle T, Wurster AL, Suto A, Michaud M, Zhang D, et al. Interleukin-21 is required for the development of type 1 diabetes in NOD mice. Diabetes. 2009;58(5):1144-55.
237. King HW, Wells KL, Shipony Z, Kathiria AS, Wagar LE, Lareau C, et al. Integrated single-cell transcriptomics and epigenomics reveals strong germinal center-associated etiology of autoimmune risk loci. Sci Immunol. 2021;6(64):eabh3768.
238. Balasa B, Krahl T, Patstone G, Lee J, Tisch R, McDevitt HO, et al. CD40 ligand-CD40 interactions are necessary for the initiation of insulitis and diabetes in nonobese diabetic mice. J Immunol. 1997;159(9):4620-7.
239. Vaitaitis GM, Olmstead MH, Waid DM, Carter JR, Wagner DH, Jr. A CD40-targeted peptide controls and reverses type 1 diabetes in NOD mice. Diabetologia. 2014;57(11):2366-73.
240. Matsumoto M, Mariathasan S, Nahm MH, Baranyay F, Peschon JJ, Chaplin DD. Role of lymphotoxin and the type I TNF receptor in the formation of germinal centers. Science. 1996;271(5253):1289-91.
241. Levisetti MG, Suri A, Frederick K, Unanue ER. Absence of lymph nodes in NOD mice treated with lymphotoxin-beta receptor immunoglobulin protects from diabetes. Diabetes. 2004;53(12):3115-9.
242. Degn SE, van der Poel CE, Firl DJ, Ayoglu B, Al Qureshah FA, Bajic G, et al. Clonal Evolution of Autoreactive Germinal Centers. Cell. 2017;170(5):913-26 e19.

243. DeFranco AL. Germinal centers and autoimmune disease in humans and mice. Immunol Cell Biol. 2016;94(10):918-24.
244. Hu CY, Rodriguez-Pinto D, Du W, Ahuja A, Henegariu O, Wong FS, et al. Treatment with CD20-specific antibody prevents and reverses autoimmune diabetes in mice. J Clin Invest. 2007;117(12):3857-67.
245. Boldison J, Da Rosa LC, Buckingham L, Davies J, Wen L, Wong FS. Phenotypically distinct anti-insulin B cells repopulate pancreatic islets after anti-CD20 treatment in NOD mice. Diabetologia. 2019;62(11):2052-65.
246. Serreze DV, Chapman HD, Niens M, Dunn R, Kehry MR, Driver JP, et al. Loss of intra-islet CD20 expression may complicate efficacy of B-cell-directed type 1 diabetes therapies. Diabetes. 2011;60(11):2914-21.
247. Smulski CR, Eibel H. BAFF and BAFF-Receptor in B Cell Selection and Survival. Front Immunol. 2018;9:2285.
248. Marino E, Villanueva J, Walters S, Liuwantara D, Mackay F, Grey ST. CD4(+)CD25(+) T-cells control autoimmunity in the absence of B-cells. Diabetes. 2009;58(7):1568-77.
249. Wang Q, Racine JJ, Ratiu JJ, Wang S, Ettinger R, Wasserfall C, et al. Transient BAFF Blockade Inhibits Type 1 Diabetes Development in Nonobese Diabetic Mice by Enriching Immunoregulatory B Lymphocytes Sensitive to Deletion by Anti-CD20 Cotherapy. J Immunol. 2017;199(11):3757-70.
250. Hamad AR, Ahmed R, Donner T, Fousteri G. B cell-targeted immunotherapy for type 1 diabetes: What can make it work? Discov Med. 2016;21(115):213-9.
251. Pescovitz MD, Greenbaum CJ, Krause-Steinrauf H, Becker DJ, Gitelman SE, Goland R, et al. Rituximab, B-lymphocyte depletion, and preservation of beta-cell function. N Engl J Med. 2009;361(22):2143-52.
252. Vecchio I, Tornali C, Bragazzi NL, Martini M. The Discovery of Insulin: An Important Milestone in the History of Medicine. Front Endocrinol (Lausanne). 2018;9:613.
253. Collin R, Dugas V, Pelletier AN, Chabot-Roy G, Lesage S. The mouse idd2 locus is linked to the proportion of immunoregulatory double-negative T cells, a trait associated with autoimmune diabetes resistance. J Immunol. 2014;193(7):3503-12.
254. Hillhouse EE, Beauchamp C, Chabot-Roy G, Dugas V, Lesage S. Interleukin-10 limits the expansion of immunoregulatory CD4-CD8- T cells in autoimmune-prone non-obese diabetic mice. Immunol Cell Biol. 2010;88(8):771-80.
255. Capone M, Curnow J, Bouvier G, Ferrier P, Horvat B. T cell development in TCR-alpha beta transgenic mice. Analysis using V(D)J recombination substrates. J Immunol. 1995;154(10):5165-72.
256. Barrett JC, Clayton DG, Concannon P, Akolkar B, Cooper JD, Erlich HA, et al. Genome-wide association study and meta-analysis find that over 40 loci affect risk of type 1 diabetes. Nat Genet. 2009;41(6):703-7.
257. Wicker LS, Clark J, Fraser HI, Garner VE, Gonzalez-Munoz A, Healy B, et al. Type 1 diabetes genes and pathways shared by humans and NOD mice. J Autoimmun. 2005;25 Suppl:29-33.
258. Maier LM, Wicker LS. Genetic susceptibility to type 1 diabetes. Curr Opin Immunol. 2005;17(6):601-8.

259. Wicker LS, Todd JA, Peterson LB. Genetic control of autoimmune diabetes in the NOD mouse. Annu Rev Immunol. 1995;13:179-200.
260. Rioux JD, Goyette P, Vyse TJ, Hammarstrom L, Fernando MM, Green T, et al. Mapping of multiple susceptibility variants within the MHC region for 7 immune-mediated diseases. Proc Natl Acad Sci U S A. 2009;106(44):18680-5.
261. Noble JA, Erlich HA. Genetics of type 1 diabetes. Cold Spring Harbor perspectives in medicine. 2012;2(1):a007732.
262. Todd JA, Bell JI, McDevitt HO. HLA-DQ beta gene contributes to susceptibility and resistance to insulin-dependent diabetes mellitus. Nature. 1987;329(6140):599-604.
263. Singer SM, Tisch R, Yang XD, Sytwu HK, Liblau R, McDevitt HO. Prevention of diabetes in NOD mice by a mutated I-Ab transgene. Diabetes. 1998;47(10):1570-7.
264. Ridgway WM, Peterson LB, Todd JA, Rainbow DB, Healy B, Burren OS, et al. Gene-gene interactions in the NOD mouse model of type 1 diabetes. Adv Immunol. 2008;100:151-75.
265. Herold KC, Vignali DA, Cooke A, Bluestone JA. Type 1 diabetes: translating mechanistic observations into effective clinical outcomes. Nat Rev Immunol. 2013;13(4):243-56.
266. Hinman RM, Smith MJ, Cambier JC. B cells and type 1 diabetes ...in mice and men. Immunol Lett. 2014;160(2):128-32.
267. O'Neill SK, Liu E, Cambier JC. Change you can B(cell)eive in: recent progress confirms a critical role for B cells in type 1 diabetes. Curr Opin Endocrinol Diabetes Obes. 2009;16(4):293-8.
268. Ferris ST, Carrero JA, Mohan JF, Calderon B, Murphy KM, Unanue ER. A minor subset of Batf3-dependent antigen-presenting cells in islets of Langerhans is essential for the development of autoimmune diabetes. Immunity. 2014;41(4):657-69.
269. Hamilton-Williams EE, Martinez X, Clark J, Howlett S, Hunter KM, Rainbow DB, et al. Expression of diabetes-associated genes by dendritic cells and CD4 T cells drives the loss of tolerance in nonobese diabetic mice. J Immunol. 2009;183(3):1533-41.
270. Turley S, Poirot L, Hattori M, Benoist C, Mathis D. Physiological beta cell death triggers priming of self-reactive T cells by dendritic cells in a type-1 diabetes model. J Exp Med. 2003;198(10):1527-37.
271. Audiger C, Rahman MJ, Yun TJ, Tarbell KV, Lesage S. The Importance of Dendritic Cells in Maintaining Immune Tolerance. J Immunol. 2017;198(6):2223-31.
272. Calderon B, Carrero JA, Unanue ER. The central role of antigen presentation in islets of Langerhans in autoimmune diabetes. Curr Opin Immunol. 2014;26:32-40.
273. Jansen A, van Hagen M, Drexhage HA. Defective maturation and function of antigen-presenting cells in type 1 diabetes. Lancet. 1995;345(8948):491-2.
274. Morel PA. Dendritic cell subsets in type 1 diabetes: friend or foe? Front Immunol. 2013;4:415.
275. Marleau AM, Summers KL, Singh B. Differential Contributions of APC Subsets to T Cell Activation in Nonobese Diabetic Mice. J Immunol. 2008;180(8):5235-49.
276. Hillhouse EE, Collin R, Chabot-Roy G, Guyon MJ, Tessier N, Boulay M, et al. Nearby Construction Impedes the Progression to Overt Autoimmune Diabetes in NOD Mice. J Diabetes Res. 2013;2013:620313.
277. Bolger AM, Lohse M, Usadel B. Trimmomatic: a flexible trimmer for Illumina sequence data. Bioinformatics. 2014;30(15):2114-20.

278. Dobin A, Davis CA, Schlesinger F, Drenkow J, Zaleski C, Jha S, et al. STAR: ultrafast universal RNA-seq aligner. Bioinformatics. 2013;29(1):15-21.
279. Li B, Dewey CN. RSEM: accurate transcript quantification from RNA-Seq data with or without a reference genome. BMC Bioinformatics. 2011;12:323.
280. Garrison EP, Marth GJaG. Haplotype-based variant detection from short-read sequencing. 2012.
281. Cingolani P, Platts A, Wang le L, Coon M, Nguyen T, Wang L, et al. A program for annotating and predicting the effects of single nucleotide polymorphisms, SnpEff: SNPs in the genome of Drosophila melanogaster strain w1118; iso-2; iso-3. Fly (Austin). 2012;6(2):80-92.
282. Ritchie ME, Phipson B, Wu D, Hu Y, Law CW, Shi W, et al. limma powers differential expression analyses for RNA-sequencing and microarray studies. Nucleic Acids Res. 2015;43(7):e47.
283. Battegay M, Cooper S, Althage A, Banziger J, Hengartner H, Zinkernagel RM. Quantification of lymphocytic choriomeningitis virus with an immunological focus assay in 24- or 96-well plates. J Virol Methods. 1991;33(1-2):191-8.
284. Mathieu M, Duval F, Daudelin JF, Labrecque N. The Notch signaling pathway controls short-lived effector CD8+ T cell differentiation but is dispensable for memory generation. J Immunol. 2015;194(12):5654-62.
285. Virostko J, Radhika A, Poffenberger G, Dula AN, Moore DJ, Powers AC. Bioluminescence imaging reveals dynamics of beta cell loss in the non-obese diabetic (NOD) mouse model. PLoS One. 2013;8(3):e57784.
286. Serreze DV, Bridgett M, Chapman HD, Chen E, Richard SD, Leiter EH. Subcongenic analysis of the Idd13 locus in NOD/Lt mice: evidence for several susceptibility genes including a possible diabetogenic role for beta 2-microglobulin. J Immunol. 1998;160(3):1472-8.
287. Kachapati K, Adams DE, Wu Y, Steward CA, Rainbow DB, Wicker LS, et al. The B10 Idd9.3 locus mediates accumulation of functionally superior CD137(+) regulatory T cells in the nonobese diabetic type 1 diabetes model. J Immunol. 2012;189(10):5001-15.
288. Dooley J, Tian L, Schonefeldt S, Delghingaro-Augusto V, Garcia-Perez JE, Pasciuto E, et al. Genetic predisposition for beta cell fragility underlies type 1 and type 2 diabetes. Nat Genet. 2016;48(5):519-27.
289. Soderstrom I, Bergman ML, Colucci F, Lejon K, Bergqvist I, Holmberg D. Establishment and characterization of RAG-2 deficient non-obese diabetic mice. Scand J Immunol. 1996;43(5):525-30.
290. Makino S, Harada M, Kishimoto Y, Hayashi Y. Absence of insulitis and overt diabetes in athymic nude mice with NOD genetic background. Jikken Dobutsu. 1986;35(4):495-8.
291. Marino E, Batten M, Groom J, Walters S, Liuwantara D, Mackay F, et al. Marginal-zone B-cells of nonobese diabetic mice expand with diabetes onset, invade the pancreatic lymph nodes, and present autoantigen to diabetogenic T-cells. Diabetes. 2008;57(2):395-404.
292. Honjo T, Kinoshita K, Muramatsu M. Molecular mechanism of class switch recombination: linkage with somatic hypermutation. Annu Rev Immunol. 2002;20:165-96.
293. Reboldi A, Cyster JG. Peyer's patches: organizing B-cell responses at the intestinal frontier. Immunol Rev. 2016;271(1):230-45.

294. Lombard-Vadnais F, Collin R, Daudelin JF, Chabot-Roy G, Labrecque N, Lesage S. The Idd2 Locus Confers Prominent Resistance to Autoimmune Diabetes. J Immunol. 2022;208(4):898-909.
295. Smink LJ, Helton EM, Healy BC, Cavnor CC, Lam AC, Flamez D, et al. T1DBase, a community web-based resource for type 1 diabetes research. Nucleic Acids Res. 2005;33(Database issue):D544-9.
296. Prochazka M, Serreze DV, Worthen SM, Leiter EH. Genetic control of diabetogenesis in NOD/Lt mice. Development and analysis of congenic stocks. Diabetes. 1989;38(11):1446-55.
297. Collin R, Dugas V, Pelletier AN, Chabot-Roy G, Lesage S. Evidence of genetic epistasis in autoimmune diabetes susceptibility revealed by mouse congenic sublines. Immunogenetics. 2021.
298. Collin R, Dugas V, Chabot-Roy G, Salem D, Zahn A, Di Noia JM, et al. Autoimmunity and antibody affinity maturation are modulated by genetic variants on mouse chromosome 12. J Autoimmun. 2015;58:90-9.
299. Nutt SL, Tarlinton DM. Germinal center B and follicular helper T cells: siblings, cousins or just good friends? Nat Immunol. 2011;12(6):472-7.
300. Banday VS, Lejon K. Elevated systemic glutamic acid level in the non-obese diabetic mouse is Idd linked and induces beta cell apoptosis. Immunology. 2017;150(2):162-71.
301. Vomund AN, Lichti CF, Peterson OJ, Arbelaez AM, Wan X, Unanue ER. Blood leukocytes recapitulate diabetogenic peptide-MHC-II complexes displayed in the pancreatic islets. J Exp Med. 2021;218(6).
302. Kendall PL, Case JB, Sullivan AM, Holderness JS, Wells KS, Liu E, et al. Tolerant anti-insulin B cells are effective APCs. J Immunol. 2013;190(6):2519-26.
303. Stebegg M, Kumar SD, Silva-Cayetano A, Fonseca VR, Linterman MA, Graca L. Regulation of the Germinal Center Response. Front Immunol. 2018;9:2469.
304. Yeh CH, Nojima T, Kuraoka M, Kelsoe G. Germinal center entry not selection of B cells is controlled by peptide-MHCII complex density. Nat Commun. 2018;9(1):928.
305. Schaum N, Karkanias J, Neff NF, May AP, Quake SR, Wyss-Coray T, et al. Single-cell transcriptomics of 20 mouse organs creates a Tabula Muris. Nature. 2018;562(7727):367-72.
306. Brink R, Phan TG. Self-Reactive B Cells in the Germinal Center Reaction. Annu Rev Immunol. 2018;36:339-57.
307. Tian J, Zekzer D, Lu Y, Dang H, Kaufman DL. B cells are crucial for determinant spreading of T cell autoimmunity among beta cell antigens in diabetes-prone nonobese diabetic mice. J Immunol. 2006;176(4):2654-61.
308. Banday VS, Thyagarajan R, Lejon K. Contribution of both B-cell intrinsic alterations as well as non-hematopoietic-derived factors in the enhanced immune response of the NOD mouse. Autoimmunity. 2017;50(6):363-9.
309. Uhlen M, Fagerberg L, Hallstrom BM, Lindskog C, Oksvold P, Mardinoglu A, et al. Proteomics. Tissue-based map of the human proteome. Science. 2015;347(6220):1260419.
310. Kim U, Qin XF, Gong S, Stevens S, Luo Y, Nussenzweig M, et al. The B-cell-specific transcription coactivator OCA-B/OBF-1/Bob-1 is essential for normal production of immunoglobulin isotypes. Nature. 1996;383(6600):542-7.
311. Heng TS, Painter MW, Immunological Genome Project C. The Immunological Genome Project: networks of gene expression in immune cells. Nat Immunol. 2008;9(10):1091-4.

312. Hess J, Nielsen PJ, Fischer KD, Bujard H, Wirth T. The B lymphocyte-specific coactivator BOB.1/OBF.1 is required at multiple stages of B-cell development. Mol Cell Biol. 2001;21(5):1531-9.
313. Samardzic T, Marinkovic D, Nielsen PJ, Nitschke L, Wirth T. BOB.1/OBF.1 deficiency affects marginal-zone B-cell compartment. Mol Cell Biol. 2002;22(23):8320-31.
314. Nielsen PJ, Georgiev O, Lorenz B, Schaffner W. B lymphocytes are impaired in mice lacking the transcriptional co-activator Bob1/OCA-B/OBF1. Eur J Immunol. 1996;26(12):3214-8.
315. Qin XF, Reichlin A, Luo Y, Roeder RG, Nussenzweig MC. OCA-B integrates B cell antigen receptor-, CD40L- and IL 4-mediated signals for the germinal center pathway of B cell development. EMBO J. 1998;17(17):5066-75.
316. Siegel R, Kim U, Patke A, Yu X, Ren X, Tarakhovsky A, et al. Nontranscriptional regulation of SYK by the coactivator OCA-B is required at multiple stages of B cell development. Cell. 2006;125(4):761-74.
317. Corcoran LM, Hasbold J, Dietrich W, Hawkins E, Kallies A, Nutt SL, et al. Differential requirement for OBF-1 during antibody-secreting cell differentiation. J Exp Med. 2005;201(9):1385-96.
318. Bartholdy B, Du Roure C, Bordon A, Emslie D, Corcoran LM, Matthias P. The Ets factor Spi-B is a direct critical target of the coactivator OBF-1. Proc Natl Acad Sci U S A. 2006;103(31):11665-70.
319. Su GH, Chen HM, Muthusamy N, Garrett-Sinha LA, Baunoch D, Tenen DG, et al. Defective B cell receptor-mediated responses in mice lacking the Ets protein, Spi-B. EMBO J. 1997;16(23):7118-29.
320. Basso K, Dalla-Favera R. BCL6: master regulator of the germinal center reaction and key oncogene in B cell lymphomagenesis. Adv Immunol. 2010;105:193-210.
321. Shakya A, Goren A, Shalek A, German CN, Snook J, Kuchroo VK, et al. Oct1 and OCA-B are selectively required for CD4 memory T cell function. J Exp Med. 2015;212(12):2115-31.
322. Sauter P, Matthias P. The B cell-specific coactivator OBF-1 (OCA-B, Bob-1) is inducible in T cells and its expression is dispensable for IL-2 gene induction. Immunobiology. 1997;198(1-3):207-16.
323. Yosef N, Shalek AK, Gaublomme JT, Jin H, Lee Y, Awasthi A, et al. Dynamic regulatory network controlling TH17 cell differentiation. Nature. 2013;496(7446):461-8.
324. Skarnes WC, Rosen B, West AP, Koutsourakis M, Bushell W, Iyer V, et al. A conditional knockout resource for the genome-wide study of mouse gene function. Nature. 2011;474(7351):337-42.
325. Rodriguez CI, Buchholz F, Galloway J, Sequerra R, Kasper J, Ayala R, et al. High-efficiency deleter mice show that FLPe is an alternative to Cre-loxP. Nat Genet. 2000;25(2):139-40.
326. Ogilvy S, Metcalf D, Gibson L, Bath ML, Harris AW, Adams JM. Promoter elements of vav drive transgene expression in vivo throughout the hematopoietic compartment. Blood. 1999;94(6):1855-63.
327. Georgiades P, Ogilvy S, Duval H, Licence DR, Charnock-Jones DS, Smith SK, et al. VavCre transgenic mice: a tool for mutagenesis in hematopoietic and endothelial lineages. Genesis. 2002;34(4):251-6.

328. Mueller K, Quandt J, Marienfeld RB, Weihrich P, Fiedler K, Claussnitzer M, et al. Octamer-dependent transcription in T cells is mediated by NFAT and NF-kappaB. Nucleic Acids Res. 2013;41(4):2138-54.
329. Wolfer A, Bakker T, Wilson A, Nicolas M, Ioannidis V, Littman DR, et al. Inactivation of Notch 1 in immature thymocytes does not perturb CD4 or CD8T cell development. Nat Immunol. 2001;2(3):235-41.
330. Moulton VR, Bushar ND, Leeser DB, Patke DS, Farber DL. Divergent generation of heterogeneous memory CD4 T cells. J Immunol. 2006;177(2):869-76.
331. McAllister EJ, Apgar JR, Leung CR, Rickert RC, Jellusova J. New Methods To Analyze B Cell Immune Responses to Thymus-Dependent Antigen Sheep Red Blood Cells. The Journal of Immunology. 2017;199(8):2998-3003.
332. Hwang SS, Kim LK, Lee GR, Flavell RA. Role of OCT-1 and partner proteins in T cell differentiation. Biochim Biophys Acta. 2016;1859(6):825-31.
333. Karnowski A, Chevrier S, Belz GT, Mount A, Emslie D, D'Costa K, et al. B and T cells collaborate in antiviral responses via IL-6, IL-21, and transcriptional activator and coactivator, Oct2 and OBF-1. J Exp Med. 2012;209(11):2049-64.
334. Zwilling S, Dieckmann A, Pfisterer P, Angel P, Wirth T. Inducible expression and phosphorylation of coactivator BOB.1/OBF.1 in T cells. Science. 1997;277(5323):221-5.
335. Brunner C, Sindrilaru A, Girkontaite I, Fischer KD, Sunderkotter C, Wirth T. BOB.1/OBF.1 controls the balance of TH1 and TH2 immune responses. EMBO J. 2007;26(13):3191-202.
336. Hogenbirk MA, Heideman MR, Velds A, van den Berk PC, Kerkhoven RM, van Steensel B, et al. Differential programming of B cells in AID deficient mice. PLoS One. 2013;8(7):e69815.
337. Chisolm DA, Cheng W, Colburn SA, Silva-Sanchez A, Meza-Perez S, Randall TD, et al. Defining Genetic Variation in Widely Used Congenic and Backcrossed Mouse Models Reveals Varied Regulation of Genes Important for Immune Responses. Immunity. 2019;51(1):155-68 e5.
338. Trub M, Barr TA, Morrison VL, Brown S, Caserta S, Rixon J, et al. Heterogeneity of Phenotype and Function Reflects the Multistage Development of T Follicular Helper Cells. Front Immunol. 2017;8:489.
339. Weinstein JS, Bertino SA, Hernandez SG, Poholek AC, Teplitzky TB, Nowyhed HN, et al. B cells in T follicular helper cell development and function: separable roles in delivery of ICOS ligand and antigen. J Immunol. 2014;192(7):3166-79.
340. Weinstein JS, Hernandez SG, Craft J. T cells that promote B-Cell maturation in systemic autoimmunity. Immunol Rev. 2012;247(1):160-71.
341. Siegemund S, Shepherd J, Xiao C, Sauer K. hCD2-iCre and Vav-iCre mediated gene recombination patterns in murine hematopoietic cells. PLoS One. 2015;10(4):e0124661.
342. Gies V, Guffroy A, Korganow AS. [Thymic B cells: not simple bystanders of T cell lymphopoiesis]. Med Sci (Paris). 2017;33(8-9):771-8.
343. Yamano T, Steinert M, Klein L. Thymic B Cells and Central T Cell Tolerance. Front Immunol. 2015;6:376.
344. Lundqvist C, Camponeschi A, Visentini M, Telemo E, Ekwall O, Martensson IL. Switched CD21(-/low) B cells with an antigen-presenting phenotype in the infant thymus. J Allergy Clin Immunol. 2019;143(4):1616-20 e7.
345. Rother MB, Schreurs MW, Kroek R, Bartol SJ, van Dongen JJ, van Zelm MC. The Human Thymus Is Enriched for Autoreactive B Cells. J Immunol. 2016;197(2):441-8.

346. Sebzda E, Mariathasan S, Ohteki T, Jones R, Bachmann MF, Ohashi PS. Selection of the T cell repertoire. Annu Rev Immunol. 1999;17:829-74.
347. Miyama-Inaba M, Kuma S, Inaba K, Ogata H, Iwai H, Yasumizu R, et al. Unusual phenotype of B cells in the thymus of normal mice. J Exp Med. 1988;168(2):811-6.
348. Isaacson PG, Norton AJ, Addis BJ. The human thymus contains a novel population of B lymphocytes. Lancet. 1987;2(8574):1488-91.
349. Yuseff MI, Pierobon P, Reversat A, Lennon-Dumenil AM. How B cells capture, process and present antigens: a crucial role for cell polarity. Nat Rev Immunol. 2013;13(7):475-86.
350. Ramsdell F, Fowlkes BJ. Clonal deletion versus clonal anergy: the role of the thymus in inducing self tolerance. Science. 1990;248(4961):1342-8.
351. Atkinson MA, Eisenbarth GS, Michels AW. Type 1 diabetes. Lancet. 2014;383(9911):69-82.
352. Aubin AM, Lombard-Vadnais F, Collin R, Aliesky HA, McLachlan SM, Lesage S. The NOD Mouse Beyond Autoimmune Diabetes. Front Immunol. 2022;13:874769.
353. Yagi H, Matsumoto M, Kunimoto K, Kawaguchi J, Makino S, Harada M. Analysis of the roles of CD4+ and CD8+ T cells in autoimmune diabetes of NOD mice using transfer to NOD athymic nude mice. Eur J Immunol. 1992;22(9):2387-93.
354. Roep BO. The role of T-cells in the pathogenesis of Type 1 diabetes: from cause to cure. Diabetologia. 2003;46(3):305-21.
355. Thomas-Vaslin V, Damotte D, Coltey M, Le Douarin NM, Coutinho A, Salaun J. Abnormal T cell selection on nod thymic epithelium is sufficient to induce autoimmune manifestations in C57BL/6 athymic nude mice. Proc Natl Acad Sci U S A. 1997;94(9):4598-603.
356. Kishimoto H, Sprent J. A defect in central tolerance in NOD mice. Nat Immunol. 2001;2(11):1025-31.
357. Zucchelli S, Holler P, Yamagata T, Roy M, Benoist C, Mathis D. Defective central tolerance induction in NOD mice: genomics and genetics. Immunity. 2005;22(3):385-96.
358. Dong M, Audiger C, Adegoke A, Lebel ME, Valbon SF, Anderson CC, et al. CD5 levels reveal distinct basal T-cell receptor signals in T cells from non-obese diabetic mice. Immunol Cell Biol. 2021;99(6):656-67.
359. Pinto AI, Smith J, Kissack MR, Hogg KG, Green EA. Thymic B Cell-Mediated Attack of Thymic Stroma Precedes Type 1 Diabetes Development. Front Immunol. 2018;9:1281.
360. Evans DE, Munks MW, Purkerson JM, Parker DC. Resting B lymphocytes as APC for naive T lymphocytes: dependence on CD40 ligand/CD40. J Immunol. 2000;164(2):688-97.
361. Van Gool SW, Vandenberghe P, de Boer M, Ceuppens JL. CD80, CD86 and CD40 provide accessory signals in a multiple-step T-cell activation model. Immunol Rev. 1996;153:47-83.
362. Brandle D, Muller S, Muller C, Hengartner H, Pircher H. Regulation of RAG-1 and CD69 expression in the thymus during positive and negative selection. Eur J Immunol. 1994;24(1):145-51.
363. Breed ER, Watanabe M, Hogquist KA. Measuring Thymic Clonal Deletion at the Population Level. J Immunol. 2019;202(11):3226-33.
364. Tan Q, Tai N, Li Y, Pearson J, Pennetti S, Zhou Z, et al. Activation-induced cytidine deaminase deficiency accelerates autoimmune diabetes in NOD mice. JCI Insight. 2018;3(1).
365. Gagnerault MC, Luan JJ, Lotton C, Lepault F. Pancreatic lymph nodes are required for priming of beta cell reactive T cells in NOD mice. J Exp Med. 2002;196(3):369-77.

366. Wan X, Vomund AN, Peterson OJ, Chervonsky AV, Lichti CF, Unanue ER. The MHC-II peptidome of pancreatic islets identifies key features of autoimmune peptides. Nat Immunol. 2020;21(4):455-63.
367. Honjo T, Muramatsu M, Fagarasan S. AID: how does it aid antibody diversity? Immunity. 2004;20(6):659-68.
368. Zaheen A, Boulianne B, Parsa JY, Ramachandran S, Gommerman JL, Martin A. AID constrains germinal center size by rendering B cells susceptible to apoptosis. Blood. 2009;114(3):547-54.
369. Daley SR, Hu DY, Goodnow CC. Helios marks strongly autoreactive CD4+ T cells in two major waves of thymic deletion distinguished by induction of PD-1 or NF-kappaB. J Exp Med. 2013;210(2):269-85.
370. Akkaraju S, Ho WY, Leong D, Canaan K, Davis MM, Goodnow CC. A range of CD4 T cell tolerance: partial inactivation to organ-specific antigen allows nondestructive thyroiditis or insulitis. Immunity. 1997;7(2):255-71.
371. Mariathasan S, Bachmann MF, Bouchard D, Ohteki T, Ohashi PS. Degree of TCR internalization and Ca2+ flux correlates with thymocyte selection. J Immunol. 1998;161(11):6030-7.
372. Hase K, Takahashi D, Ebisawa M, Kawano S, Itoh K, Ohno H. Activation-induced cytidine deaminase deficiency causes organ-specific autoimmune disease. PLoS One. 2008;3(8):e3033.
373. Perera J, Huang H. The development and function of thymic B cells. Cell Mol Life Sci. 2015;72(14):2657-63.
374. Castaneda J, Hidalgo Y, Sauma D, Rosemblatt M, Bono MR, Nunez S. The Multifaceted Roles of B Cells in the Thymus: From Immune Tolerance to Autoimmunity. Front Immunol. 2021;12:766698.
375. Spencer J, Choy M, Hussell T, Papadaki L, Kington JP, Isaacson PG. Properties of human thymic B cells. Immunology. 1992;75(4):596-600.
376. Butler JE, Sun J, Weber P, Ford SP, Rehakova Z, Sinkora J, et al. Antibody repertoire development in fetal and neonatal piglets. IV. Switch recombination, primarily in fetal thymus, occurs independent of environmental antigen and is only weakly associated with repertoire diversification. J Immunol. 2001;167(6):3239-49.
377. Haba S, Nisonoff A. IgE-secreting cells in the thymus: correlation with induction of tolerance to IgE. Proc Natl Acad Sci U S A. 1992;89(11):5185-7.
378. Liu W, Meckel T, Tolar P, Sohn HW, Pierce SK. Intrinsic properties of immunoglobulin IgG1 isotype-switched B cell receptors promote microclustering and the initiation of signaling. Immunity. 2010;32(6):778-89.
379. Martin SW, Goodnow CC. Burst-enhancing role of the IgG membrane tail as a molecular determinant of memory. Nat Immunol. 2002;3(2):182-8.
380. Torres M, Casadevall A. The immunoglobulin constant region contributes to affinity and specificity. Trends Immunol. 2008;29(2):91-7.
381. Ratiu JJ, Racine JJ, Hasham MG, Wang Q, Branca JA, Chapman HD, et al. Genetic and Small Molecule Disruption of the AID/RAD51 Axis Similarly Protects Nonobese Diabetic Mice from Type 1 Diabetes through Expansion of Regulatory B Lymphocytes. J Immunol. 2017;198(11):4255-67.

382. Okazaki T, Okazaki IM, Wang J, Sugiura D, Nakaki F, Yoshida T, et al. PD-1 and LAG-3 inhibitory co-receptors act synergistically to prevent autoimmunity in mice. J Exp Med. 2011;208(2):395-407.
383. Safavi S, Larouche A, Zahn A, Patenaude AM, Domanska D, Dionne K, et al. The uracil-DNA glycosylase UNG protects the fitness of normal and cancer B cells expressing AID. NAR Cancer. 2020;2(3):zcaa019.
384. Revy P, Muto T, Levy Y, Geissmann F, Plebani A, Sanal O, et al. Activation-induced cytidine deaminase (AID) deficiency causes the autosomal recessive form of the Hyper-IgM syndrome (HIGM2). Cell. 2000;102(5):565-75.
385. Quartier P, Bustamante J, Sanal O, Plebani A, Debre M, Deville A, et al. Clinical, immunologic and genetic analysis of 29 patients with autosomal recessive hyper-IgM syndrome due to Activation-Induced Cytidine Deaminase deficiency. Clin Immunol. 2004;110(1):22-9.
386. Durandy A, Cantaert T, Kracker S, Meffre E. Potential roles of activation-induced cytidine deaminase in promotion or prevention of autoimmunity in humans. Autoimmunity. 2013;46(2):148-56.
387. Lebel ME, Coutelier M, Galipeau M, Kleinman CL, Moon JJ, Melichar HJ. Differential expression of tissue-restricted antigens among mTEC is associated with distinct autoreactive T cell fates. Nat Commun. 2020;11(1):3734.
388. Van Parijs L, Peterson DA, Abbas AK. The Fas/Fas ligand pathway and Bcl-2 regulate T cell responses to model self and foreign antigens. Immunity. 1998;8(2):265-74.
389. Paul S, Lal G. The Molecular Mechanism of Natural Killer Cells Function and Its Importance in Cancer Immunotherapy. Front Immunol. 2017;8:1124.
390. Moore CB, Guthrie EH, Huang MT, Taxman DJ. Short hairpin RNA (shRNA): design, delivery, and assessment of gene knockdown. Methods Mol Biol. 2010;629:141-58.
391. Basit A, Tang W, Wu D. shRNA-Induced Gene Knockdown In Vivo to Investigate Neutrophil Function. Methods Mol Biol. 2016;1407:169-77.
392. Kendall PL, Yu G, Woodward EJ, Thomas JW. Tertiary lymphoid structures in the pancreas promote selection of B lymphocytes in autoimmune diabetes. J Immunol. 2007;178(9):5643-51.
393. Cerchietti LC, Ghetu AF, Zhu X, Da Silva GF, Zhong S, Matthews M, et al. A small-molecule inhibitor of BCL6 kills DLBCL cells in vitro and in vivo. Cancer Cell. 2010;17(4):400-11.
394. Bunting KL, Melnick AM. New effector functions and regulatory mechanisms of BCL6 in normal and malignant lymphocytes. Curr Opin Immunol. 2013;25(3):339-46.
395. Allen CD, Cyster JG. Follicular dendritic cell networks of primary follicles and germinal centers: phenotype and function. Semin Immunol. 2008;20(1):14-25.
396. Wu X, Jiang N, Fang YF, Xu C, Mao D, Singh J, et al. Impaired affinity maturation in Cr2-/- mice is rescued by adjuvants without improvement in germinal center development. J Immunol. 2000;165(6):3119-27.
397. McCulloch L, Brown KL, Bradford BM, Hopkins J, Bailey M, Rajewsky K, et al. Follicular dendritic cell-specific prion protein (PrP) expression alone is sufficient to sustain prion infection in the spleen. PLoS Pathog. 2011;7(12):e1002402.
398. Hill NJ, Lyons PA, Armitage N, Todd JA, Wicker LS, Peterson LB. NOD Idd5 locus controls insulitis and diabetes and overlaps the orthologous CTLA4/IDDM12 and NRAMP1 loci in humans. Diabetes. 2000;49(10):1744-7.

399. Kim H, Perovanovic J, Shakya A, Shen Z, German CN, Ibarra A, et al. Targeting transcriptional coregulator OCA-B/Pou2af1 blocks activated autoreactive T cells in the pancreas and type 1 diabetes. J Exp Med. 2021;218(3).
400. Pepin G, Ferrand J, Honing K, Jayasekara WS, Cain JE, Behlke MA, et al. Cre-dependent DNA recombination activates a STING-dependent innate immune response. Nucleic Acids Res. 2016;44(11):5356-64.
401. Allen CD, Okada T, Tang HL, Cyster JG. Imaging of germinal center selection events during affinity maturation. Science. 2007;315(5811):528-31.
402. Deenick EK, Ma CS, Brink R, Tangye SG. Regulation of T follicular helper cell formation and function by antigen presenting cells. Curr Opin Immunol. 2011;23(1):111-8.
403. Deenick EK, Ma CS. The regulation and role of T follicular helper cells in immunity. Immunology. 2011;134(4):361-7.
404. Lund FE. Cytokine-producing B lymphocytes-key regulators of immunity. Curr Opin Immunol. 2008;20(3):332-8.
405. Roux KJ, Kim DI, Burke B, May DG. BioID: A Screen for Protein-Protein Interactions. Curr Protoc Protein Sci. 2018;91:19 23 1-19 23 15.
406. Methot SP, Di Noia JM. Molecular Mechanisms of Somatic Hypermutation and Class Switch Recombination. Adv Immunol. 2017;133:37-87.
407. Geisberger R, Crameri R, Achatz G. Models of signal transduction through the B-cell antigen receptor. Immunology. 2003;110(4):401-10.
408. Xu Y, Xu L, Zhao M, Xu C, Fan Y, Pierce SK, et al. No receptor stands alone: IgG B-cell receptor intrinsic and extrinsic mechanisms contribute to antibody memory. Cell Res. 2014;24(6):651-64.
409. Wang J, Lin F, Wan Z, Sun X, Lu Y, Huang J, et al. Profiling the origin, dynamics, and function of traction force in B cell activation. Sci Signal. 2018;11(542).
410. Torres M, May R, Scharff MD, Casadevall A. Variable-region-identical antibodies differing in isotype demonstrate differences in fine specificity and idiotype. J Immunol. 2005;174(4):2132-42.
411. Teng G, Papavasiliou FN. Immunoglobulin somatic hypermutation. Annu Rev Genet. 2007;41:107-20.
412. Dunn-Walters DK, Howe CJ, Isaacson PG, Spencer J. Location and sequence of rearranged immunoglobulin genes in human thymus. Eur J Immunol. 1995;25(2):513-9.
413. Hidalgo Y, Nunez S, Fuenzalida MJ, Flores-Santibanez F, Saez PJ, Dorner J, et al. Thymic B Cells Promote Germinal Center-Like Structures and the Expansion of Follicular Helper T Cells in Lupus-Prone Mice. Front Immunol. 2020;11:696.
414. Vetters M, Barclay RS. The incidence of germinal centres in thymus glands of patients with congenital heart disease. J Clin Pathol. 1973;26(8):583-91.
415. Sims GP, Shiono H, Willcox N, Stott DI. Somatic hypermutation and selection of B cells in thymic germinal centers responding to acetylcholine receptor in myasthenia gravis. J Immunol. 2001;167(4):1935-44.
416. Di Niro R, Lee SJ, Vander Heiden JA, Elsner RA, Trivedi N, Bannock JM, et al. Salmonella Infection Drives Promiscuous B Cell Activation Followed by Extrafollicular Affinity Maturation. Immunity. 2015;43(1):120-31.

417. Trivedi N, Weisel F, Smita S, Joachim S, Kader M, Radhakrishnan A, et al. Liver Is a Generative Site for the B Cell Response to Ehrlichia muris. Immunity. 2019;51(6):1088-101 e5.
418. William J, Euler C, Christensen S, Shlomchik MJ. Evolution of autoantibody responses via somatic hypermutation outside of germinal centers. Science. 2002;297(5589):2066-70.
419. Elsner RA, Shlomchik MJ. Germinal Center and Extrafollicular B Cell Responses in Vaccination, Immunity, and Autoimmunity. Immunity. 2020;53(6):1136-50.
420. Matsumoto M, Lo SF, Carruthers CJ, Min J, Mariathasan S, Huang G, et al. Affinity maturation without germinal centres in lymphotoxin-alpha-deficient mice. Nature. 1996;382(6590):462-6.
421. Sundling C, Lau AWY, Bourne K, Young C, Laurianto C, Hermes JR, et al. Positive selection of IgG(+) over IgM(+) B cells in the germinal center reaction. Immunity. 2021;54(5):988-1001 e5.
422. Zahn A, Daugan M, Safavi S, Godin D, Cheong C, Lamarre A, et al. Separation of function between isotype switching and affinity maturation in vivo during acute immune responses and circulating autoantibodies in UNG-deficient mice. J Immunol. 2013;190(12):5949-60.
423. Brink R, Paus D, Bourne K, Hermes JR, Gardam S, Phan TG, et al. The SW(HEL) system for high-resolution analysis of in vivo antigen-specific T-dependent B cell responses. Methods Mol Biol. 2015;1291:103-23.
424. Fujihara C, Williams JA, Watanabe M, Jeon H, Sharrow SO, Hodes RJ. T cell-B cell thymic cross-talk: maintenance and function of thymic B cells requires cognate CD40-CD40 ligand interaction. J Immunol. 2014;193(11):5534-44.
425. Guerri L, Peguillet I, Geraldo Y, Nabti S, Premel V, Lantz O. Analysis of APC types involved in CD4 tolerance and regulatory T cell generation using reaggregated thymic organ cultures. J Immunol. 2013;190(5):2102-10.

Appendix A

Authorization for use of published figures

SPRINGER NATURE LICENSE
TERMS AND CONDITIONS

Feb 16, 2022

This Agreement between Mr. Felix Lombard ("You") and Springer Nature ("Springer Nature") consists of your license details and the terms and conditions provided by Springer Nature and Copyright Clearance Center.

License Number	5250850424491
License date	Feb 16, 2022
Licensed Content Publisher	Springer Nature
Licensed Content Publication	Nature Reviews Immunology
Licensed Content Title	Developing a new paradigm for thymus organogenesis
Licensed Content Author	C. Clare Blackburn et al
Licensed Content Date	Apr 1, 2004
Type of Use	Thesis/Dissertation
Requestor type	non-commercial (non-profit)
Format	electronic
Portion	figures/tables/illustrations
Number of figures/tables/illustrations	1
High-res required	no

SPRINGER NATURE LICENSE
TERMS AND CONDITIONS

Feb 16, 2022

This Agreement between Mr. Felix Lombard ("You") and Springer Nature ("Springer Nature") consists of your license details and the terms and conditions provided by Springer Nature and Copyright Clearance Center.

License Number	5250850964989
License date	Feb 16, 2022
Licensed Content Publisher	Springer Nature
Licensed Content Publication	Nature Reviews Immunology
Licensed Content Title	The who, how and where of antigen presentation to B cells
Licensed Content Author	Facundo D. Batista et al
Licensed Content Date	Dec 31, 1969
Type of Use	Thesis/Dissertation
Requestor type	non-commercial (non-profit)
Format	electronic
Portion	figures/tables/illustrations
Number of figures/tables/illustrations	1

ELSEVIER LICENSE
TERMS AND CONDITIONS

Feb 16, 2022

This Agreement between Mr. Felix Lombard ("You") and Elsevier ("Elsevier") consists of your license details and the terms and conditions provided by Elsevier and Copyright Clearance Center.

License Number	5250841377650
License date	Feb 16, 2022
Licensed Content Publisher	Elsevier
Licensed Content Publication	Immunity
Licensed Content Title	Positive selection of IgG+ over IgM+ B cells in the germinal center reaction
Licensed Content Author	Christopher Sundling,Angelica W.Y. Lau,Katherine Bourne,Clara Young,Candy Laurianto,Jana R. Hermes,Rosemary J. Menzies,Danyal Butt,Nike J. Kräutler,David Zahra,Dan Suan,Robert Brink
Licensed Content Date	May 11, 2021
Licensed Content Volume	54
Licensed Content Issue	5
Licensed Content Pages	19
Start Page	988